2021

Improving visual field tests for populations with advanced glaucoma and visual field loss in the periphery

Catherine Bain

PHD

Improving visual field tests for populations with advanced glaucoma and visual field loss in the periphery

Bain, Catherine

Award date:
2021

Awarding institution:
University of Plymouth

Copyright statement

UNIVERSITY OF
PLYMOUTH

Improving visual field tests for populations with advanced glaucoma and visual field loss in the periphery

by

Catherine Bain

A thesis submitted to the University of Plymouth

in partial fulfilment for the degree of

DOCTOR OF PHILOSOPHY

School of Health Professions

November 2020

Acknowledgements

Firstly I would like to thank my family, partner and his family for their ongoing support throughout the PhD. Keeping me positive and motivated during the whole process.

I would also like to thank my supervisors, Eleni Papadatou, Antonio Del Aguila-Carrasco and Lisa Bunn, for all of their support, guidance and expertise shared with me during unforeseeable circumstances. Also a special mention to Iván Marín-Franch and Paul Artes for their guidance and help with the Kinetic perimetry experimental R programming and design.

A big thank you must also go to all my research companions from FF01 who have support me throughout the PhD, but also became my friends and made my time in Plymouth all that more enjoyable.

Huge thank you to the School technicians, for their tireless assistance in all my projects, and to Fight for sight for funding my PhD and Plymouth University for allowing me this great opportunity.

This thesis is a reflection on my family's and my own belief in my abilities. My parents have shown continued belief that I would be able to do this and even more. A special mention to my partner Mathew Burnett who has had put up with the stress and tears of this PhD from me, but always somehow put a smile back on my face.

Authors Declaration

At no time during the registration for the degree of Doctor of Philosophy has the author been registered for any other University award without prior agreement of the Doctoral College Quality Sub-Committee. Work submitted for this research degree at the University of Plymouth has not formed part of any other degree either at the University of Plymouth or at another establishment. This study was financed with the aid of a studentship from Fight for Sight.

Presentations at conferences:

1. **Catherine Bain; Iván Marín-Franch; Paul H Artes**. Ultra-wide field (UWF) perimetry of the temporal-inferior visual field. British Congress of Optometry and Vision science, Plymouth, September 2017.
2. **Catherine Bain; Iván Marín-Franch; Andrew Ian McNaught; Paul H Artes**. The limits of the far peripheral visual field. The association of research in vision and ophthalmology (ARVO), Hawaii, April 2018.
3. **Catherine Bain; Iván Marín-Franch; Rizwan Malik; Lisa Bunn; Andrew Ian McNaught; Paul H Artes**. Adaptive kinetic perimetry of the peripheral visual field. The association of research in vision and ophthalmology (ARVO), Vancouver, April 2019.
4. **Catherine Bain; Iván Marín-Franch; Paul H Artes**. Clinical application of an adaptive kinetic perimetry algorithm, in advanced glaucoma. British Congress of Optometry and Vision science, Plymouth, September 2019.

Word count of main body of thesis: 50,038

Signed: 

Dated: 30/11/2020

Abstract

Improving visual field tests for populations with advanced glaucoma and visual field loss in the periphery

Catherine Bain

The visual field can extend up to 100° in the temporal visual region; however, in patients with glaucoma and other diseases that affect peripheral vision, only the central 30° of the visual field is monitored regularly in clinical practice using static perimetry. These static tests are rapid and robust against human errors due to their testing strategies. However, approximately 80% of the rest of the visual field is less regularly examined due to the length of time it takes to measure, using both static and kinetic stimuli. Currently, there is not an established automated kinetic test to measure the visual field within the same duration, and precision as a central static perimetry test.

The peripheral visual field is important for aspects such as attention, balance, and mobility, thus examination of this visual region may provide important information. This Thesis focuses on the development and clinical application of automated kinetic peripheral visual field tests, designed to rapidly measure the peripheral visual field.

In the first study, the outer limits of the far peripheral visual field were examined using kinetic stimuli by adapting a commercial Octopus 900 perimeter (Haag-Streit, Koniz, Switzerland) with an extended fixation device. The results confirmed research from a century ago and the distribution of responses provided the framework to develop kinetic perimetry strategies.

With this perimeter adaptation, we investigated the effect of cataract surgery on the extent of the peripheral visual field and if negative dysphotopsia can be detected. This was undertaken in 30 post-cataract surgery patients, using a stimulus that moved both inwards towards the fixation point and outwards from the fixation point. The results suggested implantation of intraocular lenses reduces the extent of the peripheral visual field. Negative dysphotopsia was detected in a patient, with shrinkage of the capsular bag being identified as the possible cause.

Simulations of responses to kinetic stimuli formed a kinetic test that was used to measure the outer visual boundary in participants with advanced glaucoma. Simulation results showed good precision, and a test duration similar to a static central test. Clinical application of this kinetic strategy test in a group of 12 participants with advanced glaucoma showed faster results than simulation estimates, and isopter estimates were precise to within ±4°.

I investigated the effect of vision loss from glaucoma on postural sway stability. Participant postural stability was measured in 11 participants with glaucoma and 12 aged matched controls, using accelerometers (Xsens MTw, Awinda, Holland). Participants viewed different visual scenes, to compare the role of central and peripheral visual fields on stability. The impact of proprioceptive feedback on stability and the contribution of vision was measured by using different standing surfaces. The results of this study confirmed a decrease of postural stability with vision loss, an increased reliance on proprioceptive feedback in glaucoma participants, and lack of input of the peripheral visual field outside of 60° on standing balance.

Contents page

Contents

List of Tables

List of Figures

List of abbreviations

ACG	Angle-Closure Glaucoma
ADVS	Activities of Daily Vision Scale
ADRV	Assessment of Disability Related to Vision
AGIS	Advanced Glaucoma Intervention Study
Asb	Apostilbs
CS	Contrast sensitivity
dB	Decibels
EGPS	European Glaucoma Prevention Study
EMGT	Early Manifest Glaucoma Trial
ETDRS	Early Treatment Diabetic Retinopathy Study
FL	FixationLoss
FN	False Negatives
FP	False Positives
GCP	Glaucoma Change Probability
GHT	Glaucoma Hemifield Test
GON	Glaucomatous Optic Neuropathy
GPI	Glaucoma Progression Index
GSS	Glaucoma Staging System
HFA	Humphrey Field Analyser
IOL	Intra-Ocular lens
IOP	Intra-Ocular Pressure
MD	Mean Deviation
MIP	Mean Isopter Position
MIR	Mean Isopter Radius
MREH	Manchester Royal Eye Hospital
NTG	Normal Tension Glaucoma
OAG	Open-Angle Glaucoma
OHTG	Ocular Hypertension Glaucoma
OHT	Ocular Hypertension
ONH	Optic Nerve Head

OPI	Open Perimetry Interface
PD	Pattern Deviation
PGA	Prostaglandin Analogue
PSD	Pattern Standard Deviation
POAG	Primary Open-Angle Glaucoma
RMS	Root-Mean-Square
RMSE	Root-Mean-Square Error
SAP	Standard Automated Perimetry
SD	Standard Deviation
SITA	Swedish Interactive Testing Algorithm
TD	Total Deviation
VA	Visual Acuity
VEGF	Vascular endothelial growth factor
VFI	Visual Field Index

1 Chapter 1: Thesis motivation and outline

The design of perimetry methods, to measure the extent and sensitivity of the visual field have developed greatly over time such as for example the development from early Bjerrum screens (Riddoch 1917), which used manual kinetic stimuli, to computerised automated kinetic perimetry devices such as the Octopus perimeter (Haag Streit AG, Koeniz, Switzerland). Despite this development in technology, difficulties remain in visual field acquisition because these tests are notoriously challenging for the patient, particularly if they suffer substantial vision loss (Chauhan et al., 2008)(Mönter, Crabb et al. 2017). One way to account for the degree of difficulty perceived by an individual with poor visual performance, is to reduce the test duration. An example of such a test is the Swedish Interactive Testing Algorithm (SITA) Fast on the Humphrey Field Analyser (HFA, Carl Zeiss Meditec, Dublin, CA).

The current standard method used to examine the visual field of a patient with glaucoma is static perimetry using the SITA standard test strategy on a HFA. However, this method only measures up to 30° of the visual field, representing only approximately 20% of vision (Bengtsson, Olsson et al. 1997). Thus, there remains a substantial area of vision that is left unexamined in patients. For detecting the early stages of glaucoma, this central static strategy method is favourable, however is difficult to undertake, and highly variable in its results when used in patients with substantial vision loss (Bengtsson and Heijl 1998, Artes, O'Leary et al. 2014).

In view of the current limitations of contemporary perimeters, there is a need for research developments designed to improve visual field assessments, for instance duration, and to increase the reliability of testing strategies. This is essential not only for monitoring glaucoma progression in the more advance stages, but also to

determine other ocular effects in the peripheral visual field, such as the impact of intraocular lenses (IOLs) on visual field extent (Simpson 2016), or visual phenomena such as negative dysphotopsia (Davison 2000). This development of better and easier visual field tests may lie in physically adapting current perimetry devices and in terms of test strategies. Such an approach would potentially reduce costs, and current clinical strains caused by lengthy testing procedures. In addition to these visual field test developments, incorporating other standard testing strategies for monitoring glaucoma such as visual acuity charts e.g. Early Treatment Diabetic Retinopathy Study (ETDRS), and Contrast Sensitivity (CS) could provide further information of the effects the later stages of glaucoma have on patients' vision.

Mobility and balance are additional factors that could be examined in individuals with advanced vision loss caused by diseases such as glaucoma. Measuring balance could allow us to determine the relationship between certain areas of visual field loss and the individuals' balance, and how this impacts the patient's daily activities (de Luna, Mihailovic et al. 2017). This could provide an alternative method of monitoring the progression of advanced glaucoma over time, and provide information in regards to patient risks in relation to extent of vision loss.

It is essential to keep tracking the progress of glaucoma at all stages, in order to preserve vision. By incorporating additional testing methods such as CS, VA and balance, a more detailed review of the patients' vision can be undertaken, monitoring of any further effects on vision could be more easily detected, compared to current methods. The aim of this thesis is to develop new kinetic visual field testing strategies, thus as to improve patient experience, and provide a method to accurately monitor the peripheral vision of advanced glaucoma patients, and healthy

individuals. This research will potentially influence the importance of peripheral visual field, and the role it plays in everyday life activities. It will also provide support for the use of peripheral visual field tests more frequently within a clinical environment.

1.1 Thesis outline

Chapter 1 introduces glaucoma, an ocular disease which causes severe and irreversible damage to visual function, and is prevalent in an older population. It will describe the pathophysiology of Primary Open-Angle Glaucoma, as this is the most common form (Cook and Foster 2012), the prevalence, the incidence and risk factors across different populations and ethnicities, and additionally the current treatment strategies for the disease. It will also examine the effects glaucoma has on other visual functions and everyday activities, such as reading and balance. This chapter will also discuss the current perimetry methods (static and kinetic) used to measure the extent of the visual field. It will also cover the pattern of visual field damage caused by glaucoma. An overview of advanced glaucoma will follow to cover aspects such as the progression to this stage of the disease and the risk factors associated with it. The problems with current monitoring strategies used for individuals with advanced vision loss will be described as well as alternative measures which could be used to improve the monitor of the progression of vision loss in advanced glaucoma.

Chapter 2 presents the design and built of an extended fixation device, which can bit fitted and calibrated with Octopus 900 perimeter. This device offers the possibility to measure a greater area of the peripheral visual field. By building devices such as

this, a commercial perimeter can be adapted to compensate for the design and limitations of the perimeter bowl when measuring the peripheral visual field.

Chapter 3 discusses the design and implementation of a new kinetic perimetry visual field test, designed to measure the furthest limits of the far-peripheral visual field in a group of healthy individuals. This is due to current limitations caused by the perimetry bowl shapes, which limit the extent of the peripheral visual field that can be measured. This kinetic perimetry test uses ascending and descending methods of limits to determine a spatial threshold in which a true isopter location would be located.

Chapter 4 investigates the performance of the new quick far-periphery kinetic perimetry test on post-cataract surgery participants. The aim of this study was to measure the peripheral visual field threshold in patients who had had cataract surgery to define the possible effects of an IOL on the extent of the temporal visual field. This experiment also attempted to locate negative dysphotopsia, which sometimes occurs after cataract surgery. This aftereffect is poorly understood and there is currently no conventional quick perimetry method to identify it. Using the new far-periphery kinetic test the position of the shadow in the temporal visual field was mapped.

Chapter 5 is a simulation chapter and is built upon the results in chapter 3. Kinetic perimetry tests are lengthy, thus participants tend to experience fatigue, causing response errors. This chapter aimed to describe the response behaviour by participants in a kinetic perimetry test. Using this distribution of response, we simulated a number of different kinetic strategies, differing on number of responses and how an isopter position was quantified. These strategies would help develop a

new kinetic algorithm that will allow measurement of the outer peripheral visual region within a short test duration while maintaining a high level of accuracy and precision. This test is designed for individuals with advanced vision loss, who currently find central static visual field tests difficult to undertake.

Chapter 6 discusses the performance of the new kinetic test strategy (designed in chapter 5) in a glaucoma population, and its suitability to be used in a clinical environment. The performance of the test is measured in terms of its test re-test variability and the test duration compared to current static visual field tests. This chapter also identifies the clinical relevance of measuring the temporal inferior visual fields, in terms of postural sway measurements in the glaucomatous population.

Chapter 7 describes an experiment which investigated the relationship between vision loss caused by glaucoma, and postural sway. This study aimed to provide relevance of the peripheral visual field for balance control and also the overall impact of vision loss on postural sway instability. This experiment used multiple surface and visual conditions and compared these results to control participants.

Chapter 8 sums up the work in the thesis, noting the novel contributions to the field of work, and gives suggestions for future work.

1.2 Glaucoma

1.2.1 Definition

Glaucoma is defined as a group of ocular disorders connected by common features including optic nerve head changes and visual field loss (Quigley, 2011). It is often, but not always, associated with increased intraocular pressure caused by

impediments in drainage of the aqueous humour fluid. As a result, glaucoma can lead to progressive vision loss and blindness (Boland et al., 2013, Thylefors and Négrel, 1994, Cook and Foster, 2012). It affected approximately 60 million people as of 2010, a number expected to increase to 80 million by the end of 2020, of whom approximately 10% of individuals are estimated to be bilaterally blind (Quigley and Broman, 2006).

1.2.2 Classification

The classification of glaucoma is most often based upon the anatomical structure of the angle between the cornea and iris, known as iridocorneal angle. Angle-closure glaucoma (ACG) is caused by a narrow angle between the cornea and iris which blocks the drainage pathway of the aqueous humour fluid. When the angle is open, but there is still a great deal of resistance of the drainage through the trabecular meshwork due to a build-up of particles, this is defined as open angle glaucoma (OAG). The majority of the time glaucoma presents as a primary disease, meaning no other cause, accounting for 92% of all presentations (de Moraes et al., 2016). However, it can on occasion be secondary due to trauma, inflammation and pupillary block in the eye (de Moraes et al., 2016).

Glaucoma is also classified in terms of intra-ocular pressure (IOP) levels. Normal tension glaucoma (NTG) is the presence of OAG with an IOP within the normal range i.e. 10-24mmHg (Weinreb, Aung et al. 2014). This accounts for an estimated 25-50% of glaucoma cases (Weinreb and Khaw, 2004). Ocular hypertension (OHT) describes the IOP levels elevated above normal range > 24mmHg, when no structural or functional damage is observed. OHT is distinct from glaucoma, but it is estimated that 1-2% of OHT patients will go on to develop OAG (Weinreb and Khaw 2004). In

those who do, glaucoma tends to progress faster, in terms of increased vision loss, thought to be due to the high IOP levels (Ocular hypertension study, OHTS) (Kass et al., 2002)(Thakur and Juneja 2018). For the purpose of this thesis, we will only discuss in depth the pathophysiology and risk factors of primary open angle glaucoma.

1.2.3 Diagnosis

The diagnosis of individuals with OAG is extremely important, as both a positive or negative diagnosis can produce a severe result for the individual. A diagnosis of OAG is undertaken by measurement using visual field tests, ophthalmoscopy, corneal thickness and IOP. Other optic neuropathies should also be excluded before declaring a diagnosis of OAG (Jacobs, Trobe et al. 2016). Epidemiological studies have shown that more than 50% of glaucoma cases remain undiagnosed, even in developed countries. This prevelance of undiagnosed population is consistent with the lack of cost-effective screening methods for glaucoma (Tielsch, Katz et al. 1994).

1.2.4 Open-angle glaucoma

As OAG is asymptomatic (Weinreb and Khaw 2004), there are no reports of pain. The only signs of progressing OAG is gradual vision loss and optic nerve head changes, thus vision loss can go undetected at first. Structural diagnosis of OAG is determined by excavation or cupping of the optic nerve head, termed as glaucomatous optic neuropathy (GON), where the retinal nerve fibres die and the cup becomes larger. An illustrated representation of GON can be seen in Figure 1.1. OAG is additionally characterised by the inhibition of aqueous humour outflow through the anterior chamber of the eye, at the iridocorneal angle. This reduced outflow sometimes precipitates a rise in IOP (Weinreb, Aung et al. 2014).

OAG is not caused by increased IOP levels, as it has been found that optic nerve head damage and visual field loss can occur regardless of IOP level (Foster, Buhrmann et al. 2002). As OAG progresses, damage is observed as thinning of the neuroretinal rim, to advanced cupping of the optic nerve head (see in Figure 1.1), resulting in typical patterns of visual field loss, thought to be due to the death of retinal ganglion cells (Smith, Katz et al. 1996, Ratican, Osborne et al. 2018). The definitive mechanism of damage to ganglion cell axons is not fully known. OAG presents as a bilateral condition, however, the visual field loss is often asymmetric at the point of detection (Weinreb et al., 2014, Weinreb and Khaw, 2004).

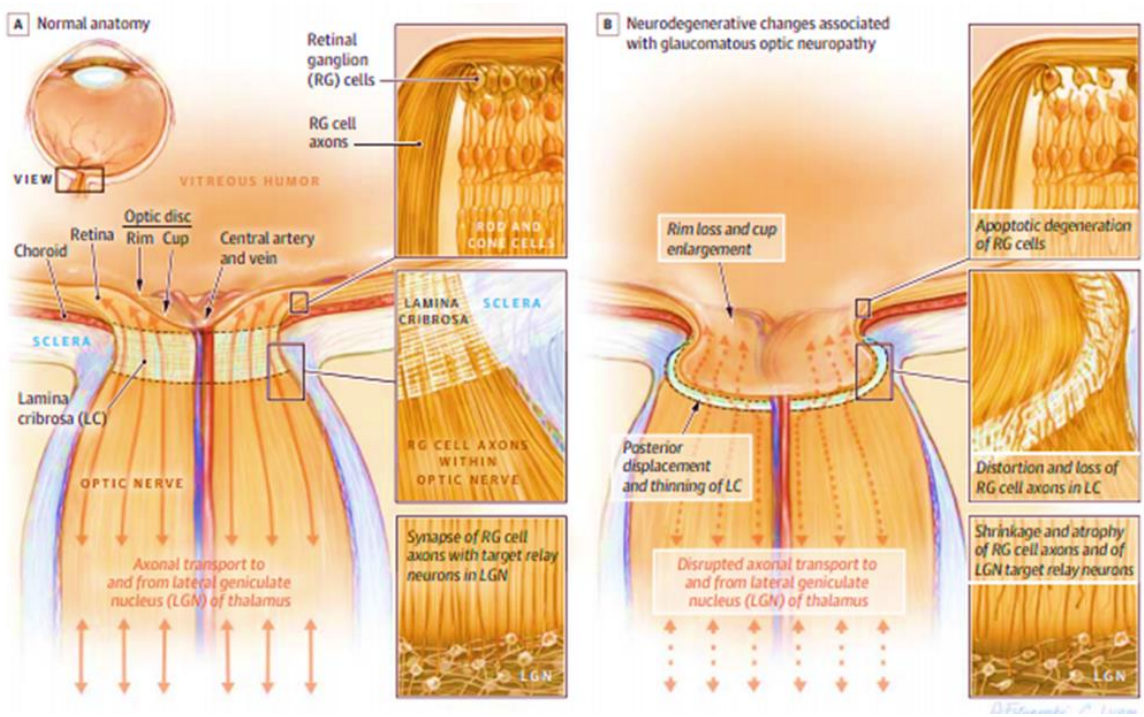

Figure 1.1: Adapted illustrated image of the anatomy of the optic nerve head. Panel A depicts the normal optic nerve head, and panel B shows the structural changes associated with glaucomatous optic neuropathy (Weinreb, Aung et al. 2014).

1.2.5 Epidemiology

The number of people with glaucoma was estimated at 60 million people across the world in 2010 (Cook and Foster 2012). Glaucoma is the second leading cause of blindness after cataract (Cook and Foster 2012). However, unlike cataracts once

vision loss has occurred, it cannot be restored through treatment. Certain forms of glaucoma and its subtypes are more prevalent than others. OAG accounts for at least three quarters of cases worldwide (Harasymowycz et al., 2016). However prevalence can differ depending on factors such as gender and ethnicity (Cook and Foster 2012). Thus, it is said that population-based screening for glaucoma types is not recommended due to these factors (Cook and Foster, 2012).

1.2.5.1 Prevalence

Prevalence is defined as the percentage of a population that is affected by the disease at any given time. This is calculated by comparing the total number of people with the disease in the population by the number of the overall population, producing a ratio. With an increasing ageing population worldwide, an accurate future prediction of prevalence is critical for the development appropriate health tailored policies for all populations (Tham, Li et al. 2014). However, prevalence differs among different populations. This is due to risk types varying between race and countries: for example, individuals who are black have a higher prevalence of OAG than individuals who are white (Friedman, Jampel et al. 2006) (see Figure 1.2). Thus population prevalence differing incurs limitations for studies to provide an accurate overall estimation of OAG prevalence (due to differing population ages, race and geographical regions etc.), resulting in a challenging approach to monitoring OAG trends for future reference.

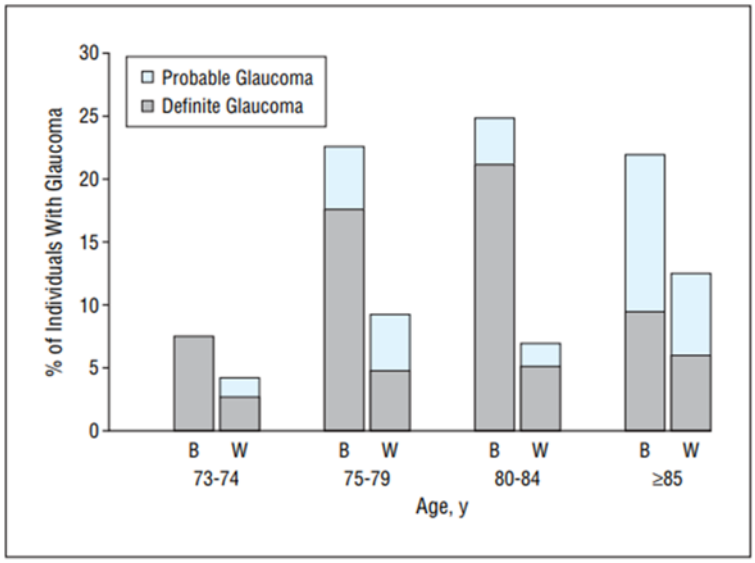

Figure 1.2: Prevalence of OAG in black and white ethnicities in the US (Friedman et al., 2006).

1.2.5.2 Incidence

The incidence of glaucoma can be defined as the rate of new cases in a population, over a given period. The incidence of glaucoma is generally studied using a cross sectional survey where a sample of the population is examined for the number of cases of glaucoma. This survey is later repeated after a number of years. Calculating the increase of new cases over that allotted period of time, in regards to the sample size of population, and number of new people identified at high risk, is defined as a percentage of incidence (Cook and Foster, 2012). Incidence percentage increases with factors such as ageing, and like prevalence differs between populations due to risk factors such as race. A review study conducted by Quigley and Vitale (1997) found that individuals of a black race in the United states' have diagnosis of OAG at a younger age, 27% longer with the condition in terms of years, than individuals who are white, with incidence increasing with age (see Figure 1.3.)

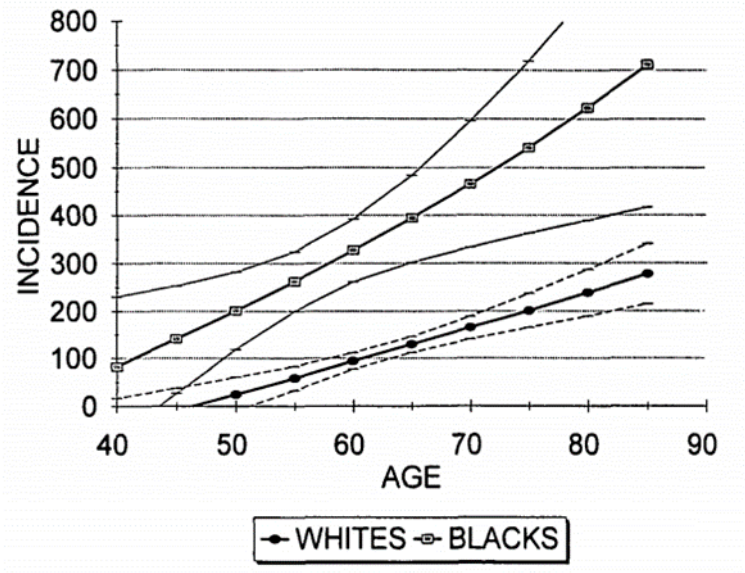

Figure 1.3: Incidence levels of OAG in black and white individuals in the United States, with increasing age (Quigley and Vitale 1997).

1.2.6 Risk factors

A list of risk factors has been identified through a large number of observational and clinical studies. These include factors such as intraocular pressure or family history, all suggestive of leading to a higher risk of developing glaucoma.

1.2.6.1 Demographic factors

Demographic factors consist of variables such as age and ancestry. These factors have been consistent throughout studies with a positive link to an increased risk of developing glaucoma (Quigley and Vitale 1997, Allison, Patel et al. 2020).

1.2.6.1.1 Age

Age is a risk factor prominent in today's society, with a large proportion of countries experiencing an increased ageing population (Coleman and Miglior, 2008). An ageing population is defined as an increasing median age compared to previous years due to increasing life expectancy (Tinker, 2002). With a longer life expectancy, there is an increase in the prevalence of glaucoma. This has been most notably seen in European countries where the odds of developing glaucoma have greatly increased

over the decades (Leske, 2007). The number of patients receiving treatment for glaucoma (e.g. drops/surgery), also increases with age, where patients aged 85 years and above, are 13 times more likely to receive glaucoma therapy then those aged between 40 to 64 years (Cook and Foster, 2012).

1.2.6.1.2 Ancestry

As ascertained, different cultures/ancestry are at more risk of developing glaucoma, more notably different forms of the glaucoma such as ACG over OAG (Friedman, 2007). The Barbados study (Leske et al., 1994) is a prime example which identified the relationship between race and prevalence of glaucoma. They identified that 1 in 11 adults, older than 50 years present with OAG in their study population, with this ratio increasing to 1 in 7 when adults are over the age of 70 years and from a black-Caribbean ethnicity.

An individual of African American descent has an increased risk of developing glaucoma (59%) in comparison to other ethnicities (Gordon, Beiser et al. 2002). This is thought to be due to African races having a significantly larger ONH, and generally a higher IOP level (Weinreb and Khaw 2004, Leske, Wu et al. 2008). They also more frequently present with bilateral glaucoma (Boland and Quigley, 2007). The onset of glaucoma has also shown to develop earlier in Africans in comparison to other ethnicities, such as Chinese and Hispanic (Gordon, Beiser et al. 2002).

1.2.6.1.3 Gender

Gender is a potential risk factor for OAG, however with many contradictory theories. Studies such as Mark (2005) found that females have a higher risk of ACG than males. This is was also found in OAG cases, however was only related in females who had early onset of menopause (Hulsman, Westendorp et al. 2001). One

theory predicts that female sex hormones may affect the shape of the ONH, with these hormones also influencing IOP levels (Drance, Anderson et al. 2001, Patel, Harris et al. 2018). Another suggests it is a decreased exposure to estrogen which increases the risk of developing OAG (Vajaranant et al., 2010). Thus, with the ever changing hormonal cycles of females, this increases the potential risk of the onset of glaucoma. An additional role that gender plays is the increased longevity of age in females in comparison to males (Barford, Dorling et al. 2006).

1.2.6.2 Genetic factors

Statistics show a higher risk of developing glaucoma if a first-degree relative has glaucoma. Prevalence within the family for OAG is estimated at 10.4% in siblings, and 1.1% in offspring of individuals with OAG (Wolfs, Klaver et al. 1998, Runyal and Din 2018). A positive family history has be found in as much as 60% of patients (Tielsch, Katz et al. 1994, McNaught, Allen et al. 2000, Green, Kearns et al. 2007). The population attributed risk of glaucoma is 16.4%, taking into account risk for relatives and individuals with no family history (Wolfs et al., 1998).

When identifying inheritance as a risk factor, there are numerous theories in regard to what affected genes lead to an increased risk of glaucoma. It is said approximately 3% to 5% of OAG is attributed to a defect in the MYOC coding of myocillin (Leske 2007), whereas other studies have identified mutations on the OPA1/OPTN genes for normal tension glaucoma (Wiggs 2007). However, these gene defects only account for a small percentage of the population with OAG, thus OAG likely arises due to a combination of genetics and other factors.

1.2.6.3 Systemic factors

1.2.6.3.1 Vascular

Studies have listed vascular risk factors as having positive links to an increase risk of developing OAG. Such conditions include systemic hypertension and atherosclerosis, and vasospasm (Bonomi et al., 2000). Blood pressure, has a well-known association with IOP levels (Wu, Nemesure et al. 2006). The fluctuation of ocular perfusion pressure (blood pressure minus IOP) causes perfusion at the ONH (Caprioli et al., 1987), thus it is suggested that IOP is more relevant than blood pressure itself in the increased risk of glaucoma development. There is also an association of the vascular role with migraines and ocular blood flow (Leske, 2007), with a migraine causing a rise in IOP and reducing ocular blood flow around the eyes.

1.2.6.3.2 Diabetes

Diabetes is an additional systemic factor, supported and unsupported for the association with OAG (de Voogd et al., 2006). Diabetes causes microvascular changes and has a strong association with high IOP levels. The high IOP is caused due to retinal vessels becoming damaged due to blood sugar levels and as a response to hypoxia (Zhao, Cho et al. 2015). New weak vessels are then formed due to VEGF factors (Osaadon, Fagan et al. 2014). These VEGF factors can travel to front of the eye and cause the formation of new blood vessels on the iris, resulting in blockage of aqueous humour flow (Zhao, Cho et al. 2015). However the direct relationship of diabetes and OAG has been hard to distinguish across studies (Leske 2007). A number of large studies are debating this question through the use of cross-sectional and case control studies such as the Ocular Hypertension Treatment Study

(Gordon, Beiser et al. 2002) which actually found that diabetes mellitus was protective against development of OAG, research is still undecided.

1.2.6.4 Ocular factors

1.2.6.4.1 IOP

The most important risk factor known to increase the risk of OAG is IOP. The relationship between OAG and IOP is best interpreted in population based incidence levels. A prominent example is from the longitudinal Barbados study (Leske, Wu et al. 2007) where incidence levels increased as baseline IOP levels increased. High IOP levels are defined as greater than 24mmHg, and individuals who present with an IOP above these levels are diagnosed with ocular hypertension (Leske, 2007). However glaucomatous damage may occur at any level of IOP, and only 5% to 10% of the population present with high IOPs (Leske 2007), thus a high IOP cannot directly be associated with OAG (see in Figure 1.4).

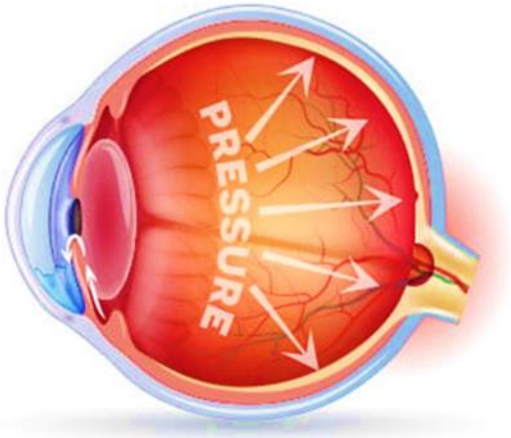

Figure 1.4: Image of cross sectional diagram of eye and points affected by increased pressure, adapted from Nariani et al, (2016).

IOP is the only factor which is modifiable, as it has been found in numerous studies, such as the Early manifest glaucoma trial (EMGT), the European Glaucoma Prevention Study (EGPS) and the Advanced Glaucoma Intervention Study (AGIS), that a reduction in IOP levels resulted in delay of glaucomatous progression. However, as only a small percentage of the population have high IOP, the relationship between lowering IOP and glaucoma progression may suggest the diverse relationship between IOP and the susceptibility of developing OAG across populations. This emphasises the possible effects of additional vascular or ocular factors.

1.2.6.4.2 Myopia

An ocular risk factor for OAG is myopia (near sightedness where light focuses in front of the retina) (Raviola and Wiesel, 1985)(Nitta, Sugiyama et al. 2017). Large studies such as the Blue Mountains Eye Study (Mitchell et al., 1999) and the Beijing Eye Study (Xu et al., 2007) have found an increased risk of glaucoma in the presence of high myopia (if refractive error exceeds -6D). Additionally an axial length > 24mm is considered to be a risk factor for glaucoma development (Marcus, de Vries et al. 2011). Thus, due to the structural differences that predispose an eye to myopia, this incurs an increased risk of damage to the optic nerve due to elevated IOP levels (Weinreb and Khaw, 2004).

1.2.6.4.3 Corneal thickness

Corneal thickness of greater than <535 μm is suggested as a risk factor for developing glaucoma (Herndon, Weizer et al. 2004).This risk further increases when coupled with an IOP >21mmHg (Gordon, Beiser et al. 2002). There has been differences shown between black and white individuals in corneal thickness

(Racette, Wilson et al. 2003, Herndon, Weizer et al. 2004) with the argument that a thinner corneal is a strong predictor of an individual developing OAG who also has ocular hypertension (Gordon, Beiser et al. 2002). The Barbados incidence study also inferred that ethnicity can differ in corneal thickness (Leske, Wu et al. 2007). However, issues identified with cornea thickness as a risk factor of OAG are from readings from tonometry, leading to clinicians underestimating IOP, thus the relationship between corneal thickness and IOP is unclear.

1.2.6.4.4 Optic nerve head

The size and ratio of cupping of the ONH can be a predictor and risk factor for developing glaucoma. With the structural measures of the ONH correlating with a loss of visual function in some patients (Boland and Quigley, 2007). Structural features which relate to a higher risk of glaucoma are a larger disc, resulting in a reduce ability to withstand stress (Boland and Quigley 2007). Although with a larger ONH, there is a greater number of nerve fibres, reducing the affect that damage has on vision loss (Quigley, Coleman et al. 1991, Jonas, Schmidt et al. 1992),Varma et al, (1995) found that individuals of African ethnicity have larger optic discs but with fewer nerve fibres, thus a greater risk of functional vision loss.

1.2.7 Physiology of Open-angle glaucoma

The physiology of glaucoma differs dependant on the type. OAG is not fully understood but current research suggests a relationship between intraocular pressure and retinal ganglion cell death, resulting in ONH damage and visual field loss. This section will discuss two pathophysiological theories on the cause of damage in OAG.

1.2.7.1 Mechanical theory

The mechanical theory is based upon the hypothesis of an elevated IOP, resulting in structural damage in and around the ONH due to compression (Yanagi, Kawasaki et al. 2011). Fluctuating or consistently high IOP is caused by a deficiency in the trabecular meshwork in managing the aqueous humour outflow, (see Figure 1.5). The fluid is secreted posterior of the iris from the ciliary body and flows anteriorly into the anterior chamber (Weinreb and Khaw, 2004). This results in a loss of lining cells, blockage of outflow (Weinreb et al., 2014) and a lack of nutrients. This obstruction is seen in individuals with ACG, where the anterior chamber angle is blocked by the iris and causes an increase in IOP. However, the anterior chamber angle can still remain "open" as seen in OAG and still cause a rise in IOP levels due to a build-up of particles preventing fluid drainage.

The precise pathophysiological relationships among elevated IOP, glaucomatous ON damage, and retinal ganglion cell death are poorly understood, however there have been observations which show that pressure-induced mitochondrial dysfunction contributes to retinal ganglion cell death and ON degeneration in glaucoma (Ju, Liu et al. 2007). Elevated IOP levels can cause compression to the ONH, due to this compression the axoplasmic transport of axons within the retinal nerve fibres is reduced, resulting in the death of the retinal ganglion cells. The death of these cells then lead on to structural damage such as thinning of the neuroretinal rim and cupping of the ONH (Flammer, Orgül et al. 2002, Weinreb, Aung et al. 2014). The process of retinal ganglion cell death through elevated IOP is known as apoptosis. Apoptosis is characterised as deoxyribonucleic acid (DNA) fragmentation, chromatin condensation and cell shrinkage (Farkas and Grosskreutz 2001). This process also

allows for activation of glial cell degeneration, through astrocytes changing the axon environment and producing milieu which prevents the survival of healthy retinal ganglion cells (Abu-Amero, Morales et al. 2006)(Weinreb and Khaw, 2004). This theory relates with other research (Gordon, Beiser et al. 2002), where the reduction of IOP even when within normal limits, reduces the progression of OAG.

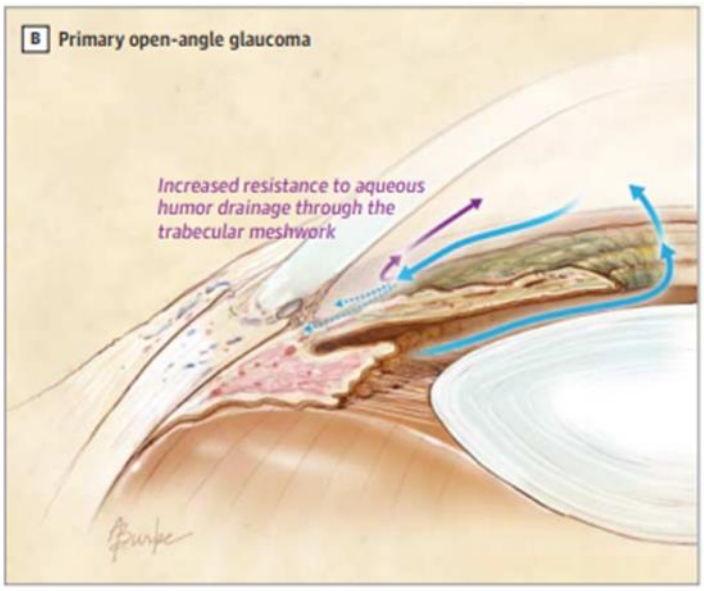

Figure 1.5: Aqueous Humour Drainage Pathway of eye with open-angle glaucoma (Weinreb, Aung et al. 2014)

1.2.7.2 Vascular theory

The vascular theory suggests that damage caused to the ONH is caused by reduced ocular blood flow, either through increased IOP or other systemic factors such as systemic hypertension (Yanagi, Kawasaki et al. 2011). As blood flow is reduced, this may incur tissue hypoxia which produces increased reactive oxygen species which can damage the ONH. Oxidative stress also causes an increase in endothelin-1, which is known to play a role of the death of retinal ganglion cells, and documented within individuals with OAG (Yanagi, Kawasaki et al. 2011, Weinreb, Aung et al. 2014). An additional aspect to the vascular theory is the decrease of cerebrospinal fluid pressure in the optic nerve subarachnoid space (Weinreb, Aung et al. 2014).

This change of pressure across the optic structures, may cause damage to the lamina, which is identified as the weakest point in the retinal nerve fibre layer, thus causing damage to the ONH.

1.2.8 Monitoring and treatment of glaucoma

When individuals are initially diagnosed with glaucoma they are placed on a treatment plan or a monitoring schedule dependant on the type of glaucoma diagnosis. The only course of treatment currently used in OAG is to reduce the IOP. This is still undertaken even when the patient has NTG as it has been found to reduce the progression of the disease, regardless of baseline IOP. By reducing this pressure by as much as 20%, visual field loss progression in reduced by half (Jampel et al., 2011). One of the first forms of treatment to reduce IOP are eye drops; currently prostaglandin analogue (PGA) eye drops are the first to be prescribed (NICE guidelines, 2017). These drugs work by reducing outflow resistance thus increasing aqueous humour flow through the uveoscleral pathway (Weinreb et al., 2014). The use of eye drops is dependent on the patients' reaction, or additional medications that they may be on.

If treatment with drops is unsuccessful, and the disease continues to progress, then an alternative therapy is used. Alternative treatment can be in the form of laser intervention to the trabecular meshwork or surgery. One form of laser treatment is trabeculoplasty. This procedure has an excellent safety profile and can be performed in a short period of time with the patient going home on the same day (Weinreb et al., 2014). Nevertheless, this treatment has shown to decrease in terms of efficiency over time. Another more invasive surgical intervention, a trabeculectomy, is the most common procedure undertaken. This procedure involves a small incision in the

trabecular meshwork to provide an alternative drainage output, thus reducing the IOP, however carries a higher risk of complications such as infection (Weinreb, Aung et al. 2014).

1.2.9 Real-world visual disabilities in glaucoma

Real-world world visual functions are activities such as walking, driving, object recognition, and reading. These are daily processes who many take for granted, but the role of vision is highly dependent on the performance (Ramulu 2009). An example is the role that our peripheral vision has on an activity such as crossing the street, and if there is central visual loss, then an individual relies heavily on the peripheral vision to detect a hazard. However even with this preserved peripheral visual region the ability to detect hazards is still greatly affected (Crundall, Underwood et al. 2002, Lee, Black et al. 2017). This makes daily activities difficult for individuals with vision loss from glaucoma. The aim of this section is to give a brief outline of the quality of life of individuals with glaucoma and some of the everyday tasks affected.

1.2.10 Quality of life and visual disability

Quality of life is frequently evaluated in patients with glaucoma. This is undertaken through questionnaires such as the NEI-VFQ 25 (Marella, Pesudovs et al. 2010). The purpose of this questionnaire is to observe an individual's perception of their vision, and how they feel about it. An example of one of these questions is "How much time do you worry about your eyesight?" These results can then be correlated with visual functions such as visual fields, hence establishing a relationship between how a patient is feeling, and how bad their vision loss actually is (Spaeth, Walt et al. 2006). This observation is important due to some patients sometimes feeling that their

vision is getting worse, resulting in them being less confident in undertaking certain activities. However on occasion there is no evidence from tests to suggest progression of vision loss. Thus, the mental health of patients should be monitored as well as their vision. However there is relatively little work on quality of life and visual disability currently, but there is a growing interest (Crabb, Smith et al. 2013, Murata, Hirasawa et al. 2013).

Another questionnaire to measure quality of life, is the Activities of Daily Vision Scale (ADVS), which measures how difficult an individual feels certain daily tasks are. These types of measures are effective at observing different types of vision loss and how they related with activities such as walking/balance performance (Murata, Hirasawa et al. 2013). Freeman et al, (2008) found that when using the ADVS questionnaire, individuals with bilateral glaucoma reported more difficulties than those with unilateral glaucoma.

Studies that utilise these types of questionnaires have provided evidence that patients with glaucoma struggle with activities such as reading, and that vision loss has an effect on their mobility (Ramulu, 2009). Additional findings have also related glaucoma to the increased levels of depression and other mental health issues (de Moraes et al., 2016). However, these questionnaires are only useful for detecting the aspects of visual functions that glaucoma patients feel they struggle with. These answers are subjective to a number of factors such as for example mental health at the time of questioning (Jampel, Schwartz et al. 2002). Measuring these visual functions would provide a more reliable performance of these tasks, and the effect that glaucoma has on them.

1.2.11 Reading

Being able to read is one of the main anxieties reported by glaucoma patients (Burton, Crabb et al. 2012). This is an unexpected finding due to glaucoma rarely affecting the central vision until the later stages of the disease. One factor recorded is the correlation between reading performance in glaucoma patients under poor lighting conditions (Burton et al., 2012). As already seen, patients with glaucoma have lower contrast thresholds (Owsley 2003, Pelli and Bex 2013) that deteriorateas the disease progresses. Thus it has been shown that reading performance as well as other visual functions are affected more when lighting conditions are poor (Nelson, Aspinall et al. 2003) relating to their contrast sensitivity visual function.

The pattern of visual field loss has also been shown to affect reading speed performance. A study by Ramulu et al, (2013) indicated that patients with binocular glaucomatous visual field loss had reduced reading speed during silent reading conditions. Burton et al, (2014) additionally found that advanced bilateral vision loss affects the speed of reading in glaucoma patients. As glaucoma progresses there is evidence that eye movements' characteristics change as vision loss increases, in comparison to healthy individuals (Smith, Glen et al. 2014).

1.2.12 Spatial visual search

Patients with glaucoma have shown to take longer when locating a visual target, in comparison to healthy subjects (Smith, Crabb et al. 2011). This functional mechanism is not understood very well, but one theory is that glaucoma has an effect on eye movements (Smith et al., 2012). Crabb et al, (2010) found that glaucomatous patients show different eye movement characteristics in comparison to healthy subjects, when observing a hazard perception test. They suggested

patients produced significantly more saccade eye movements. However, a study by Smith et al, (2012) found that patients made fewer saccades. They found that the stage of the disease and the contrast sensitivity score of the patient affected the amount of saccades manifesting. These results suggest that glaucomatous patients struggle with spatial visual search due to their visual field loss/scotomas obstructing their field of view. This could also interpret Crabb et al, (2010) results that an increase of eye saccades helps quicken visual search tasks for some patients with these patterns of vision loss.

1.2.13 Mobility, balance and risk of falling

To safely navigate through complex environments, an individuals' vision is essential. If visual input is decreased then the risks of falling is increased (Dhital, Pey et al. 2010) due to not having the ability to plan and avoid obstacles in a route (Black, Wood et al. 2011). With the elderly population already having a 30% risk of falling at least once in a year (Yuki, Asaoka et al. 2015), it is suggested that glaucoma patients with significant vision loss are at a significantly higher risk than the general age matched population. However there is currently no significant research to suggest that glaucoma patients do fall more (Dhital, Pey et al. 2010). This is due to additional risk factors which can lead to falls, such as body-mass index, age and general health. As a large proportion of glaucoma patients are over the age of 60, it is hard to distinguish what factor is causing the falls or if it is a combination of many. It has been observed that falls are more likely to occur if the inferior visual field is lost over the superior (Yuki et al., 2015, Black et al., 2011). This is thought to happen due to limited information in regards to steps/ramps being seen by the individual,

increasing their chances of tripping over obstacles. An additional factor, which may predict why vision loss leads to a higher risk of falls, is postural stability.

Postural stability involves the processing of information from vestibular, somatosensory, visual and musculoskeletal systems, with addition of cognitive factors attention, and reaction time (Shabana, Cornilleau-Pérès et al. 2005). Testing measures of balance in individuals' and the elevated risk of falling is essential in current and future work. Studies such as Kotecha et al, (2012) found that due to glaucoma patients having less visual input, they re-weighted on other postural controls, and were found to sway less than the control group when standing on a firm surface. When placed on a soft/foam surface, somatosensory input was reduced, resulting in glaucoma patients having worse postural sway. Relating this to real-world environments would suggest walking on grass or sand would be very difficult for glaucoma patients with reduced vision, as their somatosensory system is compromised temporarily.

Patients with glaucoma have shown to have reduced walking speed when they have significant visual field loss (Friedman, Freeman et al. 2007). This vision loss has also be associated with an increased fear of falling, resulting in a lower engagement in physical activity thus lower physical fitness (Ramulu 2009). Impoverished depth perception has been identified as a risk factor for reduced mobility and an increased risk of falls in glaucoma patients (Gupta, Krishnadev et al. 2006). This would suggest that glaucoma patients who have severe vision loss in just one eye are at a higher risk of falling, due to missing binocular cues for depth perception, such as stereopsis.

From the research discussed it would be suggested that the preservation of vision is essential for maintain a greater quality of life in patients. Current research have

conflicting findings in regards to the true extent vision loss has on aspects such as balance, thus this area of work should be developed.

1.3 Visual fields

The field of vision can be defined as the portion of the external environment from which an observer can obtain visual information when fixating without head or eye movement (Smythies 1996, Racette, Fischer et al. 2016). The purpose of measuring the visual field is to observe any vision loss or scotomas caused by disease or trauma, to either the eye or brain (Harwerth and Quigley, 2006). The constriction of the visual field having a negative impact on individual's quality of life.

1.3.1 Physiology of the visual field

The measured extent of the visual field can differ between observers dependant on age (Haas, Flammer et al. 1986, Vonthein, Rauscher et al. 2007). However in general the visual field extends approximately 100° temporally, 70° inferiorly, and 50-70° superiorly/nasally (Traquair and Scott 1957). Each individual has what is called a monocular field of vision, from one eye, and a binocular visual field formed from the morphing of both monocular fields (Nelson-Quigg et al., 2000). The visual field is separated into two regions, superior and inferior, across the horizontal midline, and two regions, temporal and nasal, across the vertical midline. However, the structure of an individual's face can have an impact on the extent of the visual field regions. For example, the nasal and superior regions of the visual field can be affected by structures like the nose and eyelids (Racette, Fischer et al. 2016). The optic disc is represented by a blind spot approximately 13° in the temporal visual field.

The visual field is constructed by rays of light passing through the cornea, iris (controlled by the pupil), and lens, and is then focused onto the retina (Aulhorn and

Harms 1972). The retina consists of a large number of photoreceptors. These photoreceptors contain opsins, which are a group of proteins.

The light which enters the eye initiates a cellular responses in the retina that begins as a slow response of photoreceptors and then transforms into a coordinated action of potentials at the level of the retinal ganglion cells (RGCs) (Tobimatsu and Celesia 2006). The visual signals formed from the photoreceptors are then send through parallel pathways which lead to and are distributed among the diencephalon, midbrain, lateral geniculate body, primary visual cortex, and more (Skalicky 2016).

The parallel pathways can be broadly divided into three major streams, the parvocel3 lular, magnocellular, and koniocellular pathways. Each of these pathways contributes to visual processing (Skalicky 2016).

Beyond the primary visual cortex there are two streams of information which can develop. These are the dorsal stream and the ventral stream. The dorsal stream involves the detected of where objects are and motion detection. The ventral stream in more involved with identify what objects are, for example their colour, depth etc (Tobimatsu and Celesia 2006).

It is important to note that the position of the visual field is reversed when examining the position of light focusing on the retina. For example, vision loss the inferior temporal visual field in the right eye, represents damage in the superior nasal side of the retina.

1.3.2 Hill of vision

The “Hill of vision” term for the visual field was originally coined by (Traquair 1924), where he described the visual field as “an island of vision surrounded by a sea of

blindness". This hill is formed around the sensitivity of the retina during fixation, see in Figure 1.6. The characteristics of the hill of vision are derived from the use of static and kinetic perimetry, measuring the luminance sensitivity at different positions in the visual field. This is usually measured by contrast sensitivity rather than absolute sensitivity due to the differences across regions, and measured in decibels (dB). By measuring this sensitivity it gives us a clear view of the normal sensitivity threshold range and also age-related effects, or abnormalities on the visual field (Katz, Gilbert et al. 1997). It is the 50% point of probability that is used to define the threshold (i.e. the chance of the threshold being detected 50% of the time), and thus determining the position of a point in the hill of vision (Schiefer, Strasburger et al. 2001). The hill of vision can be divided into three different levels; central peak 0 to 15°, mid-plateau 15° to 25° eccentricity and the peripheral 25° and onwards (Jacobs and Patterson 1985). Eccentricity is expressed as the visual angle, between the central fixation and the position of a target located on the visual field.

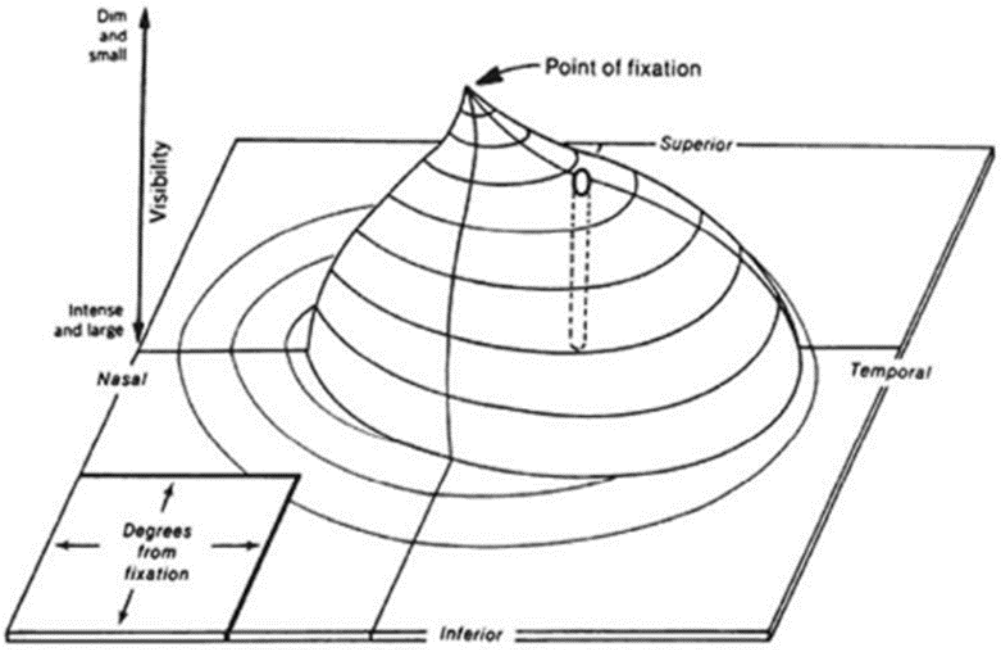

Figure 1.6: Illustrated diagram of the Hill of vision, example of a right eye (Anderson 1987).

1.3.3 Peripheral visual field

The peripheral visual field, described as the area outside the central 30° of vision when fixating (Strasburger, Rentschler et al. 2011), allows to detect objects and movement outside of the direct line of vision (central vision). The peripheral visual field can further be separated into two regions “far” and “mid” periphery (Bock, 1993)(Racette, Fischer et al. 2016), with mid subtending 30° to 60°, and far subtending beyond 60°, see Figure 1.7.

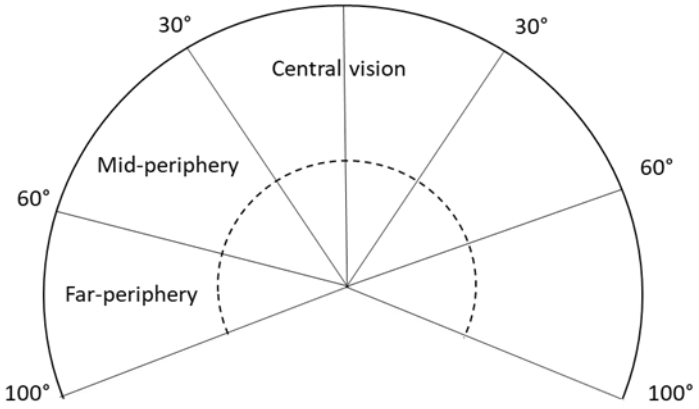

Figure 1.7: Diagram of peripheral and central visual field limits from a binocular perspective.

The peripheral area of the visual field is made up of less rods and cones in comparison to the central region (Swienton and Thomas 2014). Thus, contrast sensitivity is reduced in this region, hence the shape of the hill of vision becomes steeper as seen in Figure 1.6. The visual representation in the visual cortex is also reduced for the periphery, in comparison to the fovea region due to the decreased density of ganglion cells located in this area (Strasburger, Rentschler et al. 2011). Further visual functions, which are reduced due to density of rods and cones in the periphery, are colour vision and shape discrimination. In accordance to motor control, the peripheral vision is said to be responsible for processing ambient vision,

which is concerned with detecting spatial characteristics in the surrounding visual world (Berencsi, Ishihara et al. 2005).

1.3.4 Central visual field

The central visual field is measured from the point of fovea central fixation, up to 30°. This area of the eye has the largest in-take of light, focusing it at the retina, with the highest sensitivity at the fovea. This is due to the majority of retinal ganglion cells located in this area (Gibson 1950)(Hannibal, Christiansen et al. 2017). The fovea makes up 3° of the central visual field and the macular makes up to 10°. The central visual field in terms of motor control is said to be responsible for distinguishing physical characteristics of environmental objects (Berencsi, Ishihara et al. 2005).

1.3.5 Glaucomatous visual field loss

A visual field defect or vision loss is referred to as a loss of light sensitivity across the whole or part of the visual field (Cook and Foster 2012). Vision loss in glaucoma patients is irreversible, with most patients unaware of the loss of vision until the later stages of the disease, when it has an effect in everyday functions such as reading (Jampel, Schwartz et al. 2002).

1.3.5.1 Patterns of visual field loss

Although there is not set pattern of visual field loss across all glaucoma patients, typically loss occurs around the arrangement of the retinal nerve fibre layers as they pass through to the optic disc (Shaarawy, Sherwood et al. 2014). Those fibres, which enter at the temporal retina, are at most risk of damage, thus vision loss occurs more frequently in the superior hemisphere. Glaucomatous visual field loss is usually bilateral but mostly asymmetric between eyes, where one eye presents with twice as much damage as the other (Quigley, 2011). This damage usually starts around 10°

to 20° in the paracentral region, with the far peripheral and central regions not affected until the later stages of the disease.

1.3.5.1.1 Diffuse vision loss

Vision loss can initially appear as diffuse depression over the whole visual field or a large proportion, with vision loss not located to just one hemifield (Shaarawy, Sherwood et al. 2014). The appearance is sometimes referred to as a "sinking island of vision", however there is controversy with diffuse vision loss, as is not a specific glaucomatous sign (Caprioli et al., 1987) and could be a result of uncorrected refractive error when undertaking a visual field test.

1.3.5.1.2 Localised vision loss

Localised vision loss generally begins as a paracentral defect (scotoma), which develops into a paracentral arcuate defect where it progresses towards the blind spot (Shaarawy, Sherwood et al. 2014). Additional loss of arcuate nerve fibres results in this arcuate defect to arch over the fixation point and end in the nasal region. Often in the later stages of glaucoma these scotomas merge together, causing a ring scotoma. Additional patterns of vision loss are temporal wedge, nasal step and generalised constriction (Caprioli et al., 1987, Nevalainen et al., 2009). Nasal steps can appear step-like when observed using kinetic perimetry due to their asymmetric appearance on the border between the inferior and superior regions. See figure 1.8 for progression vision loss from OAG.

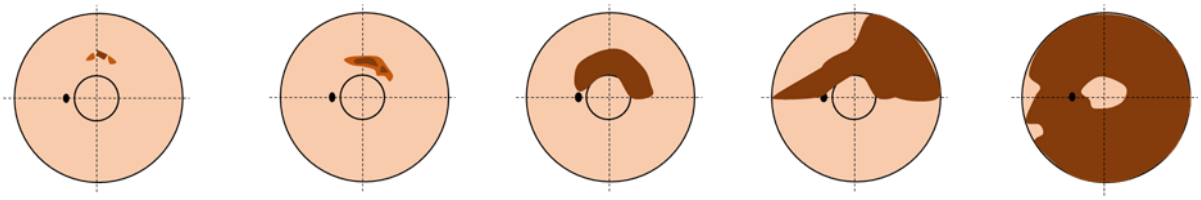

Figure 1.8: Schematic showing worsening visual field loss within 30° in a left eye with open-angle glaucoma.

1.4 Perimetry

The term perimetry is used to describe the investigation of an individual's visual field through different techniques and strategies. The purpose of perimetry is to map out the areas of the external environment, which are perceived, and also to quantify the functional capacity of the visual system (Aulhorn and Harms, 1972). This is undertaken by measuring the luminance sensitivity across the visual field in a systematic and standardised manner (Racette, Fischer et al. 2016). During steady fixation of a target, an individual is presented with light stimuli of set luminance and size, within their field of vision. The individual is instructed to respond when they see the source of light. These stimuli can either be in the form of static (static spot of light) or kinetic (moving spot of light). These can be adjusted by a number of different luminance intensities and sizes dependant on the location being measured in the visual field. The most commonly used test condition is to present a white stimulus upon a white background which must be dimmer than the stimulus (white-on-white) (Racette, Fischer et al. 2016). Other developments of perimetry use blue on yellow testing background (blue stimuli on yellow background), although this has had reports of higher test variability.

To perform a perimetry test an individual is sat in front of the perimeter with their head stabilised on a chin rest, and asked to indicate if they see a light stimulus. If the individual cannot see the light source then another is produced in the same location

but of a higher intensity. The minimum light intensity that an individual responds to is defined as the light sensitivity threshold (Aulhorn and Harms 1972, Anderson and Patella 1992, Racette, Fischer et al. 2016). Perimetry tests are primarily carried out on one eye at a time with the other eye covered during the test, unless measuring binocular vision (Jampel, Friedman et al. 2002). Using this technique the hill of vision can be mapped out, however perimetry can be a time consuming procedure, thus more efficient strategies based on threshold estimates have been developed over the years (Artes, Iwase et al. 2002, Turpin, McKendrick et al. 2002).

When measuring the sensitivity to light across the visual field, the decibel scale (dB) is used as a clinical interpretation of the results in a clinical environment (Racette, Fischer et al. 2016). The range of stimulus intensities differ between devices but general ranges from 0 to 32 dB in the fovea, where a threshold value of 0 dB indicates that an individual is not able to see the most intense stimulus that the device displays (Fankhauser, Spahr et al. 1977, Racette, Fischer et al. 2016). However, the actual measurement of stimulus intensity is defined as luminance. This is expressed in terms of candelas per meter squared (cd/m^2) or in apostilb (asb). The conversion of candelas to apostilb is $1cd/m^2$ to 3.14asb, however this is an older unit and not used often in current times (Short 1976, Saunders and Grum 1977, Brigell, Bach et al. 1998).

1.4.1 Static automated perimetry

Static perimetry quantifies the sensitivity of an individual's peripheral vision using different testing strategies. The static stimuli used have a constant size but varying luminance to determine an individuals' sensitivity threshold (Heijl, Patella et al. 2012). The standard size used is Goldmann size III (diameter 0.43°). The aim of static

perimetry is to confirm that visual function is not below the normal range through quantification (Heijl, Patella et al. 2012). Static threshold measurements are sensitive to shallow depression of the visual field, which increases detection of early glaucoma deficits compared to manual tests such as confrontation (Johnson, Keltner et al. 1979, Heijl, Lindgren et al. 1989).

1.4.1.1 Testing grid patterns

The most common testing patterns for this type of static perimetry are 30-2, 24-2 and 10-2, consisting of grids with 76, 54, 73 and 68 testing locations (see in Figure 1.9). The 30-2 tests the central 30° of the visual field made up of 76 locations, formed on a square matrix of 6°, displaced from the horizontal and vertical midlines by 3°. The 24-2 programme consists of 54 test locations, extending to 24°, apart from two points, which are located 27° nasally. It benefits from being faster than the 30-2, and has less interference from the lens rim artefact which can sometimes show as vision loss in the larger 30-2 test, thus has become more generally used in practice (Heijl and Krakau 1975, Guo, Kwon et al. 2017). The 10-2 testing pattern is generally used for patients with specific ocular diseases, such as macular degeneration or advanced glaucoma. This grid pattern has test points space equally 2° apart (Heijl, Patella et al. 2012).

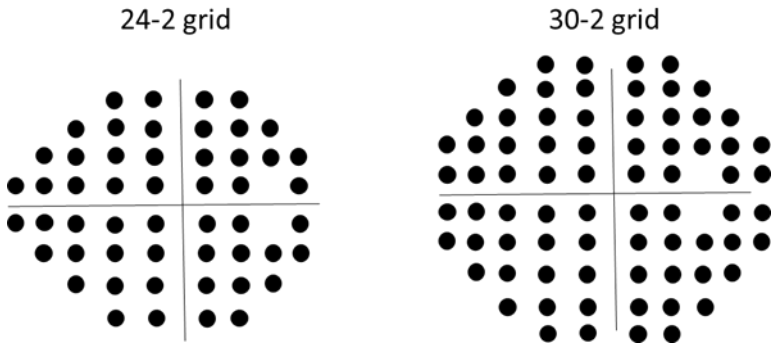

Figure 1.9: Grid patterns for 24-2 and 30-2 static automated perimetry.

1.4.1.2 Threshold estimation in static perimetry

When using static perimetry, the procedure of estimating the threshold value can have an effect on both the duration and detail of the test. Adaptive threshold strategies have been developed to use in static perimetry based upon efficiency in accuracy and precision, and the following section will discuss the most frequently used (Turpin, McKendrick et al. 2002).

1.4.1.2.1 Full threshold

The aim of Full threshold is to estimate the threshold of sensitivity through step down/up (staircase) techniques. Stimuli are presented at a pre-determined location, and of selected intensity based on a normative dataset (Artes, Iwase et al. 2002). This staircase algorithm is based on the responses to the stimuli. The stimulus intensity is adjusted in steps of 4dB, until the first response reversal occurs, where the stimulus is then adjusted in steps of 2dB. An estimation of these results is based on the last seen stimulus in a given test location, after there have been two response reversals (Artes, Iwase et al. 2002). This is the standard method used and widely accepted around the world. However this test strategy has a long duration and can be hard for patients to undergo (Johnson, Chauhan et al. 1992), with inconsistent responses. Increased sensitivity means more noise in the measurements thus it is difficult to determine a real change in the visual field from fluctuations of the test (Heijl, Lindgren et al. 1989, Artes, Iwase et al. 2002).

1.4.1.2.2 SITA Standard & SITA Fast

The SITA (Swedish Interactive Threshold Algorithm) threshold strategies were developed to produce the same quality of results which can be obtained with the full threshold method, but within a shorter test duration (Bengtsson, Heijl et al. 1998). Within the SITA test strategies the threshold values and measurement errors

are estimated continuously throughout the test. This is through maximum posterior probability calculations from established visual field models (Bengtsson, Heijl et al. 1998). The SITA strategies use the same staircase method to establish luminance sensitivity, however are interrupted when measurement errors have been reduced to a pre-determined level. Through this method the test time duration is greatly reduced when using the SITA Standard strategy (Artes, Iwase et al. 2002), but the SITA Fast strategy is even shorter in duration. Additional aspects of the SITA test which allow for a faster test duration is, adaption of the interstimulus interval to the individuals response speed by estimation of false positive rates (Bengtsson, Olsson et al. 1997, Artes, Iwase et al. 2002).

The difference between the SITA Standard and SITA Fast is the level of certainty required to end the test (Bengtsson, Olsson et al. 1997). The test-retest variability is lower in the SITA standard compared to Full threshold. Whereas the SITA fast only has lower variability in high sensitivity areas (Artes et al., 2002). Thus overall the SITA standard is a more reliable threshold strategy for routine tests.

1.4.1.2.3 FASTPAC

FASTPAC threshold is determined by a single reversal using an increment of 3dB, the threshold is defined as the last seen stimulus luminance. The FASTPAC algorithm takes 35% of the time taken to complete the full threshold, however is a lot less reliable (25%) for detecting visual field defects (Wild et al., 1999).

1.4.1.2.4 Suprathreshold

Suprathreshold is a fast strategy used to detect visual field defects without having to quantify the depth of the visual field. It is a widely used approach, and stimulus intensities are based upon the normative “Hill of vision” threshold values. If the

stimulus is seen then it is assumed that there is no significant vision loss in that test location. The suprathreshold stimuli used are of an intensity of pre-determined brightness, produced at each test location, usually in accordance to patient's age. Sensitivity of the patients' response at each location is unknown, but it is assumed that there is no substantial damage to that region of the eye if the stimulus is seen (Artes et al., 2003). It is important to note that the intensity of the stimulus is not too high or low, resulting in the test becoming insensitive or giving false-positive responses. This type of threshold testing is an attempt to measure the dimmest stimulus that can be detected 50% of the time by the patient, and is designed to be completed in a shorter amount of time than the full threshold, with fewer patient errors and less need for "practice" tests before obtaining reliable results.

A suprathreshold test will mark an area of the visual field defective when two stimulus presentations are missed. This method reduces false positive rates, however lowers overall sensitivity as a result (Artes et al., 2003). Artes et al (2003) found that dependent on a pass/fail criteria a better sensitivity and specificity could be obtained when between 3 to 5 presentations were missed, although this would extended the duration of the test (Mckendrick and Turpin 2005).

1.4.1.3 Interpretation of static perimetry output.

1.4.1.3.1 Grayscale

The estimated values of sensitivity across the central visual field are illustrated as a grayscale plot. Each shade of gray in the plot represents a different sensitivity value ranging from 0 to 5 dB. Normal sensitivity is shown as light gray, whereas absolute sensitivity (no detection of light) is seen as black. The grayscale plot is not age or

eccentricity corrected, and does not represent early visual field loss accurately, however is more useful in end stage visual field loss see figure 1.10.

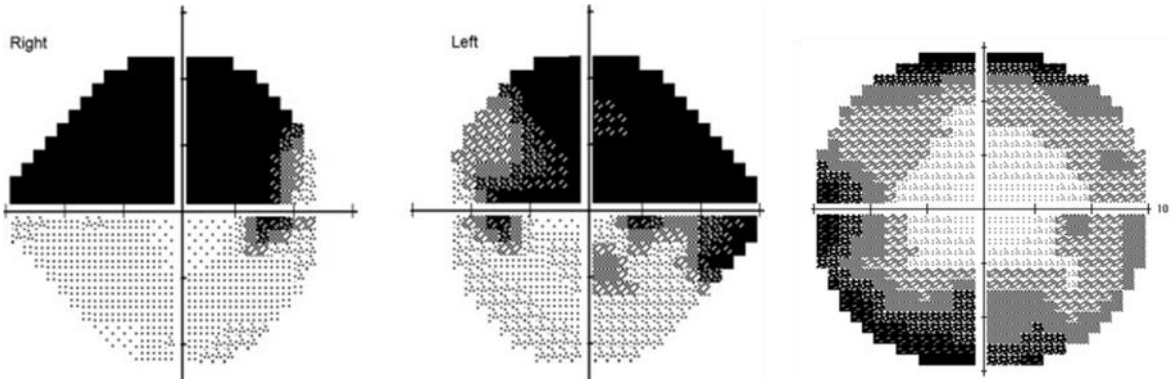

Figure 1.10: From left to right: Gray scale plots from two 24-2 grid patterns for right and left eye, and 30-2 grid pattern.

1.4.1.3.2 Probability plots

The probability plots on the central field printout are the Total Deviation (TD) and Pattern Deviation (PD) probability values. The TD probability level is displayed at each stimulus location. It is associated with the age-corrected deviation from the normal estimated sensitivity of the eye. The difference between this value and the normal range is indicated as sensitivities that are worse than the 5th, 2nd, 1st and 0.5th percentile of the normal range according to age. The PD probability value is calculated in the same way as the TD, however it takes into account the overall elevation or reduction in sensitivity. This method is useful for detecting localised field defects, however is unreliable for distinguishing between diffuse and generalised field loss.

1.4.1.3.3 Global indices

The global indices are the Mean Deviation (MD), Pattern Standard Deviation (PSD), and the Visual Field Index (VFI). These are a summary of measures of estimated sensitivity across all test locations.

The MD is the weighted mean difference across all stimulus locations in comparison to a healthy age-corrected (threshold sensitivity decreases with age) visual field. It is the average of the deviations shown in the TD plot. As the visual field worsens the MD becomes increasingly negative, where a MD of -25dB is defined as functional blindness. However, the MD can be effected from ocular factors such as cataracts. The PSD is again calculated across all stimulus locations, and represents more localised defects in the visual field. It is calculated as the standard deviation of the TD. It differs from the MD as it becomes more positive with the advancing of visual field loss. As previously stated the PSD, becomes unreliable when there is advanced visual field loss.

The VFI was designed to counteract factors such as cataracts, which can influence the appearance of generalised visual field loss (Bengtsson and Heijl, 2008). The VFI can be calculated using two different methods dependant on the MD value. When the MD is equal to or better than -20dB, VFI is calculated from the sum of the sensitivity values at each test location from the PD probability plot. If the MD is worse than -20dB then the sum is taken from the TD probability plot. The VFI is scored in percentages, with 100% representing a normal sensitivity at each test location, 0% is scored when there is absolute loss at a location.

1.4.1.3.4 Reliability indices

There are three reliability indices on the HFA printout. They are Fixation loss (FL), False-positives (FP) and False-negatives (FN). FL rates are estimated by presenting a stimulus of maximum contrast in the patients' blind spot. If fixation changes during this presentation it is recorded as a FL. A FP is recorded as a response to a non-existing stimulus. The response rates are estimated during the introduction of catch trials in the test procedure, the device will produce the same sound as when producing a normal stimulus. They are additionally calculated through the number of responses that occur too early before presentation. High rates of FP make a test outcome unreliable and can indicate high threshold values, these patients are also known as "trigger happy". The rates of FN are calculated when there is no response to a previously seen stimuli. Usually through the presentation of suprathreshold stimulus (very bright) at already measured locations in the visual field to determine if there is vision in that region or not. However the rates of FN need to be examined carefully if there are large areas of visual defects. Attention rates of the individual during the procedure can also effect the outcomes of FN. The reliability of FP and FN has been set at cut off points of 33%, and FL at 20%. However at present there is no evidence to support these figures (Heijl, Patella et al. 2012).

1.4.1.3.5 Glaucoma Hemifield Test

The Glaucoma Hemifield Test (GHT) is based upon the pattern of visual field loss often seen in static threshold visual field tests from glaucoma patients (Åsman and Heijl 1992). This pattern presents asymmetrically across either the superior and inferior hemifields. Analysis is measured using the PD probability across five zones superior of the horizontal midline and then five inferior of this line (see in Figure

1.11). These zones are correlated with the distribution of axons in the retinal nerve fibre layer. If one of these zones scores significantly different from their corresponding zone in the other hemifield, then the GHT classes it as “Outside of normal limits”. If there is only a small difference then this is classed as “Borderline”. If points in all zones are affected then it is classed as “General Depression of sensitivity”; “Abnormally high sensitivity” is the presence of a high threshold estimate across the zones, and “Within normal limits” is when the threshold estimates of the zones all fall within the normal range of a health individual (Artes, Chauhan et al. 2010). A repeatable measure of abnormality in the GHT outcome is a strong indicator of the presence of glaucoma. GHT provides a method to analyse the relationship between the structural and functional aspects of glaucoma and can be used to map the visual field loss due to ONH damage (Katz et al., 1995).

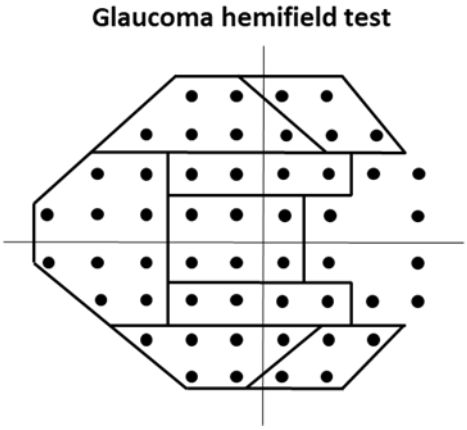

Figure 1.11: Illustrated diagram of Glaucoma hemifield test

1.4.1.4 Progression analysis of static perimetry results

Progression analysis is used to define the progression and rate of vision loss. The following section will discuss four types of this progression analysis: clinical judgement, defect classification, trend analysis, and event analysis for OAG. It should be noted that none of these methods are universally recognised as a quantitative technique for measuring glaucomatous change overtime.

Clinical judgement consists of a simple subjective observation of visual field test results over numerous visits (Tanna, Budenz et al. 2012). It is faster than other methods due to no need for a computer, and flexible due to clinicians taking into account other factors, such as ONH and other non-clinical factors such as time of day tests were undertaken. However, this method suffers from inter-observer variability, as different clinicians will use different criteria for deciding on progression, and agreement between experienced clinicians often does not occur. This is particularly hard when observing changes in patients with advanced visual field loss, thus unreliable.

The classification analysis divides visual field defects into stages. This is based on the eccentricity and extent of defect locations. Stages used to define the progression of the disease are mild, moderate and severe. There are a number of Standard Automated Perimetry (SAP) staging systems that have been developed. One common criteria used is by Hodapp, Parish and Anderson. This system considers two criteria: the overall extent of vision loss using the MD value, and the number of points of reduced sensitivity in the PSD map, with the addition of the proximity of the defects to the fixation (Susanna Jr and Vessani 2009). The definition of advanced glaucoma, at the beginning of the next section, is chosen from this staging system. The Advanced Glaucoma Intervention Study (AGIS) suggested a more continuous staging system, where the visual fields of patients were divided into 20 stages, in order to increase the likelihood of detecting progression in patients with more extensive vision loss (Investigators 1994, Susanna Jr and Vessani 2009). The scoring system for this is taken from the TD plot of a HFA Statpac2 package. These classification systems are important to divide patients into subtypes and stages to

establish the risk of progression, optimising treatment, and the ability to monitor the functional vision.

Trend analysis follows the test parameters sequentially over time, to determine the magnitude and significance of patterns within the data. The first version of the Statpac package (Heijl, Lindgren et al. 1987) that was used on the HFA, determines whether the MD of an individual is increasing over time, using a linear regression. The first two visual field tests are used as a baseline, and further tests completed over time to compare to them. The rate of glaucoma progression is measured with the changes of the MD value per year. In the Statpac2 package the first result taken from a series of tests is disregarded if it deviates substantially from the trend, avoiding any learning effects (Morgan, Feuer et al. 1991). Issues with this package is the effect of factors such as cataracts and refractive error on the MD. To reduce these effects Bengtsson and Heijl (2008) developed the Glaucoma Progression Index (GPI) to evaluate the progression of glaucoma, expressed as a percentage rather than in dBs. For advanced damage (MD > -20dB) analysis uses the TD due to define this percentage. This test reduces the effects from optical opacity, however suffers from large variability in advanced damage groups (Rao, Jonnadula et al. 2013) suggesting it is not an effective method for monitoring the progression of visual field changes in advanced vision loss.

Event analysis or Glaucoma Change Probability (GCP) identifies the threshold estimate at any given location of any visual field test examination, and correlates it to the original threshold estimates of the first two baseline tests (Morgan, Feuer et al. 1991, Leske, Heijl et al. 2003). This result is compared to the test re-test variability thresholds in any location, from individuals who have stable glaucoma.

Progression is noted as the significant reduction of sensitivity in 3 or more locations in the visual field, compared to the two baseline tests, or if visual decay in locations is less than 5% of this re-test value. However this analysis has shown to be unreliable for determining the rate of progression, influenced by the test re-test variability (Artes, O'Leary et al. 2014)

1.4.2 Kinetic perimetry

Kinetic perimetry is an alternative method to static perimetry where a spot of light, or a solid target is moved from an area of non-seeing (from the periphery) to an area of seeing (towards a central fixation point). This trajectory of the stimulus is called a vector (Racette, Fischer et al. 2016). The visual field location in which a patient responds to a stimulus is recorded as the threshold of their visual field sensitivity (Johnson and Keltner 1987, Schwartz, Dobson et al. 1987) and has a sensitivity threshold equal to the specific light intensity used along the vector. Further responses to the same stimulus intensity on additional vectors are connected to form an isopter, known as a boundary of equal sensitivity (Traquair and Scott 1957, Racette, Fischer et al. 2016). An isopter is similar in appearance to contour lines found on a topography map, which indicates areas of elevation, but isopters are a representation of threshold sensitivity in the visual field. Isopters mapped using different stimulus intensities together form the hill of vision, where higher threshold values indicate greater sensitivity. Any defects to this isopter shape could be interpreted as a reduction of sensitivity indicating visual field loss. However defects can also be due to anatomical structures intruding on the visual field such as having a large nose that reduces the extent of the nasal visual field (Traquair and Scott 1957).

To produce a plot which covers the whole area of the visual field, multiple stimuli are used of varying intensity. These stimuli are either adjusted by size or luminance intensity (Munnerlyn, Joba et al. 1981, Racette, Fischer et al. 2016). This will produce a plot of several isopters representing the threshold sensitivity across the visual field. Isopter positions can be affected by the velocity of the stimulus trajectory. Typically stimuli presented in the periphery are set at a speed of 5°/s, whereas in the central visual field, it is suggested that a slower velocity of 1°/s is used due to the difference in sensitivity between the two regions (Vonthein, Rauscher et al. 2007).

1.4.2.1 Goldmann manual kinetic perimetry

Goldmann manual kinetic perimetry was first introduced in 1945 (Goldmann 1946). Its use was to detect visual field damage such as scotomas, in the peripheral and central visual field. This was a big step towards quantifying perimetry as it provided a uniform setup and procedure for clinicians to follow. It is a relatively short procedure and provides a good overview of any profound visual field defects (Nowomiejska, Vonthein et al. 2005). It is accepted as a method for monitoring progression, stability, or improvement of visual field defects in individuals suffering from concentric constriction of the visual field (Grover, Fishman et al. 1998).

The background illumination used in manual kinetic perimetry was established as a luminance of 10cd/m² (31.4asb). This luminance was established as the minimal brightness needed for photopic vision, which depends on the function of rods and cones (Heijl et al., 2012).

When performing manual kinetic perimetry, the examiner can change the stimulus size and intensity used, dependant on their individuals visual condition (low vision), through standardised filters. The visual field is recorded on a set chart print out (see

Figure 1.12,) whereby responses are marked out by using a pantograph, which moves the stimulus intensity selected. The examiner will move the stimulus from an area of non-seeing to an area of seeing, at an approximate speed of 5°/s. Between 8-12 vectors are generally used per isopter, separated by 30-45° but more vectors can be used if necessary. Different sizes and contrast filters are selected to map out the area of visual field, starting with either the largest or brightest stimulus first. If there is a wide spread between two isopters then another filter adjusted stimuli will be used to map out that area between them (Pineles, Volpe et al. 2006).

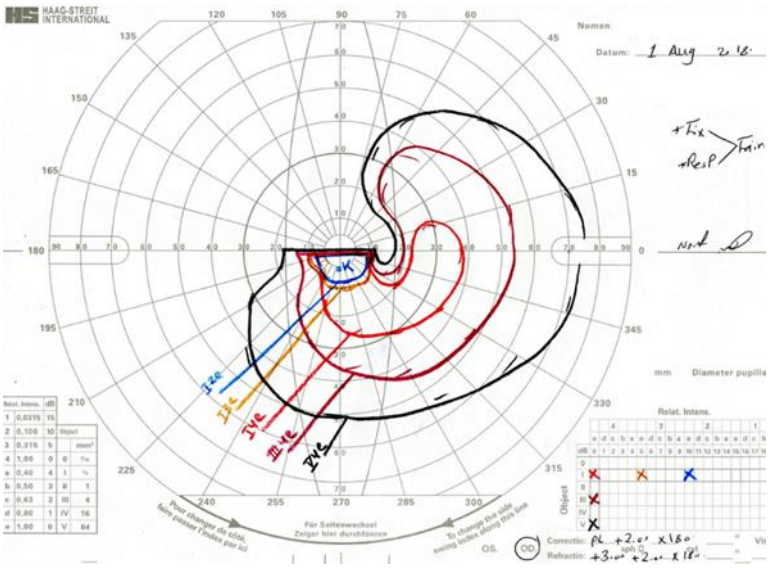

Figure 1.12: Manual Goldmann perimetry output, for glaucoma patient with reduced superior and nasal visual field. Different colours represent the different stimulus intensities used. This example shows a defect in the superior nasal region which extends inferiorly.

This technique is preferred over static tests when observing larger areas of visual field damage, and when trying to define the shape of absolute scotomas (Nowomiejska et al., 2005)(Phu, Kalloniatis et al. 2018). There is significant patient preference for Goldmann over static perimetry in patients with a wide range of glaucomatous visual field loss (Pineles, Volpe et al. 2006, Ramirez, Chaya et al.

2008). Previous research (Ramirez, Chaya et al. 2008) has shown that patient preference between static, kinetic and a combined static kinetic test was in favour of the kinetic. Kinetic perimetry is better suited for those who suffer from depressed central vision, and cognitive disorders which effect fixation control, due to better control by examiner interaction during examination (Ramirez et al., 2008) and also faster overall when measuring the periphery. However, the disadvantages of using Goldmann manual kinetic perimetry are first, the discontinued production of Goldmann perimeters since 2007 and the need for well-trained examiners to undertake the examination. Without proper training examiners may move the stimulus faster than 5°/s or have a delay in marking the response, thus effecting the output. It takes approximately up to three months of training before an examiner is comfortable with the procedure (Racette, Fischer et al. 2016). The results could also differ dependant on the examiners comprehension of the patients' responses, with variability between different examiners (Nowomiejska, Vonthein et al. 2005). An additional disadvantage is the quantification of the isopter outputs, due to the lack of standardization of equipment and methods (Berry, Drance et al. 1966).

1.4.2.2 Semi-automated and automated kinetic perimetry

Semi-automated automated kinetic perimetry was designed to counteract the disadvantages of the manual kinetic perimetry Goldmann test. This resulted in the development of new software techniques, used in devices such as the Octopus 101 (Haag-Streit, Koeniz, Switzerland). This procedure allows for almost all of the visual field to be measured using stimuli which can be presented in any direction (Ramirez, Chaya et al. 2008). There are automatic set programs, but the device also allows for custom programs to be performed.

The automated kinetic test has the advantage of better comparisons between tests due to the digitalisation of the data and the standardised programs used (Nowomiejska, Vonthein et al. 2005, Ramirez, Chaya et al. 2008). The device has set normative values dependant on age of the patient, which has been established during the development of kinetic perimetry (Vonthein, Rauscher et al. 2007).

1.4.2.3 Goldmann stimuli

In kinetic perimetry, the stimuli used to map out the visual field varies in size and intensity (Racette, Fischer et al. 2016), as can be seen in Tables 1.1 and 1.2. When the manual Goldmann perimeter was developed it contained one light source which could be adjusted in luminance through filters (Goldmann 1946). The stimuli can be adjusted according to greyscale filters, which allow the logarithmic decadal gradation of the stimuli luminance to be determined (Racette, Fischer et al. 2016). There are two greyscale filters, the first ranges from 1 to 4, adjusting in luminance values from 15dB to 0 dB in steps of 5dB. This can also be expressed in terms of luminance absorption from 31.5, 100, 315 and 1000asb. The second filter ranges from a to e, which equal luminance values of 4dB to 0dB in steps of 1dB. In terms of absorption these are 400, 500, 630, 800 and 1000asb. These filters can be incorporated into 20 different combinations of stimulus luminance (Racette, Fischer et al. 2016).

Table 1.1: Range of Goldmann sizes shown in millimetres squared area and diameter in terms of degrees.

Goldmann size	*Stimulus in mm²*	*Stimulus diameter in °*
I	0.35	0.11
II	1	0.22
III	4	0.43
IV	16	0.86
V	64	1.72

Table 1.2: Table of target luminance with applied Goldmann filters.

Indications	*1*	*2*	*3*	*4*
Transparencies	0.0315	0.10	0.315	1.00
Intensities (asb)	31.5	100	315	1000

Indications	*a*	*b*	*c*	*d*	*e*
Transparencies	0.40	0.50	0.63	0.80	1.00
Intensities (asb)	400	500	630	800	1000

1.4.2.4 Interpretation of results

There is no set automated analysis of kinetic test results like in static perimetry. The results of these test outputs are generally evaluated by observation, or by customised programs set by the researchers (Johnson and Keltner 1987, Schiefer, Schiller et al. 2001). However results can be compared to normative values collected from healthy participants (Vonthein, Rauscher et al. 2007). In the Octopus 900 these plotted isopters are compared against normative regions, which are age and stimulus intensity corrected.

Kinetic perimetry isopters can be quantified by a few methods. The area of the isopter can be described as the square degrees of visual angle (Nowomiejska et al., 2005) or as cm^2 on a standard chart (Ramirez et al., 2008). Another method is to measure the visual field in terms of volume. This uses contrast sensitivity as part of the measure. Through these methods, examiners are also able to monitor the variability of patients' responses. These responses are proven to be reproducible (Vonthein et al., 2007), and provide clinical information of visual field results when

used in conjunction with static central visual fields (Nowomiejska et al., 2014, Nowomiejska et al., 2015).

1.4.3 Reliability of visual field tests in glaucoma

The variability of using visual field tests to monitor glaucoma is considerably high, even with the development of new analysis models to counteract for variability factors. Visual field tests can show both intra-test (short term) and inter-visit (long term) variability (Heijl 1987). Short term fluctuation is computed from the variability of threshold values found on repeated measurements during the same examination (Urata, Mariottoni et al. 2020), whereas long term fluctuation or inter-test variability is defined as the variability in threshold values among examinations performed over time, corrected for short-term fluctuation in the absence of clinically detectable pathology (Khan, Ishaq et al. 2017) The more advanced visual field damage a patient has, the higher variability (Investigators 1994). The rate of FP during the examinations is also high, as seen in De Moraes et al (2016) who found a rate of 57% FP on initial testing of glaucoma patients. With repeated testing this percentage did declined to 2%. However the increased need for multiple visual field tests increases clinician workload and costs to the health sector (de Moraes, Liebmann et al. 2016).

Patient factors can affect the outcome of visual field tests reliability. Learning effects have been demonstrated in advanced glaucoma patients, with the largest difference between first and second examinations (Heijl et al., 2012). These patients with greater visual field damage take longer to complete the tests, and produce higher FP and FN scores (de Moraes, Liebmann et al. 2016). Fatigue effects are an additional factor observed in visual field tests. It has be shown by Heijl and Drance (1983) that there is a decrease in threshold sensitivity in relation to test times in glaucoma patients. These effects are larger in more defective areas and also

increase with patients' age (Heijl and Drance, 1983). With a better understanding of the additional factors such as learning and fatigue affects, more reliable visual field tests could be developed, allowing better monitoring of glaucomatous visual field progression (De Moraes, Liebmann et al. 2013).

1.4.4 Contrast sensitivity in glaucoma

Contrast sensitivity is the ability to detect the difference between two areas, in terms of luminance (Hawkins et al., 2003). There are two types of CS. First is spatial contrast, where two different luminance areas are next to each other, with the transition at the edge of an image that delineates the existence of an object/pattern (Owsley, 2003). The second type is where two different contrast areas occur sequentially; this is called temporal CS. When using perimetry to measure visual field loss in glaucoma patients, contrast is generally measured in dB or in percentages from 0 to 100%, in detection of the stimuli/object from the background luminance. The level in which an individual can just detect a difference in luminance in order to see a target is called the threshold.

CS tests can be used to measure vision loss, due to the loss of retinal ganglion cells within the eye, when an individual has glaucoma. This is due to damage caused to the axons of these cells, as they exit the eye through the lamina cribrosa. One of the uses of CS, particularly in glaucoma, is the detection of hidden losses in visual function, which may not be detected through other tests such as visual acuity. Visual impairment classification by CS is marked as LogCS values of less than 1.50 logMAR. When observing visual disability there is a higher correlation with CS over visual acuity, when measuring the mobility of patients with glaucoma (Richman, Lorenzana et al. 2010). CS has been found to be a useful method in monitoring progression in glaucoma patients (de Moraes, Liebmann et al. 2016). This is measured in patient-

outcome tasks such as reading, visual task performance, facial recognition and vision related quality of life (Owsley 2003).

There are many factors which can effect an individual's contrast sensitivity, some physiological and others due to external factors. The most common cause in the decline of contrast sensitivity is due to ageing, with CS decreasing every decade by approximately 0.5 decibels (Owsley, Sekuler et al. 1983, Elliott 1987, Hou, Lesmes et al. 2016). Additional factors such as refractive errors can effect sensitivity, thus the refraction must be adjusted dependent on distance of presentation (Arundale 1978). Pupil size can also effect the amount of light going into the eye. If the pupil is less than 2mm then both CS and visual acuity have been shown to be affected, particularly under mesopic conditions (Alfonso, Fernández-Vega et al. 2007). Cognitive functions which contribute to reduced measures of contrast sensitivity are fatigue and loss of attention, resulting in a number of FP and FN responses which occur during visual field tests (Owsley 2003).

The use of CS in glaucoma patients has shown to be beneficial when observing real-world visual problems (Richman, Lorenzana et al. 2010), when used in conjunction with other tests to monitor the progression of glaucoma (de Moraes, Liebmann et al. 2016). Although as a detection method on its own, CS is highly variable with many factors other than the disease affecting reliability of CS scores (Owsley, Sekuler et al. 1983).

1.5 Problems in advanced glaucoma

Monitoring patients with OAG on a regular basis is essential. Doing so helps identify patients where treatment plans may not be working, thus they are at risk of have progressive visual field loss, and potential risk of blindness. The aim for clinicians

when they treat glaucoma is to halt or slow down the progression of the disease, preserving visual function. However, this is not possible for all individuals. Some patients, despite therapy, end up progressing to a later stage of the disease, with advanced vision loss.

Advanced OAG patients are in imminent danger of losing their remaining vision, and as a result may face additional socioeconomic challenges such as stigmatization and unemployment. Furthermore, with this ever decreasing vision, it can also have a negative impact on the patients' mental health. These issues from advanced glaucoma can ultimately result in an increase in morbidity and mortality (de Moraes, Liebmann et al. 2016).

The workload on the health care system is increasing from advanced OAG patients. A survey completed by Lee et al (2006), in the USA in 2005, found that with the increasing severity of OAG, and the impact it can have on the individual, medical costs and every increasing. Patient treatment costs approximately $600 per year, when the individual is diagnosed with early or suspect glaucoma, whereas a patient with advanced stage glaucoma this cost is approximately 4 times greater per patient per year (Lee, Walt et al. 2006).

The following section with discuss the above issues. I will present a definition of advanced glaucoma, and how many people are affected. I will also discuss the current methods used to monitor vision in advanced glaucoma patients, and causes which lead to this stage of the disease.

1.5.1 Definition of advanced OAG glaucoma

There are various definitions of advanced OAG from the output of static automated perimetry. One definition is a Mean Deviation worse than -12 dB. Advanced

glaucoma can also be defined as having 1 or more points in the central 5° with a sensitivity of 0 dB, or multiple points within 5° with a sensitivity less than 15 dB, in both the superior and inferior regions (de Moraes et al., 2016). Other researchers define advanced glaucoma as total cupping of the optic nerve either with or without severe vision loss within 10° of fixation (Gessesse and Damji 2013). This thesis will adopt the definition by Hodapp (Hodapp, Parrish et al. 1993) for the classification of advanced glaucoma.

1.5.2 Epidemiology of advanced glaucoma

1.5.2.1 Prevalence, incidence & prognosis

There is a scarcity of data on the prevalence of advanced OAG in the general population. However it has been suggested from one study that between 10-40% of glaucoma patients, will present with advanced visual field damage in at least one eye (King, Stead et al. 2011).

The predicted incidence of advanced glaucoma in the USA is based upon the incidence of glaucoma patients who have gone blind. Out of 100,000 patients, 6 will go blind as a result of glaucoma. From these figures it is then predicted that as many as 10 times more patients are actually living with advanced glaucoma (de Moraes et al., 2016). The rate of progression to advanced glaucoma, in relation to visual fields, is a mean loss of 3.6% per year, according to the mean deviation index (MDI) (Broman, Quigley et al. 2008, Chauhan, Garway-Heath et al. 2008). However this is disputed by early research which suggests a slower rate of 1.3% per year (Kwon, Kim et al. 2001).

As vision loss progresses in OAG, there is a substantial risk of an individual going blind in at least one eye (Fraser, Bunce et al. 1999). WHO (World health

organisation) estimated by the year 2010 glaucoma would be the cause of 12% of all blindness. Whereas other research suggests that on their last visit to their clinician, prior to death (median age at death 88 years), 16.4% of glaucoma patients were bilaterally blind, and 42.2% were unilaterally blind (Peters, Bengtsson et al. 2013, Peters, Heijl et al. 2015).

1.5.3 Causes of advanced glaucoma

It is essential to recognise patients who are at a higher risk of progressing to the advanced stage of OAG or blindness, taking appropriate steps to try slow and halt the disease. Factors which contribute to the late presentation of the disease, rate of progression, and how those factors relate with unsuccessful therapy interventions will be discussed.

1.5.3.1 Late presentation

One of the most important and highly recognised risk factors for an individual developing advanced OAG, is the late presentation of the disease. Late presentation is described as when a patient first presents to either an optometrist or GP, with substantial visual field loss, and cupping of the ONH. Presenting late with OAG has an effect on the prognosis for the patient. Research suggests that when a patient presents with already existing advanced vision loss, the deterioration of vision loss is predicted to be 11.7 times faster, than if there was little to no vision loss on first detection of the disease (Fraser et al., 1999).

Initial diagnosis of OAG, when and who it was by, is a key element of late presentation. In the UK approximately 90% of all glaucoma cases are referred by community optometrists. This leaves approximately 10% who are referred by their GP or from hospital departments such as A&E (Sukumar, Spencer et al. 2009). This

usually occurs when the patient starts to recognise that their vision is being affected. The patients referred by the GP etc. are more likely to present with advanced vision loss. This is confirmed by the registration of blind patients, as a result of glaucoma, at the Manchester Royal Eye Hospital (MREH). They found a high percentage of these patients registered as blind, were directly referred from there GP. This finding suggests a poor utilisation of optometrists, and the care they provide by some individuals in society, resulting in advanced vision loss (Sukumar et al., 2009). Fraser et al, (1999) suggested that the 10% of glaucoma patients who are not referred by optometrists, or are not correctly referred, either through wrong diagnosis, or not attending a vision test, are 4.5 times more likely to present late, and at a more severe stage of OAG. A clinical study in the UK recorded that the number of newly diagnosed glaucoma patients identified as having advanced glaucoma was 38% (48 patients out of a sample of 126) (Ng, Agarwal et al. 2010), this figure further supports the prediction of advanced glaucoma prevalence by King et al, (2011).

A study by Grant and Burke (1982) calculated that one third of patients who end up blind from glaucoma, had already reached this advanced stage before seeking medical attention. Elkington et al, (1982) reported that 33% of individuals with glaucoma were delaying medical attention. Further research found 10% of those with glaucoma were severely visually impaired at first examination, whereas Sheldrick et al, (1994) suggested that up to 20% of patients presented with severe impairment at first examination. Individuals from an African-Caribbean origin were more likely to attend a sight test with advanced glaucoma in comparison to a white population (Fraser et al., 1999). This finding suggests that cultural background may also play an affect in seeking initial medical attention. These figures imply that the

risk of developing or going blind from advanced glaucoma is greater when patients do not seek healthcare (e.g. seeing an optometrist regularly or are not referred appropriately).

An important risk factor for the late presentation of OAG is the socioeconomic status of the patient. Fraser et al, (1999) found that individuals from a higher socioeconomic background were least likely to present late with glaucoma. This finding is further supported by Sukumar et al, (2009), who found a strong association between damage at diagnosis and an area-based measure of deprivation. The compliance and access of medical care for patients has also been linked to socioeconomic status, this is prominently more noted for screening of diseases such as cancer. However low attendance to regular eye tests is associated with a higher risk of vision loss (Fraser et al., 2001). This implies individuals of low socioeconomic status are at greater risk of having vision loss. Compliance, care regime of patients, and the increased risk of developing the advanced stage of the disease will be discussed more in-depth in the unsuccessful therapy section.

1.5.3.2 Rapid progression

There are a number of risk factors that could contribute to the rapid progression of OAG. An initial risk factor is the type of glaucoma. As this thesis is observing only OAG, I will only discuss different types of this classification. Pseudoexfoliation glaucoma is a common identifiable cause of rapid progression. The exact composition of the exfoliation material is still unknown, however it is known that it causes a chronic accumulation that blocks the anterior chamber, increasing IOP. This high level of IOP is what is thought to cause the rapid progression of the disease (Shaarawy et al., 2009). The clinical signs are often over looked, resulting in less than

ideal management. Leske et al, (2003) found in the Early Manifest Glaucoma Trial (EMGT) that individuals with pseudoexfoliation glaucoma had a higher baseline IOP on initial visit. Out of 19 patients in the study with pseudoexfoliation, 18 of them had OAG progression. In ocular hypertensive patients' exfoliation has shown to be a risk factor for progression to OAG (Grødum, Heijl et al. 2005).

In terms of incidence level and progression, if an individual has an IOP of 21-25mmHg then the average time taken to progress is 14.4 years from the earliest detection to the advanced stage of OAG (Gessesse and Damji 2013). It takes 6.5 years on average for an IOP of 25-30mmHg, and 2.9 years if IOP is greater than 30mmHg (Gessesse and Damji 2013). Thus if a patient has an IOP of 25mmHg or greater, then it is estimated that on average, without treatment, they will progress to the advanced stage of glaucoma in 3.6 years (Gessesse and Damji, 2013). This incidence of progression can however differ dependant on the population being measured. Quigley et al, (1996) found that the rate of progression was higher in a black population, with a progression of 0.23 field score units a year compared to a white population, which progressed at 0.11 units per year.

As previously noted in the OAG risk factors section, the relation between the axial length and the presence of myopia are risk factors for the development of OAG. However, they also may play a role in the progression of glaucoma, due to the appearance of the ONH. Distinguishing changes of the ONH from the result of myopia or glaucoma can be difficult (Bussel, Wollstein et al. 2014). Changes such as bundles of papillomacular are found highly in myopic eyes, but are also indicative of early glaucomatous development. In terms of visual fields, a large proportion of myopic discs are tilted with peripapillary atrophy, causing glaucoma like visual field

defects (Chang and Singh 2013). Thus distinguishing between the two conditions can be a challenge for clinicians, and possibly result in the progression of OAG going unnoticed.

Other risk factors are ethnicity and age. As previously discussed, the ethnic background of an individual can increase their risk of developing glaucoma e.g. a higher prevalence of OAG in blacks compared to whites. When looking at the progression of the disease, research suggests that an individual with a high IOP >31mmHg, and is of African origin, above the age of 60, is more likely to progress to the advanced stage of OAG, than an individual of same criteria but non-African ethnicity (Gessesse and Damji, 2013).

1.5.3.3 Unsuccessful therapy

When patients are first diagnosed with OAG, depending on their stage of disease, and additional health issues, they are put on a certain treatment regime. All current therapies work through reducing IOP levels, reducing IOP to under 24mmHg using either eye drops or surgery. Even when a patient reacts well to a treatment therapy, and complies with the care regime afterwards, there is still some progression of vision loss occurring (Leske 2007).

IOP levels have been correlated numerous times with the progression of OAG. Hong et al, (2007) stated that a patient who's IOP fluctuates, progresses with visual field loss at a higher rate than a patient with a consistently stable IOP. In one study an IOP mean between (15.4± 2.7 mmHg to 24.5 ± 6.9 mmHg) resulted in stable vision, compared to (21.3 ± 3.2 mmHg and 39.2 ± 11.0 mmHg), where patients vision worsened. The variance in these patients IOP was lower in the stable group (Stewart, Chorak et al. 1993, Stewart, Day et al. 2006).

The compliance and care regime of a patient during and after a therapy treatment is essential to its outcome (Weinreb, Aung et al. 2014). As previously discussed, the socioeconomic status of an individual can affect the point in which they seek medical attention. This can also play a role in the management of the disease by the patient e.g. not consistent with follow up eye tests (Ntim-Amponsah, Amoaku et al. 2004). If the country that individual resides in does not provide free medical care, then the costs of treatment i.e. eye drops can be too much for some individuals (Gessesse and Damji, 2013). This issue may arise in less developed countries where access to medicines or medical centres is restricted, due to distance or funds.

In care regime a common issue heard by many doctors when they ask about how a patient is getting on with taking their drops is “I take my drops everyday, unless I forget” (Weinreb, 1992). Due to the nature of OAG, patients generally feel of good health, thus do not feel the need to take their medication. Some medications can evoke side effects, meaning patients purposely miss doses. Patients then try to make up these missed doses by doubling up, however this can cause more substantial systemic side effects, due to some medications consisting of Beta blockers (Weinreb et al., 2014). Although some treatments can cause side effects, compliance with these treatments, whether surgical or eye drops, is essential for potentially slowing the progression of vision loss caused by OAG, to the advanced stages, or even blindness. As previously noted even when IOP levels are kept stable, there can still be a small amount of progression of the disease, despite good care regime.

1.5.4 Monitoring vision in advanced glaucoma

In recent decades there have been many new developments with technology to detect and monitor the early stages of OAG. These modern technologies such as

static automated perimetry, Optical Coherence Tomography (OCT), and disc photography are useful for early detection, however are limited in their abilities to monitor advanced glaucoma. This raises issues with a clinician's ability to preserve and monitor the remaining vision left in a patient with this stage of the disease, increasing the patients' risk of going blind. The following sections will discuss methods currently used to monitor the progression of OAG in the advanced stages.

1.5.4.1 Visual fields in advanced glaucoma

Visual field measurements are the most frequently used method to monitor OAG progression (Bengtsson and Heijl 2008). It is suggested that visual field changes are the only evidence of reliable progression in advanced glaucoma (Gessesse and Damji, 2013). However it is noted that the use of visual fields is highly variable, and it is not yet known the frequency of tests needed to reliable confirm worsening of the visual field (Nouri-Mahdavi, Hoffman et al. 2004). The following will discuss the different visual field methods used to define progression in OAG.

SAP remains the standard of clinical assessment to measure visual function in a patient with advanced OAG (de Moraes et al., 2016). This method has a high test-retest variability when used on individuals with more severe vision loss, and many more repeated tests are needed to determine progression. This uses up a great deal of clinicians' time, cost to the healthcare system, and is not a reliable method to monitor progression. Advanced glaucoma patients usually have a small degree of central vision remaining, thus the use of testing programs such as the 10-2 on the HFA, in conjunction with the current 24-2/30-2 programs may allow for better detection of changes over time (De Moraes, Liebmann et al. 2013, de Moraes, Liebmann et al. 2016). The 10-2 program focuses on a small area encompassing

approximately 30% of retinal ganglion cells, and relates to over 60% of the visual cortex (de Moraes et al., 2016). This program allows 68 test points to be measure over a 10° area, thus increasing sensitivity for detecting paracentral damage (Racette, Fischer et al. 2016). This can be further improved by replacing the standard Goldmann size III stimulus, with the larger size V stimulus, increasing the stimulus intensity. By increasing the sensitivity of detecting further vision loss (Gessesse and Damji, 2013), and reducing the variability, ensures tests are more reliable for detecting progression (de Moraes et al., 2016).

Kinetic perimetry, both manual and automated, is an important method for monitoring the vision in advanced glaucoma patients. As the visual function of patients gradually reduces, the ability to undergo SAP tests becomes increasingly harder. Kinetic perimetry is the favoured method when trying to define the edge of visual field loss (Nowomiejska, Vonthein et al. 2005). It allows almost the full field of vision to be measured, and the shape and extent of the visual field defect can be detected, along with any change to this shape over time. Kinetic perimetry is useful for monitoring progression in patients suffering from a constricted visual field (e.g. from advanced retinal nerve fibre layer loss or hemianopia etc.) (Nowomiejska et al., 2005). The test-retest variability is lower than that of static perimetry (Nevalainen, Paetzold et al. 2008). It is the preferred visual fields testing method by patients with advanced glaucoma (60%), due to the patient/examiner interaction, and less fatiguing to complete (Nowomiejska et al., 2005, Nevalainen et al., 2008(Nowomiejska, Kiszka et al. 2018)).

1.5.4.1.1 Rates of visual field progression in advanced glaucoma

The rate of visual field progression can differ between diagnostic groups. The Early Manifest Glaucoma Trial found that different factors between these groups lead to different rates of progression. OHT patients' visual fields have shown to progress at a faster rate than NTG, due to a high mean IOP during the monitoring period of their study (Leske et al., 2003). For every unit of mmHg above the baseline (21mmHg), rate of visual field progression increased by 5%. The EMGT study listed these diagnostic groups in terms of hazard ratio (HR) of visual field progression. OHT patients had a HR = 1.70 in comparison to NTG patients HR = 0.50. Patients who have pseudoexfoliation have an increased HR = 2.31. These results support the importance for certain diagnostic groups to be monitored more frequently to reduce the risk of advanced glaucoma, or blindness if patients first present with advanced glaucoma.

The overall rate of OAG visual field progression is said to be slowed at 1.3% per year, or in-terms of decibels 0.35dB (Kwon et al., 2001). However, when observing eyes which already have substantial damage this rate of visual progression increases to 2.1% or 0.48dB. It should be noted that additional factors such as age, late presentation and other ocular conditions such as cataracts, as discussed in the rapid progression section, effect the rate of visual field progression.

1.5.4.2 Visual acuity and contrast sensitivity in advanced glaucoma

The use of best corrected visual acuity routinely at appointments, may help in detecting vision loss. A fluctuation of two lines in the Snellen chart of best corrected visual acuity is expected between routine appointments, thus an increase of this at

follow up visits should increase a level of suspicion that the disease is possibly progressing (de Moraes et al., 2016).

Richman et al, (2010) compared patients of all glaucoma severity, between visual acuity, and contrast sensitivity, using a performance based test (e.g. Assessment of Disability Related to Vision -ADREV). The results suggest there is a strongly correlation with binocular VA and CS. The ADREV measures the visual function of patients, and how their vision affects daily life activities. Studies such as Richman et al, (2010), and Haymes et al, (2006) support the use of these tests in monitoring glaucoma, especially in the advanced stages when visual fields and ONH assessment are not reliable on their own for detecting progression. Kiser et al, (2005) looked at the reliability of visual function tests such as VA and CS in severe vision loss patients. They examined the variability of these tests to determine whether deviations of the measures were indicative of visual change, or just inherited variability (Kiser, Mladenovich et al. 2005). They found that both VA and CS results showed repeatable measures, thus a deviated score is a likely estimate of glaucoma progression in severe vision loss patients.

1.5.4.3 Optic nerve head progression

Different forms of photography are used to examine the ONH, such as Fundus photography and OCT. Although there is an apparent clinical judgment variability of the appearance of the ONH, it is still a widely used method to monitor the progression of OAG. Once the disease reaches the later stage, this progressive change is difficult to be defined. Aspects such as loss of neuroretinal rim tissue and peripapillary nerve fibres make this observed change extremely hard even for well-trained clinicians (de Moraes et al., 2016).

Disc haemorrhages have been consistently shown in clinical trials and longitudinal studies as important predictors of glaucoma progression (de Moraes et al., 2016). Two factors that influence the detection are the use of fundus photography of the optic disc, and frequency of examination. Due to the nature of disc haemorrhages being transient, the frequency of assessment may lead to an increased likelihood of detection of advanced glaucoma progression, although it has been shown that disc haemorrhages are not always linked to glaucoma progression (Chauhan, Nicolela et al. 2009). The incidence of these occurring in the advanced stage are rare, thus evidence of one can be a surrogate measure of possible future progression (de Moraes et al., 2016).

Due to optic disc photography being highly subjective, and subject to poor repeatability, it possess a challenge for monitoring progression in advanced glaucoma (Artes and Chauhan 2005, Chauhan, Hutchison et al. 2005). Automated alternation flicker has been developed to detect small changes in the optic nerve structures (Syed, Radcliffe et al. 2011, Syed, Radcliffe et al. 2012). These would otherwise be missed when trying to flick between previous images from examinations by clinicians (de Moraes et al., 2016). This technique aligns two images from different examinations, by identifying vascular intersections and other features. It superimposes the images at a subpixel level and alternates the images using a user-dictated frequency. Longitudinal studies are still needed to assess the reliability of this technique. It could be useful for detecting structural or visual field changes in advanced glaucoma.

1.5.4.4 Alternative methods for monitoring progression in advanced glaucoma

Observing a physical change in the structure of the eye, or in visual fields has shown to be highly variable, and reliant on clinician judgement. Using alternative methods for observing vision loss in conjunction with these current techniques could strengthen reliability of suspected progression in advanced glaucoma. A few of these alternative methods are used to measure physical performance in patients, as well as observing other daily activities such as reading etc. The knowledge of when and how glaucoma produces disability allows for the judgement of how aggressively to treat a patient (Ramulu, 2009).

One method to measure rate of disability, due to vision, is to combine visual fields tests from the left and right eye. This is undertaken via an Esterman binocular supra-threshold field or by overlapping data from individual visual fields. This method is prominent when observing reading performance in advanced glaucoma patients. It has been shown that patients with bilateral visual field damage have more difficultly reading (Ramulu, Swenor et al. 2013). Thus measuring aspects such as reading speed at routine follow-up visits could identify possible OAG progression.

Postural sway is an additional method recently implemented for examining the effects of advanced visual field loss. Postural stability involves the neural processing of visual, vestibular and somatosensory inputs (Shabana et al., 2005). The role of vision on postural sway can reduce the performance by up 25-75% in normal sighted patients. Thus it is suspected that patients who have visible reduce vision from advanced OAG will have an increased postural sway. Issues however is the role of somatosensory inputs. Advanced glaucoma patients have shown to make better use of this input, in the absence of vision (Kotecha, Richardson et al. 2012). Placing them

on a foam like surface removes this input and gives a better prediction of the role of vision in postural sway (Shabana et al., 2005). Using this method could indicate progressive vision loss in advanced glaucoma patients in conjunction with visual fields and other visual function tests.

Unlike early and moderate stage glaucoma, advanced glaucoma patients are symptomatic as visual field loss progresses. Asking patients, at this stage of the disease, if they have noticed any change while undertaking general daily activities, could be essential in detecting vision loss progression (Gessesse and Damji, 2013). A number of visual function questionnaires have been developed in order to measure patients' responses. Example of questions are "how well do you find items" or "how do you feel about the quality of your vision". They also take the mental health of the patient into consideration, measuring the effects of glaucoma on their quality of life. Examples of some of these tests are the Activities of Daily Vision Scores, National Eye Institute-Visual Functioning Questionnaires, and the Visual Functioning 14 Questionnaire (Nelson et al., 2003). The results from these questionnaires give an indication of specific visual disability as a result of advanced glaucoma. Thus used as a key measurement of either treatment success, or possible progression of OAG.

1.5.5 Summary of advanced glaucoma

From the information which has been discussed in this chapter (i.e. late presentation, rate of progression, and methods used for monitoring advanced glaucoma), it can be concluded that much more research is needed in the field of advanced glaucoma. The progression rates to blindness worldwide are estimated at 12%, suggesting that for every blind person as a result of glaucoma, there are 10 times as many individuals in the advanced stages of the disease. Methods with low

variability are needed to detect the progression to this stage more accurately, with the current focus primarily on visual fields.

All diagnostic methods currently used to monitor glaucomatous changes become more challenging, and less reliable in the late stages of the disease. This is a crucial issue as the number of patients diagnosed with OAG estimated to increase in the next few years (Tham, Li et al. 2014). This leaves an ever-increasing socioeconomic pressure and burden on the current health care system.

Developing a visual field test which is patient friendly in terms of duration and performance is desirable. Ideally, a visual field test for an advanced glaucoma patient should not take any longer than approximately 7 minutes, to counteract for factors such as attention and fatigue which can effect results. This could be in the form of a kinetic and static combined test, which examines the visual field as a whole, but can identify small changes through more sensitive stimuli. The kinetic stimuli will monitor the outer bounds of the visual field, which could be correlated with the performance of patient balance. The static function will focused on potential scotomas located within the rest of the visual field. Incorporating visual acuity, and contrast sensitivity could also be of benefit at detecting progression in advanced glaucoma, at low cost to the healthcare system. Attributing these aspects to the measurement of the visual field of an advanced glaucoma patient, can give a better understanding to the risk towards possible falls, thus affecting quality of life. By measuring balance and vision loss, it could allow identification of specific visual field damage, which influences this loss in balance. Overall, these outputs could lead to a better understanding of the effects advanced glaucoma has on an individual, and how we can better monitor the progression to the benefits of the patient.

1.6 Conclusions

This section of the thesis highlights the current limitations of visual field tests in a population with substantive visual field loss. In view of these issues, it is evident that more research is required to produce visual field tests which can monitor the progression of late stage glaucomatous disease combined with alternative methods such as balance tests. It is also critical that the design of perimeters allow for the full extent of the visual field to be examined, thus allowing a more in depth picture of the effects that different ocular conditions have on the periphery, but also the role the periphery has in everyday activities.

The overarching aim of this thesis is to develop new visual field test, which can measure the outer limits of the peripheral visual field. This visual field test should be able to examine visual phenomena within this far peripheral region. The visual field tests should be fast, while maintaining precision in the results. The primary objective of this Thesis is to examine different methods and strategies of kinetic perimetry, and incorporate these findings into a test which can measure the peripheral visual field in patients with advanced glaucoma. Moreover, secondary objectives include to design a test which helps to identify other peripheral visual field phenomena. This test should be robust to patient errors and can be performed within a short time duration. Another object of this Thesis will be also to investigate the impact of advanced vision loss in both the central and peripheral visual field, caused by glaucoma, on postural sway.

2 Chapter 2: Design and build of extended fixation device on an Octopus 900.

2.2 Introduction

The “hill of vision” was a term first coined by Traquair (1924) as a representation of the visual field. The gradient of the hill is defined as a threshold value to luminance levels, with the peak of the hill being the most sensitive part of our visual field (Traquair 1924, Broadway 2012). The shape of this hill can be affected by a number of ophthalmic and neurological diseases and also by the ageing process. To map out this hill, different techniques can be used, such as kinetic perimetry. This method was initially used with a Bjerrum screen, where an examiner would move an object of certain size, from outside the patient’s visual field to an area where the object was first seen. A verbal response was given when the stimulus was detected by the observer. This technique has been used in a number of early studies, with measured responses in the temporal visual field up to and beyond 100° (Druault 1898, Ronne 1915, Hartridge 1919).

A more standardised version of kinetic perimetry was later developed by Goldmann (1945). This method of perimetry is still used today, although only within a small number of clinics with trained examiners. The method consists of a bowl with a set background illumination of 31.4 asb (10 cd/m²) and stimuli presented are controlled by an examiner. Patients sit with their chin on a chin rest, at a set distance (30 cm) from the bowl (Goldmann 1946). The edge of the bowl extends to 90° of the patient’s visual field. More recently, a computerised version of kinetic perimetry was developed to provide a more standardised method, which was less affected by examiner performance. These new devices, such as the Octopus 900 (Haag Streit, Switzerland), used the same concept of producing stimuli on a

hemispherical bowl, but the process is automated, and stimuli and test programs can be easily adjusted on a connecting computer.

One of the main differences between the original perimetry methods and newer computerised methods is the extent of the visual field that can be measured. By using a hemispherical bowl, which only extends up to 90°, measurements across the visual field are limited. With the biological structure of the face, monocular visual fields are reduced to approximately 60° nasally, 60° superiorly, and 70° inferiorly (Drake and Hetherington 1990). However, from the measurements taken using the original Bjerrum screen, it was found that the temporal/inferior regions of the visual field can extend past this 90° limit at approximately 100° (Traquair 1924) (Ronne 1915, Hartridge 1919).

The aim of this study was to develop a fixation device, which could be attached or incorporated into the bowl of an Octopus 900, to be able to measure a greater extent of the visual field. This procedure will allow for replication of early Bjerrum screen measurement responses, but in an automated fashion.

In this chapter, I discuss the development of this fixation device. This was undertaken in collaboration with the School of Engineering, Computing and Mathematics at the University of Plymouth. Some of the parts and design for the new device were sourced from an already existing OWL robot project (https://www.plymouth.ac.uk/research/robotics-neural-systems/plymouth-owl), from the centre of Robotics and Neural systems at University of Plymouth.

2.3 Methods

2.3.1 Purpose

The device had to be lightweight and small enough so that it did not encroach on the visual field, so that it did not affect the visual field measurements. It also had to be automated, to ensure repeated measures were standardised and unaffected by human error. The device had to control the direction and presentation of a fixation stimulus, with a large range of movement to cover the extent of the visual field.

2.3.2 Hardware

The extended fixation device consisted of 3D printed brackets which held a pair of MKS DS65k high-speed digital servos motors (MKS Instruments, Inc, UK) that could move with a frequency of 333 Hz period. The period of the pulse wave used by the Pulse-Width Modulation (PWM) was 3 ms and the pulse had a width between 850 µs and 2150 µs. This range allows up to 160° of rotation by each servo motor. The servos were controlled by a Raspberry Pi (Raspberry Pi Foundation, UK) compute module using the library PiGPIO which allows control of the GPIO inputs/outputs on the PI module (Figure 2.1). The Raspberry Pi compute module runs an IP server program (available as either Python script or C-code program) which creates an IP socket over the host USB connection using the Transmission Control Protocol (TCP). The script, which determines the position of the motors, waits by a 24-byte packet, which holds six 4-digit decimal integer numbers in an ASCII string separated by spaces. These are the new servo positions instructed by the host computer. Servo positions were calibrated dependent on visual field positions (e.g. for the measurements on the 180° horizontal temporal meridian, the servo was positioned 15° along the X axis in the nasal region). Fixation positions had eccentricities of 15°,

21° or 0°, to measure around the whole visual field. The host computer was installed with PuTTY (version 0.70), which is an open source software that is available with source code. This configures a connection to secure shell (SSH) software package whereby a terminal window is opened and the script on the Pi module is securely transferred, can be run or adjusted.

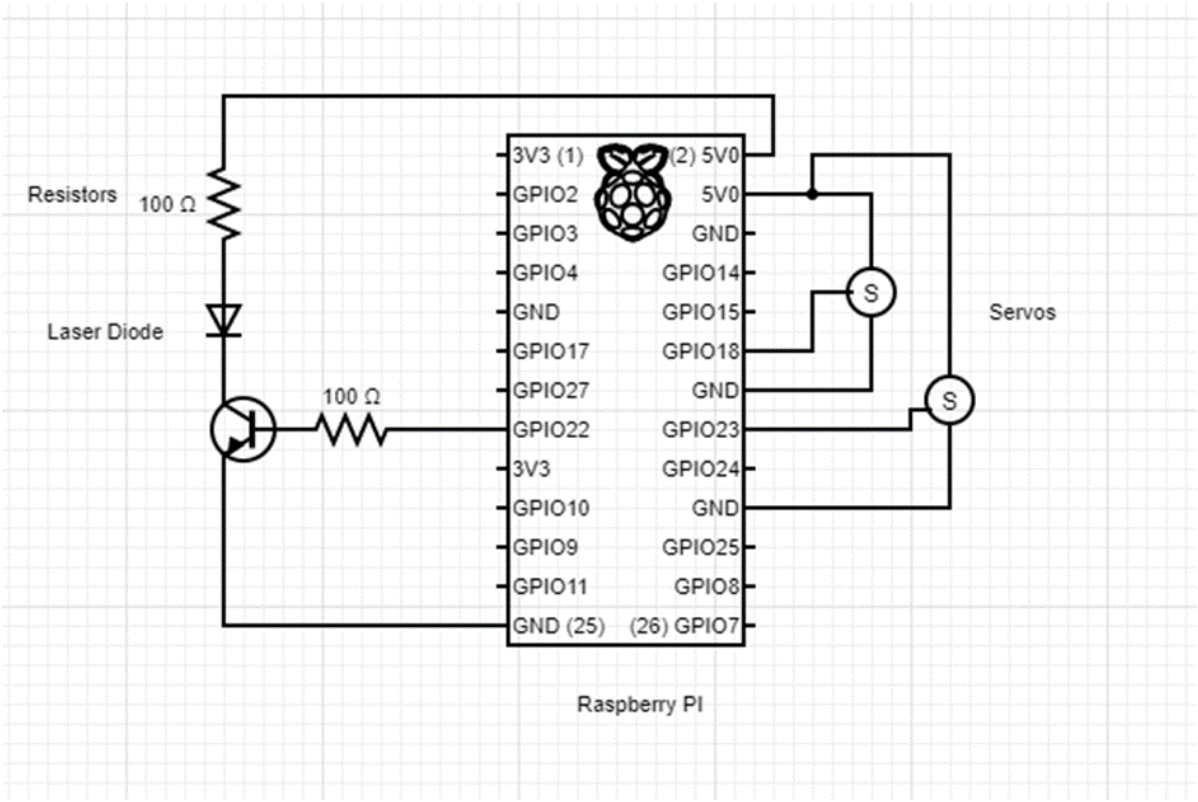

Figure 2.1: Technical drawing of circuit set up of raspberry PI module with servo and laser diode connections. Resistors allow a 3 Volt continuous current through the laser diode, with transistor switch to control on/off of diode.

A fixation point was created by a 10 mm diameter laser diode (Class 1) with a neutral density filter to reduce reflections. A current limiting resistor was also attached to the diode, so that it could be operated continuously. This diode was mounted in a 3D printed holder (Figures 2.2 and 2.3) that could be rotated in horizontal and vertical directions by the servos.

The device was mounted on the inside upper left corner of the Octopus 900. The Pi module was attached on the front, under the outer shell panel. USB cables connecting to the Pi module were fed through an opening and connected to the host computer. One USB cable powered the Raspberry Pi and another USB cable was used for connecting it to the host (Figure 2.4).

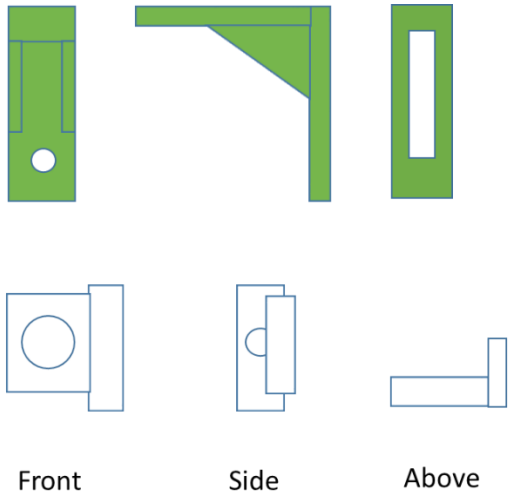

Figure 2.2: Schematic drawing of 3D printed brackets and holder for MKS servos and laser diode. Diagram shows front, side, and view from above of servo brackets (green) and laser diode holder (white).

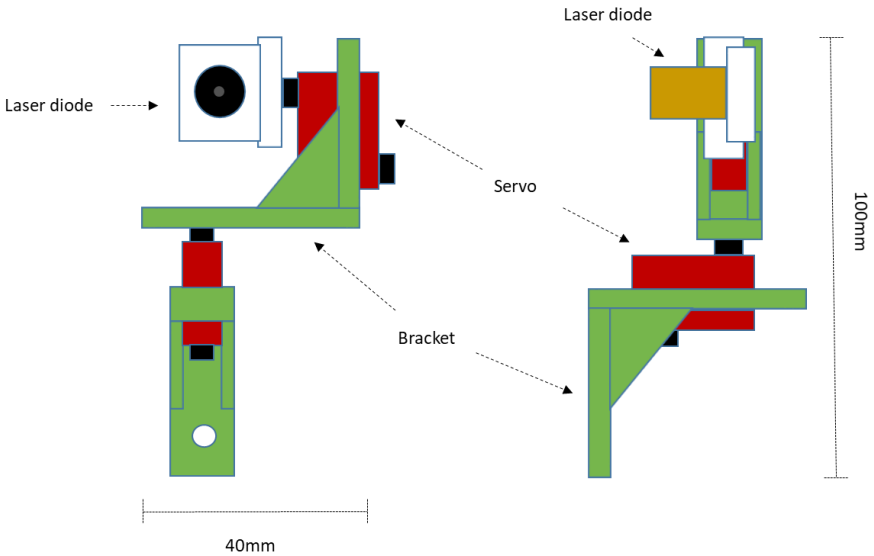

Figure 2.3: Technical drawing diagrams of extended fixation device. Diagram shows position of servos (red) and laser diode (gold) fitted with 3D printed brackets (green) and holder (white).

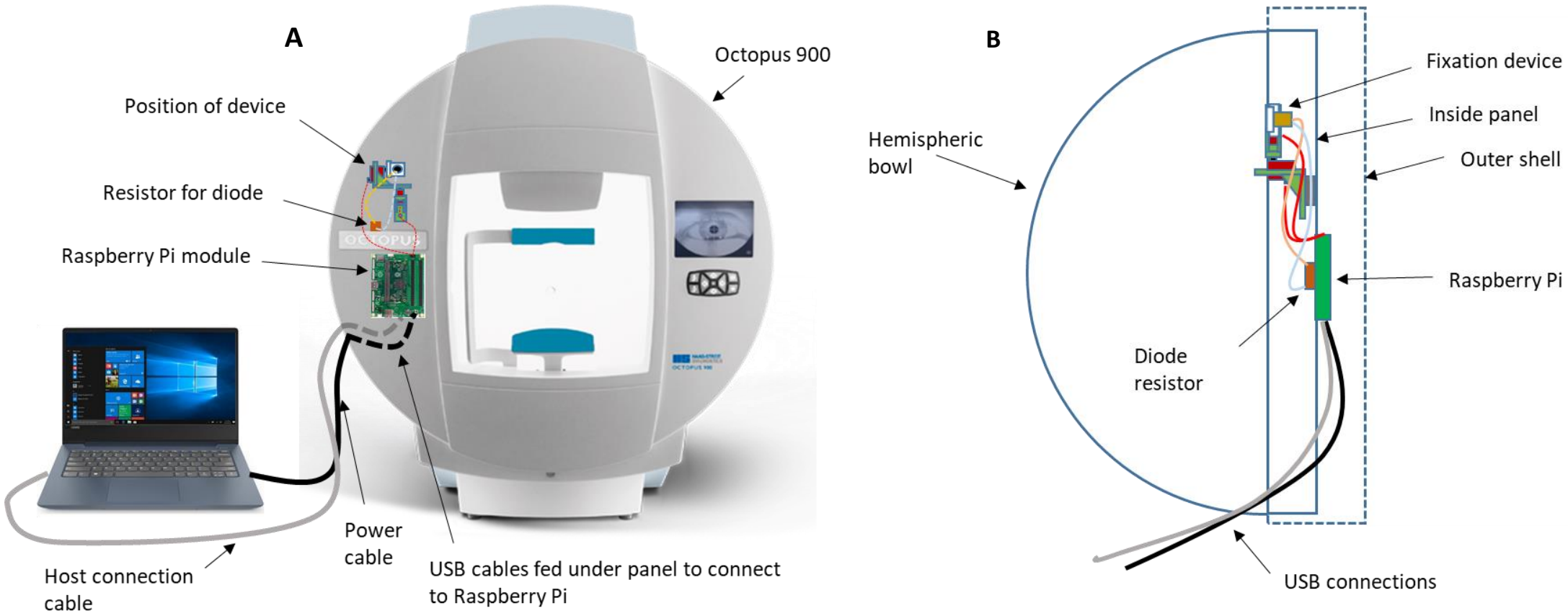

Figure 2.4: Illustrative diagram of position of fixation device and Raspberry Pi module within the Octopus 900. Panel A shows front view with connection to host computer. Panel B shows side and internal view of placement of devices.

2.4 Discussion

This extended fixation device provides a simple method for measuring the limits of the visual field in an automated fashion. Due to the small size of the device and its placement within the Octopus 900, there is no infringement on the visual field. Additionally, with the movement limits of the motors fixation points can be produced within a relatively large area of the bowl.

By using an extended fixation stimulus, a greater area of the perimeters bowl can be utilised to generate responses which will correspond to areas if the visual field beyond 90°. The extent of fixation should be controlled for patient comfort. When an individual focus on a point outside of the natural line of sight, it creates strain on the ocular muscles (Sommerich, Joines et al. 2001). The length of time should also be considered when using an extended fixation stimulus, as prolonged fixation/muscle tension has been found to leads to increased eye strain and fatigue (Collins, O'Meara et al. 1975). We suggest that fixation positions should be change every few presentations of a stimulus to reduce eye strain and maintain the observer's attention throughout the procedure. This method will also allow for a more reliable measurement of the extent of the visual field compared to the manual methods currently used, such as the tangent corner test (TCT) (Johnson, Wall et al. 2016), due to observers being unable to predict stimulus direction. A neutral density filter should also be applied to the front of the diode to reduce the reflection within the bowl for eye safety.

A couple of issues have been identified with this initial device build. Firstly, due to the motors used, the fixation stimulus makes very small movements, approximately 1 mm, when the motors are extended to their limits. However, these movements

did not seem to effect fixation in the study this device was applied in, and it should also be noted that some observers preferred this small movement as it improved concentration and helped to maintain fixation (Engbert and Kliegl 2004, Krauzlis, Goffart et al. 2017). Further research is required to determine if the small movements of a fixation point could affect overall fixation, however more advanced servos could be used in future device developments to counteract for this movement. Another issue was that this device was soft mounted to the Octopus 900. In case of possible movement of the fixation device, fixation positions were calibrated before use to ensure reliable results, however this was time consuming. Using a hard mount on which the device could be attached and detached from, would allow for a more standardised test and enable the possibility of making changes to the device and the replacing parts without the need to recalibrate fixation positions.

The overall performance and feasibility of the extended fixation device was assessed. The model that we have developed is both cost effective, and easily applied to any perimeter and host computer through open source software. By using this simple extended fixation stimulus, future research is not restricted by the physical bowl boundaries and test programs currently found in commercial perimeters.

3 Chapter 3: The outer limits of the far peripheral visual field

3.1 Introduction

The outer limits of the far-periphery visual field have not been yet studied with automated perimetry in a systematic manner. Previous measurements of the limits of the visual field were undertaken over a century ago and described responses beyond 100° in the temporal visual field (Rönne 1915). These measurements were undertaken manually with a tangent screen, on an undisclosed number of observers. In commercial perimeters, measurements of the far-peripheral visual field are currently limited to 90°. In this study, we aim to measure the limits of the far-peripheral visual field using an adapted automated perimeter to confirm findings on the limits of the temporal visual fields from over a hundred years ago (Rönne 1915).

Understanding the limits of the outer visual field could help contribute to the knowledge of the already established role of the far-peripheral field. Vision in the far periphery is used to guide attention (Webster and Haslerud 1964, Posner 1980, Gwinn and Jiang 2020). Vision contributes to the detection of objects, enabling individuals to allocate them within their central vision where resolution is at its highest (Simpson 2017, Simpson and Muzyka-Woźniak 2018). Moreover, it has a significant role in connecting awareness of human self-motion, providing important information in regards to awareness of where we are, and how we are moving within our external environment (Brandt, Dichgans et al. 1973, Schmitt, Schwenk et al. 2021). In terms of clinical management, the far-peripheral visual field could contribute to the understanding of ocular and retinal degenerations, such as glaucoma and retinitis pigmentosa, or visual phenomena such as negative dysphotopsia, which can occur after cataract surgery (Simpson 2017).

The definition of far-peripheral visual field is inconsistent throughout the literature, with many studies considering far only as parts of the visual field beyond 90° away from the fovea (Webster and Haslerud 1964), and others beyond only 60°(Simpson 2017). In this paper, we define the far-peripheral visual field as the visual region which extends beyond 60° (Simpson, 2017).

Currently, the peripheral visual field is not measured frequently, due to a lack of fast and accurate standardised testing procedures (Nowomiejska, Vonthein et al. 2005). Some of the perimetry options used to measure the peripheral visual field are the Humphrey Field Analyzer (HFA, Carl Zeiss Meditec, Jena, Germany), Octopus instruments (Haag-Streit, Koniz, Switzerland) and Goldmann manual perimetry, among others. These perimeters offer a number of testing strategies, consisting of static or kinetic stimuli, to measure peripheral regions up to 90°. However, these tests can be lengthy in duration and as such, are at risk of inducing ocular fatigue and deterioration of observers' attention, both of which can affect test results and reliability. The hemi-spherical shape of the bowl also restricts the measurement of the far-peripheral visual field beyond 90° or even less since the background light in the bowl become increasingly non-homogenous for areas far from its centre.

Only a few papers, some from over a century ago, have previously examined the lateral margin of the visual field. They observed that the visual field can extend to more than 100° (Druault 1898, Ronne 1915, Hartridge 1919). This limit however could only be measured using a large intense stimulus. For example, Rönne (1915) used a test-object at a visual angle of 9° to measure the furthest extent. A large target is required to measure this visual region due to the reduction of effective area of pupil, and sensitivity of the retina decreasing with eccentricity (Traquair and Scott

1957). More recent studies have examined the border of peripheral visual field (Johnson et al., 2016 and Nowomieiska et al., 2005) using both manual and kinetic perimetry techniques. The manual technique by Johnson et al. (2016) used a tangent corner test, where a black tennis ball subtending a visual angle of 4° was presented horizontally along a wall until seen. Nowomiejska et al. (2005) examined the peripheral visual field with automated kinetic perimetry up to 90°, however there is currently not an automated method to measure beyond 90°.

In this paper, we aimed to confirm the findings by Rönne (1915) in a larger group of observers. This study will also compare the variability of responses to kinetic perimetry, using ascending and descending methods of limits. To this end, we adapted a perimeter and a devised automated kinetic perimetry strategy for measuring the outer limits of the far-peripheral visual field.

3.2 Methods

3.2.1 Participants

For this study, 10 healthy observers, with a mean age of 27 years, range 25 – 37 years, were recruited from students and staff at the University of Plymouth. Participants were examined at the University vision lab. The exclusion criteria for this study were history of ocular surgery or disease (strabismus), medications that affect peripheral vision, and refractive error of spherical ametropia greater than 6 dioptres (D) or astigmatism greater than 2D. Refractive errors were not corrected to avoid lens rim artefacts, and it has been shown that, in eyes with refractions in this range, correction of the refractive error has no influence on the position of peripheral isopters (Niederhauser and Mojon 2002). Ethical approval was obtained

from the University of Plymouth and followed the tenets of the Declaration of Helsinki. Informed consent was obtained from each participant.

3.2.2 Apparatus

We used the Octopus 900 automated perimeter (Haag Streit, Switzerland) in this study, which has a hemispherical bowl with a radius of 300 mm, and a background luminance of 10 cd/m² (Haag-Streit, Koniz, Switzerland).

To create new fixation points, a laser diode, with a neutral density filter placed over it to dim the diode intensity, was mounted on two motors (MKS D565K servos) controlled by a programmable motherboard (Raspberry Pi Model 3), inside of the opening of the Octopus 900 (see Chapter 2 for a more detail description of the build of the fixation device). Figure 3.1 shows pictures of the montage. The laser device was controlled using custom-written scripts in Python programming language (Python software Foundation version 3.6.4). We used the Open Perimetry Interface (OPI) (Turpin, Artes et al. 2012) and the R programming language (R core team 2018), to present the kinetic stimuli from the far periphery towards the new fixation point projected with the laser diode (see Appendix 1 for R code). Fixation was monitored through a separate small video system, consisting of an infrared camera that was fixed to the chin and headrest, and a small display unit, which allowed the examiner to observe the eye being tested.

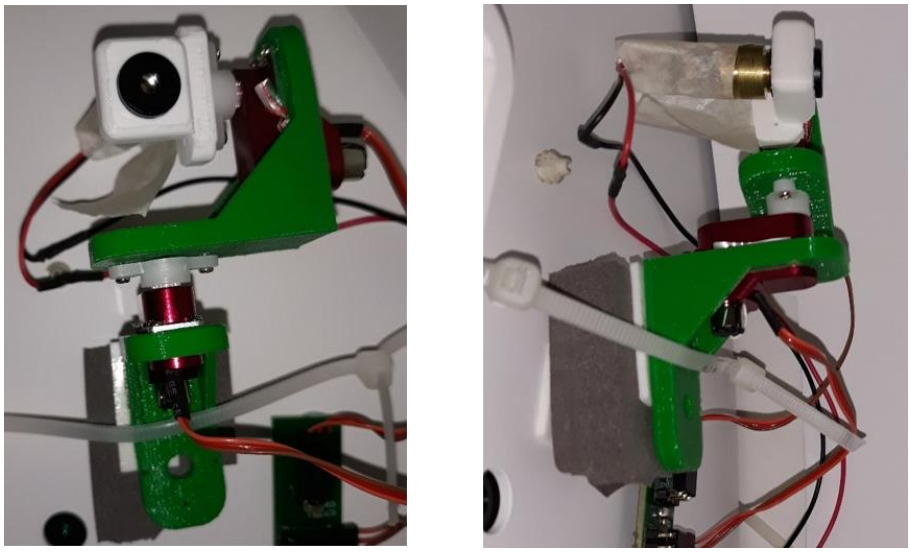

Figure 3.1: Images of laser diode moved by MKS D565K servos which were control by a Raspberry PI model 3. This laser was placed on the inside top left corner of an Octopus 900.

3.2.3 Fixation locations

We produced six fixation points with eccentricities of (15°, 15°), (15°, 0), (0°, 0°), (-15°, 0°), (-15°, 15°) and (0°, 15°) to measure the whole visual field. Figure 3.2 shows the position of the fixation points; these are colour and letter coded with the angles of meridians. Depending on the position of the fixation, presentations would only appear on certain meridians. A central fixation point was used to measure the superior hemisphere due to anatomical features restricting the limits, which can be measured when using an extended fixation.

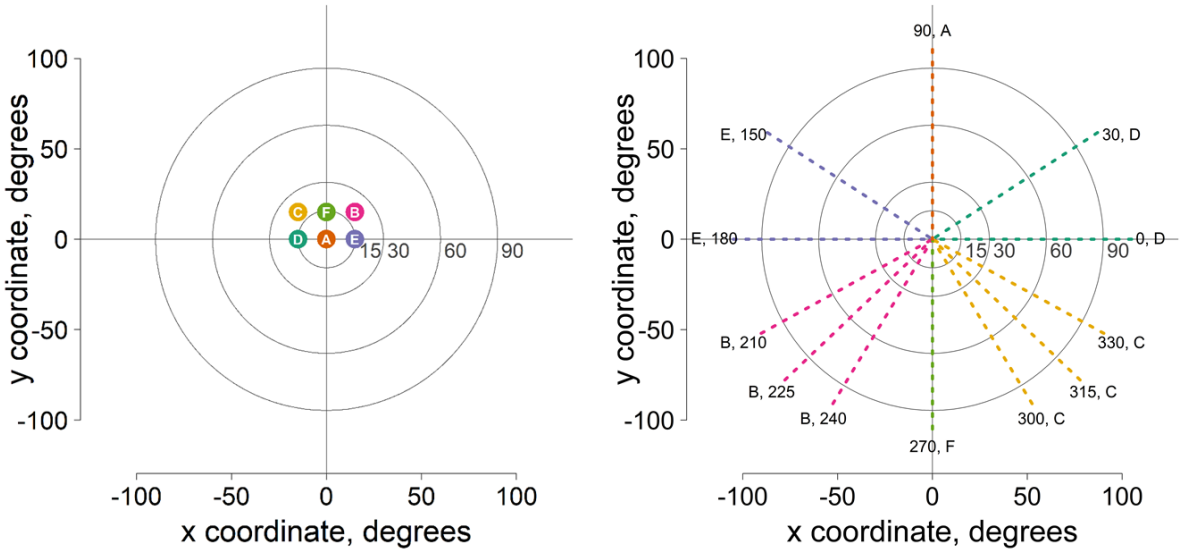

Figure 3.2: Left panel shows fixation positions and right panel shows the meridians measured per fixation point (colour and letter coded). Labels equal meridian angle in degrees.

3.2.4 Kinetic visual field test

Kinetic stimuli were presented at 12 meridians (see right panel in Figure 3.2). The projected stimuli had sizes and intensities that followed the Goldmann standards. Three stimuli were used: I-4e, subtending 0.108°, III-4e subtending 0.43°, and V-4e subtending 1.73°. The luminance for all stimuli were 1000 apostilbs or 318.3 cd/m². The stimulus moved at a speed of 5°/s. There were 10 stimuli presentations per meridian. The order of fixation location and meridians measured were assigned at random.

Stimuli presentations moved either outwards from the centre so the subject could see it at the beginning of the trial, or inwards from the far periphery until the subject could see it. Pros and cons for each method of presentation are explained in detail in Blackwell (1946), Guilford (1954), Herrick (1965), and Engen (1988), however both methods are affected by the error of expectation and error of habituation introduced by the observer. For each method, participants were given practice trials

until they were comfortable with the test procedure. Participants underwent a total of 720 trials, corresponding to 10 repetitions for each of the 12 meridians at each of the 3 stimulus sizes and the 2 presentation methods.

3.2.5 Experimental protocol

For each participant the left eye was selected. This eye was selected due to the set-up of previous versions of the extended fixation device, however, testing of the right eye would have equally worked using this studies device version. For each participant 6 kinetic examinations were performed of the peripheral visual field. All tests took place over 3 sessions, with 2 examinations per session, taking approximately 1 hour including breaks per session. Altogether, the study procedure took approximately 3 hours per participant.

Participants were briefed on the aim of the study and asked to position themselves in front of the perimeter in a comfortable position. A stimulus size, fixation position and direction on stimulus presentation were chosen at random to reduce an order effect on results. To make the test easier for participants, once a stimulus size and direction were chosen, all fixation points were undertaken under these conditions to form an isopter before randomly choosing another condition.

In conditions where the stimulus would move inward, the start of the presentation was positioned far enough out to ensure the participant would not see it straight away. The participant was instructed to click the response button when they were aware of the stimulus. For the outwards conditions, the starting position was in a region where the participant would be able to see the stimulus initially, and the participant was instructed to press the response button when they were no longer aware of the stimulus.

During each fixation position, the participant was made aware that the stimulus would only come from a small number of angles, see Figure 3.2, however it was still randomised across those angles. The participants' pupil was aligned before starting testing each position. Once the presentations for that position were finished the participant was given a short break of approximately 2 minutes or until they were ready to continue. This procedure was repeated until all stimulus sizes and stimulus directions were completed, forming 6 isopters which represent the threshold to that stimulus intensity on the outer border of the visual field.

3.2.6 Data analysis

The mean isopter radius (MIR) was used as the global summary, and the reproducibility of an individual participant's responses was summarized as the median absolute deviation (MAD) of responses from the final isopter. The mean isopter was defined from the median response per isopter position for each participant. The variability between the two presentation methods per stimulus size was compared via a Wilcoxon's signed rank test. The variability of the scatter of responses between the two methods per stimulus size was compared using a Wilcoxon's signed rank test, and the scatter of responses across all isopter positions was compared using a Friedman's test.

3.3 Results

3.3.1 Comparison between ascending and descending method of limits

Table 3.1 shows the difference between inward and outward stimulus presentation. Outward presentation (from seen to not seen) yielded on average a greater MIR than inward presentation (from not seen to seen). Nevertheless, the average difference decreased with stimulus size, from 9° (corresponding to a 15% increase)

for Goldmann I-4e stimulus to 5° for III-4e (a 7% increase), and only 2° for V-4e (a 3% increase). The MIR were significantly different for sizes I (p = 0.002, effect size = 1.3) and III (p = 0.002, effect size = 0.8), but not for size V. Figure 3.3 shows individual plots of isopters obtained with inwards and outward presentation methods.

Table 3.1: MIR of size I, III & V for both outward (not seen to seen) and inward presentation strategies (seen to not seen). Table shows mean, range and difference between MIR for the methods of limits.

	Mean isopter radius (MIR)				
Stimulus size	**Outwards Mean**	**Outwards Range**	**Inwards Mean**	**Inwards Range**	**Difference**
I-4e	**62°**	**58-68°**	**71°**	**67-76°**	**9°**
III-4e	**71°**	**63-76°**	**76°**	**72-81°**	**5°**
V-4e	**75°**	**67-80°**	**77°**	**73-82°**	**2°**

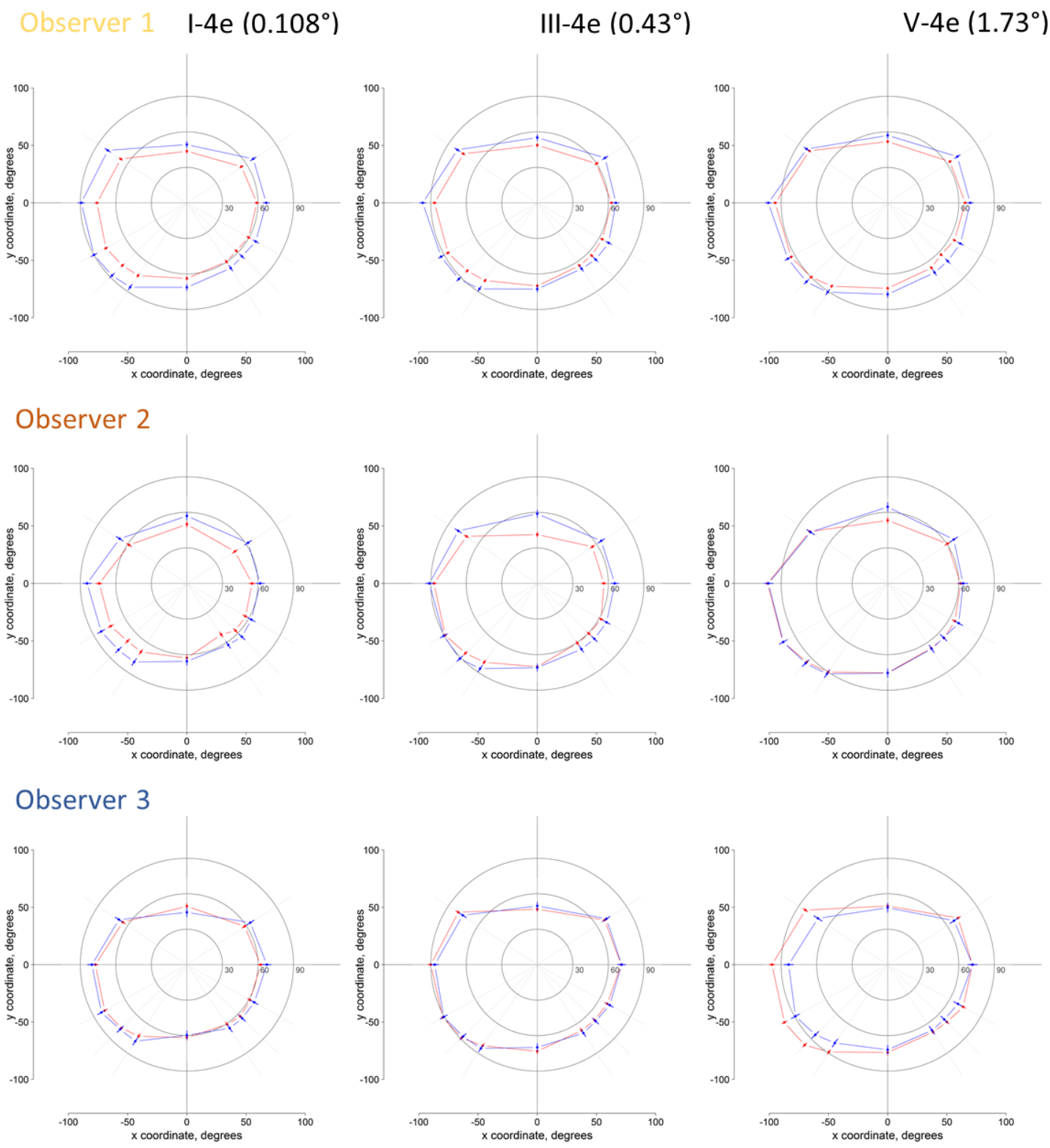

Figure 3.3: Examples of 3 participants, colour coded for reference in further plots. These plots illustrate the difference between ascending and descending method of limits, for all 3 stimulus intensities. The isopter derived from the ascending (non-seeing to seeing) method of limits is shown in red, for the descending (seeing to non-seeing) method of limits it is shown in blue. Error bars indicate the precision of participants represented as the median absolute deviation (MAD).

Table 3.2 shows the scatter of responses according to stimulus size and stimulus presentation direction. The scatter of responses was larger for the inward method than for the outward method for all stimulus sizes and those differences were statistically significant. For size I-4e there was a 0.5° difference, which corresponds to a 50% increase ($p = 0.002$, effect size = 1.2). For size III-4e there was a difference of 0.5°, which corresponds to a 60% increase ($p = 0.002$, effect size = 0.9), and for size V-4e there was a 0.6° difference, which corresponds to a 75% increase ($p = 0.002$, effect size = 1.2).

Figure 3.4 shows the scatter of responses for both inward and outward presentation directions for size V-4e for each participant. It also shows the overall distribution of responses for both conditions, fitted with a normal distribution curve. For all stimulus sizes in the inward condition there was a significant difference in distribution $p < 0.001$ ($D = 0.14$, 0.18, and 0.13). For the outward condition there was also a significant difference for stimulus sizes I-4e and III-4e $p < 0.001$ ($D = 0.1$, 0.17) and V-4e $p = 0.004$ ($D = 0.07$).

Table 3.2: Median absolute deviation of spread of participant's responses for stimulus size I, III & V. Table shows median and range of median absolute deviation.

Median absolute deviation (MAD)				
Stimulus size	**Outwards Median**	**Outwards Range**	**Inwards Median**	**Inwards Range**
I-4e	**1.5°**	**1.3 – 2.0°**	**1.0°**	**0.8 – 1.6°**
III-4e	**1.4°**	**1.0 – 2.2°**	**0.9°**	**0.5 – 1.9°**
V-4e	**1.4°**	**0.9 – 2.2°**	**0.8°**	**0.5 – 1.2°**

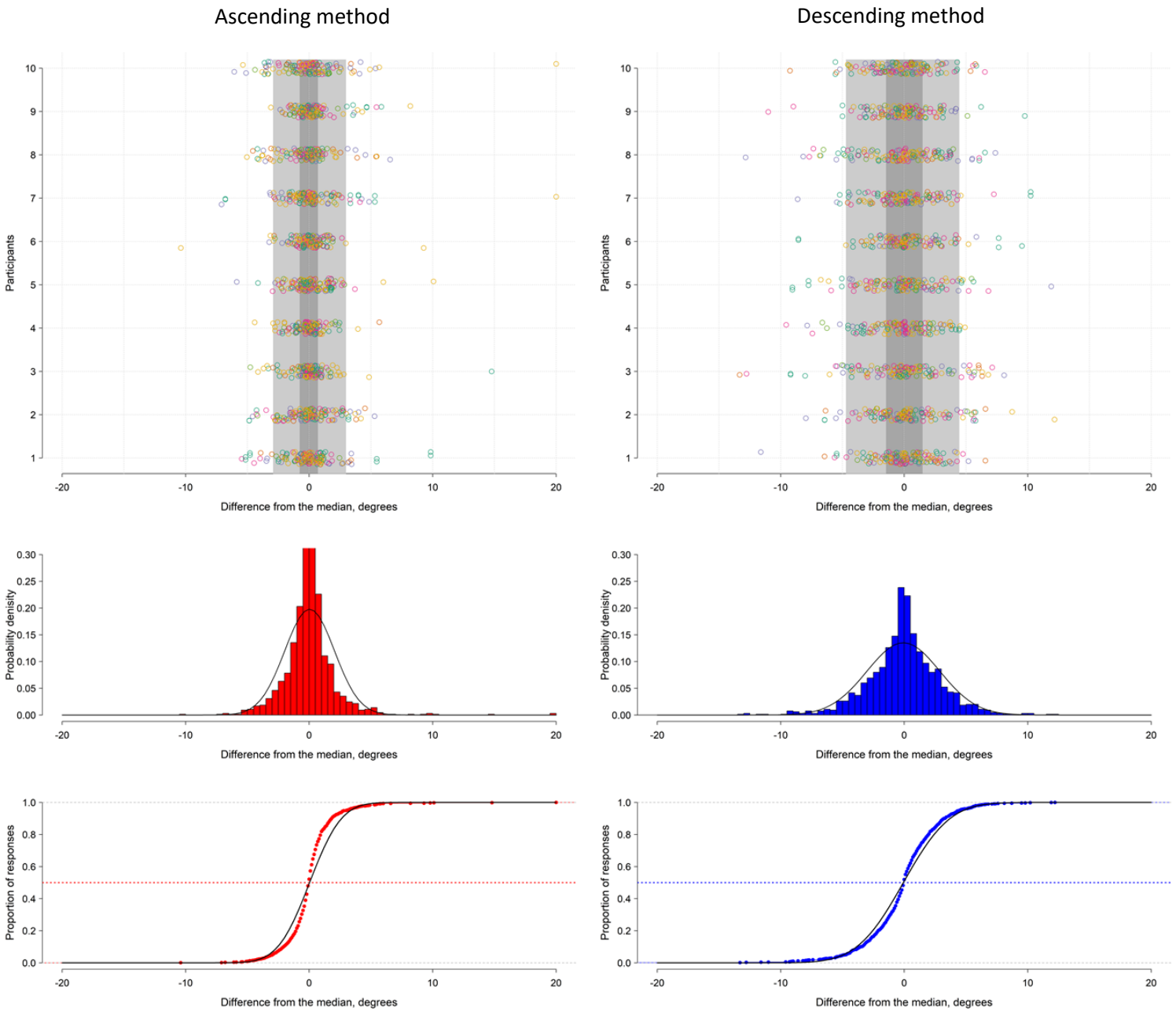

Figure 3.4: First column represents the ascending method, and the second column illustrates the descending method. Top row: Scatter of responses from the median (V-4e) for each participant. Points are colour coded by angle of direction (see Figure 3.2). Light grey bar indicates 90% interval, dark grey is 50% interval. Points at 20° on x axis equals 20+ degrees. Points jittered in Y axis. Middle row: Histogram of overall scatter of responses from the median, black line illustrates a normal distribution. Bottom row illustrates a cumulative distribution, with dotted middle line representing the 50-percentile point of detection, and black line the normal distribution.

3.3.2 Temporal limits of the kinetic visual field

Figure 3.5 shows the overall mean isopter per stimulus size and the individual estimated isopter per observer using the conventional inward method. This also shows the inter-individual difference which was found to not be significantly different across isopter positions. The point of furthest extent was found on the 210° meridian. With increasing stimulus intensity resulting in a mean isopter position increased, with I-4e at 79°, III-4e 93° and V-4e at 100°.

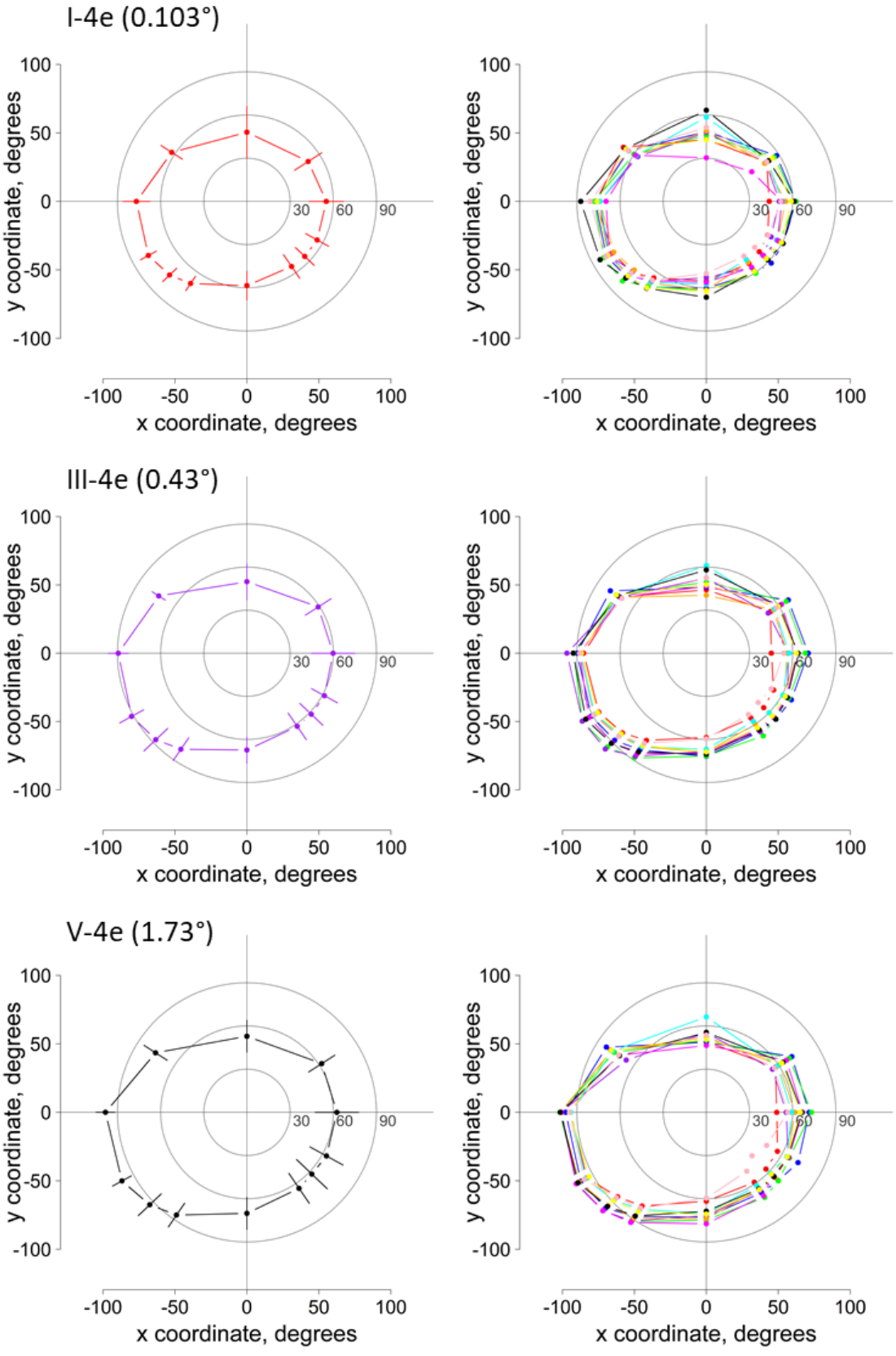

Figure 3.5: Left panel: Mean isopter of the group. Error bars indicate 2 standard deviations. Right panel: Isopters to Goldmann size I-4e, III-4e & V-4e stimulus (1.73°, 0.43° & 0.108°, 318cd/m2), in 10 healthy observers.

3.4 Discussion

The objective of this study was to develop a method to measure the outer border of the far-peripheral visual field. Our results show that it is possible to measure beyond 90° in the inferior temporal visual field, by using a simple fixation adaption on a commercial Octopus 900 perimeter.

This study replicated closely the findings of Rönne (1915), with detected stimuli within the temporal region on average up to and beyond 100° using the large V-4e stimulus. Measurements up to 108° were found on the 180°meridian. The less intense stimulus III-4e found detected stimuli between 86° to 100°, thus even with a less intense stimulus measurements beyond 90° are feasible. It should be noted that these extreme responses were only found in the inferior temporal visual field.

When observing the outer border of the visual field in other visual regions, the extreme limits are affected by facial features, such as the nose and eyelids. Visual regions most affected by facial features are the superior and nasal regions. These features differ greatly between observers, thus the measured extent of these regions is limited. With extended fixation, the results of the nasal visual region did not differ from using a central fixation. This could be explained in terms of the extension of the nose blocking light from entering the pupil, thus even with fixation extension the nose still blocks light entering the pupil beyond an angle on average of 60° (Lewis and Maurer 1992).

When using a conventional central fixation, the isopter difference between stimulus intensities V-4e and III-4e, within 90° are relatively small (Niederhauser and Mojon 2002). However, in our study we found on average a 7° difference between isopter positions, within an inferior temporal position using the ascending

technique. This follows on from Druault (1898), Rönne (1915), and Hartridge (1919) who could only measure this position by using a stimulus of large intensity. Our findings also support the hypothesis that there is a drop in sensitivity in the far-periphery beyond 90° due to the effective area of the pupil, thus only a size V-4e stimulus would be effective at measuring this visual area.

By using a large number of presentations, we were able to examine the distribution of responses in the far-peripheral visual field. The results demonstrated that there were no significant differences in response scatter between isopter locations, allowing us to pool responses to a particular stimulus intensity, across the entire visual field. The responses to kinetic stimuli show a non-normal distribution and this distribution showed “long tails” and a “high peak”. The shape of this distribution would suggest that on average participants are precise in their responses, creating this “high peak”, however on occasions they do produce some extreme “outlier” responses (Lynn 1991), resulting in “long tails”. Future research, for example via computer simulations, using this distribution could allow for the development of a more efficient strategy for measuring the far-peripheral visual field.

Results of the study identified small differences in isopter sizes between ascending and descending methods of limits. The largest difference was found with the I-4e stimulus, where the descending method produced on average a 9° larger isopter. For the III-4e stimulus, this difference with descending methods was 5°, and with stimulus V-4e the difference was 2°. These results are not consistent with those of Phu et al. (2016), who identified much larger differences between isopters. However this was found in the central visual field, where response times have a greater effect

on isopter positions compared to the peripheral visual field (Schiefer, Schiller et al. 2001). A number of factors in kinetic perimetry could attributed to a spatial difference between isopters. A high variability in response times between participants is common (Schiefer, Schiller et al. 2001) along with an increase in response times with eccentricity and fatigue (multiple test in one day).

With the descending method (seeing to non-seeing) the isopters were larger, but the responses were more variable in comparison to the traditional ascending (non-seeing to seeing) method. This can be seen from the MAD of responses, with the descending method producing a larger response variability across all stimulus sizes, see table 2. Works by Blackwell (1946), Pelli (1980), and Robson and Graham (1981) found that the detectability of a stimulus reduces with eccentricity, unless it is accounted for by increasing the stimulus intensity. One theory for this increase of response variability is the uncertainty factor, where an increase of uncertainty reduces stimulus detection (Pelli 1985). A more in-depth explanation of models of contrast detection and uncertainty factors can be found in Pelli (1985). These results suggest an overall isopter defined using the descending method is less reliable than an isopter using the ascending method. Thus, the conventional ascending method should be favoured for future measurements in the far-peripheral visual field.

This study has shown that it is possible to examine the far-periphery beyond 90°, with responses up to approximately 108° found in the inferior temporal region. Through the use of the OPI and R code, this procedure can easily be adapted to existing commercial perimeters. Precise measurements of the extreme limits of far-peripheral vision, beyond 90° of fixation, are feasible with a simple modification of existing projection perimeters. Established feasibility of this novel kinetic perimetry

method could be applied for examining and quantifying any retinal or neurological diseases, which affect the peripheral visual field (Mönter, Crabb et al. 2017). For future measurements of the far-peripheral region, a strategy using fewer presentations, a size V-4e stimulus, and the conventional ascending methods of limits, would be suffice define an overall isopter position.

4 Chapter 4: Measuring the extent of the peripheral visual field and identifying negative dysphotopsia in pseudophakic patients.

4.1 Introduction

Negative dysphotopsia is a rare and poorly understood condition; however, some patients do report some form of the phenomenon as a shadow in the periphery, right after undergoing cataract surgery (Davison 2000, Osher 2008). Negative dysphotopsia was first reported by Davison (2000), where patients self-reported observations of dark shadows in a crescent shape, within the temporal side of their vision. However, the aetiology of negative dysphotopsia is still under debate and the underlying cause still unknown (Henderson, Yi et al. 2016). This phenomenon is different from positive dysphotopsia, which presents as optical disturbances in the form of light streaks and halos. For a small number of individuals, negative dysphotopsia remains persistent, although some patients are eventually able to ignore the shadow (Henderson, Yi et al. 2016), or the phenomenon can spontaneously resolve itself through neuro-adaption (Masket, Rupnik et al. 2019). The latter happens in the majority of cases, once both eyes have undergone the cataract surgical procedure (Frank and Gupta 2016, Safran 2017). For others, the phenomenon is severe and bares resemblance to retinal detachment and vascular occlusion (Bournas, Drazinos et al. 2007). This persistent visual disturbance leads some individuals to consider surgical intervention.

The aim of cataract surgery is to replace the crystalline lens of the eye, which has become cloudy overtime, with a new artificial clear IOL. The procedure is relatively uncomplicated, with an extremely high success rate, and results in improved visual acuity and contrast sensitivity for patients (Kessel, Andresen et al. 2016). The optical

diameter of the IOL is smaller than that of the crystalline lens (6 mm compared to about 9.5 mm), and it is also thinner (0.8 mm compared to approximately 5 mm). When the natural lens is removed the iris is moving posteriorly (Simpson and Muzyka-Woźniak 2018). However, the reduced thickness of a new implanted IOL causes a larger gap between the IOL and the iris. This gap between the IOL and iris can be beneficial in patients with glaucoma, because the outflow of aqueous fluid is increased thus lowering the intraocular pressure (Yang and Hung 1997). However, others believe that the formation of this gap is an underlying cause of negative dysphotopsia. The following sections will discuss possible causes for negative dysphotopsia and perimetry methods used to detect it.

A possible cause of negative dysphotopsia, which is based upon the size of the IOL, is the effect of pupil size on the amount of light that reaches the retina and the angle at which light rays enter the eye. Using Zemax ray tracing software (Optic Studio, Kirkland, WA), it has been found that when light enters the eye at a large angle (e.g. 85°), part of it bypasses the IOL. This is due to the light entering from the side rather than the centre of the pupil and passing through the gap between the iris and the lens (Figure 4.1). The shadow (non-illuminated area on the retina) is thought to occur between the last ray of light that is focused by the lens and the point where rays first miss the IOL (Holladay and Simpson 2017, Simpson 2017).

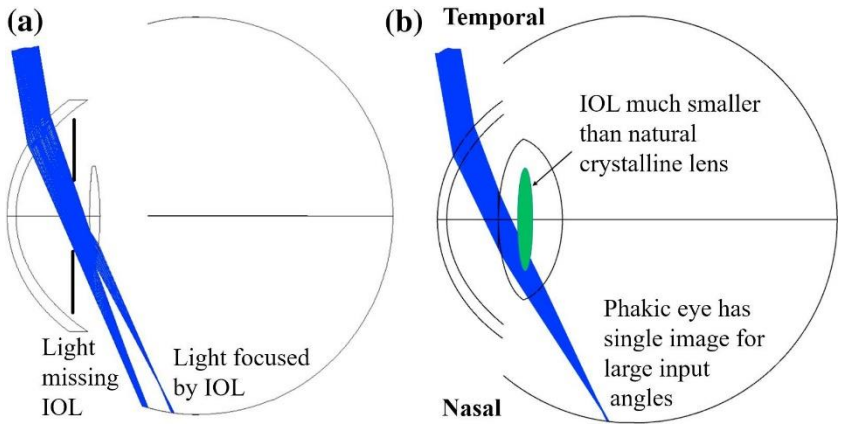

Figure 4.1: Drawing showing how light bypasses the new IOL implanted in an eye Simpson (2017).

An additional theory for the cause of negative dysphotopsia is based upon the design of the IOL. Vignetting occurs when light enters the eye and hits off the edge of the IOL, creating a dark area in the periphery of the visual field (Simpson 2015, Simpson 2016). This occurrence is thought to be prevalent when an individual has a small pupil diameter because some areas of the peripheral retina can be non-illuminated due to the reduction of light entering the eye (Holladay and Simpson 2017). Some studies have found that the symptoms of negative dysphotopsia are reduced with pupil dilation (Masket and Fram 2011), thus enhancing the idea that pupil size has a crucial role in negative dysphotopsia.

During cataract surgery a small incision (typically less than 3 mm) is typically made in a superotemporal or temporal location of the cornea to remove and replace the crystalline lens (Osher 2008), however incisions can be made in alternative positions to compensate for corneal astigmatism. A study by Osher (2008) followed up patients after cataract surgery to investigate the relationship between the location of corneal incision and negative dysphotopsia. All patients in the study had either a superotemporal incision made in the right eye, or a temporal incision in the left eye. If patients perceived a shadow, they were asked to indicate its location in their visual

field. These patients were followed up after 1 year, and those who still perceived a shadow underwent additional tests to investigate possible causes. The results of this study showed that individuals who had cataract surgery performed on their left eye reported a higher incidence of a temporal shadow after 1 year compared to the ones who had the right eye operated. This is thought to be due to the exposure of the incision, as superotemporal incisions are usually covered by the upper eye lid whereas temporal incisions are left exposed. This finding is further supported by a study of Davison (2000) who found that all individuals with negative dysphotopsia received a temporal clear incision in their left eye during cataract surgery. However, as negative dysphotopsia is also reported in eyes with superotemporal incisions, this suggests that incisions are not the primary cause of this phenomenon.

In cataract surgery, the IOL is placed within the capsular bag remnant following an overlying continuous circular anterior capsulotomy (Powell and Olson 1995). One possible cause of negative dysphotopsia is due to the anterior capsulotomy edge causing a reflection on the nasal retina. The optical relationship between the anterior nasal region of the capsulotomy and anterior surface of the new IOL is thought to cause this visual phenomenon in the temporal visual field (Masket, Fram et al. 2018). Support for this theory comes from a surgical intervention study which found that by removing a portion of the overlying nasal anterior capsulotomy with the Neodymium–doped yttrium aluminium garnet (Nd:YAG) laser, removed the effect of negative dysphotopsia in a patient (Cooke, Kasko et al. 2013). An additional surgical procedure is to add on a piggyback IOL in the ciliary sulcus, however this procedure has varying effects on negative dysphotopsia (Masket and Fram 2011).

A method used to map the shadow caused by negative dysphotopsia is perimetry. Previous studies have attempted to use static perimetry, using the conventional 24-2/30-2 grid patterns (Narváez, Banning et al. 2005, Kim, Ha et al. 2014). However, these tests did not detect negative dysphotopsia probably because the shadow was located in the outer visual field, beyond 30°. Lengthy procedures, such as Goldmann manual and automated kinetic perimetry, have previously been successful at measuring the extent of the shadow, which is usually detected at approximately between 60° to 80°in the temporal visual field (Makhotkina, Berendschot et al. 2016, Makhotkina, Dugrain et al. 2018, Masket, Rupnik et al. 2019).

Makhotkina et al. (2016) used the manual Goldmann technique to establish the difference in visual field extent before and after cataract surgery. They found there was a small reduction of the visual field in the temporal region. This was more noticeable in patients who reported negative dysphotopsia. These patients had approximately a 10° reduction in visual field extent in the temporal area. One of their patients with negative dysphotopsia was able to see the size V-4e Goldmann stimulus at the outer edge of the shadow. The visibility of the stimulus was then partially obstructed by the shadow and then the stimulus was visible again on the inner edge of the shadow. However, it is unclear whether this is the case for all patients, or if the shadow *per se* is actually the outer edge of their peripheral visual field. One reason for this uncertainty is the limitation of perimeters, which can only measure the visual field up to 90°, whereas the temporal visual field is extended beyond this point, up to approximately 105° (Simpson 2017). This outlines the need for an alternative method in order to measure the full extent of the temporal visual field in these patients.

Masket et al. (2019) found shadows in the temporal inferior region using kinetic perimetry but nowhere else. Their theory was that the superior defect could be reduced by the upper eyelid, obscuring the amount of light coming in.

The aims of this study was to identify the extent of the temporal visual field of pseudophakic patients and compare against an age matched population who has not had cataract surgery. This will be undertaken by means of automated kinetic perimetry, using an alternative kinetic perimetry technique for detecting the presence and the extent of negative dysphotopsia in the temporal visual field.

4.2 Methods

4.2.1 Participants

This study is a retrospective cross-sectional study involving 30 patients (mean age 73 ± 5 years, range 61 to 83 years) who have undergone cataract surgery between November 2018 and July 2019. Using convenience sampling, potential participants were identified from the routine post-operative cataract clinics of the Royal Eye Infirmary and Nuffield Hospital at Plymouth. If the patients met the criteria and were willing to participate in the research project, they were invited to attend a single study visit at the University of Plymouth Peninsula Allied Health Centre. The study obtained HRA and REC approval ref15/SS/0141, and was approved by the Ethics Committee of University of Plymouth and adhered to the tenets of the Declaration of Helsinki.

4.2.2 Study criteria

The inclusion criteria for the study were participants who had undergone routine cataract surgery using a standard, sutureless, micro-incision, phacoemulsification

technique under topical anaesthesia. They were aged over 18 years and were capable of giving the informed consent. The exclusion criteria included amblyopia, pupil deformation or a dilated pupil smaller than 5 mm, existent macular pathology or other retinal disease, glaucoma, corneal disease, iris abnormalities, and any previous corneal or intraocular surgery other than cataract surgery. Moreover, any patient who had surgical complications such as posterior capsule opacity or macular oedema, was also excluded from participation in the study.

4.2.3 Procedure

Each participant attended one study visit approximately 1 to 3 months post-surgery. During this visit the eye of the participant the surgery was undertaken on was evaluated. Visual acuity (VA) was measured using a ETDRS chart, and pupil size was measured under scotopic conditions using an auto-refractor (OPD-Scan lll, Nidek, Japan). A custom-made questionnaire (Figure 2, left panel) was used to identify participants with a presence of a shadow in their vision. If they did report a shadow, they were asked to indicate its location in their visual field and a basic sketch was made (Figure 4.2, right panel) based on the description.

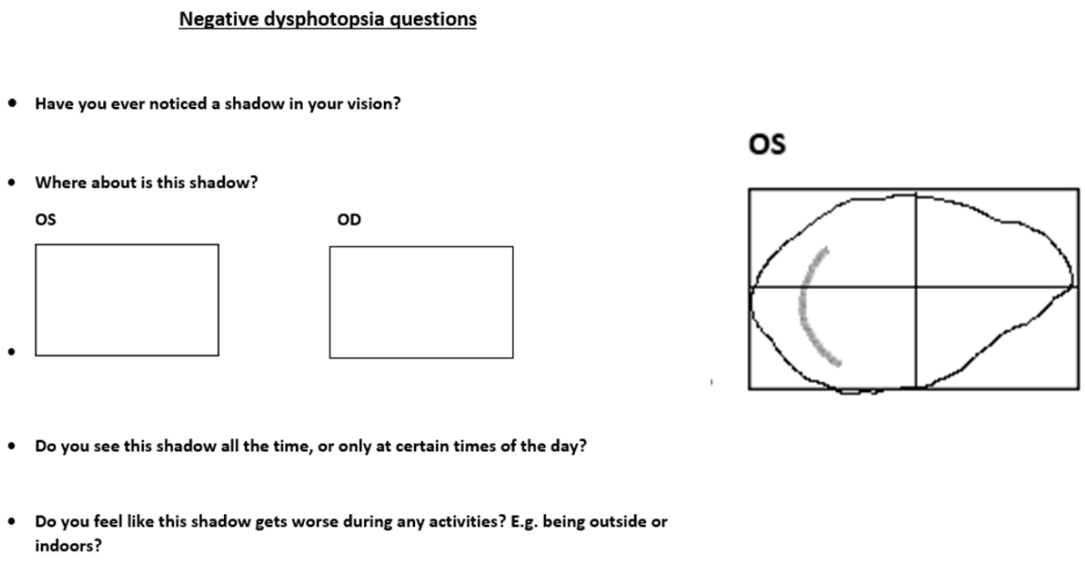

Figure 4.2: Negative dysphotopsia questionnaire. Left panel shows the questions asked to ask patient before undergoing a perimetry test. The right panel shows in detail an example of how a sketch was drawn of the negative dysphotopsia as described by the patient. This example showed an arc shape shadow in the temporal side of the left eye.

Then, automated kinetic perimetry was performed using an Octopus 900 perimeter controlled by the OPI, using a size III-4e stimulus (0.43° diameter, 1000 asb) which moved at 5°/s with a background luminance of 31.4 asb, see appendix 2 for R script. An extended fixation point was used to allow approximately 100° of the temporal field to be measured within the bowl of the Octopus 900, which is usually limited to 90°. During the test participants were asked to fixate on a red laser diode, which had a neutral density filter applied to it. The point of the laser diode extended fixation towards the nasal region. For a more detailed description of the set up please see chapter 2. To identify the outer boundary of the visual field and the possible inside edge location of a shadow if present, two methods of limits were used. The III-4e stimulus was first directed from a non-visible area to a visible area (conventional ascending method of limits (AML)) and then from a visible area to a

non-visible area (descending method of limits (DML)). Only three meridians were measured in the temporal visual field region: on the horizontal meridian at an angle of either 180° or 0° and another two angles subtending 30° superior and inferiorly (see right panel of Figure 4.3). These three meridians were measured six times using the ascending method and six times using the descending method, with the addition of 4 false positive trials in the ascending condition. False positives were used to ensure patients were not guessing or trigger happy. Before undergoing the test, participants were given a quick practice session to get familiar with kinetic perimetry. After kinetic perimetry was finished, patients' study eye was dilated using phenylephrine 2.5% and tropicamide 1.0%, and a period of 30 minutes or more was provided for the full effect of dilation to take place. After this period, the previously described tests were repeated.

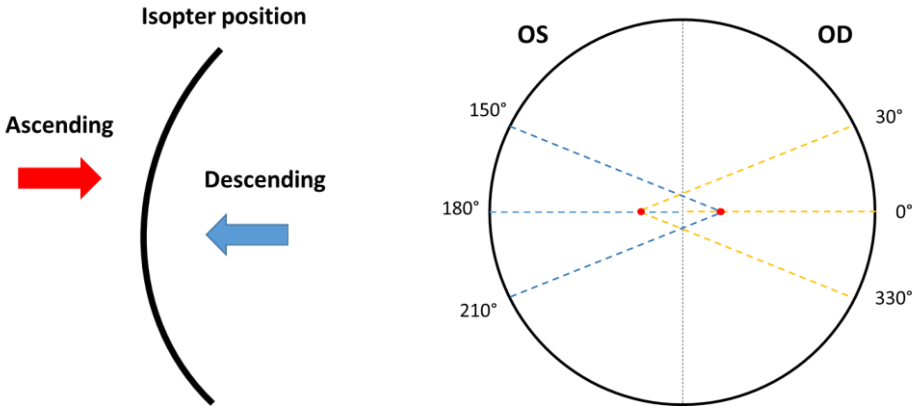

Figure 4.3: Stimulus position and directions. Left panel indicates direction of stimuli, with ascending (red) stimuli heading towards the fixation point and descending (blue) heading away from the fixation point. Right panel shows vectors measured for the left (blue) and right (orange) eye. Position of the fixation point for left and right eye indicated by red point.

4.2.4 Statistical analysis

The data was collected in Excel software (Microsoft Office 2010, Microsoft Corp.) and analysed using R core software (2016). Of the 6 responses per vector, the median was used to define the isopter position. The scatter of responses was defined by the median absolute deviation (MAD) to account for extreme values. These isopter positions were quantified globally using the mean isopter position (MIP) per method of limits and pupil size condition. Tests which resulted in three or more false positives were identified as unreliable and not used in the overall analysis. A Wilcoxon's signed rank test was used to compare if there was a significant difference between MIP of ascending and descending methods and pupil condition, and between MIP of ascending and normative isopter values defined by Vonthein et al. (2007).

4.3 Results

Patients' demographics of age, visual acuity and un-dilated and dilated pupil size can be found in Table 4.1.

Table 4.1: Patient parameters.

PARAMETER	CATARACT PATIENTS (MEAN, RANGE)
AGE (YEARS)	75 (61 to 83)
VISUAL ACUITY (LOGMAR)	0.1 (-0.14 to 0.44)
UN-DILATED PUPIL SIZE (MM)	4.7 (2.89 to 6.49)
DILATED PUPIL SIZE (MM)	7.1 (5.21 to 8.58)

4.3.1 Ascending and descending methods comparison

A comparison was made between AML and DML for un-dilated and dilated pupil size (Tables 4.2 & 4.3). The results for un-dilated pupil size showed that for all angles, the DML produced a slightly larger isopter position. A Wilcoxon's signed rank test found

a significant difference between overall mean isopter position (p = 0.0187, effect size 0.44), between the two methods.

Table 4.2: Mean MIP values, range and difference of ascending and descending methods for un-dilated pupil size and for the three angle conditions. SD stands for standard deviation.

NORMAL PUPIL	**ASCENDING**		**DESCENDING**		
ANGLE (°)	MIP (SD °)	Range	MIP (SD °)	Range	Difference
30	58 (±14)	30 – 95	62 (±9)	36 - 75	4
0	79 (±7)	70 – 102	80 (±14)	37 – 96	1
-30	78 (±7)	66 – 100	80 (±14)	37 - 95	2

The results for a dilated pupil size (Table 4.3) were similar to the normal pupil size with DML resulting again in slightly larger isopter positions at all angles. The Wilcoxon's signed rank test found a significant difference in overall isopter positions between DML and AML, (p < 0.001, effect size 0.64).

Table 4.3: Mean MIP values, range and difference of ascending and descending methods for a dilated pupil size for the three angle conditions. SD stands for standard deviation.

DILATED PUPIL	**ASCENDING**		**DESCENDING**		
ANGLE (°)	MIP (SD °)	Range	MIP (SD °)	Range	Difference
30	60 (±7)	47 - 72	63 (±10)	37 - 79	3
0	75 (±5)	58 - 84	79 (±12)	37 - 93	4
-30	76 (±5)	63 - 84	79 (±12)	36 - 95	3

There were no statistically significant differences between un-dilated and dilated pupil in AML or DML conditions, with the dilated pupil resulting in a decrease of 2° in the AML condition and 0.4° in the DML condition.

The response variability (Tables 4.4 and 4.5) between dilated and un-dilated pupil sizes was measured using the median absolute deviation (MAD) to account for outliers. It was found that although the DML produced a greater isopter position, it also incurred in a greater variability in responses in both pupil conditions. A Wilcoxon's signed rank test found this difference not significant in either the dilated or normal pupil condition.

Table 4.4: Response variability (MAD) per angle for AML and DML in the dilated pupil condition.

DILATED PUPIL	**MEDIAN ABSOLUTE DEVIATION (RANGE)**	
ANGLE (°)	Ascending (range °)	Descending (range °)
30	1.8 (0.2 – 6)	1.9 (0.1 – 10)
0	1.3 (0.2 – 11)	1.6 (0.4 – 10)
-30	1.2 (0.1 – 7)	1.4 (0.3 – 4.4)

Table 4.5: Response variability (MAD) per angle for AML and DML in the un-dilated pupil condition.

NORMAL PUPIL	**MEDIAN ABSOLUTE DEVIATION**	
ANGLE (°)	Ascending (range)	Descending (range)
30	1.7 (0.6 – 16)	1.7 (0 - 14)
0	1.2 (0.1 – 4)	1.7 (0.2 – 8)
-30	1.5 (0.1 – 5)	1.8 (0.3 – 5)

4.4 Normative versus post-cataract visual field limits

In accordance to Simpson (2017), the visual angle produced by the IOL after cataract surgery is smaller than that of the original lens. Using the mathematical model designed by Vonthein et al. (2007), which estimates visual field limits of healthy individuals based on age, stimulus size and stimulus speed, we compared the limits

of the temporal visual field at the three meridians used in our experiment between post-cataract surgery patients and this mathematical model which represents the results of healthy patients. It should be noted that Vonthein's model is based upon the results from a healthy population, none of which had undergone cataract surgery. Due to the conventional method of kinetic perimetry, we only compared the results using the AML with a normal pupil against the normative results. Our results in Table 4.6 show that our group of post-cataract surgery patients had on average a 10° smaller isopter position in the temporal region compared against the normative age matched model.

Table 4.6: Mean isopter position and difference per angle for cataract patients and aged matched healthy patients.

ANGLE (°)	ASCENDING MIP	NORMATIVE MIP	DIFFERENCE
30	58°	70°	12°
0	79°	85°	6°
-30	78°	89°	11°

4.4.1 Detection of negative dysphotopsia

The results from the questionnaire found that in this study's patient group, approximately 20% occasionally experienced a phenomenon similar to negative dysphotopsia. This was reported as a line or shadow noticed in the visual field early after surgery, however, it was only perceived when the patient was situated inside, normally against a light coloured wall. In the majority of these cases, the phenomenon disappeared after a few weeks, or the patient was not aware of it at the time of the study visit.

Two patients (A & B) with IOLs implanted in their left eyes, reported that they felt like they could see the edge of the lens at all times. Both were aware of the

phenomenon at the time of the appointment. When they placed their chin on the chin rest in the perimeter, they both were still aware of the line in the side of the temporal visual field, while under illumination from the perimetry bowl. In both these cases, under the un-dilated pupil size condition, the DML produced a smaller isopter at two angles (Figure 4.4). In patient B, the upper lid reduced the superior visual field substantially. The results suggested that there was a visual phenomenon at a MIP of 71° in patient A and 50° in patient B, which disrupted the kinetic stimulus.

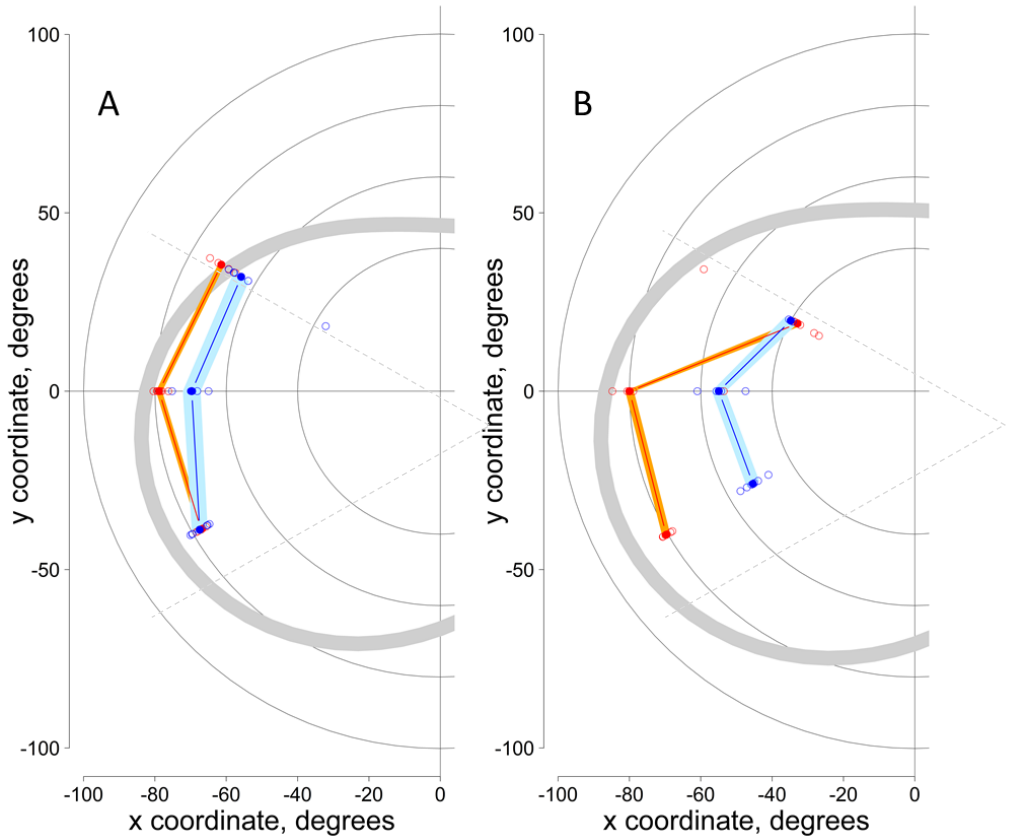

Figure 4.4: Diagrams of kinetic perimetry isopters using DML (blue) and AML (red) in the un-dilated pupil condition for patients A (left panel) and B (right panel). Points in plot are adjusted to account for extended fixation. The light blue and orange bands around isopters represent the 90% interval of response variability. Light gray isopter represents the age match normative expected values. In panel B, the superior angle (30°) was greatly affected by the upper eyelid.

Under dilated pupil conditions (Figure 4.5), both patients were no longer aware of the line in their vision. However, for patient A the gap between the DML and AML isopters increased, with the MIP of the phenomenon now appearing at approximately 62°, whereas for patient B the isopters overlapped in most positions suggesting the phenomenon no longer had an effect on the isopter position using DML.

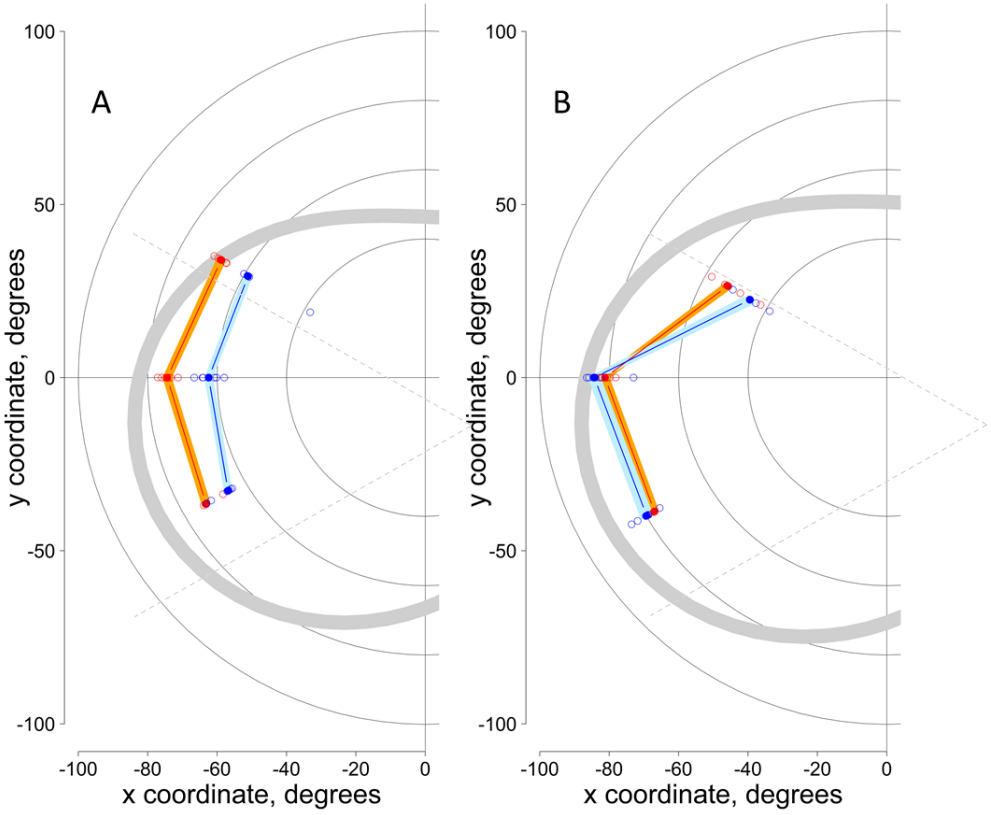

Figure 4.5: Diagrams of kinetic perimetry isopters of DML (blue) and AML (red) in the dilated pupil condition for patients A (left panel) and B (right panel). In the left panel, there is still a gap between isopters suggesting an affect by a visual phenomenon whereas in panel B the gap has disappeared suggesting that the visual phenomenon is no longer present.

4.5 Discussion

Negative dysphotopsia remains a meaningful concern for patients and surgeons. Although the incidence level of this phenomena is low, some individuals who are left with a permanent shadow in their vision find it bothersome, and results in a secondary surgery such as implantation of a piggyback IOL to try to eliminate it.

The results of this study found that the visual field in the temporal region is reduced by approximately 10° compared against an age match population (Vonthein, Rauscher et al. 2007). This finding supports that of Simpson (2017), which suggested that light passing through a small IOL cannot produce images at large angles. Our findings also closely support the results of Makhotkina et al. (2016) who used manual Goldmann perimetry to measure the extent of the visual field before and after cataract surgery. They found a decrease of the temporal visual region between 1 and 5°. In this study, we found twice as much. This doubling in difference could be due to the use of an extended fixation allowing larger visual fields to be measured. Makhotkina et al. (2016) also found an increase of the nasal visual field region, thus future studies using our automated technique to assess the extent of the nasal visual field could provide additional information. Additionally, a larger sample is required to increase the reliability of results and to study the clinical relevance of our findings of this visual field difference.

In this study, we found no effect of pupil size on the extent of the temporal visual field. Only this part of the visual field was measured due to previous research (Makhotkina, Berendschot et al. 2016) indicating this area for appearance of negative dysphotopsia. The DML technique produced slightly larger isopters in both pupil conditions compared to the traditional AML technique. This is consistent with

our findings in Chapter 3. Additionally, the results showed that the response variability in DML was larger than in AML, which supports the uncertainty model (Pelli 1985) in an older population.

Within this study, the aim of using DML was to detect an estimated inside edge location of the shadow caused by negative dysphotopsia that can occur after cataract surgery. In this study population, we identified two patients who reported observing a shadow or "the edge of the lens" at all times. Approximately 20% of patients reported observing this type of phenomena straight after cataract surgery, however the perception of the shadow reduced significantly by the time of the study visit, where it was only observed on occasion; e.g. when walking into a room, or it was not perceived anymore. These percentages are similar to the findings of (Osher 2008).

Both patients who observed the shadow permanently, perceived it in the left eye. This is in agreement with (Osher 2008), who also found negative dysphotopsia occurring more frequently in left eyes, possibly due to temporal incisions. However, this study did not attempt to identify incision positions. Our kinetic perimetry test was able to pick up an estimated location of the shadow in both patients. Patient B perceived a shadow and had had both eyes operated on before their initial study visit. On the other hand, patient A had only one eye operated on at the time of the first visit.

For patient B, the shadow was no longer perceived or detected using the kinetic perimetry method when their pupil was dilated. This would suggest that a possible cause for the negative dysphotopsia in this patient was the pupil size. However, in this patient the undilated pupil was 4.58 mm, which does not abide by Holladay &

Simpson's (2017) Zemax simulations that negative dysphotopsia would occur with a small pupil size of 2.5mm. Another explanation of the persistent occurrence of negative dysphotopsia in patient B could be due to the morphology of the capsular bag in which the IOL was placed in. In Figure 4.6, it is observed what looks like part of the anterior capsular bag across the front surface of the IOL. This could possibly be due to shrinkage of the bag after implantation, resulting in a partial covering of the IOL. Another explanation is that the capsule was too small and the implantation of the new IOL caused a tear in accordance with previous research, such as the works from (Masket and Fram 2011) and (Folden 2013), who found that surgical correction of the capsule results in resolution of negative dysphotopsia.

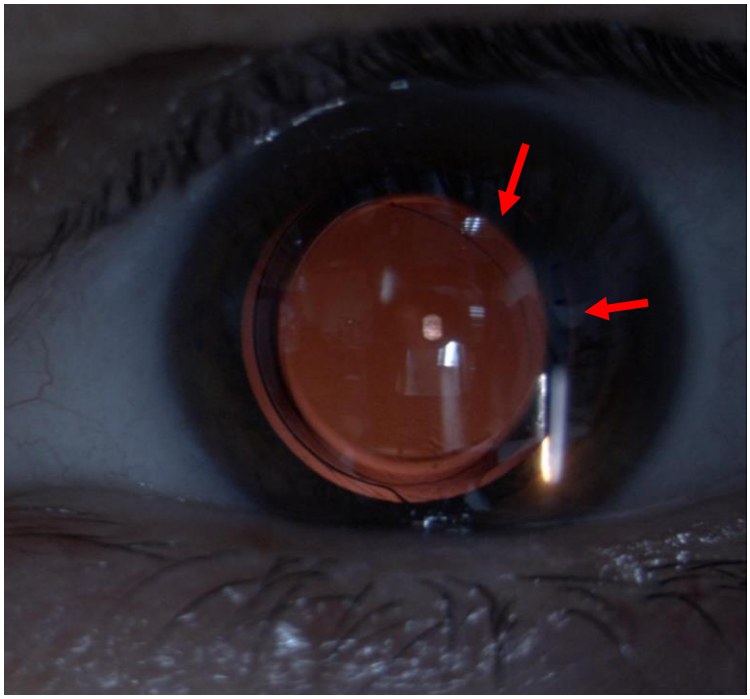

Figure 4.6: Image of dilated left eye of Patient B who perceives a shadow in the temporal visual field. From the image we can see part of the anterior capsule bag covering part of the IOL indicated by red arrow.

By using the extended fixation technique, we were able to measure the full extent of the temporal visual field which is known to extend beyond 90° (Ronne 1915,

Traquair and Scott 1957, Niederhauser and Mojon 2002). This is an improvement with regards to the study from Makhotkina et al. (2016), who were limited in their estimations of the temporal region, due to the limitations of the manual Goldmann perimetry device, not allowing them to measure beyond 90° in some patients. In our study, we identified two patients who had overall isopter positions located up to 102°. In the patients with constant negative dysphotopsia, we were able to identify intact peripheral visual field beyond the estimated position of the shadow. This suggests that the visual phenomena did not extend out to the visual field edge "like wearing horse blinkers" as some studies have reported (Davison 2000, Masket and Fram 2011). However, it supports the results from one patient in the study of Makhotkina et al. (2016) who detected a size V-4e stimulus on the outer side of the temporal shadow.

Our study has several limitations. Firstly, the sample size and incidence of patients with negative dysphotopsia was small. To further support the reliability of our automated kinetic perimetry technique in estimating the position of the shadow in negative dysphotopsia, a follow up study would need to undertake the procedure in more patients with negative dysphotopsia. This could be achieved by seeing patients soon after surgery where the incidence of the phenomena was reported as high as 20%.

Kinetic perimetry is not a routine test undertaken in clinical settings, thus patients are unfamiliar with it. Additional training sessions could allow for more reliable results, less variability, and less drop out of patients due to poor test results.

In this study, we only observed patients after cataract surgery and used Vonthein's et al. (2007) mathematical model to compare age-matched visual field positions. In

future research the extent of patients' visual field should be measured before and after surgery to have a more reliable prediction of the reduction of visual field extent caused by the IOL.

The addition of more meridians could allow for obtaining the position of the shadow with a higher precision. However, with this increase of positions the test duration would increase, resulting in possible fatigue, and thus a drop in patient attention. Then, to prevent a long duration of the test, a reduction in the number of presentations would need to be implemented.

In conclusion, in this study we provided strong evidence that in cataract surgery the temporal visual field is reduced, due to the smaller IOL size. We also showed that by using an extended fixation technique, we were able to measure functional visual field beyond 90°, with both ascending and descending techniques. Additionally, we could estimate the position of the shadow in patients with negative dysphotopsia. These findings support the use of kinetic perimetry in future observations of negative dysphotopsia, providing more precise estimates in regards to the position and shape of the shadow.

5 Chapter 5: Simulating response behaviours to kinetic perimetry: an adaptive algorithm

5.1 Introduction

The objective of kinetic perimetry is to produce an accurate and precise isopter of the visual field by using the minimum amount of presentations, and within a reasonable testing time. In a clinical environment short test durations are essential. An ideal approach would be to produce a strategy which is robust to varying degrees of patient response errors. Several approaches have been applied to perimetry in recent years in order to obtain a balance between test time and accuracy, but most of this work has been done with static rather than kinetic automated perimetry (Bengtsson, Olsson et al. 1997, Zeman, McKendrick et al. 2017, Heijl, Patella et al. 2019).

Current automated kinetic perimetry is based upon the earlier manual Goldmann kinetic perimetry, where an examiner would manually move a stimulus of set intensity and size, from an area of non-seeing to seeing, marking the verbal response of the patient on a record sheet. This technique is flexible, but it is hard to standardise, and therefore differs between examiners. In recent years a new software technique was developed as a computerised automated version of Goldmann perimetry, called semi-automated kinetic perimetry (SKP) (Schiefer, Schiller et al. 2001) to reduce the need for highly trained examiners, and the test could be performed more accurately. This semi-automated kinetic test procedure was first available on the Octopus 101 device (Haag Streit AG, Koeniz, Switzerland) and is also available on the Octopus 900 (Haag Streit AG, Koeniz, Switzerland). These devices offer built-in tests in their software, but also allow for customised programs.

Due to the marked reduction of result variability (Nowomiejska, Vonthein et al. 2005) by the automated versions of kinetic perimetry, there is strong support for the replacement of manual procedures, both in clinical and research environments. Although automated perimetry has been widely used in research, and there have been developments to estimate the normative isopter outputs dependant on age and stimulus size/intensity (Vonthein, Rauscher et al. 2007), the variability of kinetic perimetry is still relatively high (Schiefer, Strasburger et al. 2001, Hirasawa and Shoji 2014). It is also prone to patient error, e.g. outlier responses from the norm. There has been little research on the minimum number of presentations needed in order to produce an accurate and precise isopter to represent a patients' visual field.

Computer simulations have been extensively used to quantify threshold estimations of procedures in static automated perimetry, to estimate accuracy or compare the efficiency of different test procedures (Turpin, McKendrick et al. 2003). Many of these simulations were based upon the model of the relation of response variability and contrast sensitivity (Turpin, McKendrick et al. 2003). With kinetic perimetry, the literature on simulations is less well developed. One example is by Shapiro et al. (1988), who developed the computer simulation procedure KRAKEN for both kinetic and static perimetry. They based their simulation model of kinetic perimetry from manual Goldmann examinations, where isopter locations were converted to contrast sensitivity values based on size and intensity of the Goldmann stimulus.

The work presented here is based upon the previous work conducted by Mönter et al. (2017), who examined the precision of isopters from repeated kinetic stimulus presentations. They found that a single isopter can provide a global estimate of the

peripheral visual field, with precision similar to that of the mean deviation (MD) in static perimetry in the central visual field. Their procedure used 3 presentations along 16 meridians (3 training stimuli, 48 kinetic stimuli and 6 false-positive catch trials), and the entire test took approximately 11 minutes (Mönter, Crabb et al. 2017). However they did not establish what was the best method to quantify the isopter position. In their study they used the median, which is suggested as a robust method against a non-normal distribution. However, could there be a better, more robust method specifically for kinetic perimetry, which could provide a more accurate result of the true isopter threshold location.

We aimed to establish an optimal kinetic strategy to estimate accurate and precise isopter locations with a minimum number of presentations through simulations with differing patient performance characteristics. This will form an adaptive algorithm which adjusts the procedure dependent on the input received. This procedure will then be used to simulate a fast and accurate kinetic perimetry test, whilst being robust against patients' errors, e.g. distribution of outlier responses. By simulations, we will investigate how closely this adaptive procedure will replicate patterns of vision loss from manual Goldmann perimetry plots, obtained within a clinical setting.

5.2 Methods

The kinetic response data which was used for these simulations is the same data obtained in Chapter 3. The methodology for obtaining this data is described in detail in the Methods section of that Chapter. All simulations in this chapter were undertaken using R core software (2016), and used the response data obtained in chapter 3.

The response variability between the participants from this dataset varies between 0.5° and 1.2° MAD with a median of 0.8°. To account for the differences, and in order to pool the data together, the data was normalised dependent on the participants MAD. Figure 5.1 shows the distribution of responses from the isopter position before and after normalisation for each participant, along with the participants responses pooled together in a histogram and fitted with a Gaussian kernel.

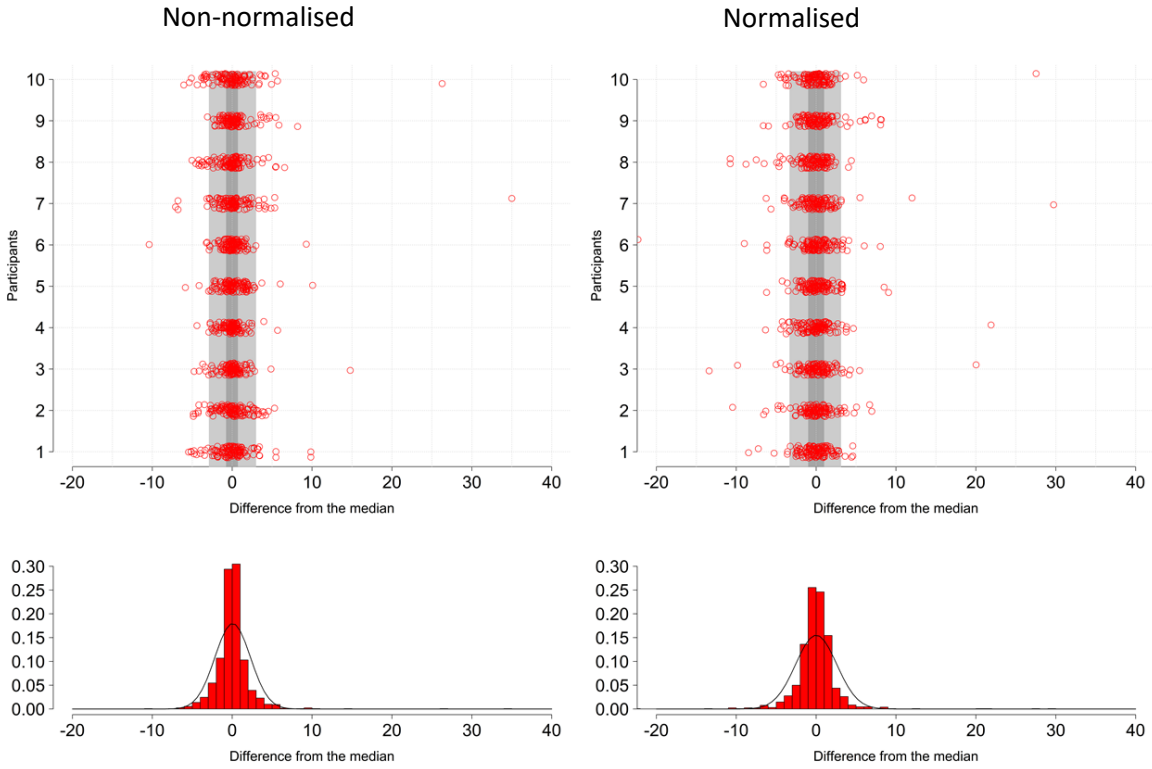

Figure 5.1: Scatter of responses around the isopter position for each participant. Numbers on y axis to identify participants match those from far-periphery study. Left: Scatter of responses around the isopter position for each participant. Light grey bar indicates 90% interval and dark grey indicates 50% interval. Histogram underneath shows the overall scatter of responses fitted with a Gaussian kernel. Right: Normalised scatter of responses around the isopter position for each participant. Histogram fitted with a Gaussian kernel.

After normalising the data by each participant, the data was then pooled together to show the overall distribution pattern of responses which was used for all the simulations.

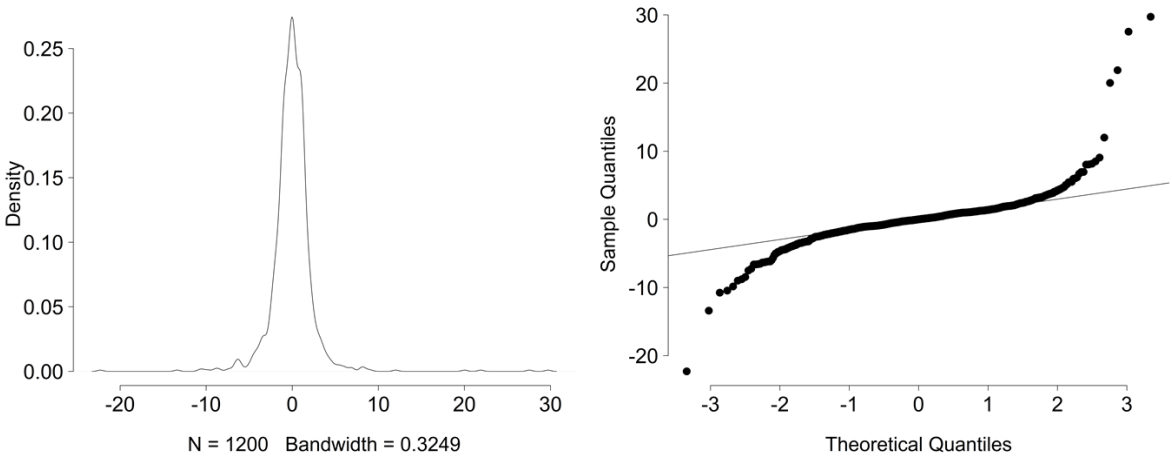

Figure 5.2: Normalised scatter of responses from the isopter position. Left: Distribution of responses from the isopter position. Negative values on the x-axis indicate responses occurring within the estimated isopter and positive values indicate responses outside of the estimated isopter. The distribution is non-normal and has long tails and indicates that a vast majority of responses are closely spaced to isopter locations while occasional responses occur at larger distances from the isopter. Right: The q-q plot compares the distribution of the responses, around the isopter, to a normal distribution. Points deviating off the line indicate that some responses occur at large distances, both inside and outside the isopter.

As seen in figure 5.2 the normalised data does not fit a normal distribution, with long tails deviating outside of 10° and -10° from the isopter position. To describe the normalised distribution we used a mixture of Gaussian distributions to provide a best fit in which the simulations would be based from, see appendix A3 for R script. These tails suggest that occasionally responses occur further outside the isopter position more often that within the isopter. During a kinetic perimetry test the participant is instructed to respond when a target is detectable in their peripheral vision, after the participant responds the target disappears, this response is suggested as their threshold point of detection. From this distribution it could be suggested that further presentations would be expected to fall on or before this

point, but not after unless participants have a dip in attention resulting in a response after the threshold. The next set of simulations use this distribution of kinetic response behaviour.

5.3 Simulation 1: estimating the isopter position

How we estimate an isopter position from a small number of responses is essential for test precision. Conventionally the median is used to estimate the isopter position, as it is robust against extreme values (outliers). However, in kinetic perimetry we cannot assume that a response was a “bad response” contrarily to static perimetry, where we can determine false positives/false negatives. Then, is there another alternative method which could be used to define the estimated isopter position with as much or even better precision? We used the distribution of kinetic response behaviour to conduct simulations with to estimate the best method to quantify the isopter position with increasing number of responses. These simulations of 10,000 iterations compared methods such as the mean and trimmed mean (outer points removed), to the currently used median.

Figure 5.3 shows the results from these simulations. There is little difference in the precision of the estimated isopter position when comparing the trimmed mean to the median up to 5 presentations. When dealing with a small number of responses it is very hard to find a method which is completely robust (Huber 1972). The trimmed mean is very similar to the median due to the fact that a trimmed mean, where the outer two responses are removed, of 3 and 4 presentations equals that of the median of 3 and 4 presentations. The trimmed mean only differs from the median when there are 5 or more presentations. The trimmed mean is most beneficial with 5 presentations or more, however in terms of precision it is overtaken by the

Hodges-Lehmann method at 7 or more presentations. The results from this simulation suggest that either of the methods (median, trimmed mean or Hodges-Lehmann) are suitable for estimating the isopter position. For this adaptive procedure the median is most favourable in terms of precision, as using a trimmed mean or Hodges-Lehmann is only beneficial over the median for 5 responses or more which is unlikely to occur very often within a kinetic test due to time limitations.

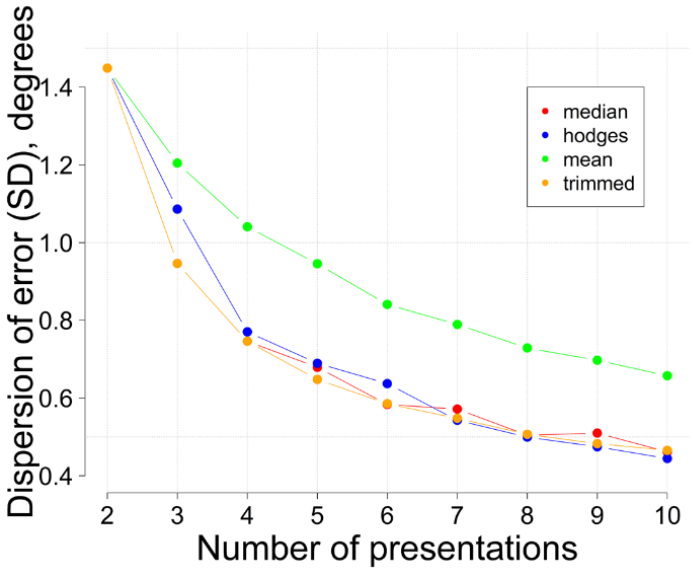

Figure 5.3: Precision of estimating isopter position with the median, mean, Hodges-Lehmann and trimmed mean for 2 to 10 presentations. Increase of precision (decrease in standard deviation) is expected with an increase of presentations. The median and trimmed mean performance is almost identical up to 5 presentations.

5.4 Simulation 2: precision and accuracy of kinetic perimetry

In order to define the number of kinetic presentations which will provide the greatest accuracy and precision, we simulated the scatter of responses around a "true" isopter position with increasing number of presentations. This simulation used the distribution of responses and median response variability of participants from Figure 5.4. The number of presentations per meridian increased from (2 to 5 in steps of 1) and 10,000 iterations were simulated for each presentation condition.

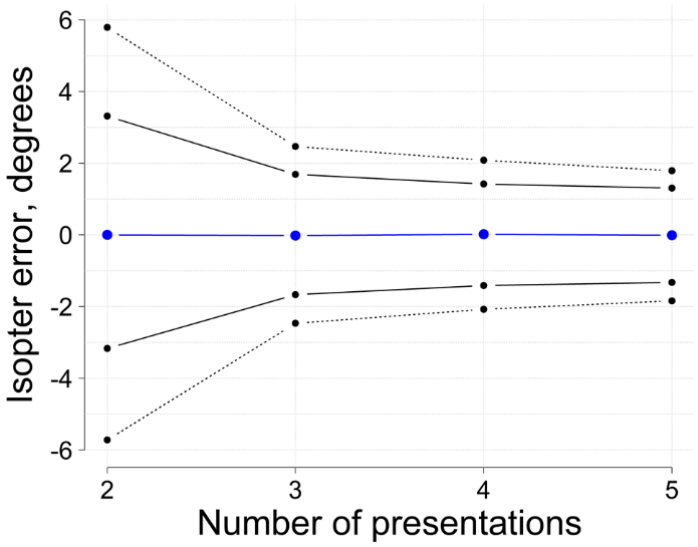

Figure 5.4: Precision of isopter location with increasing number of presentations per meridian. Dispersion of the estimated isopter location from the true isopter location (error). Increasing the number of presentations per meridian decreases the dispersion of error. Negative values indicate estimated isopter locations within the true isopter location. Blue points represent the 50% percentile of error. Black lines indicate the 95th percentile of error from the estimated to the true isopter location, and the dotted black line indicates the 99th percentile.

The median absolute error between the estimated and the "true" isopter location was 0.6° with 2 presentations per meridian, 0.55° with 3 presentations, and 0.5° with 4. The 95% and 99% intervals in Figure 5.4 suggest that there is a relatively large increase in isopter precision by increasing the number of presentations per meridian from 2 to 3 (approximately 50%), however the gain in precision with more than 3 presentations is small. These results suggest that the largest gain of precision is achieved by presenting a third stimulus.

The response variability of the participants in this distribution was relatively small (MAD = 0.8), due to individuals having healthy vision, and a mean age of 27 years. Individuals who have substantial vision loss, and are of an older age, will most likely have larger response variabilities. With an individual of high response variability, the

use of two or three presentations may not be enough to produce an isopter which is precise. However, increasing the number of presentations increases the test duration, possibly making it unsuitable for a clinical environment. Thus additional simulations using the exact same criteria as the last simulation, however with a two larger response variabilities. As seen in Figures 5.5 and 5.6, with increasing response variability the error of responses around the "true" isopter increases, this results in the requirement of more than 3 presentations in some instances. The results from these simulations suggest that two presentations per meridian is not always enough to produce an isopter which is precise, especially in circumstances where an observer is highly variable in their responses. However by increasing presentations, this increases the test time, thus a strategy is required to determine when more presentations are required, which balances the line between precision and duration for a test.

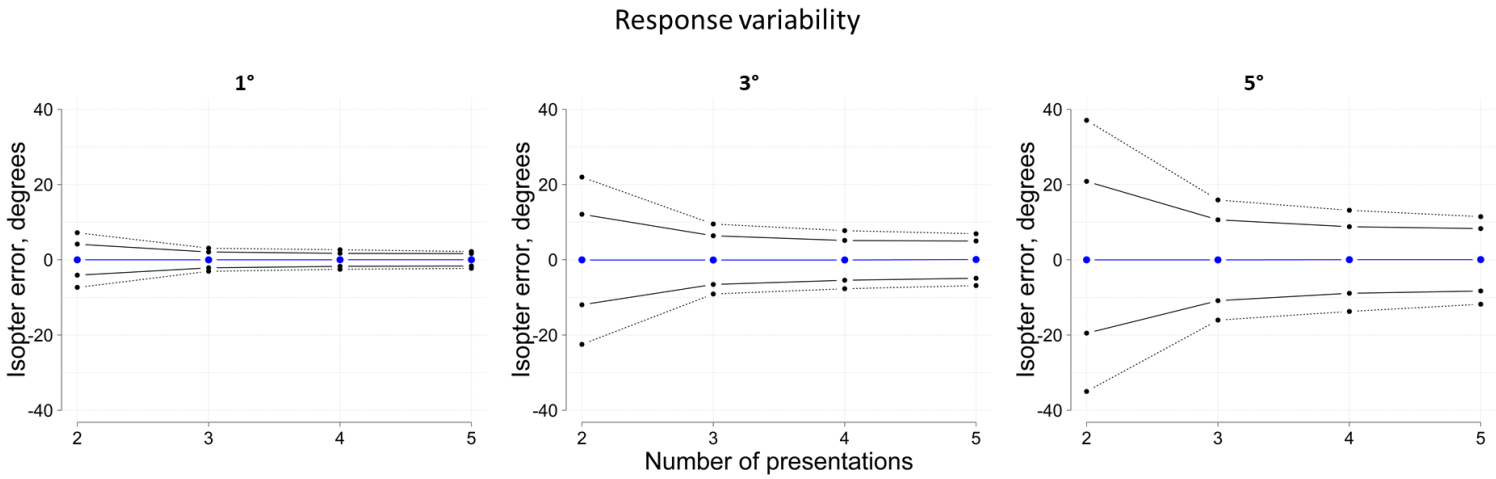

Figure 5.5: Dispersion of the estimated isopter location from the true isopter location (error). Increasing the number of presentations per meridian decreases the dispersion of error. Plots increase by response variability (MAD = 1°, 3° and 5°) from left to right. With increasing response variability the precision around the true isopter decreases. Negative values indicate estimated isopter locations within the true isopter location. Blue points represent the 50% percentile of error. Black lines indicate the 95th percentile of error from the estimated to the true isopter location, and the dotted black line indicates the 99th percentile.

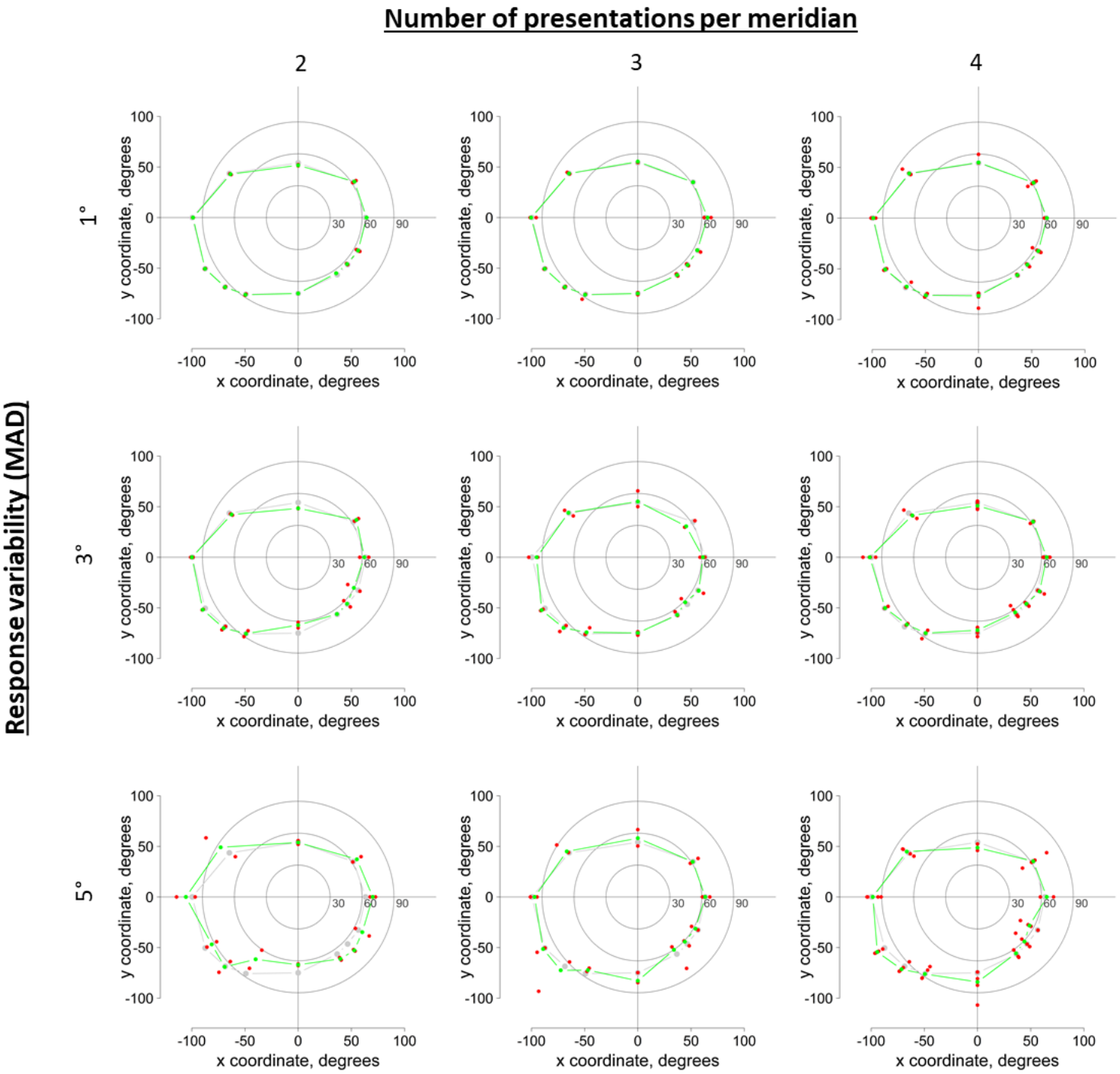

Figure 5.6: Examples of simulated isopters with increasing numbers of presentations and response variability. The true isopter is shown in grey, the estimated isopter in green, and the individual responses around the isopter position in red. The first row shows simulated isopters of increasing number of responses of a participant with a low response variability of MAD = 1°. Second row, simulated participant with a response variability of MAD = 3°. Third row shows participant with a high responses variability MAD = 5°.

5.5 Simulation 3: strategy for additional presentations

We know that the minimum number of presentations needed per meridian is two in order to determine an isopter position based on an average. Thus if an isopter was compiled of 12 meridians this would mean a minimum of 24 presentations to define an isopter. We can also determine from the previous simulations that little precision is gained after 4/5 presentations for all levels of response variability, thus a maximum of 5 presentations would account for more highly variable observers. The next step is to design a strategy to establish a procedure for additional presentations within this minimum and maximum presentation limits.

5.5.1 Strategy 1

A strategy which could be applied to kinetic perimetry is to base the number of presentations required to define an isopter position on the distance between responses. If the distance between the first two responses is greater than a certain number of degrees (the criterion), then a third presentation would be required. When there are two responses there is one distance between them; however, with three responses there are two distances among them to measure. We have suggested that if the minimum of the two distances between responses is less than the criterion, then no additional presentations are required for that meridian, as seen in Figure 5.7. Circumstances where a fourth presentation is required can be seen in Figure 5.8.

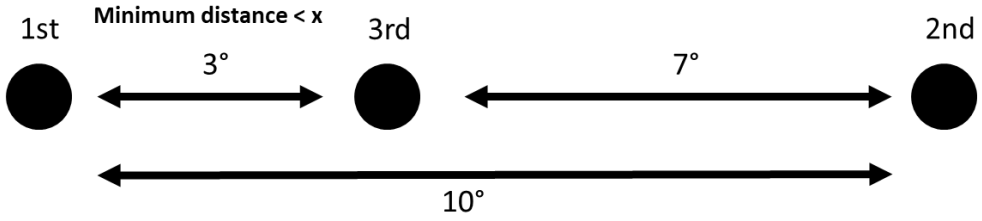

Figure 5.7: Example of third presentation and whether a fourth is required. The first and second responses have a large distance between them which is greater than x = 4°. Thus, a third presentation is required and is responded to between the two original responses. The distances between responses is now 3° and 7°, since the minimum distance is less than x a fourth presentation is not required.

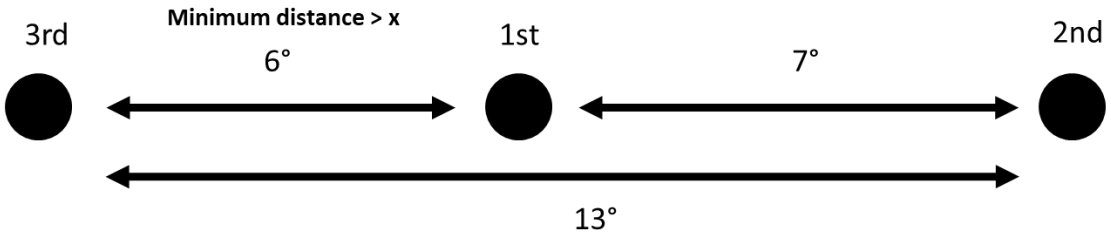

Figure 5.8: Example of third presentation and whether a fourth is required. The first and second responses have a large distance between them which is greater than x = 4°. A third presentation is required and is responded to outside the first two responses. The difference between the responses is now 6° and 7°, which is still greater than x, thus a fourth response is required.

Simulations were conducted in order to determine the value of x, as to determine whether a third presentation is required. Simulations of this procedure used the distribution of responses in Figure 5.2 with increasing response variability per 10,000 iterations.

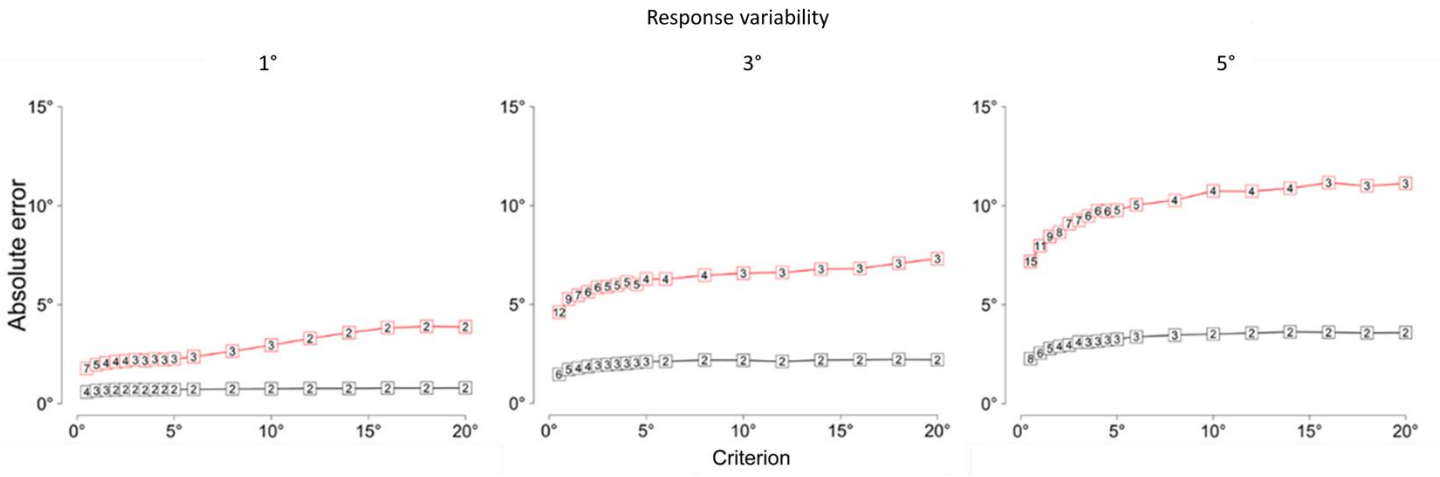

Figure 5.9: Simulations of the absolute error from the true isopter with increasing levels of criterion value (distance between responses) for additional presentations. Local regression lines show absolute median error (grey) and 95th percentile (orange). Numbers on local regression lines indicate the mean number of presentations required over 12,000 iterations for the median and 95th percentile. As the criterion for an additional presentation increases the absolute median error increases slightly. As expected, with increased response variability the precision around the true visual field is decreased.

As previously stated, the strategy of the adaptive algorithm would require a minimum of 2 presentations per meridian, and a maximum of 5. From Figure 5.9 we can predict that by using a criterion value of 5° for individuals with a high response variability, 50% of the time the procedure would only require 3 presentations, with an upper limit of 5 presentations at the 95th percentile. For individuals with lower response variability the number of presentations required would be less. The median absolute error also remains approximately constant with criterion values greater than 5° at the 50% percentile, thus little accuracy is achieved by using a larger criterion. By using a criterion value smaller than 5° there is a small gain in accuracy, however this is at the cost of a greater number of presentations required 50% of the time, which would incur a longer test duration. See appendix A3.1 for R script of strategy 1 simulation.

5.5.1.1 Performance of strategy 1

By using a criterion value of 5° and the upper and lower limits (2 and 5) of possible presentations, the performance of this procedure can be examined. For these simulations a manual Goldmann perimetry output was digitized to x and y coordinates for 12 locations in integers of 30°, and used as a model of the "true" visual field. The difference between this isopter and a simulated isopter of 10,000 iterations was defined as the error. The mean isopter radius (MIR) was quantified for each simulation, in addition to the error per individual isopter location. The results found that the absolute mean error of the MIR from the true visual field was 0.8° for a response variability of 3°. For individual isopter locations this absolute mean error was 2.5° with a standard deviation of 3°. Full results for other levels of response variability can be seen in Table 5.1.

Table 5.1: Accuracy and precision of simulated isopters using strategy 1, against the true visual field.

	MEAN ISOPTER RADIUS (MIR) ERROR		**ISOPTER POSITION ABSOLUTE ERROR**	
RESPONSE VARIABILITY	**Mean**	**SD**	**Mean**	**SD**
1°	0.3°	0.4°	0.9°	1.2°
3°	0.8°	0.9°	2.5°	3.3°
5°	1.2°	1.5°	4°	5.2°

5.5.2 Strategy 2

An alternative strategy which was undertaken follows the same process as strategy 1; however, rather than defining the median of all responses as the isopter position, this strategy used the median of the two responses that met the criterion value.

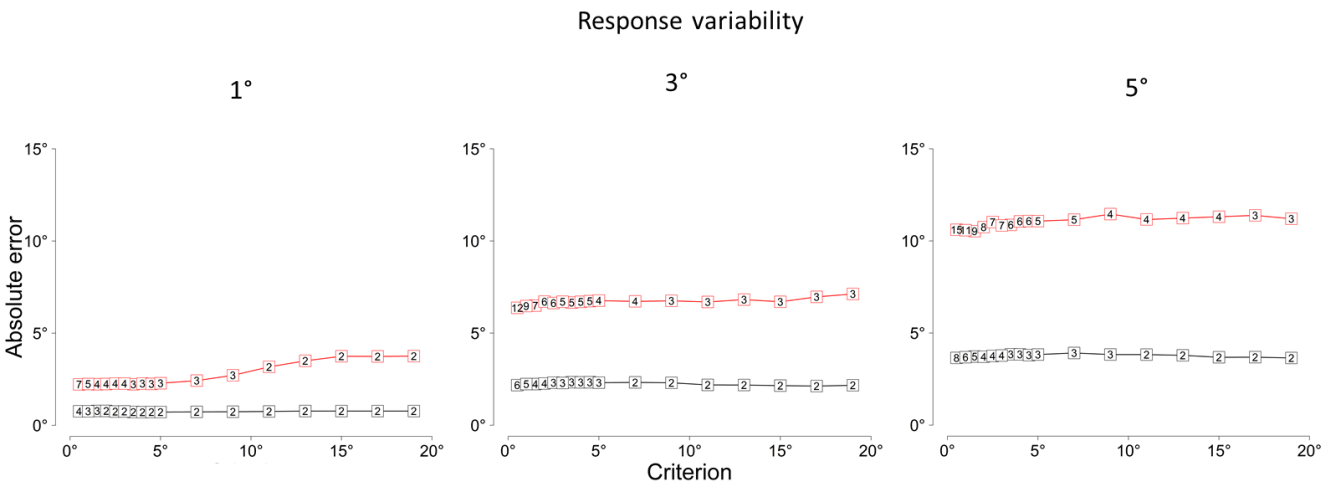

Figure 5.10: Simulations of the absolute error from the true isopter with increasing levels of criterion value (distance between responses) for additional presentations, median of two responses which meet criterion used to define isopter. Local regression lines show absolute median error (grey) and 95th percentile (orange). Numbers on local regression lines indicate the mean number of presentations required over 12,000 iterations for the median and 95th percentile. As the criterion for an additional presentation increases the absolute median error only increases slightly for low response variability. As expected, with increased response variability the precision around the true visual field is decreased.

From the results in Figure 5.10 we can predict again that by using a criterion value of 5° we can define an isopter position using 3 responses at the 50th percentile, and 5 responses at the 95th percentile for highly variable participants, with these numbers reducing for participants with lower response variability. This replicates the results of strategy 1, however when using the median of the two closest responses to define the isopter position, there is no gain in accuracy even when a large number of responses are used. See appendix A3.2 for R script of simulation for strategy 2.

5.5.2.1 Performance of strategy 2

By using a criterion value of 5° and the upper and lower limits (2 and 5) of possible presentations, the performance of this procedure can be examined. The same procedure that was used in strategy 1 was used for this one. The results found that

the absolute mean error of the MIR from the true visual field was 0.8° for a response variability of 3°. For individual isopter locations this absolute mean error was 2.8° with a standard deviation of 3.6°. Full results for other levels of response variability can be seen in Table 5.2.

Table 5.2: Accuracy and precision of simulated isopters using strategy 2, against the true visual field.

	MEAN ISOPTER RADIUS (MIR) ERROR		ISOPTER POSITION ABSOLUTE ERROR	
RESPONSE VARIABILITY	**Mean**	**SD**	**Mean**	**SD**
1°	0.3°	0.4°	0.9°	1.2°
3°	0.8°	1°	2.8°	3.6°
5°	1.3°	1.7°	4.6°	6°

5.5.3 Strategy 3

In the previous two strategies we used one criterion value to cover all levels of participant response variability. However, as we know that a minimum of two responses are required on all meridians measured, it is possible to define an individual participant criterion value based on these first responses. If we were to measure an isopter consisting of 12 meridians then it would first require 24 responses. From these 24 responses there is 12 measured distances between responses. By using the median of these distances we can define an individual criterion value where 50% of the meridians would require a third presentation. However we already know that this will not produce a good strategy test duration. If we define a criterion value by using the median plus the median absolute deviation of the distances between responses, then approximately only 25% of the meridians would require additional responses. For an illustrative example, see Figure 5.11.

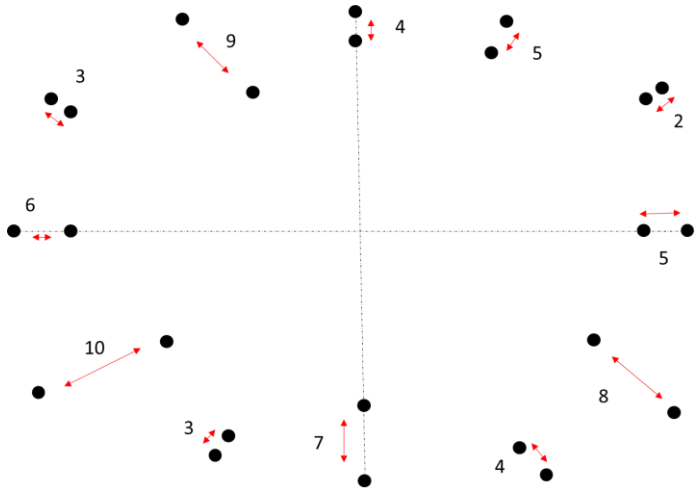

Distances = 3, 6, 10, 3, 7, 4, 8, 5, 2, 5, 4, 9

Criterion = median + mad = 7°

Figure 5.11: Diagram of strategy 3. 12 meridians consisting of 24 responses, creating 12 distances between responses. The median and median absolute deviation (MAD) is used to define a criterion value for additional responses. In this example the median is 5° with a MAD of 2°, thus the criterion for this individual participant would be 7°, thus 3 out of the 12 meridians would require additional presentations until either a max of 5 presentations are used or the distance between two of responses is less than or equal to 7°.

Due to the nature of this strategy the criterion value within the simulations cannot be predicted exactly like in strategies 1 and 2. See appendix A3.3 for R script simulation of strategy 3.

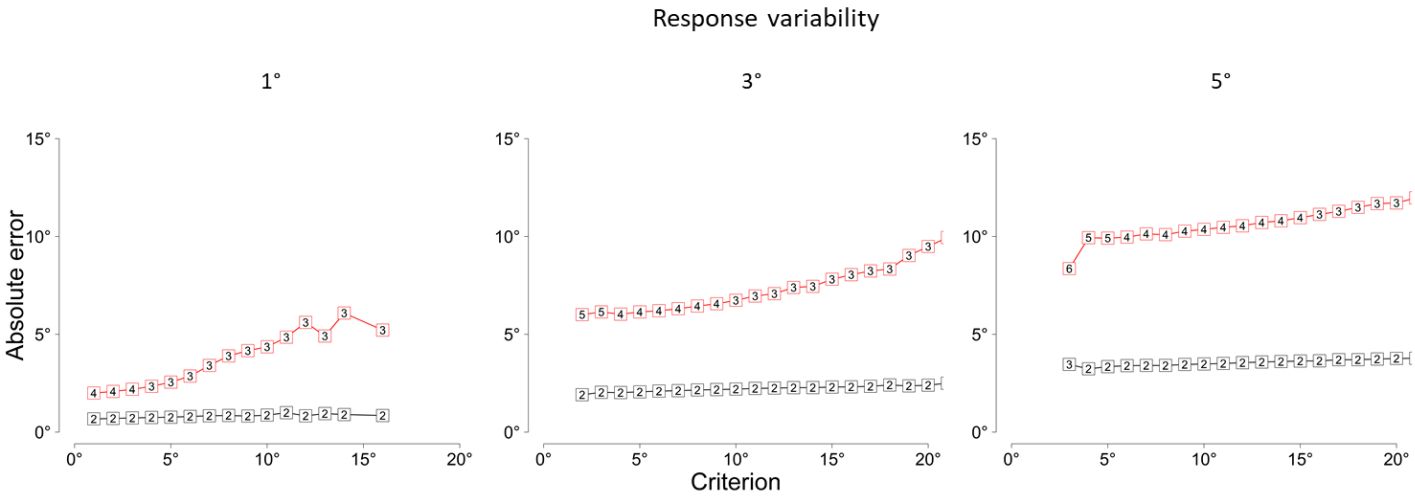

Figure 5.12: Simulations of the absolute error from the true isopter with increasing levels of criterion value (distance between responses) for additional presentations, median plus MAD of first 24 responses used to define criterion, median of all responses used to define isopter. Local regression lines show absolute median error (grey) and 95th percentile (orange). Numbers on local regression lines indicate the mean number of presentations required over 12,000 iterations for the median and 95th percentile. As the criterion for an additional presentation increases the absolute median error increases slightly for moderate and high response variability, with a more steep increase for low response variability. As expected, with increased response variability the precision around the true visual field is decreased.

From the results in Figure 12 we can predict that by using an adaptive criterion per individual we can define an isopter position using 2 responses 50% of the time, and approximately 5 responses 95% of the time for a highly variable participant, with these numbers reducing with participants of lower response variability. This replicates the results of strategies 1 and 2, however when using this strategy we cannot predict the criterion value before the test, thus there is the possibility of the procedure using a high criterion value, resulting in less precision in comparison to the other strategies.

5.5.3.1 Performance of strategy 3

As the procedure of this strategy is adaptive per individual, we cannot directly compare the performance of using a specific criterion value like in the other two strategies. However, it can be suggested from the results in Figure 5.12 that the performance of strategy 3 would be similar to that of strategy 1 with a criterion value of 5. Although the decrease of precision is more evident when increasing the criterion value compare to the other two strategies.

5.5.4 Overall strategy preference

From the results of the three strategies there is very little difference between the performances. There is a slight decrease in precision and accuracy in strategy 2 compare to strategy 1, thus suggesting the first would be more favourable. The performance of strategy 3 is difficult to compare to the others, however, due to the decrease of precision with larger criterion values compared to strategy 1, it could be suggested that for the purpose of this study, strategy 1 performs the best for all levels or response variability by using a criterion value of 5°.

5.5.5 Simulation 4: time performance of adaptive algorithm

By using strategy 1 as our adaptive algorithm we can estimate the time performance of a kinetic perimetry test consisting of 12 vectors. Simulations were conducted of 10,000 iterations and the mean and range of the number of presentations required to define an isopter for all iterations was calculated see table 5.3.

Table 5.3: Mean sum of the number of presentations required for isopters compiled of 12 vectors.

	SUM OF PRESENTATIONS PER ISOPTER	
RESPONSE VARIABILITY	**Mean**	**Range**
1°	25	24 - 31
3°	30	24 - 40
5°	34	25 - 47

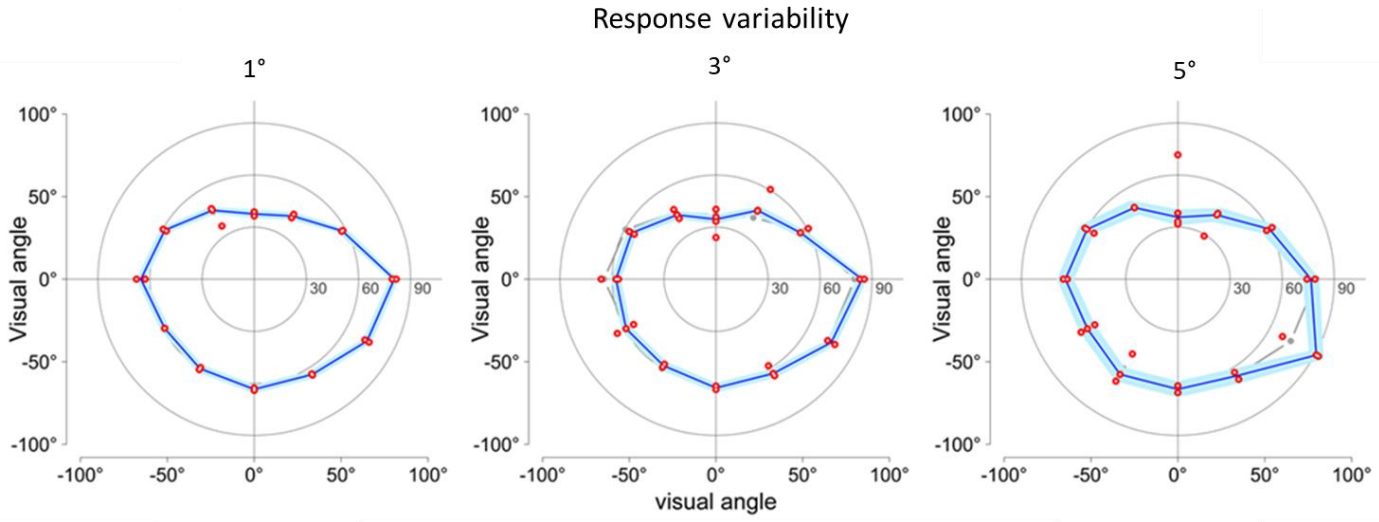

Figure 5.13: Estimated versus true isopters for 3 simulated subjects with response variabilities of MAD (1°, 3°and 5°). The light grey curve shows the true isopter and the dark blue curve shows the estimated isopter, defined from the median of individual responses per meridian (red points). An 80% confidence band is shown in light blue.

From these simulations we can predict that for an individual of moderate variability (3°), the time taken to define an isopter comprising of 30 responses across 12 vectors, would take on average approximately 6 minutes (this time is not inclusive of false positive presentations). This time frame was calculated using the test time results indicated by Mönter et al. (2017) for their kinetic perimetry test, which consisted of 16 vectors (3 training stimuli, 48 kinetic stimuli and 6 false-positives). See Figure 5.13 for graphical output of these simulations.

5.6 Discussion

Computer simulation of kinetic perimetry strategies allows for the development of accurate and precise test strategies. These investigations would not be possible in studies with human observers, due to the time it would take to undertake. The kinetic test strategy that we have developed has shown to be both accurate and precise within the restraints of test duration, and can be applied to a number of different patient groups. Doing so would allow to explore response variability, and patterns of visual defects within these patient groups. Such comparisons are essential within clinical practice/research to identify appropriate test procedures, and to understand the limitations of this strategy within certain patient groups, and how it can be further improved.

From the results of these simulations it can be assumed that between two and three presentations is the ideal number to define an isopter position, in terms of test duration and performance. To define an average isopter position, a minimum of two presentations are required, however this is not always enough. In order to determine the need of additional presentations per isopter position, our results found that by using the distance between the first two responses per meridian, we could maximise the precision of isopter positions while maintaining a suitable test duration. From the results of the simulations we found that by using a criterion value of 5° of less between responses, we could predict that 50% of the time individuals would only require 3 or less presentations to define an accurate isopter position, and the 95th percentile requiring 5 or less. As previously shown in the results very little precision is gained after 5 presentations, thus this is the maximum that would be presented per isopter position. This maximum number also keeps test

duration to a minimum without sacrificing accuracy. These results cover individuals with a high response variability, and individuals with a lower response variability would require less presentations 50% and 95% of the time. See Figure 5.14 for flow chart of the adaptive kinetic perimetry algorithm.

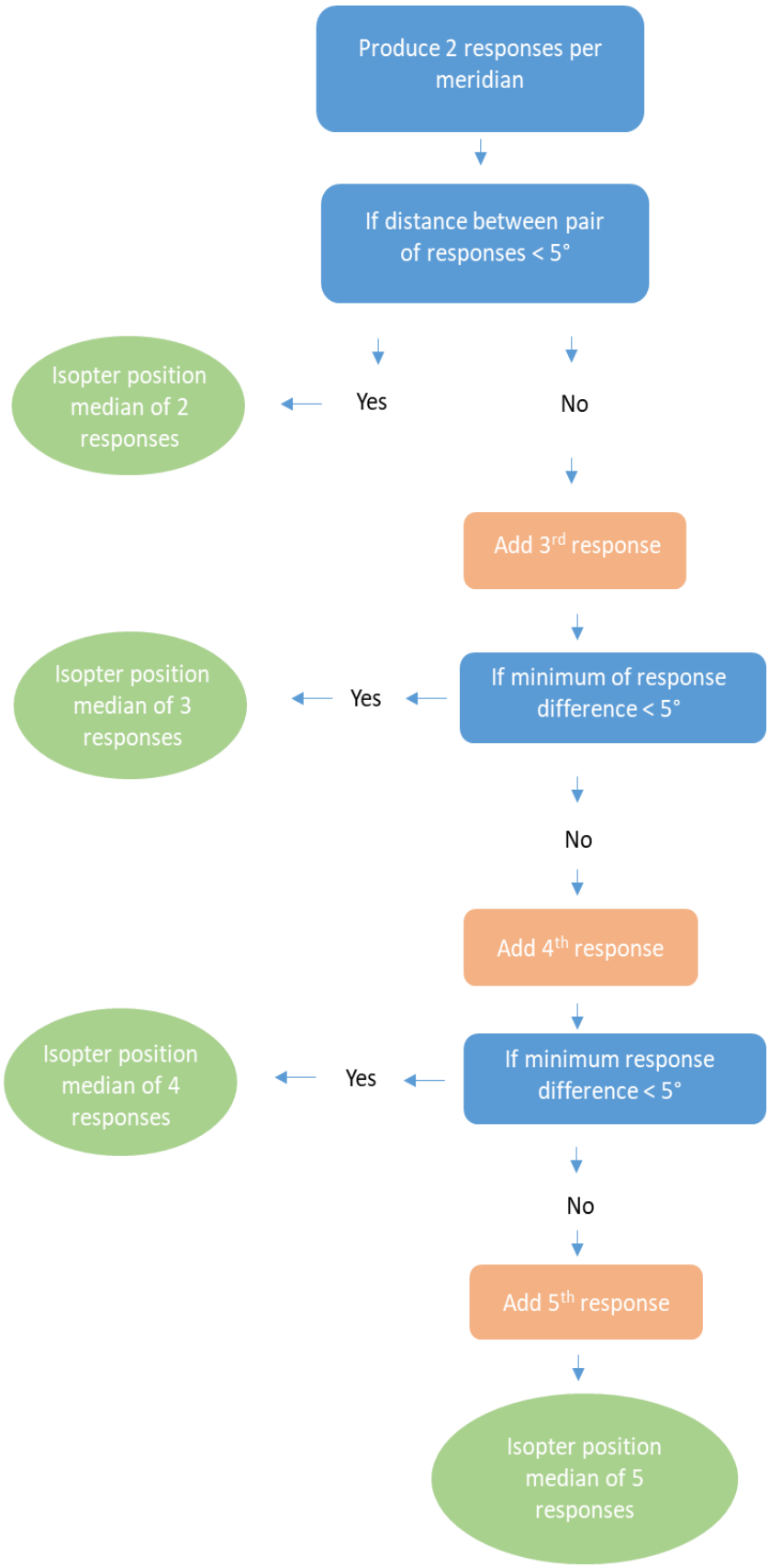

Figure 5.14: Flow chart of adaptive kinetic strategy.

One of the possible limitations of our simulations is that our model of response variability (low, moderate and high) was fixed around all isopter positions. As known, response variability increases with vision loss, thus patients may have different levels of response variability across their visual field dependent on the extent and location of vision loss. The distribution that these results were simulated from showed no significant difference of scatter between isopter positions. However, these responses were obtained from a group of individuals with healthy vision. Due to the nature of our kinetic strategy, using the distance between responses as a method for determining additional presentations would account for different levels of response variability across the visual field. Additionally, it was found that by using a criterion value of 5° we can account for all levels of response variabilities.

The procedure that we have developed will allow for the extent of the outer peripheral visual field of an individual eye, made up 12 vectors, to be measure in approximately 5 to 7 minutes on average with a high degree of precision, for all levels of response variability. This test duration is feasible in a clinical environment and will reduce the effects of fatigue or drop in attention, which is a current issue in kinetic perimetry when it is performed manually (Nowomiejska, Vonthein et al. 2005). However this test time is still long when compared to static perimetry tests such as the SITA Fast 24-2 threshold test, which on average takes approximately 4 minutes per eye.

A patient group where observations of the peripheral visual field could be important, is in patients with advanced glaucoma. Conventional static perimetry methods such as the SITA Fast/Standard 24-3 and 30-2 do not provided reliable

results in patients who have advanced vision loss, and also do not provide any important information in regards to vision loss progression outside of 30° of vision (Nouri-Mahdavi, Hoffman et al. 2004, De Moraes, Liebmann et al. 2013, Nowomiejska, Wrobel-Dudzinska et al. 2015, de Moraes, Liebmann et al. 2016). The use of kinetic perimetry to measure the peripheral visual field could provide important information about the progression of vision loss in these individuals (Nowomiejska, Vonthein et al. 2005, Nevalainen, Paetzold et al. 2008). Nevertheless, it needs to be comparable in test time to the currently used static perimetry tests.

One of the roles that the peripheral visual field plays in everyday life is providing information in regards to navigation within a visual environment, where objects are located outside of our line of sight (Strasburger, Rentschler et al. 2011). When manoeuvring by obstacles another key element is balance (de Luna, Mihailovic et al. 2017). Black et al. (2008) found that postural sway measurements were greater in individuals who had visual field loss located in the inferior region of the visual field. As a result of this increase of postural sway, individuals are more a risk of having falls, thus affecting their quality of life (Black, Wood et al. 2011). If peripheral visual field tests were focused on this region of vision, to monitor visual field loss progression, then it may be possible to help indicate the point at which individuals are more at risk of having falls, and to implement prevention strategies. By using the adaptive strategy that we have developed it may be possible to monitor the temporal inferior visual field at 7 locations in approximately 3 minutes, excluding false positives. This is in line with current static perimetry test durations. Figure 5.15 shows simulated examples of the adaptive strategy output of the temporal inferior visual region from glaucomatous manual Goldmann outputs.

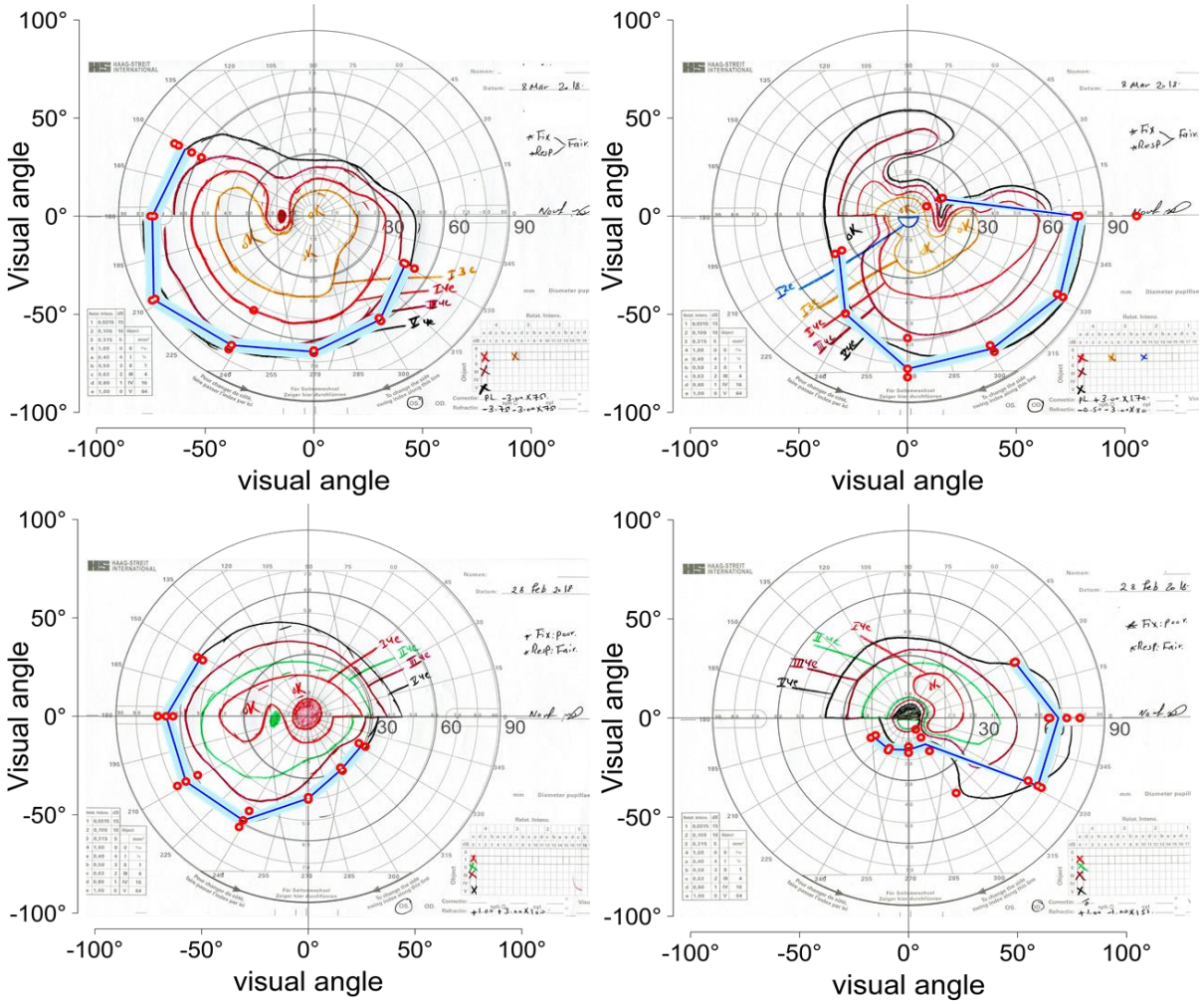

Figure 5.15: Simulated partial isopters of the temporal inferior visual field, using the size V-4e Goldmann stimulus and of moderate response variability. Dark blue curve indicates estimated isopter defined from the median of responses (red points) per isopter position. Light blue band contains 80% of responses. Goldmann manual perimetry output shown in the background.

The next step on from these simulations is to implement the test strategy on real observers. When using computer simulations, assumptions are made in regards to observer responses, for example attentional lapse and fatigue, which is not always a true reflection of real observer response characteristics. Thus in order to truly validate this kinetic perimetry strategy, clinical testing is required. In summary, from our kinetic perimetry simulations, we suggest that it is possible to effectively measure certain regions of the visual field with precision, and within a reasonable

clinical test duration by using our adaptive strategy. This adaptive kinetic strategy could provide clinically relevant information in regards to the role the peripheral visual field has in relation to everyday visual functions, and promote the relevance of kinetic perimetry as a diagnostic and therapeutic method of monitoring patients with visual field loss.

6 Chapter 6: An automated kinetic perimetry algorithm: test-retest variability of measures of the inferior temporal visual field in glaucomatous visual field loss.

6.1 Introduction

The standard method for measuring the visual field in patients with glaucoma is computerised perimetry. Over the years this method has increased in sensitivity in terms of detection, and enhanced the reliability of results in follow-up tests (Fankhauser, Spahr et al. 1977, Li, Spaeth et al. 1979, Gloor, STURMER et al. 1984, Weleber, Smith et al. 2015). Two of the most commonly used computerised automated perimeters are the Octopus (Interzeag International, Bern- Koniz, Switzerland) and the Humphrey Field Analyzer (Zeiss Humphrey Systems, Dublin, California). Both of these perimeters have been found to be superior at measuring visual field loss compared to manual methods such as Goldmann manual kinetic perimetry, when examining the central 30° of vision (Heijl and Drance 1981, Mills, Hopp et al. 1986).

Due to the nature of glaucomatous visual field loss, the majority of visual defects tends to be found within the central 30° (Schiefer, Schiller et al. 2001); however, on occasion the first detectable evidence of glaucomatous visual field loss may occur outside of this central area (LeBlanc, Lee et al. 1985). For the purpose of initial diagnosis, computerised static perimetry tests are the most favoured method, with substantial research behind the development of algorithms, such as the Swedish interactive threshold algorithms (SITAs), that are commercially available for the Humphrey Field Analyzer (Bengtsson, Olsson et al. 1997, Bengtsson and Heijl 1998). These are designed to measure accurately and precisely threshold estimates across the central visual field, within a patient friendly test duration. These algorithms are

robust against patient errors and reliable, and multiple tests can be compared to track possible disease progression. The balance between accuracy and test time has been highly debated and attempted throughout the last several years (Turpin, McKendrick et al. 2003).

In cases of advanced glaucoma the standard perimetry test, e.g. SITA Standard 24-2, becomes increasingly hard for the patients, due to the progressive decline in contrast sensitivity, and provides little information in regards to visual field loss progression once vision loss has reached a certain stage (De Moraes, Liebmann et al. 2013, de Moraes, Liebmann et al. 2016). At this stage Goldmann manual kinetic perimetry can be used to measure the peripheral visual field outside 30°, however it has disadvantages, for instance the need for a skilled examiner, test duration and standardisation (Nowomiejska, Vonthein et al. 2005, Nevalainen, Paetzold et al. 2008). Thus, the introduction of a computer-driven kinetic visual field test, Automated kinetic perimetry (AKP). This test uses stimuli corresponding to that of manual Goldmann device, and is easier to standardise (Schiefer, Schiller et al. 2001). Nonetheless this method is currently not widely used outside of specialist centres due to the need for a trained examiner.

The peripheral visual field plays an important role in everyday functions such as walking and driving (Huisingh, McGwin et al. 2015, Simpson 2017), and contributes to postural sway (Berencsi, Ishihara et al. 2005, Black, Wood et al. 2008, Black, Wood et al. 2011, Kotecha, Chopra et al. 2013). This argument promotes the importance of measuring the peripheral visual field, particularly in individuals with advanced vision loss due to glaucoma. The process of measuring the entirety of the peripheral visual field is lengthy compared to current clinical static programs for the

central 30°. Thus, developments of perimetry measurements of the peripheral visual field should not only be clinically relevant, but also brief to avoid fatigue and reliability issues cause by human errors.

A part of the peripheral visual field which is suggested to be clinically relevant in terms of postural sway is the inferior temporal visual region. It has been found that glaucoma patients exhibit more postural sway than their age match counter parts (Black, Wood et al. 2008, Black, Wood et al. 2011, Ramulu, Maul et al. 2012, Ramulu, Van Landingham et al. 2012, de Luna, Mihailovic et al. 2017). As a result of this increase of sway, these individuals are possibly at more risk of falls (Haymes, LeBlanc et al. 2007). Black et al. (2008) found that when proprioceptive feedback was removed in postural sway measurements while standing on foam surface, individuals with greater inferior visual field loss incurred greater sway. It should also be noted that the temporal region has the greatest eccentricity and was also found to be one of the last regions affected by glaucoma (Freeman, Munoz et al. 2007). This finding suggests that if there is visual field loss progression in the inferior temporal visual regions, it could impact on glaucoma patients' postural stability, leading to a greater risk of falling. However, there are a number of underlying factors which contribute to falls which are poorly understood.

Although automated kinetic perimetry is an extensively used method to examine the peripheral visual field, there are issues with its automation. The method of single responses close to the threshold, which defines the sensitivity of the visual field at a particular eccentricity, are highly variable (Schiefer, Strasburger et al., 2001, Nevalainen, Paetzold et al., 2008, Mönter, Crabb et al., 2017). In manual Goldmann perimetry an examiner can disregard unusual responses which are against the

expected norm (Hashimoto, Matsumoto et al., 2015); however, a method to replicate this process in automated kinetic perimetry has yet to be established.

In this study, we have designed an automated kinetic perimetry algorithm, which aims to estimate the outer border of the peripheral visual field. This strategy aims to produce measurements with precision and accuracy whilst using the least number of presentations possible. As to relate the clinical relevance of the peripheral visual field, and to keep test time in line with current static test durations, only the temporal inferior visual region will be measured. This study also aims to report on the performance of a simple adaptive kinetic algorithm when used on patients with moderate to advanced glaucoma. Moreover, the repeatability of this test is analysed.

6.2 Methods

6.2.1 Participants

In this study, 12 glaucoma participants (median age 75y, range 69y to 80y) and 12 control participants (median age 74y, range 68y to 81y) performed the new kinetic test twice. The visual field mean deviation (MD), defined from the results of the SITA Fast test, in the worse and better eyes of the glaucoma patients was -18 (-8 to -29) dB and -8 (-2 to -20) dB. Before attending the study session both groups of participants were screened for no history of any other ocular disease, no previous eye surgery apart from uncomplicated cataracts or glaucoma related surgery. Ethical approval was obtained from the University of Plymouth and followed the tenets of the Declaration of Helsinki.

All participants at the study session were screened to ensure they had at least -6 MD moderate visual field loss due to glaucoma (glaucoma participants) in at least

one eye in any location, or did not have visual field loss (control patients) using the HFA SITA-fast 24-2 visual field test. All glaucoma participants had a clinical diagnosis of glaucoma according to their records at the Centre for eye care excellence (CEE) Plymouth. The mean deviation results of this test provided a staging criteria for glaucoma patients (Hodapp, Parrish et al. 1993). Participants were additionally screened for diabetic retinopathy through fundus images, refractive error of spherical ametropia greater than 6 dioptres (D) or astigmatism greater than 2 D. Refractive errors were not corrected to avoid lens rim artefacts, and it has been shown that, in eyes with refractions in this range, correction of the refractive error has no influence on the position of peripheral isopters (Niederhauser and Mojon 2002). Participants' were examined using their own spectacles, on the Early Treatment Diabetic Retinopathy Study (ETDRS) chart. Measures of contrast sensitivity were also taken using the Mars chart, both monocular and binocularly. Results of these tests defined whether participants were eligible to undertake the new visual field test. As participants were also asked to undertake a postural sway test in the same study session, they also had to meet the inclusion exclusion criteria list in chapter 7.

6.2.2 Visual field examinations

Both eyes of each participant were examined. The order of each eye was random and two kinetic examinations were performed on the inferior temporal peripheral visual field. Before undertaking the test participants were given a short practice test to familiarise themselves with the test procedure. All visual field tests were undertaken during one study session with a break of approximately 1 hour between the first and second examinations. Kinetic tests were performed on a projection

perimeter (Octopus 900; Haag-Streit), with a hemispherical bowl (radius 300 mm) and a background luminance of 10 cd/m2. Stimuli were circular luminance increments (Goldmann size V, subtending 1.72 degrees). The kinetic test was custom written with R core software (2016), and performed on the Octopus 900, controlled using the Open Perimetry Interface (OPI) (Turpin, Artes et al. 2012). See Appendix A4 for R script.

6.2.2.1 Kinetic adaptive visual field test

Kinetic perimetry was performed using the adaptive algorithm described in Chapter 5. This algorithm uses a set distance of 5° between responses to define if a third, fourth or fifth presentation is required to define the isopter position. A Goldmann V-4e stimulus was used at a speed of 5 °/s. According to Goldmann terms, these stimuli are circular spots subtending a visual angle of 1.72 degrees with a luminance of 318 cd/m². Kinetic stimuli started outside the normal range of visibility and moved from the periphery toward the centre and were presented in random order. The visual field was constructed of 7 meridians which covered the temporal and inferior visual regions, as shown in Figure 6.1. Two meridians are located on the horizontal midline, subtending 3 degrees to account for the pattern of visual field loss caused by glaucoma (Damgaard-jensen 1977). The final partial isopter was defined from the median of responses per isopter position. The mean position of the partial isopter (MIP) was used as a global summary measure, and the scatter of an individual's responses was defined using the median absolute deviation (MAD) of responses around the final isopter positions. False-positive catch trials (n = 4) were stimuli presented in the far nasal periphery where they were invisible to the

individual, but there was still an association with the sound of the movement of the perimeter projector.

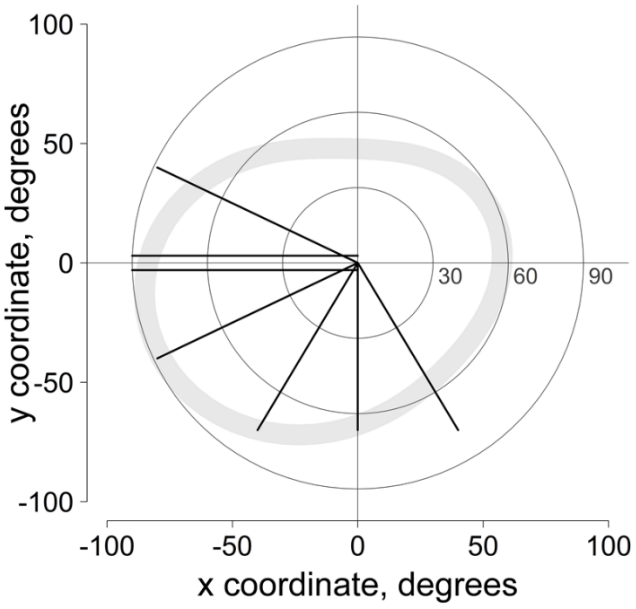

Figure 6.1: Diagram of kinetic visual field test meridians. Meridians indicated in black along the temporal and inferior visual regions of a left eye. The lightly shaded region indicates the normative response range according to Vonthein et al. (2007) of an individual 70 years of age, using Goldmann stimulus size V-4e.

6.2.3 Data analysis

The test-retest variability of the adaptive kinetic perimetry test was estimated with a modified version of Bland-Altman analysis (Bland and Altman 1986) for glaucoma patients. This analysis relates the differences between the repeated tests to the best available estimate of the ‘‘true’’ value (the mean of the repeated tests). The systematic error between tests was estimated from the median of the differences, with the retest variability defined using the MAD, due to outliers highly effecting the standard deviation. The relation between MD central damage and MIP in glaucoma patients was observed using a Spearman rank order correlation. The difference between the extent of the peripheral visual field between glaucoma and control groups was compared using a Mann Whitney U test. Graphical representations of

the visual fields and statistical analyses were performed in R statistical software version 3.4.1.

6.3 Results

Table 6.1 shows the median, range of mean deviation, visual acuity, contrast sensitivity, and age for both glaucoma and control patients that participated in this study. The majority of glaucoma patients had advanced damage, in at least one eye, in the central visual field.

Table 6.1: Summary descriptive of vision and demographic measurements of years (Y), visual acuity (VA), contrast sensitivity (CS) and mean deviation (MD).

PARAMETER	GLAUCOMA MEDIAN (RANGE)	CONTROL MEDIAN (RANGE)
AGE, Y	75 (69 to 80)	74 (68 to 81)
BETTER EYE VA (LOGMAR)	0.08 (-0.04 to 0.34)	-0.005 (-0.12 to 0.04)
WORST EYE VA (LOGMAR)	0.28 (0 to 0.5)	0.06 (-0.08 to 0.2)
BINOCULAR VA (LOGMAR)	0.08 (0 to 0.38)	0 (-0.08 to 0.02)
BETTER EYE CS	1.36 (0.84 to 1.52)	1.48 (1.2 to 1.76)
WORST EYE CS	1.16 (0.48 to 1.36)	1.40 (0.96 to 1.64)
BINOCULAR CS	1.32 (0.78 to 1.64)	1.6 (1.20 to 1.76)
BETTER EYE MD	-3.60 (-2 to -17)	-0.89 (-2.85 to 0.84)
WORST EYE MD	-17.5 (-6 to -29)	-2.22 (-4.31 to 1.55)

6.3.1 Central MD versus peripheral visual field MIP

From our results it can be demonstrated the large scatter of differences between central visual field damage and peripheral isopters. This difference in vision damage can be seen in Figure 6.2, whereby some individuals can have advanced central

visual field loss, but have a normal size isopters for their age group. In contrast, others have less central damage, yet a more constricted isopter. A Spearman rank order correlation coefficient of MIP and MD was P = -0.28, suggesting a very small negative correlation between the damage of central visual field damage and the size of a partial peripheral isopter in the inferior temporal visual field.

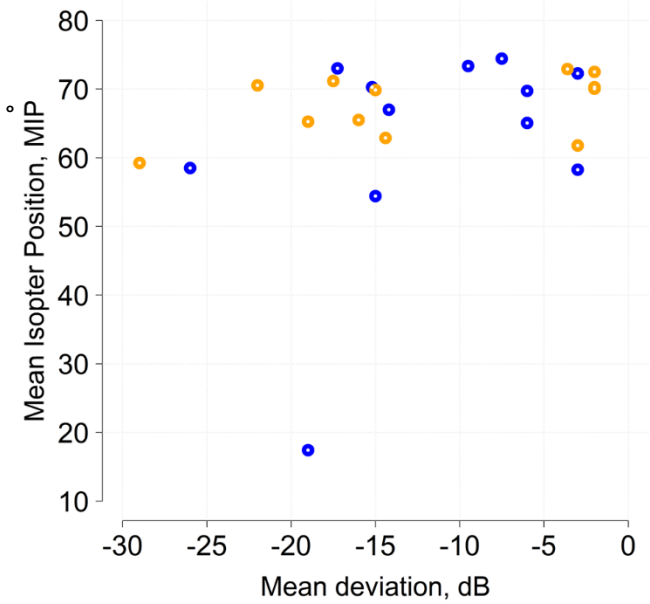

Figure 6.2: Relationship between the peripheral visual field MIP and the central visual field MD. Each point shows the mean of the repeated kinetic visual field test and the MD from the 24-2 SITA Fast HFA test. Blue points represent the right eye of participants and orange equals the left eye.

6.3.2 Test-retest variability of adaptive kinetic algorithm

The results of the test-retest variability of the adaptive kinetic algorithm for the peripheral visual field showed that there was no systematic differences, which could be a consequence of learning effects. The median test-retest difference was -0.7°. The absolute test-retest difference between MIP was 2.4° with approximately 90% of differences falling with ± 3.6° (see Figure 6.3). This result suggests the initial estimates of the peripheral visual field from the adaptive kinetic algorithm are precise.

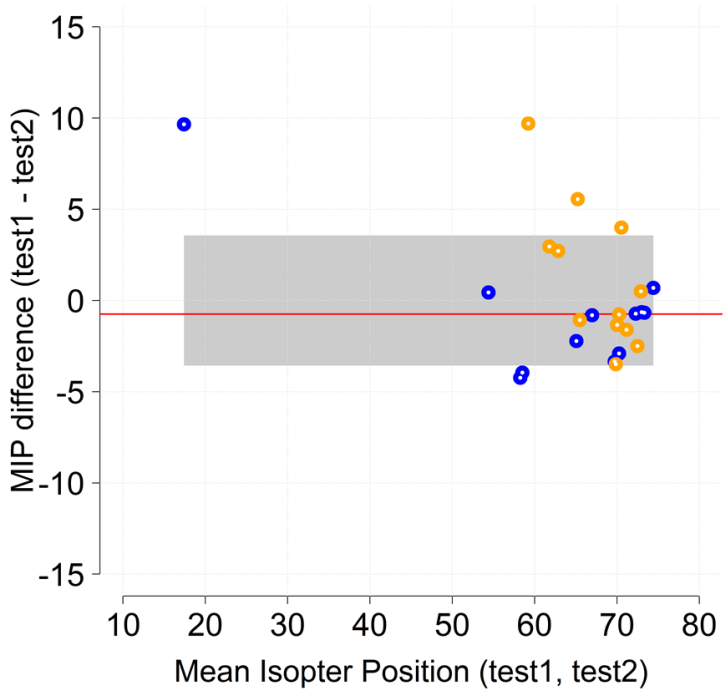

Figure 6.3: Relationship between test-retest differences in MIP and the range of peripheral visual field damage (mean of repeated test MIPs). The gray rectangle represents the 90% test-retest interval of ± 3.6° in height and the range of mean of MIPs width direction (17° to 74°). The red line indicates the median test-retest difference. Blue points represent right eyes, orange points indicate left eyes.

Figures 6.4, 6.5 and 6.6 show example responses from three individual patients, and illustrate the relationship between peripheral and central visual fields and the repeatability of the kinetic test, see appendix A4.1 for all participant plots. In these plots both the central 24-2 HFA output, and the partial isopter are shown by overlaying the grayscale representation on the central visual field with the kinetic isopter plot. The individual responses per isopter position are shown as red points (white dots within the red dots allow for easier identification of responses). The median of these red dots per isopter were used to define the final isopter, shown in dark green. The scatter of responses is represented at the MAD multiplied by 2.2 to

define a 90% confidence interval band shown in light green. Normative age values according to Vonthein et al. (2007) are shown as a light gray isopter.

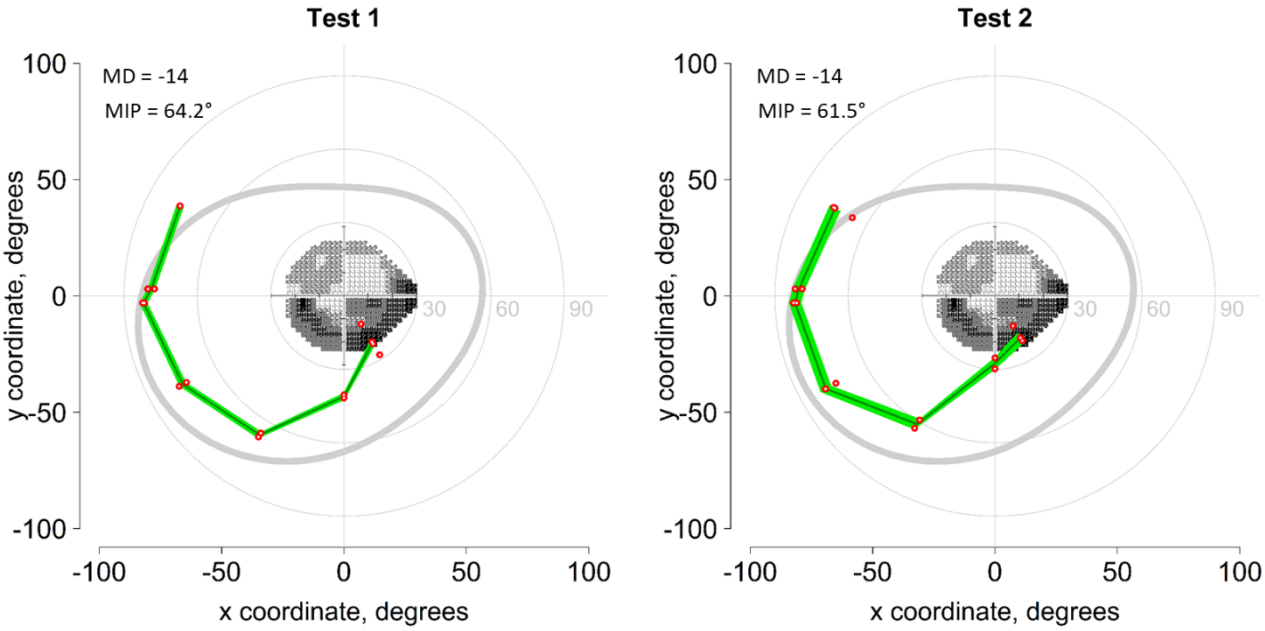

Figure 6.4: Participant 6's central field showed a dense inferior arcuate scotoma, extending above the horizontal meridian in the nasal region. The partial isopter estimated using a V-4e stimulus, shows that this inferior nasal visual field loss within the central 30° extends into the far peripheral visual field. The temporal region of the isopter was close to the expected values. Individual response were clustered closely together, apart from on the 300° meridian where vision loss was greatest. This required additional points by the adaptive algorithm. The 90% confidence band around the isopter was narrow (MAD, test 1 = ±1.5° test 2 = ±2.5°). The peripheral isopter looks similar in the first and second test.

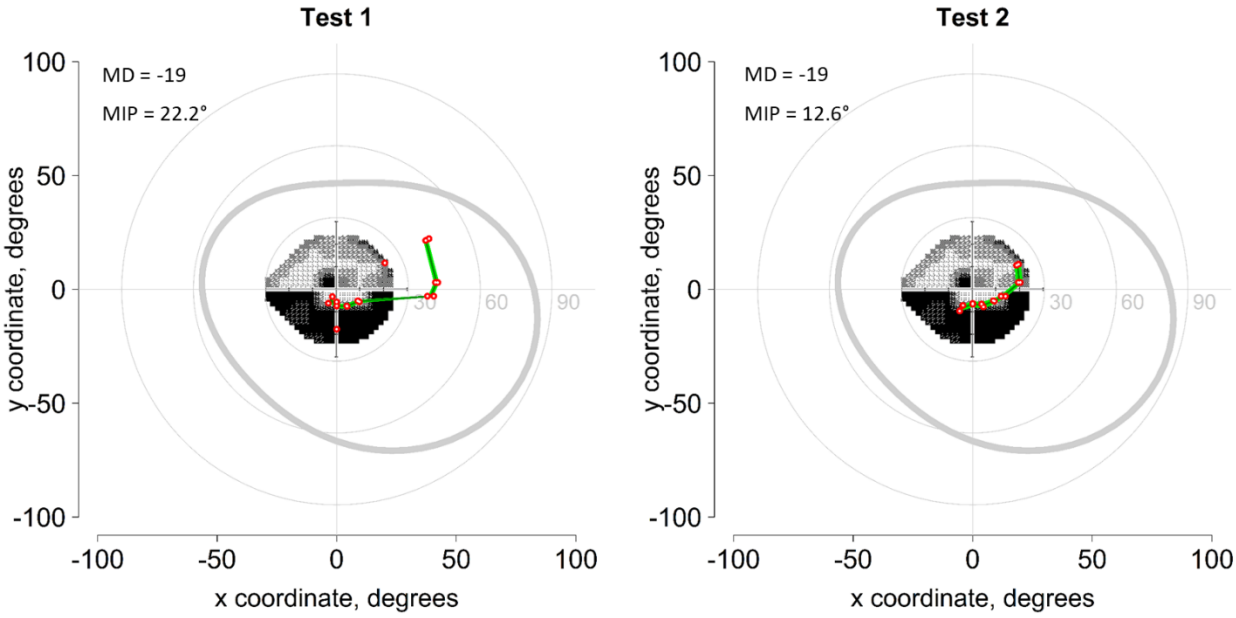

Figure 6.5: Participant 8's central field showed a very dense inferior arcuate scotoma, extending above the horizontal meridian in the temporal region. The partial isopter estimated using a V-4e stimulus, shows that this inferior visual field loss extends all the way out to the far peripheral visual field, with no intact vision detected in this area. Individual responses were clustered closely together for most of the isopter positions. The 90% confidence band around the isopter was narrow (MAD, test 1 = 0.9° test 2 = 1.3°). The peripheral isopter in the temporal region is not similar between first and second test, this suggests that the superior/temporal visual region may still have small patches of vision left.

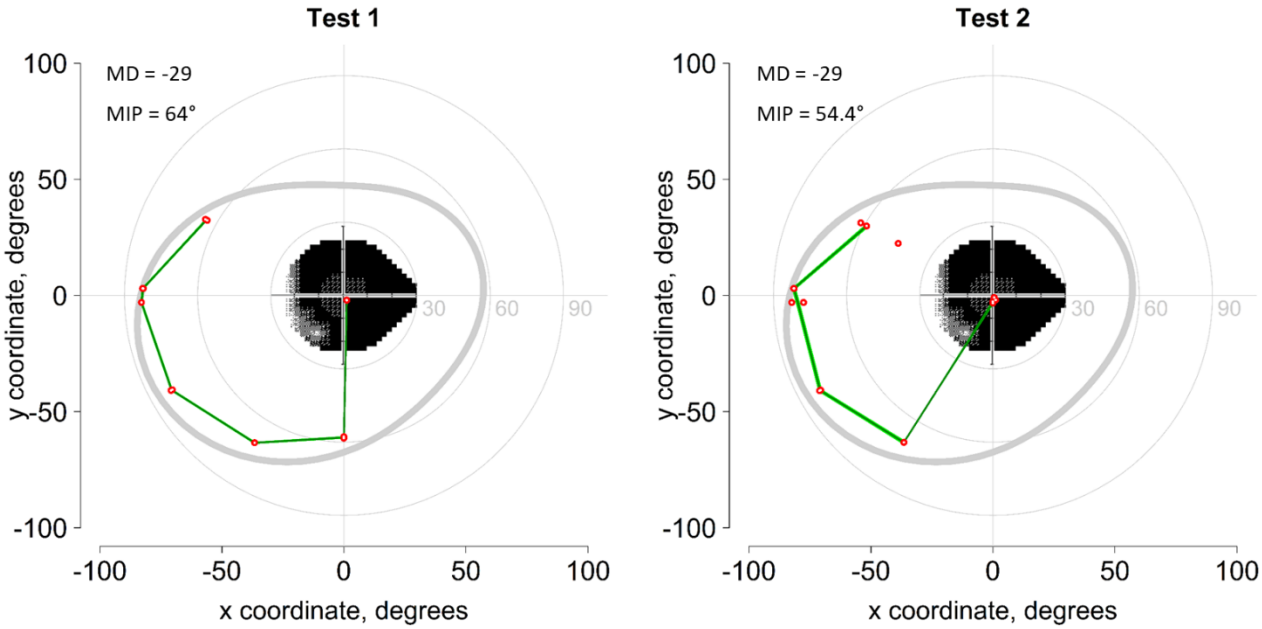

Figure 6.6: Participant 4's central field showed a very dense damage all over, with only signs of vision in the temporal border. The partial isopter estimated using a V-4e stimulus, shows that there is vision in inferior temporal visual field extending all the way out. There are no signs of peripheral vision in the nasal region. Individual responses were cluster closely together for all isopter positions. The 90 % confidence band around the isopter was narrow (MAD, test 1 = 0.3° test 2 = 0.6°). The peripheral isopter position in the inferior 270° region is not similar between first and second test, this suggests this visual region may still have small patches of vision left.

6.3.3 Performance of adaptive algorithm

Table 6.2 summarises the performance in terms of precision, number of responses required, and test duration. From these results, it can be suggested that the clinical application of this test replicates closely the results of the predictions made by the simulations (see Chapter5). On average, the 90% isopter confidence band was within ± 2° (MAD). To define an isopter consisting of 7 vectors, on average it took 15.5 responses define all 7 positions for test 1 and test 2, and with the inclusion of 4 false positive catch trials this took approximately 2 minutes, (range 1.3 – 4.7 mins). On

average to define individual isopter positions is took approximately 2.2 responses with a range of 2 to 5.

Table 6.2: Summary statistics of peripheral visual field test. The table shows the MIP and isopter confidence band measure in degrees, with the standard deviation (SD) and interquartile range (IQR) also shown. The test duration is measures in minutes and seconds (MIN:S).

	MEAN (SD)	MEDIAN (IQR)	RANGE
MEAN ISOPTER POSITION °	65.2° (11.6)	69.7° (62.6 - 71.4)	17.4 - 74.4°
ISOPTER CONFIDENCE BAND°	2 (1.2)	1.61 (1.04, 2.5)	0.3 – 5.1
TEST DURATION (MIN:S)	2.08 (0.38)	2.08 (1.59, 2.20)	1.33 – 4.42

6.3.4 Glaucoma versus control peripheral visual field

The results of a Mann Whitney U test found that there was a significant difference between the MIP of healthy and glaucoma patients, $p < 0.001$, with a large effect size 1.05, with Figure 6.7 showing that the control patients have on average a 7° larger partial isopter of the temporal inferior visual field, see Table 6.3 for full results.

Table 6.3: Summary of MIP for glaucoma and control participants.

	MEAN (SD)	MEDIAN (IQR)	RANGE
GLAUCOMA	65.2° (11.6)	69.7° (62.6 - 71.4)	17.4 - 74.4°
CONTROL	72.2° (12)	76.9° (63.1 - 82.4)	42.5 - 86.6°

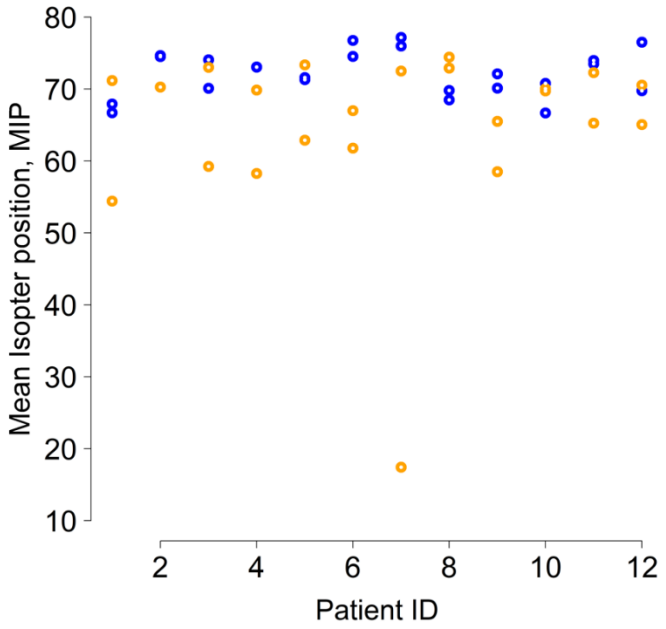

Figure 6.7: Mean isopter position for both glaucoma and control patients. Orange points represent both left and right eye measurements for glaucoma patients, and blue points show left and right eye measures for control patients.

6.4 Discussion

The objective of this study was to examine the performance of an adaptive kinetic perimetry strategy at estimating the temporal inferior border of the peripheral visual field in moderate to advanced glaucoma patients. This study also examined the relationship between central visual field damage and the extent of peripheral visual field.

The outcome of this kinetic strategy was not aimed at replicating manual Goldman perimetry isopters, which are detailed in their outputs, but rather to produce a simple kinetic test to measure a portion of the visual field within a reasonable test duration. An additional aim of our test was to try to compensate for outlier responses which can often occur in kinetic perimetry, causing “spikes” in isopter

plots (Lynn, 1991). We know from previous research that by increasing the number of presentations, precision of isopter estimation is increased (Nowomiejska, Wrobel-Dudzinska et al., 2015), however this incurs a lengthy test duration. By using our adaptive strategy we accounted for outlier responses by presenting additional stimuli up to a limit of 5, but also adjusted for precision, thus if two responses were close together we defined this as precise enough to define an isopter position.

Our results show that the adaptive kinetic strategy efficiently estimates the temporal inferior visual field in moderate to advanced glaucoma patients within a retest interval of approximately ±3.6°. This result is similar to previous works (Nowomiejska, Vonthein et al. 2005, Nevalainen, Paetzold et al. 2008, Hashimoto, Matsumoto et al. 2015, Mönter, Crabb et al. 2017), and is less than the space between points in conventional static perimetry. This result suggests that the adaptive strategy is precise, and with a small difference of -0.7° between the first and second test, there is little evidence of a learning effect occurring.

Mönter et al. (2017) used a strategy of 3 presentations over 16 meridians to cover all regions of the visual field. However, this procedure was lengthy (~11 minutes) due to the addition of false positives. With our procedure we reduced the number of meridians measured and focused only on the temporal inferior region, as this is the area of the visual field which extends the furthest out and could be a more clinically relevant visual region in the more advanced stages of glaucoma, i.e. help with mobility (Black, Wood et al. 2011). Additionally, the strategy adapted the number of presentations per meridian dependant on the distance between responses. Using this strategy this test took approximately 2 minutes. The duration of this new kinetic

test is in line with other current central visual field tests, such as SITA Fast, used in a clinical environment.

When examining the relationship between the central versus peripheral visual field damage, there was little correlation. Some individuals who have severe damage in the central visual field have relatively normal peripheral isopters. This result suggests that perimetry of the temporal inferior visual field may provide important information in conjunction with central visual field tests which could relate to an overall view of visual impairment. In addition, the peripheral visual field may provide clinically relevant information in regards to treatment decisions.

There was a significant difference in the mean isopter position between glaucoma and control patients. This finding would suggest that in the more advanced stages of glaucoma there is visual field damage occurring in the far periphery. Although it should be noted that we did not exclude patients who had undergone cataract surgery, there has been evidence to support an effect on the extent of the far-peripheral visual field in these individuals (Makhotkina, Berendschot et al. 2016). The results of Chapter 4 which used the extended fixation procedure from chapter 3 which supports this finding, thus follow up investigations would exclude participants who had undergone cataract surgery. This is an important finding due to current visual field loss progression identification procedures (Spry and Johnson 2002, de Moraes, Liebmann et al. 2016, Ernest, Schouten et al. 2016, De Moraes, Liebmann et al. 2017, Wall, Zamba et al. 2018), with current clinical procedures only examining the central visual field in the majority of cases. If a patient presents with a lot of damage in the central field, then it is hard to detect further vision loss from the results of a HFA test, and it also becomes increasingly hard for the patient to

undertake (Katz, Gilbert et al. 1997, Broman, Quigley et al. 2008). From our results it could be suggested that the implementation of a peripheral visual field test would benefit progression analysis in the more advanced stages of the disease, and provide additional information in regards to glaucomatous visual field loss patterns.

The performance of this kinetic strategy improved upon our estimations using simulations see chapter 5. When conducting the simulations the response variability was set as a consistent value across the whole visual field. However we know from previous work that response variability can differ dependent on extent of visual field damage in the visual field (Turpin, McKendrick et al. 2002). In our group of patients some individuals had visual field damage extending into the periphery only in certain regions, e.g. nasal (see participant 4 in Figure 6.6). Thus, with this response variability across the visual field, some regions performed better than others and shortened the test duration. This is an important factor to account for in future kinetic simulations.

As this kinetic strategy was designed using the Open Perimetry Interface (OPI) with an Octopus 900 perimeter, future developments to the strategy could be easily implemented. Possible adaptions could be to adjust stimulus speed dependent on its location within the visual field, e.g. slowing the speed when the stimulus gets closer to the centre. Due to the current test time it may be possible to add further locations either between current meridians, or to extend further in the superior and nasal regions, without incurring too long of a test, adding more important information about the periphery.

Our study demonstrated that precise estimates of peripheral isopters can be obtained in the temporal inferior visual field from a fully automated kinetic

approach using our adaptive strategy. Future work should aim to investigate how it can be best used in conjunction with results obtained through static perimetry, and how perimetry of the peripheral visual field can help to improve clinical decisions and treatment plans in patients with advanced glaucoma.

7 Chapter 7: Postural sway and the peripheral visual field in glaucoma.

7.1 Introduction

Balancing our body is an integral process in everyday activities such as walking and even standing (Peterka 2002). Although upright balance is often automatically undertaken independent of conscious control, a number of sensory systems are required in order to control the motor functions and balance (Mergner, Maurer et al. 2003). Upright stance is achieved through feedback mechanisms, which counteract body-sway, detected primarily by visual, somatosensory and vestibular sensory systems (Jeka, Oie et al. 2000, Peterka 2002, Kotecha, Chopra et al. 2013, Anson, Bigelow et al. 2017). In order to maintain balance, information from the three sensory systems need to integrate efficiently. Weighting of sensory inputs to determine motor responses are thought to occur in a dynamic way between visual, somatosensory and vestibular afferent inputs (Peterka 2003). Relative weighting of contributions from sensory systems differs depending on circumstances such as walking compared to standing, and as such their inputs are weighted differently depending on the activity (Redfern, Yardley et al. 2001). Even when walking the environment around us can affect the weighting of different sensory systems (Peterka 2003). For example, when an individual walks into a poorly illuminated room there is up-weighting (more dependence) to the somatosensory and vestibular system due to the reduction of vision. Also, when walking on soft ground such as sand there is less proprioceptive feedback, thus up-weighting to the visual and vestibular systems (Polastri, Barela et al. 2012, Barela, Weigelt et al. 2014).

An impairment in sensory acuity or processing of any single sensory system could lead to a balance impairment. Balance impairment can then in turn limit mobility

and activities of daily life. This can result in a decrease in participation of social activities, leading to increased levels of isolation and decrease in quality of life (Lopez, McCaul et al. 2011).

Vision enables head referenced signals from the vestibular system, and body-referenced signals from the proprioceptive system (body schema) to be contextualised relative to the environment (Taube 2007). This is fundamentally important in order to navigate during mobility. Vision is also important in providing online feedback of body sway (rate of angular change over time), and is effective when combined with an awareness of the earth-referenced visual vertical to inform postural adjustments (Kuo, Speers et al. 1998). Visual impairment is also known to increase the range and speed of postural sway, which is the movement of the centre of mass in a standing position (Redfern, Yardley et al. 2001, Horak 2006, de Luna, Mihailovic et al. 2017). This has also been observed in healthy individuals who were blindfolded or had field of view constrained (Uchiyama and Demura 2008). Studies on people with glaucoma also show that patients with more extensive visual field damage report postural instability and have increased measures of postural sway (Black, Wood et al. 2008, Kotecha, Chopra et al. 2013, de Luna, Mihailovic et al. 2017). This suggests that their balance may worsen with visual field loss. However, the true effect that the pattern of glaucomatous visual field damage has on balance remains unclear (de Luna, Mihailovic et al. 2017). Variables such as age, age-related decline in proprioceptive function, physical coordination, and cognitive abilities (Kotecha, Richardson et al. 2012), and non-miotic topical glaucoma medications (typically β-blockers) could also increase postural instability and hence impact measures of postural sway (Black, Wood et al. 2008). Thus, there is building

evidence for the need of comparative studies on glaucoma patients and aged matched controls to determine the effect of different visual field loss on increased postural sway.

When examining visual field loss in glaucoma patients, the pattern of vision loss tends to follow the path of the retinal nerve fibres, with damage initially appearing in the mid periphery around the blind spot, usually in the superior hemisphere, and arching over into the nasal region (Weinreb, Aung et al. 2014). Damage can however appear as inferior visual field loss as well (Schiefer, Papageorgiou et al. 2010). There is conflicting evidence though in regards to which visual region with visual field loss incurs greater increase of postural sway. De Luna et al, (2017) found that there was an increase in postural sway in terms of Root Mean Square (RMS) of overall sway speed, associated with visual field damage in the superior hemisphere, compared to that of inferior hemisphere damage. This challenges reports by Black et al, (2008) who found that more extensive visual field loss in the inferior region, is associated with an increase in postural sway. A review of studies which have examined the effect of location of visual field loss on postural sway, have only observed the effect of this loss within 30° of vision (Black, Wood et al. 2008, Kotecha, Richardson et al. 2012, de Luna, Mihailovic et al. 2017), neglecting a large proportion of the peripheral visual field. Despite visual field damage being associated with an increase in falls; an outcome of high levels of postural instability (Freeman, Munoz et al. 2007), few studies have explored postural sway relatively to impairments in the peripheral visual field. It should be noted that there are many other factors what influence postural sway, such as age and comorbidities (Røgind, Lykkegaard et al.

2003), and these should never be neglected when observing the effects of vision loss on increased sway.

In motor control, there are two types of vision, which distinguish different functional and processing characteristics from the environment, known as focal and ambient (Berencsi, Ishihara et al. 2005). Focal vision is associated with central vision for detecting physical objects within the environment, and ambient vision is associated with peripheral vision which is responsible for defining spatial characteristics (Berencsi, Ishihara et al. 2005). The role of central versus peripheral vision is one that is highly debated within research, with three main theories arising from this work. The "peripheral dominance theory" suggests that peripheral vision plays a greater role than central in control of postural sway (Brandt, Dichgans et al. 1973, Berencsi, Ishihara et al. 2005). The "retinal invariance hypothesis", suggests that central and peripheral vision are equally weighted in their contribution to control of postural sway (Straube, Krafczyk et al. 1994, Bardy, Warren et al. 1999). Lastly, the "functional sensitivity hypothesis", suggests that the different visual regions have different and complementary functional roles, all with the potential to contribute to control of postural sway but as yet these roles are undefined (Stoffregen, Schmuckler et al. 1987, Nougier, Bard et al. 1997).

Of the three theories, the "functional sensitivity hypothesis" goes further to suggest that the difference between the two visual regions can also be associated with directional control of postural sway. It suggests that central vision controls the lateral (medio-lateral or ''roll'', meaning side-to-side) movement of postural sway, and the peripheral vision controls the anterior-posterior (AP or ''pitch'', meaning forwards-backwards) movement of postural sway (Anson, Bigelow et al. 2017).

However, when investigating this directional control, studies have presented contradictory evidence, with many being un-comparable, due to the different study designs (Berencsi, Ishihara et al. 2005, Agostini, Sbrollini et al. 2016). For example, different types of visual stimuli e.g. static or dynamic, or even the size of the target have shown to selectively activate different visual regions (Paulus, Straube et al. 1984). It should also be noted that directional visual cues (which cue the observer towards a direction) also have an effect on the direction of stability (Balestrucci, Daprati et al. 2017) for example a visual cue pointing/moving horizontally would increase roll directional sway. Therefore these studies are limited in terms of comparability (Berencsi, Ishihara et al. 2005). This provides justification to investigate the role of visual scenes and targets in different visual regions, to explore their contribution to postural stability.

Even with the advancing of visual field loss in some individuals with glaucoma, postural stability typically remains only mildly affected until severe stages of glaucoma where extensive binocular vision loss occurs, as suggested by (Black, Wood et al. 2008). One theory derived from recent investigations of postural sway, in patients with glaucoma, suggests this relatively preserved postural stability may be explained by the initial up weighting of postural control signals, from intact proprioceptive and vestibular systems (Kotecha, Chopra et al. 2013). Indeed ‘‘normal’’ measures of body sway in people with glaucoma and healthy controls when in “quiet stance” (e.g. standing upright looking ahead with no conscious moving of arms, head, etc.), found that on a firm surface, with no visual targets there is an increase of weighting of proprioceptive and vestibular inputs (Kotecha, Richardson et al. 2012). On occasion, people with glaucoma performed even better

than controls (Kotecha, Richardson et al. 2012). This is thought to be due to the natural up weighting of the other two sensory systems because of the impaired visual system, resulting in less reliance on visual targets to stabilise themselves (Kotecha, Richardson et al. 2012).

To investigate the role of vision in postural control in people with glaucoma, methods need to be developed in order to control or systematically explore the up-weighted contributions of other sensory systems. This is important because real world functional balance often presents occasions where up-weighting of proprioceptive systems is compromised, for example when walking on a moving platform (bus, train, escalator etc.), or over uneven surfaces (sand or on deep pile carpets). Similarly, vestibular contributions may be compromised when standing on an unpredictably moving support surface, such as a boat or train. Reweighting strategies may therefore not be able to fully compensate for all real world balance activities. This provides justification to further investigate the role of vision more widely and its relationship with postural sway, in terms of visual region, for those known to have a balance impairment and episodes of falling in conjunction with visual field loss, and also to compare against control groups with an in tacked healthy visual field.

A simple method of exploring the role of vision in postural control is to record postural sway in two standardised standing positions, to observe the up weighting from the somatosensory system to the visual and vestibular. These standing positions would explore visual contribution on postural sway. The ratio difference of sway between the two visual conditions is known as Romberg's ratio (Winter 1995). Romberg's ratio is quick and simple method, but does not specifically control of the

systematic examination of the proprioceptive system. A more recently developed method is the Instrumental Clinical Test of Sensory Integration and Balance (CTSIB) test (Fling, Dutta et al. 2014) which establishes the difference between visual input (using eyes-open and eyes-closed conditions). It also identifies the role of somatosensory input on balance by measuring the difference in measures of postural sway when standing on a firm or foam (soft) surface. This method enables examination of main effects of vision and proprioception but also of interactions between manipulations of the two systems.

The use of wireless accelerometers to measure postural sway is increasing within research areas such as sports, health and exercise (Mancini, Carlson-Kuhta et al. 2012, Chen, Xu et al. 2014, Heebner, Akins et al. 2015, de Luna, Mihailovic et al. 2017), with the reliability of this method validated against other methods of postural sway measures (force platform). The placement of these sensors differ between studies as approximately 65% of studies place them within the lower back area (e.g. L3 to L5 vertebrae) (Howcroft, Kofman et al. 2013). By using this placement the centre of mass (COM) can be approximated. However a review by Cretual (2015), which discussed methods of postural sway measurement e.g. centre of pressure (COP), COM and single/double pendulum (segmental models) based on the review of (Winter 1995), found that due to technological limitations, the COP was the most largely used method ten years ago and remains the most common method. However, within this review, there is support for using the simple pendulum model, where a sensor is placed within the C7 to T1 region which denotes the cervicothoratic junction (CTJ). This method correlates sway with COP related movements and is inclusive of trunk and pelvis motion. With an anatomical higher

sensor position to that of the COM, this offers a greater sensitivity to angular change of whole body sway over time (Cretual 2015).

From the literature already discussed, there is a gap in the research, in terms of visual region and its contribution towards standing balance, and even more so in visual conditions such as glaucoma or retinitis pigmentosa. As some previous research has found an increase of postural instability in a glaucomatous population (Kotecha, Richardson et al. 2012, de Luna, Mihailovic et al. 2017), due to their decreased vision, more information of the contribution of the different visual fields (e.g. central versus peripheral) could provide a more comprehensive view. In order to do this we must also investigate the impact of visual stimuli, such as frequency, within these visual regions.

In summary, this pilot study aims to examine the relationship between vision loss and postural sway in glaucoma patients and compare overall postural sway to a control group to observe the role of vision and postural sway.

In order to meet the aim the following hypotheses will be explored:

1. **People with glaucoma will sway more in all sensorimotor standing conditions**: In order to test this hypothesis, RMS measures of angular body sway will be calculated for different test conditions, and mean measures derived for each participant. Analysis will then explore a main effect of groups (glaucoma/control) across a number of sensory factors.

2. **People with glaucoma will have a directional preponderance of body sway, in favour of the ''pitch'' direction that is associated with peripheral visual field loss, according to the functional sensitivity hypothesis**: This will be

explored by recording ''pitch'' and ''roll'' directional RMS measures of body sway, and calculating the RMS error of directional preponderance (pitch/roll) across a number of sensory factors, in both groups.

3. **People will sway more in sensorimotor standing conditions when the somatosensory system is compromised:** This will be explored by measuring the RMS of angular body sway across sensorimotor standing conditions with the same visual input and compared by firm or foam standing conditions.

4. **People will sway less in visual environments with a greater number of visual targets:** To test this hypothesis, measures of angular body sway will be calculated for different test conditions. Analysis will explore the effect of visual scene groups (i.e. no stimuli, peripheral stimuli, central stimuli and, central and peripheral stimuli) across eyes-open test conditions on firm and foam surfaces.

5. **People will sway more when visual input is unavailable:** A Romberg's ratio test will use the mean RMS measures of angular body sway in (a) eyes-open condition no stimuli, on firm surface and (b) eyes-closed on firm surface.

Balance activities can include a wide range of tasks from quite standing to climbing stairs, running and jumping. In order to ensure optimal standardisation of experimental conditions, we need to systematically examine the vision contribution in balance in people with glaucoma at an impairment level where the effect of confounding variables is minimised. This study will therefore use a simple standing task incorporating a simple pendulum model of human body sway (Mergner, Maurer et al. 2003). Body sway will be collected using a lightweight wireless motion sensor (XSens Awinda sensor, XSens, Enschede, Netherlands), which will provide measures

of speed, range and acceleration of angular motion in pitch and roll directions. Postural sway will be measured under four vision conditions (eyes-open, eyes-closed, best eye-open, worst eye-open). Monocular conditions are used due to the asymmetric damage of visual field loss caused by glaucoma (Weinreb and Khaw 2004). Postural sway will also be measured on two surfaces (firm and foam), and within four visual scenes (no stimuli, peripheral stimuli, central stimuli, and central and peripheral stimuli) to access visual cues in certain visual regions on postural stability. The sizing of the peripheral visual region will be measured up to 90°, to compare against previous work of up to 60° and to access the role of the far periphery in postural stability. This will be undertaken using a custom kinetic perimetry test (described in chapter 6) which can measure the periphery up to 90° using a quick and standardised strategy. As the kinetic perimetry test and the setup of the postural sway conditions are novel, the following will be a pilot study to evaluate any trends.

The results from the kinetic visual field test will provide a more comprehensive addition to current knowledge of the contribution of peripheral vision on the control of standing balance, by measuring an area of the visual field that is usually left unmonitored in advanced glaucoma patients. Ultimately, this procedure will provide a comparative observation of the role that visual field loss, in different visual regions, has on postural sway in people with glaucoma. The results from these tests may help in enabling more targeted future fall prevention strategies for patients with advanced vision loss.

7.2 Methods

7.2.1 Participants

After ethical approval by The University of Plymouth's Faculty of Health's Ethics and Integrity Committee, postural sway recordings were recorded from 11 glaucoma participants (median age 75 years, range = 69 to 79 years) with varying levels of visual field loss, and 12 control participants (median age 74 years, range = 68 to 81 years). Patients were screened to ensure they either have glaucoma, or do not have glaucoma (control group) see chapter 6 for more detail on this inclusion/exclusion criteria. This was defined through visual field loss using the HFA SITA-fast 24-2 visual field test (HFA, Carl Zeiss Meditec, Jena, Germany). Before attending a study session participants were screened for history of ocular disease (apart from glaucoma), no previous eye surgery apart from cataracts or glaucoma related surgery for participants with glaucoma, as they were asked to part in the additional study (chapter 6) within the same study session, and no history of comorbidities effecting lower limbs such as arthritis, hip/knee replacements or Parkinson-type disorders. This study followed the tenets of the Declaration of Helsinki.

Both groups were screened for diabetic retinopathy through the use of retinal images, analysed during the study visit, and their Best Corrected Visual Acuity (BCVA) was measured using the patient's own spectacles on the Early Treatment Diabetic Retinopathy Study (ETDRS) chart. Measures of contrast sensitivity (CS) were taken using the Mars chart, both monocular and binocularly. Eye dominance was recorded to assess the difference of eye dominance (defined a best and worst eye) on postural sway stability. An eye dominance test was used to determine the best eye in the control group, and greatest visual field loss and visual acuity was used to

define the worst eye in the glaucoma group. All participants were screened for underfoot proprioceptive loss. Participants were excluded if they had less than eight microfilament placement detections as per standard peripheral neuropathy screening using a 10gm (5.07 gauge) Jamar Semmes Weinstein test due the effects on stability. Measures of patient height and weight were recorded for the set-up and position of the sensory scene. Ascending proprioceptive thresholds using a neurothesiometer at the ankle were additionally taken. This was used as a measure of proprioceptive loss, and accessing any undisclosed ailments, which could affect proprioceptive feedback. The ascending method was chosen for less variable results. Control patients were aged matched closely against glaucoma patients to within ± 5 years.

7.2.2 Visual field evaluation

The outer border of the peripheral visual field was determined using custom designed kinetic test on an Octopus 900 control using the OPI (see chapter 5 for more detail and appendix A4 for R script). The kinetic test measured up to 90° in the temporal inferior region and 30° superiorly, as to evaluate the role of the extent of the peripheral temporal visual field on balance. The superior region above 30° can be effected by the eyelid, and this is why it is not measured in this pilot study. The test was performed twice on each eye of glaucoma patients, and only once in on each eye in the control group. It was only undertaken once in the control group as an additional study of the test/re-test of the kinetic test was only evaluated in the glaucoma group, see chapter 6 for results of this.

7.2.3 Balance evaluation

Balance data was collected using the XSens Awinda motion sensor (XSens Awinda sensor, XSens, Enschede, Netherlands), which is an accelerometer and gyroscope. This was placed on the back of the patient on the T1 vertebra, selected due to its position which is unaffected by intersegmental localised movement (e.g. arm moving, to measure whole body sway).

A standardised test of standing balance was conducted using twelve conditions, grouped by three factors: factor 1 = 4 'vision conditions' (eyes open, eyes closed, best eye open, worst eye open). Factor 2 = 2 'surface standing conditions' involving a (i) hard surface and (ii) a foam surface (10cm thickness medium density), and factor 3 = 4 'visual scenes' (no stimuli, peripheral stimuli, central stimuli, and central and peripheral stimuli). The sequence of these conditions was randomised in presentation.

Table 7.1: Visual scene, eye and surface conditions for postural sway measurements.

CONDITION NUMBER	VISUAL SCENE	EYE CONDITION	SURFACE CONDITION
1	No stimuli (1)	Eyes closed	Firm
2	No stimuli (1)	Eyes open	Firm
3	Peripheral (2)	Eyes open	Firm
4	Peripheral (2)	Eyes open	Foam
5	Central (3)	Eyes open	Firm
6	Central (3)	Eyes open	Foam
7	Cent + peri (4)	Eyes open	Firm
8	Cent + peri (4)	Eyes open	Foam
9	Cent + peri (4)	Best eye open	Firm
10	Cent + peri (4)	Worst eye open	Firm
11	Cent + peri (4)	Best eye open	Foam
12	Cent + peri (4)	Worst eye open	Foam

During each trial participants were asked to stand barefoot, to avoid the effects of shoes and/or thick socks on proprioception feedback (Robbins, Waked et al. 1995), with their arms by their sides. Feet were apart within a fixed distance (4cm) using placed markers on the floor surface which were pre-measured. Participants were asked to avoid making any conversation or purposeful voluntary movements such as head turning or arm movement during the trial (see Figure 7.1, 7.3 & 7.4 for set up). Both surfaces were cleaned between participants. Each of the 12 conditions was repeated three times to achieve an average measurement, hence 36 recordings were taken per patient (see Table 7.1 for list of conditions). All measurements were taken at a sampling frequency of 100Hz over a 40 second duration in order to measure both pitch and roll sway. The 40 second duration consisted of 5 seconds for

stabilization, 30 seconds for measurements and 5 seconds for possible fatigue. The sequence of conditions was randomized across trials to avoid habituation effects. These measurements were additionally passed through a 10Hz Butterworth low pass digital filter and a 46.1Hz Human filter, in order to remove potential noise in each recording, caused by other human factors other than the postural sway movement.

7.2.4 Visual scenes

Patients viewed four separate visual scenes (see in Figures 7.1 and 7.2). The first of these visual scenes had no visual stimuli. All visual scenes were located at a viewing distance of 70cm. The second scene was made up of 36 static dot stimuli (2cm x 2cm, with 2.5 point fade), located within 60° to 90° of the peripheral visual field (subtended at a visual angle of 30° horizontal and 60° vertically) across two boards. The third scene consisted of 36 static dot stimuli located within 60° of the central visual field (subtended at a visual angle 60° horizontal and vertically) on one board. The dot frequency was the same across the second and third scenes. The fourth scene was a combination of the central and peripheral stimuli (72 in total) located within 60° of the central visual field (subtended at a visual angle 60° horizontal and vertically) and 60° to 90° of the peripheral visual field (subtended at a visual angle of 30° horizontal and 60° vertically). The spacing of dots was equal but random, to avoid directional/pattern cues, in one corner and then mirrored into the opposite corners for equal weighting across the visual region. The contrast between the dots and the background was made high, 100%, due to glaucoma reducing contrast sensitivity (Owsley and Sloane 1987), thus dots were made highly visible to get a true effect of the visual cue on stability. These scenes were adjusted manually against the eye level height of the patients, with the central position of the scene in

line with their eyes. With this arrangement, linear horizontal and vertical structural cues could be avoided and standardised for each participant. The room illumination was approximately 25 cd/m² measured using a luminancemeter, this was achieved by having the blinds closed but room lights on during every participant measurement. This ensured that the illumination of the scenes were consistent for all participants. Participants were instructed to look straight ahead towards the middle of the board before beginning the measurement in all conditions. Once participants were positioned correctly, the measurement would begin. An eye tracker was not used in this pilot study to evaluate the gaze of participants due to the position of the peripheral cues, and the physical design of eye tracking devices. The design of eye-trackers aim central vision gaze and the outer rim would obstruct the view of the peripheral cues.

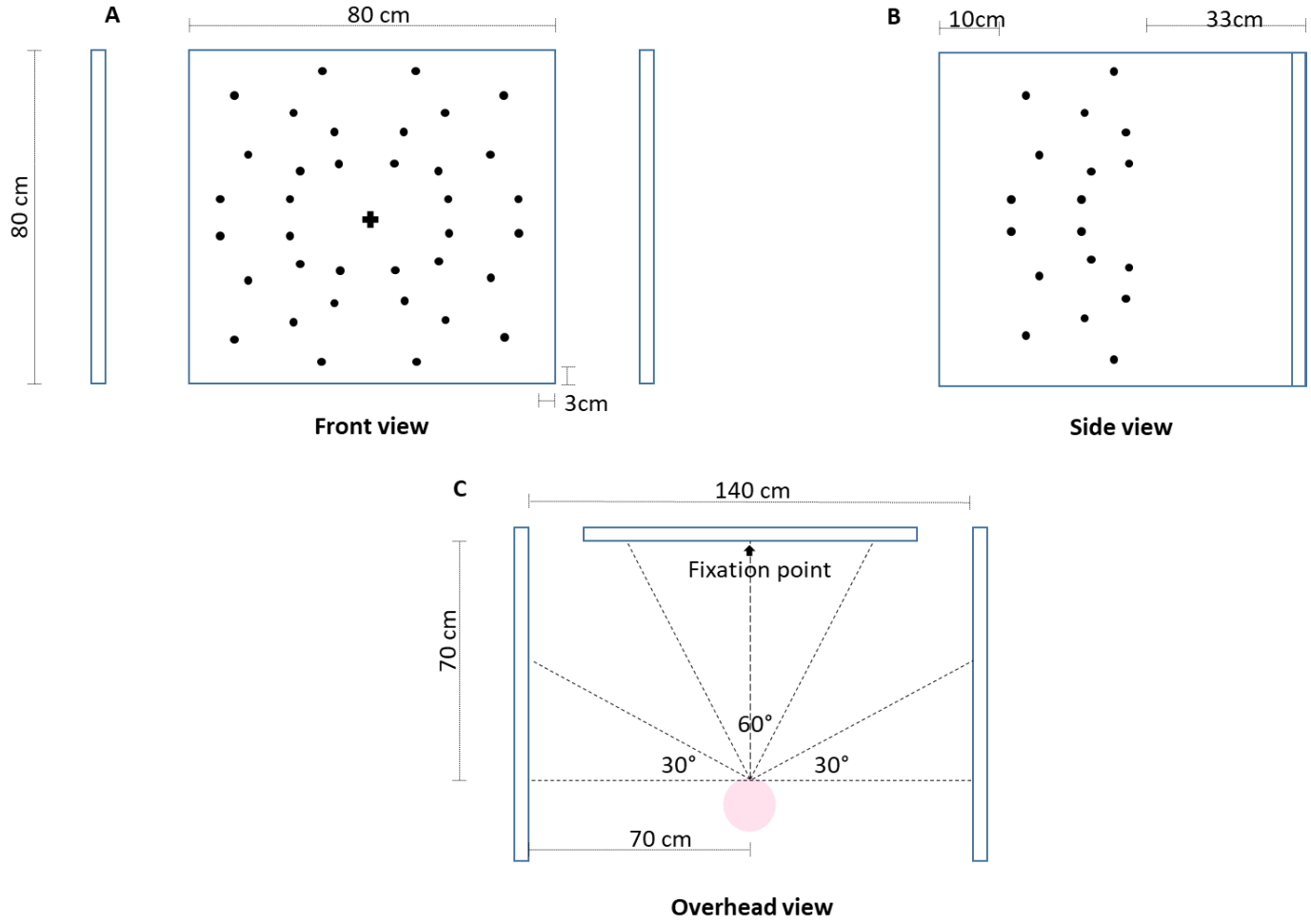

Figure 7.1: Image A shows front view the visual scene set up, with central visual field stimuli. Image B shows side view of set up with peripheral stimuli, which is mirrored on the opposite side. Image C shows overhead view of set up with angles of visual stimuli shown against participant's head position, which is denoted by the pink shaded circle. The visual environment that participants viewed is made up of 3 prepared screens aligned relative to the central head position at a standardised set distance. All scenes had no stimuli within 3 cm of the board edge.

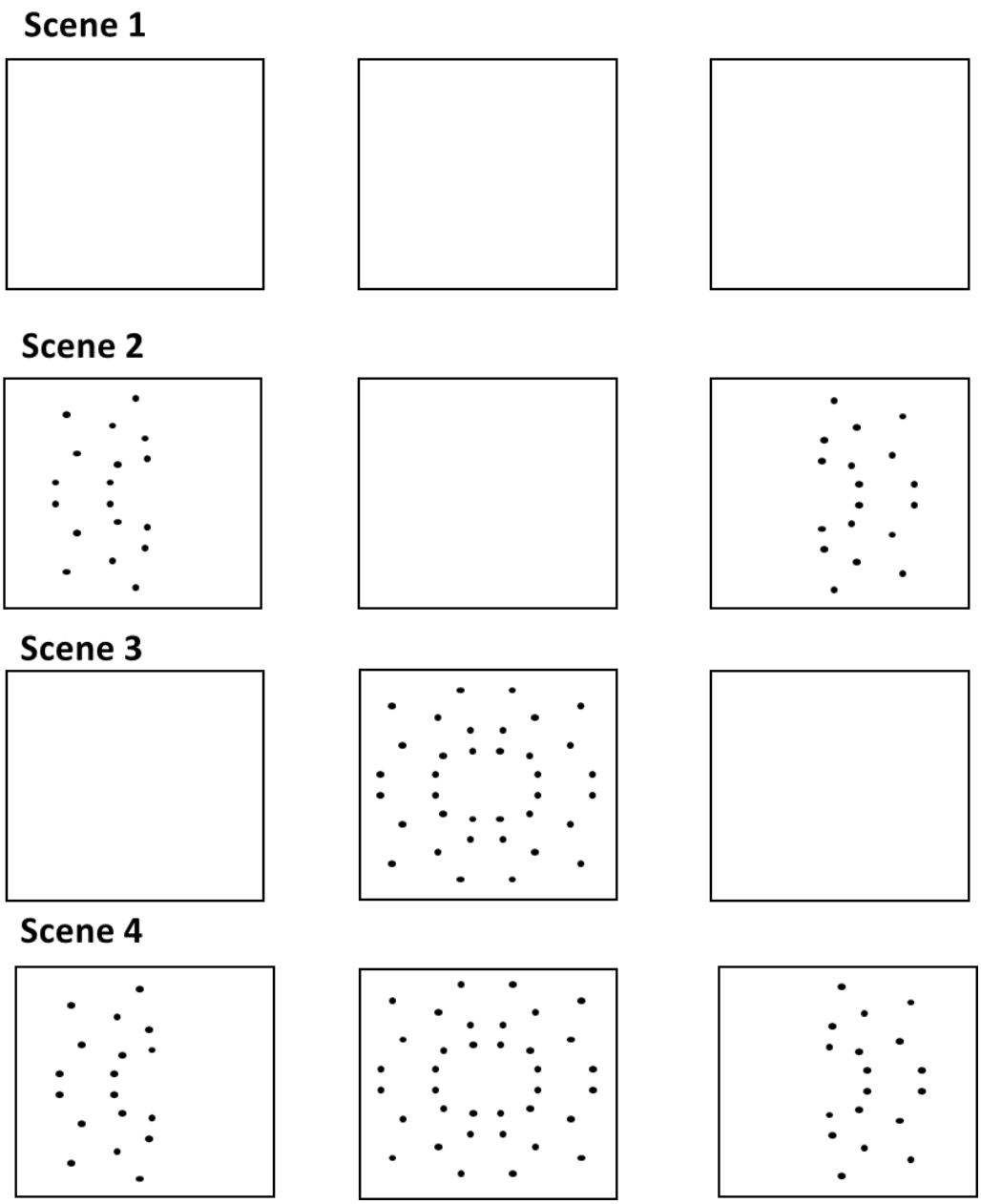

Figure 7.2: Diagram of visual scenes used for eye and surface conditions. Scene 1 is a baseline, no visual stimuli condition. Scene 2 is a peripheral visual stimuli scene, presenting stimuli within 60° to 90° of the visual field. Scene 3 presents stimuli within the central 60° of the visual field, and scene 4 presents both peripheral and central stimuli.

Figure 7.3: Postural sway set up with pilot participant standing on foam surface condition with eyes open and central + peripheral visual scene. Xsens accelerometer is attached to skin, overlying T1 vertebral spinous process, with two latex-free double sided, self-adhesive strips.

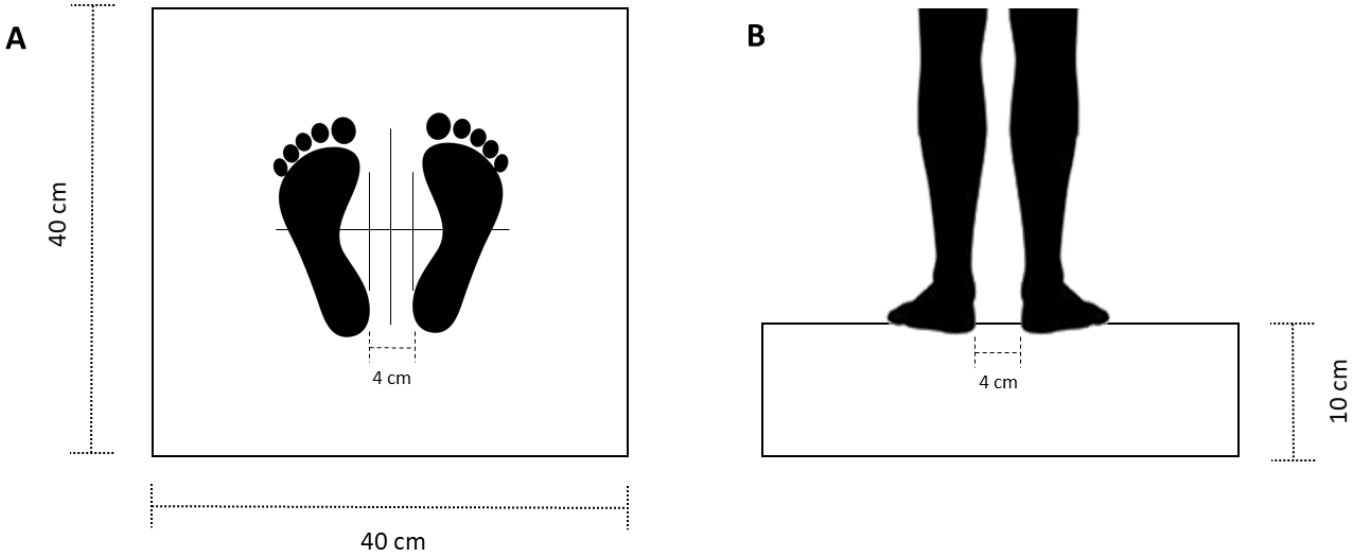

Figure 7.4: Standing position on foam surface. Panel A shows position from above, and panel B from behind. Patients were asked to stand 4cm apart. Guidelines on the firm and foam surface guided individuals towards this position before each trial. Patients undertook all trials barefoot with surfaces cleaned between use.

The mean RMS from the 30 second data collection period of body sway, and directional measures of sway in pitch and roll were evaluated across all test

conditions. Measures of sway area and mean body sway speeds represented overall measures of postural sway. RMS measures of angular ranges and directional speed measures were further explored, to test the hypothesis that participants with glaucoma sway more in the pitch than the roll directions (de Luna, Mihailovic et al. 2017), and also in general they have a greater sway speed.

7.2.5 Vision measures

To examine vision loss, the kinetic perimetry test was measured in terms of overall isopter position mean isopter position (MIP) see chapter 6 for full explanation.

7.2.6 Balance measures

To examine postural sway a measure of overall speed was used. This was derived from combined root mean squared error (RMSE) measures of directional angular velocity (angular excursion/s^2), on the post filtered data per trial and average across the three for the overall measure of RMS. Directional angular velocity was also independently assessed e.g. pitch and roll. A larger value of sway indicates more instability, as the more an individual moves the value of the measurement increases, suggesting poorer balance. Visual dependence was an additional parameter used to measure the affect vision has on postural sway; this used the Romberg's ratio, see equation below. A value exceeding 1 indicates a greater postural sway under the eyes closed condition and an up weighting of reliance on vision, this was compared against glaucoma participants and controls.

$$\textbf{Romberg's ratio} \quad \frac{\textbf{Eyes Closed (EC) RMSE}}{\textbf{Eyes Open (EO) RMSE}}$$

7.2.7 Analysis

Each patients' mean of trials was used for statistical analysis; trials, which were compromised (i.e. the full time duration was not recorded), were discarded and the mean of the remaining trials was used. The aim of the analysis was to determine if there was a difference in the amount of postural sway among the 12 conditions between and within the participant groups. The overall speed data showed a non-normal distribution, supported by Shapiro-Wilk's test which found a result ($p < 0.05$), thus the median and interquartile ranges were calculated against the hypotheses. In addition, the Romberg's ratio was calculated for overall sway measures of speed between eyes closed and eyes open conditions. A Friedman's test was used to assess within group differences. Post-hoc analysis of significant differences reported within the Freidman's test was conducted using Wilcoxon signed-rank tests with a Bonferroni correction applied due to the number of comparisons made and to control for type I error. Between, group differences across conditions were compared using a Mann Whitney U test. This analysis allowed the investigation of the practical significance for measuring postural sway in glaucoma patients. All test analysis, filtering of data and graphical output was performed using R core software (2016), the scripts for all of the above can be seen in appendix A5.

7.3 Results

As this is a pilot study, there was no pre-defined sample size determined. Approximately 50 participants were approached from a list of participants who previously consented for glaucoma research through the University of Plymouth, or participants who answered a vision research email on behalf of the University of the third age (U3A). Of those, 17 glaucoma and 13 control participants were recruited, however due to undisclosed mobility or vision issues detected during the initial

screening tests, 1 control and 6 glaucoma patients were excluded from the study. Thus, the results for 11 glaucoma and 12 control patients are reported. Any significant findings will be defined as a trend towards significance. All demographic parameters can be found in table 7.2.

Table 7.2: Demographics of glaucoma and control patients. Age is represented in years (Y), VA represents visual acuity in the best (dominant) eye and worst eye, which was measured in logMAR. Proprioceptive threshold was measured in Volts (V). Contrast sensitivity (CS) was also measured in logMAR and mean deviation (MD) used for visual field loss screening. Weight is measured in pounds (LBS) and height in centimetres (CM).

PARAMETER	GLAUCOMA (MEDIAN, RANGE)	CONTROL MEDIAN (RANGE)	MANN-WHITNEY P VALUE (EFFECT SIZE)
AGE, Y	75 (69 to 79)	74 (68 to 81)	0.5994
BETTER EYE VA	0.08 (-0.04 to 0.34)	-0.005 (-0.12 to 0.04)	0.002 (0.92)
WORST EYE VA	0.28 (0 to 0.5)	0.06 (-0.08 to 0.2)	0.005 (0.85)
BINOCULAR VA	0.08 (0 to 0.38)	0 (-0.08 to 0.02)	<0.001 (1.03)
BETTER EYE CS	1.36 (0.84 to 1.52)	1.48 (1.2 to 1.76)	0.005 (0.84)
WORST EYE CS	1.16 (0.48 to 1.36)	1.40 (0.96 to 1.64)	<0.001 (1)
BINOCULAR CS	1.32 (0.78 to 1.64)	1.6 (1.20 to 1.76)	0.010 (0.77)
BETTER EYE MD	-3.60 (-2 to -17)	-0.89 (-2.85 to 0.84)	<0.001 (1.05)
WORST EYE MD	-17.5 (-6 to -29)	-2.22 (-4.31 to 1.55)	<0.001 (1.21)
HEIGHT CM	167 (152 to 185)	172 (162 to 180)	0.621
WEIGHT LBS	134 (115 to 198)	154 (131 to 198)	0.190
THRESHOLD V	31 (23 to 39)	27 (16 to 35)	0.073

The following plot shows a graphical representation of the comparisons which will be made through this results section. Each participant had up to three individual

trials in each condition some consisted of two due to invalid trials. These trials were averaged across for overall sway speed, and also sway in pitch and roll directions.

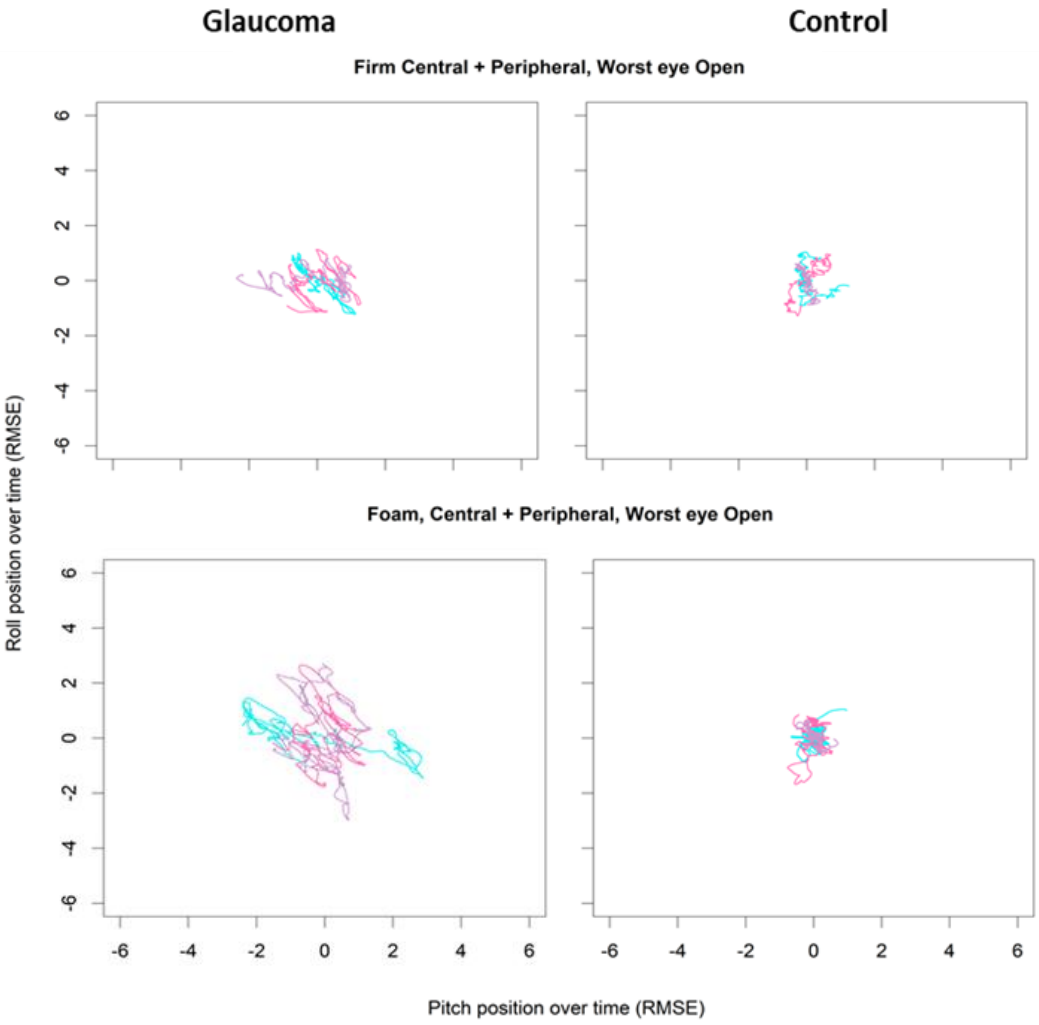

Figure 7.5: Position over time plots of a glaucoma and a control participant under the condition of central and peripheral scene, worst eye open, on firm surface (top row) and foam surface (bottom row). Different colours indicate separate trial measurements. Time measurement is 30 seconds.

7.3.1 Comparison of postural sway speed between glaucoma and control groups

When comparing overall sway speed (mm/s) between the glaucoma and control participants, there was only a trend towards significance under monocular conditions on a foam surface. A Mann-Whitney U test showed there was a significant difference (P = 0.025), for best eye open on a foam surface between

glaucoma and control participants, and a significant difference (P = 0.025) for worst eye open on foam surface between the two groups. These were both under the visual scene consisted of central and peripheral dots, and both resulted in a large effect size (0.68). These comparisons can be seen in figure 7.6. Although no other comparisons past the significance threshold of p = 0.05, there was still a trend of increased postural sway speed in the glaucoma group compared to control group across all conditions, see Figure 7.7 (see appendix A5.1 for individual condition comparisons of overall speed and in pitch and roll directions).

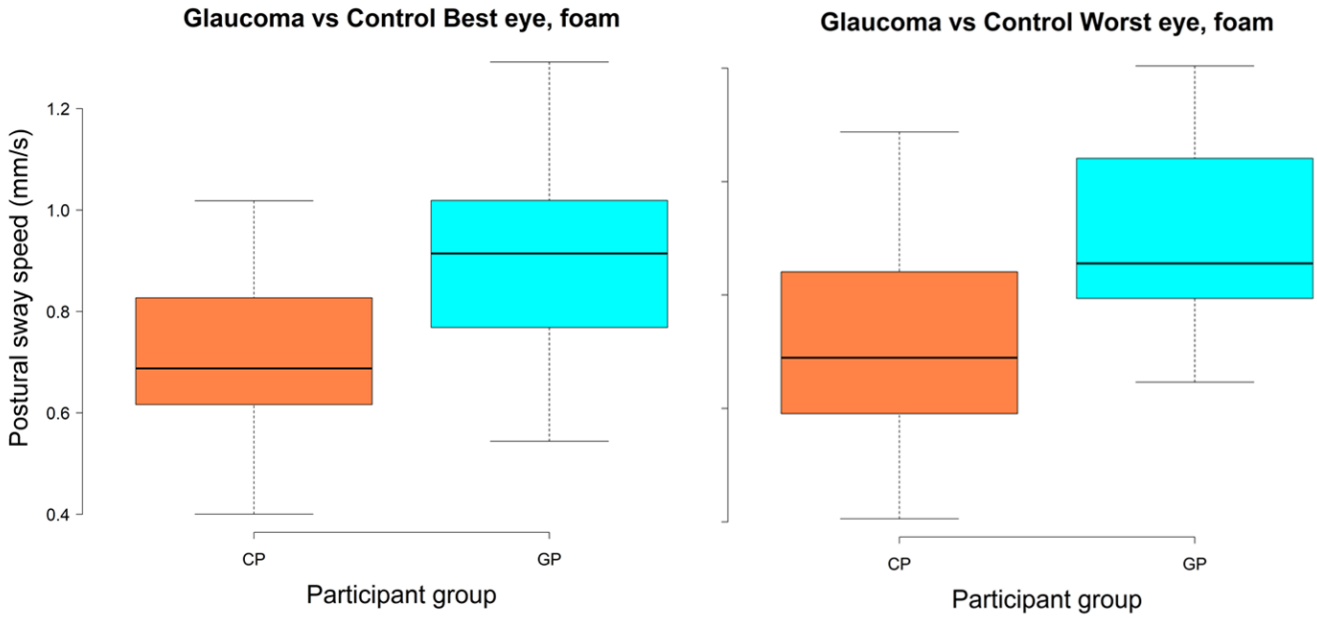

Figure 7.6: Boxplots of postural sway speed (mm/s) comparison between glaucoma (blue-GP) and control (orange-CP) groups. Left boxplots shows the difference between the groups under the best eye open condition. The right boxplot shows the difference between groups under the worst eye open condition. Both comparisons are made under the foam surface condition with the central and peripheral visual scene.

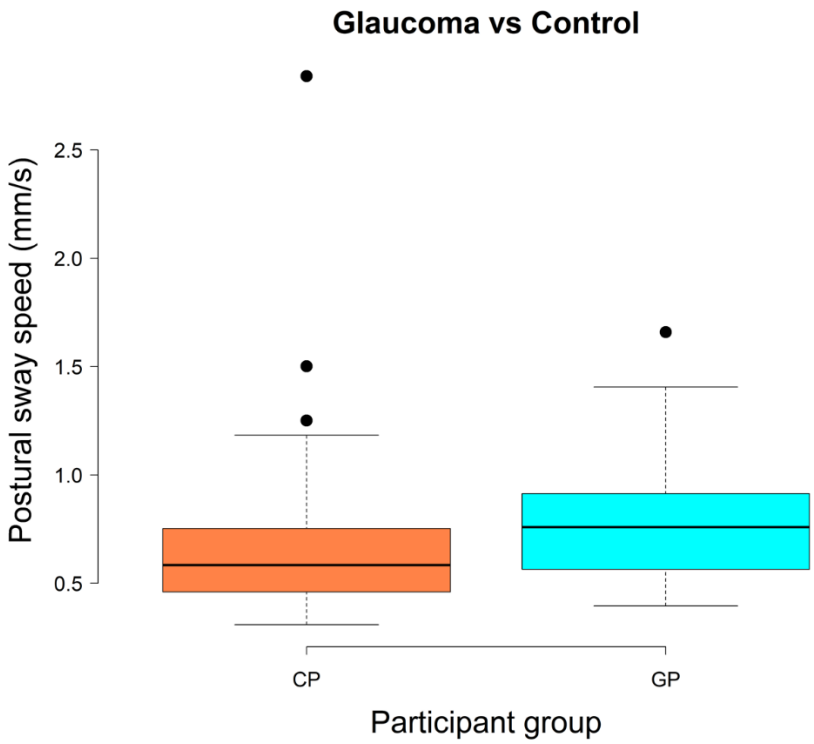

Figure 7.7: Boxplots of between group comparisons of overall postural sway spend mm/s across all 12 conditions between glaucoma (blue-GP) and control (orange-CP) participants. Black points show individuals participant outlier.

7.3.2 Glaucoma postural sway direction, pitch vs roll.

When observing directional sway RMSE (pitch/roll), no significant difference was found between the two directions of sway within the glaucoma group, although there was a small increase in the roll direction across most conditions. This does not support this study's hypothesis that the group glaucoma would sway more in the pitch direction, however might suggest a role for central vision loss within 60° in controlling roll directional sway, supportive of the functional sensitivity hypothesis.

In the control group there was a significant difference between pitch and roll in the no stimuli condition (with eyes open, firm surface), with greater sway in the roll direction, ($P = 0.024$) resulting in a large effect size 0.65. This may suggest the role of visual stimuli in the central visual field as a method for stabilising postural sway in roll in addition to proprioception. However with no peripheral stimuli in this condition either, it would be expected that there would also be increase in pitch direction resulting in no significant difference between directions, thus does not support the literature for the functional sensitivity hypothesis (Anson, Bigelow et al. 2017).

Between the glaucoma and control groups, there was an increase of directional sway in the pitch direction for the glaucoma group in all conditions. However this only showed a trend towards being statistically significant in two conditions, both eyes open, on foam with only central scene (CEOFO) ($P = 0.004$) effect size 0.86 and worst eye open on firm (CPWOF) with central and peripheral scene ($P = 0.003$) with a slightly larger effect size of 0.90. Overall sway in the pitch direction can be seen in Figure 7.8.

For the roll direction, glaucoma patients showed an increase in postural sway compared to controls. There was a trend towards significance in the conditions; peripheral scene on foam (PEOFO) (P = 0.039) effect size 0.62, and same condition again but on firm surface (PEOF) (P = 0.006) effect size 0.82. There was also a significant difference for worst eye open with central and peripheral dots on firm surface (CPWOF) (P = 0.034) effect size 0.64. See Figure 7.9 for a graphical representation of the overall difference of roll directional sway between glaucoma and control patients.

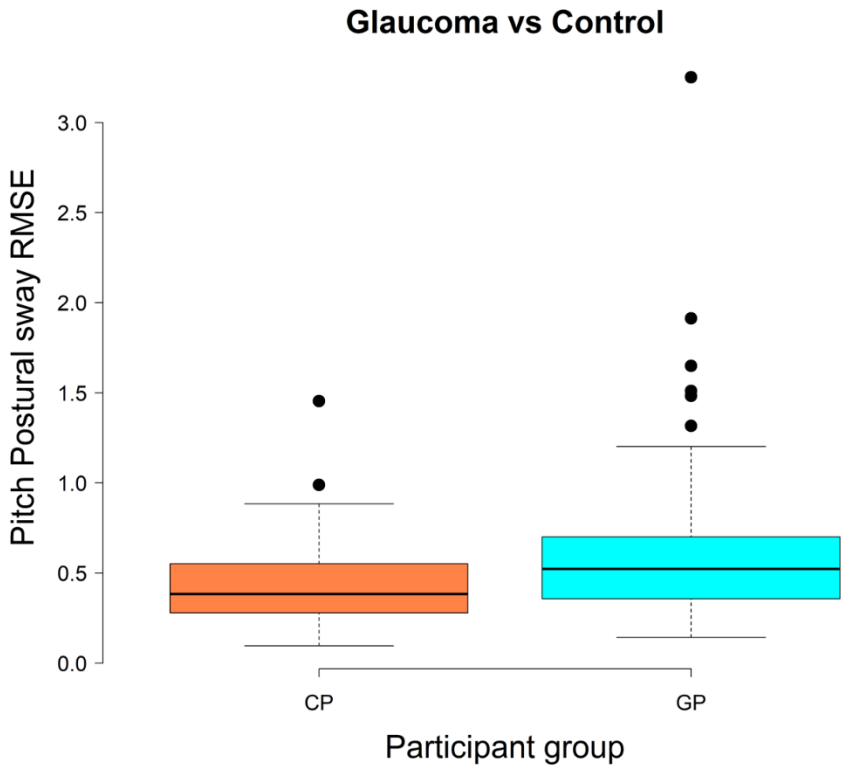

Figure 7.8: Boxplot shows RMSE of pitch sway for glaucoma (blue-GP) and control (orange-CP) groups across all conditions. Black points indicate individual outlier results.

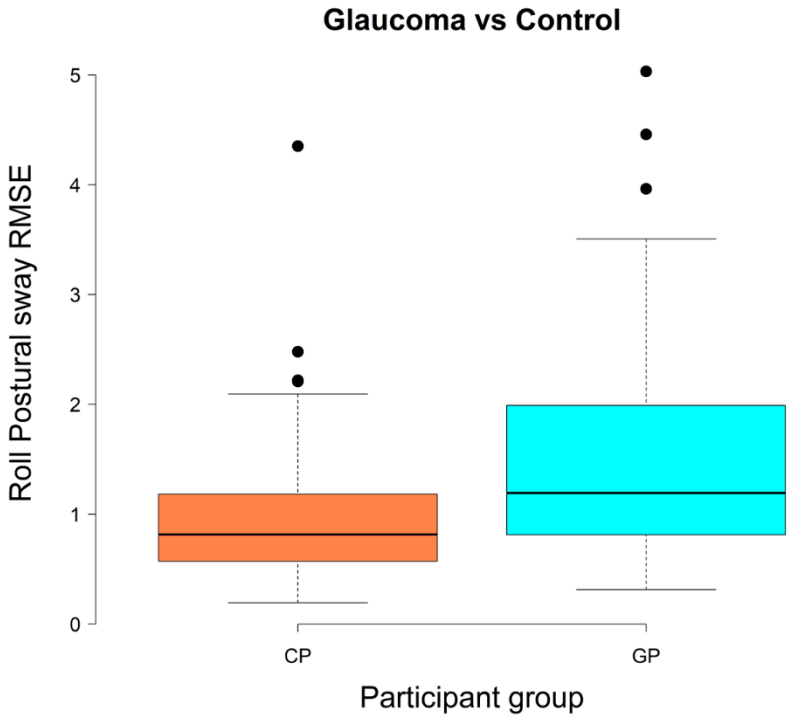

Figure 7.9: Boxplot shows RMSE of roll sway for glaucoma (blue-GP) and control (orange-CP) groups across all conditions. Black points indicate individual outlier results.

7.3.3 Firm vs Foam standing comparisons

A Wilcoxon's signed rank test was used to analyses the differences between postural sway speed in foam and firm surface conditions within groups. For glaucoma participants there was a significant difference between firm and foam surface conditions for the following visual scene conditions with both eyes open: central dots (CEOF/CEOFO) ($P = 0.015$) effect size 0.73, and central and peripheral dots (CPEOF/CPEOFO) ($P = 0.035$) effect size 0.63. The graph in Figure 7.10 shows' a side by side comparison of control and glaucoma participant's postural sway measures when standing on a firm or foam surface, under difference visual scenes. For control participants there were significant difference between firm and foam for all visual scene conditions for eyes open: peripheral dots ($P < 0.001$) effect size 0.98, central dots ($P = 0.012$) effect size 0.72, and central and peripheral dots ($P = 0.033$) effect

size 0.61. From these comparable graphs in Figure 7.10 it is possible to see the similar trend in behavior of both groups.

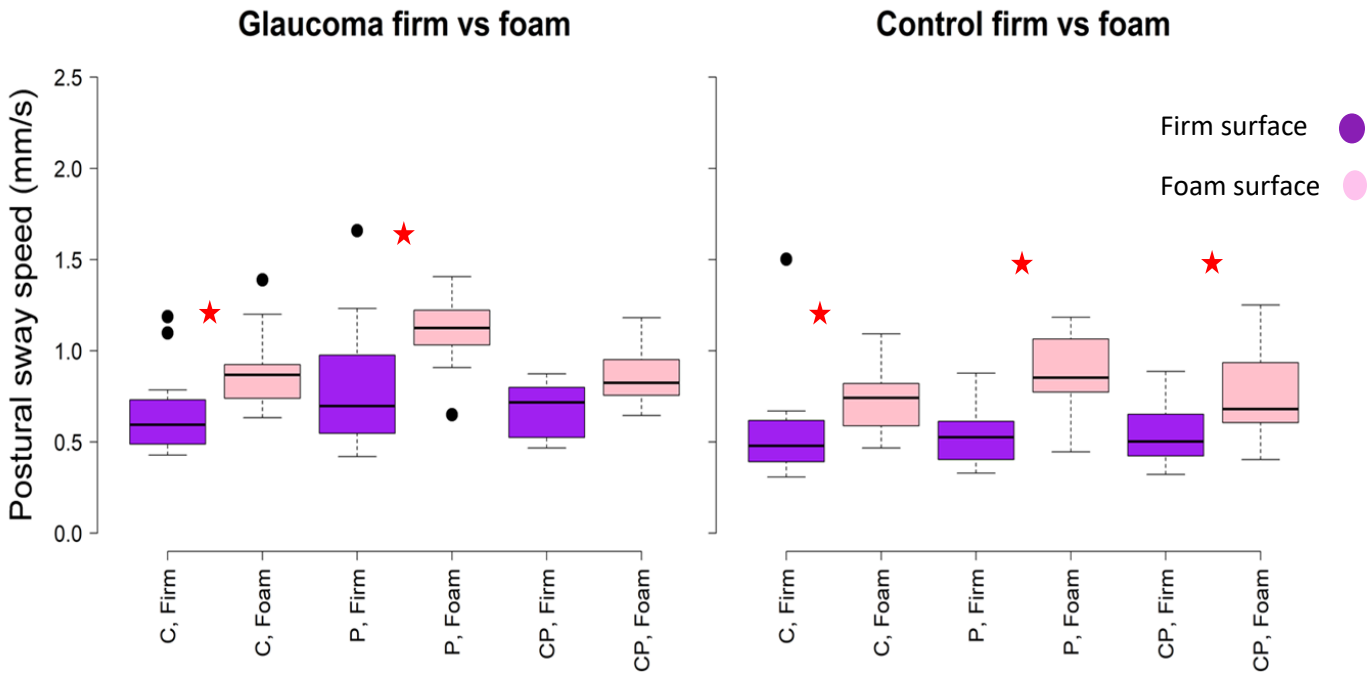

Figure 7.10: Boxplots show comparison of postural sway speed (mm/s) between firm (purple) and foam (pink) surfaces for visual scene conditions within glaucoma and control groups. C = central dots scene, P = peripheral dots scene and CP = central and peripheral dots scene. Black points indicate outliers. Significant comparisons are marked with a red star above.

7.3.4 Visual scene comparisons within and between groups.

A Friedman's test was used to analyse the differences between visual scenes in firm and foam conditions for both glaucoma and control groups under both eyes open condition. For both glaucoma and control groups there were no significant differences between visual scenes in the firm surface condition. For the glaucoma group there was a significant difference between foam conditions (P = 0.012). Posthoc analysis using a Wilcoxon's signed rank test with a Bonferroni correction found that there was only a trend towards significant difference between the central and peripheral dots, and peripheral dots visual scene (P = 0.037) effect size 0.75 (see

in Figure 7.11). There was no significant difference between visual scenes for the foam condition in the control group.

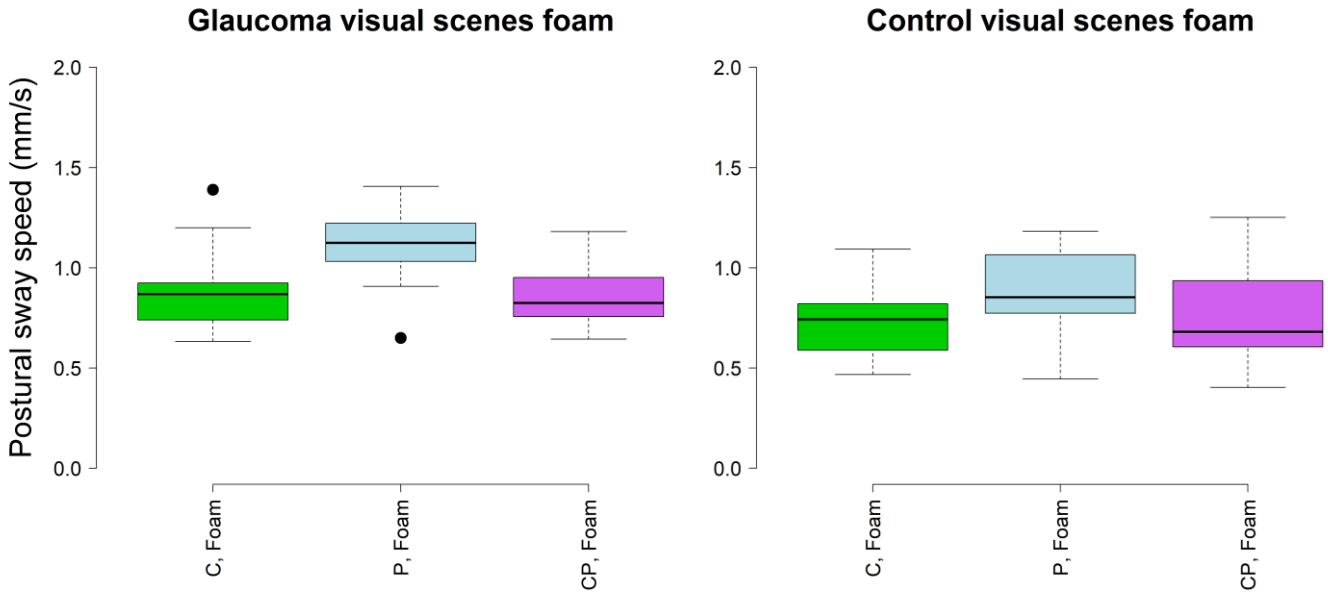

Figure 7.11: Boxplot shows comparisons of postural sway speed (mm/s) between visual scene conditions in the foam surface condition, for both glaucoma and control groups. Green = central visual scene, blue = peripheral visual scene, and purple = central and peripheral visual scene. Black points indicate outliers.

7.3.5 Visual dependence of postural sway

A Romberg's ratio test was undertaken to distinguish the visual contribution to postural sway for each patient. The median Romberg's score for glaucoma patients was 0.89, and for controls it was 1see figure 7.12 for boxplot.

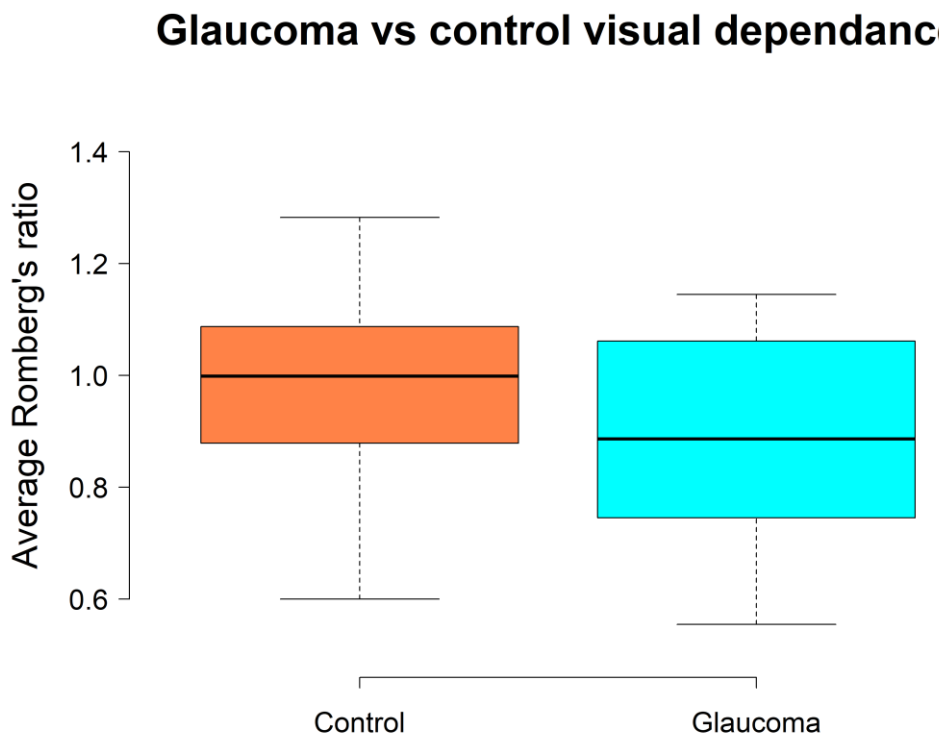

Figure 7.12: Boxplot of average Romberg's ratio for glaucoma and control groups. Orange = controls, blue = glaucoma. Control patients show more dependence on the visual system for controlling balance compared to glaucoma patients.

7.3.6 Visual field outputs in comparison to postural sway

A Spearman's rank-order correlation coefficient was undertaken to establish if there is a relationship, in the glaucoma group, between the results of the central visual field test, and the custom kinetic peripheral visual field test, with postural sway speed. These visual field outputs where correlated with the monocular visual conditions on foam and firm surfaces only as binocular visual field outputs were not determined. The results found that for the central visual field, on a foam surface there was a very small negative correlation -0.35 between best eye Mean Deviation (MD) and postural sway speed, and a very small positive correlation between worst eye MD and postural sway speed 0.02. There were also small correlations found

between MD of best and worst eye and postural sway speed on a firm surface with best eye MD and postural sway speed -0.11, and worst eye MD and postural sway speed 0.095, see figure 7.13.

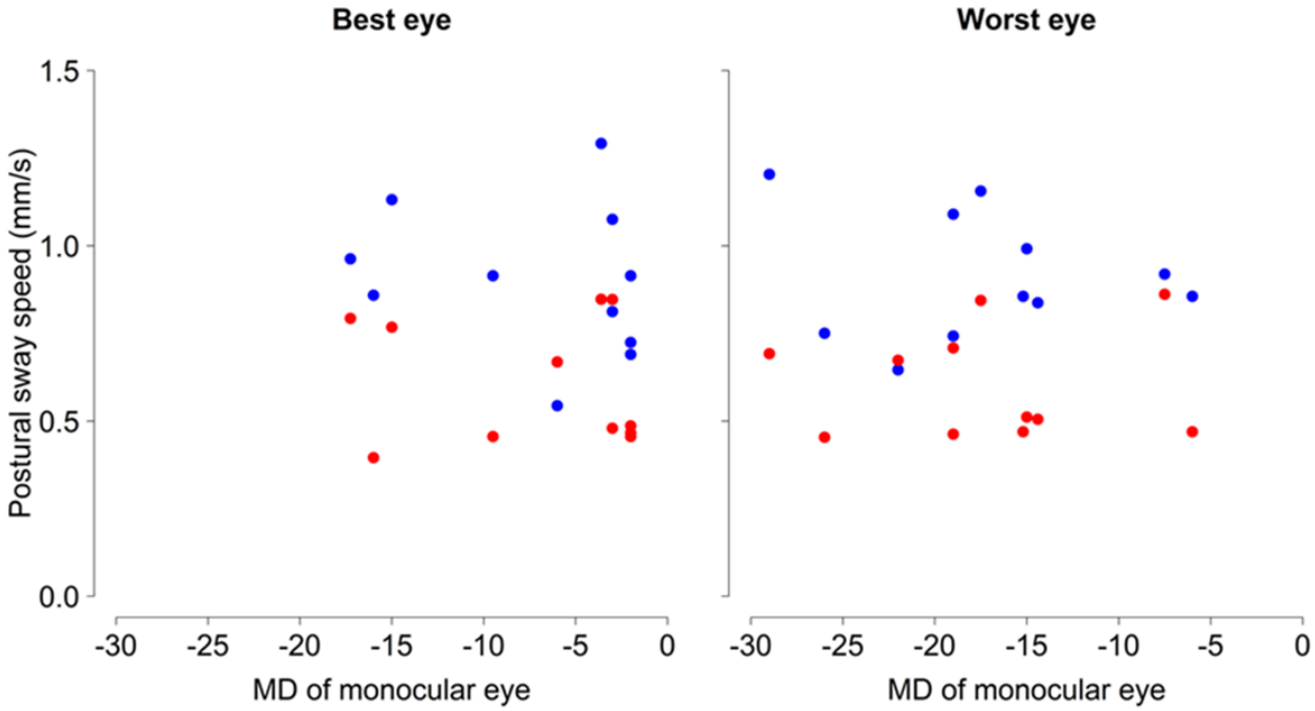

Figure 7.13: Scatterplot showing correlation between best and worst eye MD defined from the central visual field test, of glaucoma group with postural sway speed in monocular conditions (best & worst eye) on both firm (red) and foam (blue) surfaces. Y axis scales are the same for both plots.

For the kinetic test of the peripheral visual field, we used the mean isopter position (MIP, average of all positions measure) to compare the extent of the peripheral visual field against postural sway speed. A Spearman's rank-order correlation coefficient found that on a foam surface there were small negative correlation with best eye vs MIP -0.25, and worst eye vs MIP -0.35. On a firm surface there were again very small negative correlations with best eye vs MIP -0.29, and worst eye vs MIP -0.16 (see in Figure 7.14).

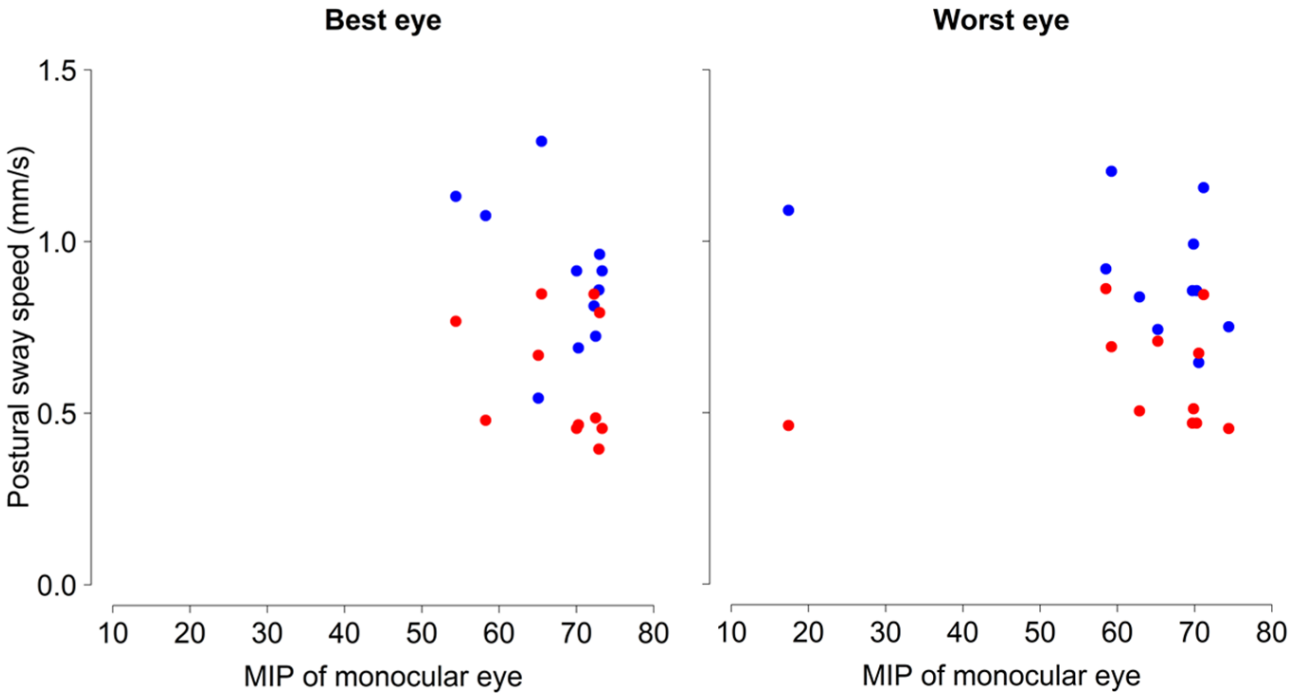

Figure 7.14: Scatter plot of correlation between MIP and postural sway speed for the glaucoma group glaucoma group with postural sway speed in monocular conditions (best & worst eye) on both firm (red) and foam (blue) surfaces. Y axis scales are the same for both plots.

7.4 Discussion

This study systematically examined the relationship between vision loss and postural sway in glaucoma patients which is inclusive of the periphery beyond 60 degrees. Consistent with past reports, participants with glaucoma were more unstable across a range of controlled visual environments and underfoot surfaces compared to age and sex matched healthy controls. This suggests that, despite the availability of largely intact proprioceptive and vestibular systems that could act in a compensatory capacity, the presence of visual impairment owing to glaucoma still translates into detectable whole body instability at an impairment level. However the contribution of the visual system is more notable in controls, as when vision is removed they are less able to rely on their proprioceptive system compared to their glaucoma counterparts. Previous findings of the peripheral visual field contributing

to pitch sway stability were not confirm, however leads to the question of what region of the periphery does contribute to balance.

The objective of this study was to evaluate the differences in postural sway under different visual and surface conditions, between healthy control and moderate to advanced glaucoma participants. This was undertaken as it has previously been seen that people with mild balance impairment caused by abnormal sensory motor control can compensate with intact single sensory systems. With this idea this study aimed to evaluate if there was overall compensated instability caused by vision loss which manifested when then compensatory ability, proprioception was reduced in a glaucomatous population. This study also evaluated the role of peripheral and central visual fields on postural sway direction and stability, with the functional hypothesis theory suggesting that central and peripheral fields control different directional postural stability, thus a glaucoma participant with vision loss located in the periphery, would sway more in a pitch direction compared to a healthy control with no vision loss. It also observed the overall impact of the central and peripheral visual field on postural stability using frequency matched visual cues.

Participants with glaucoma had increased postural sway speed across all conditions. This increase of postural instability was more noticeable across conditions where glaucoma participants were required to stand on a foam surface, where their proprioceptive input (somatosensory system) was reduced. Most noticeably there was a significant difference of postural sway measurements between glaucoma and control patients under monocular conditions on foam. This suggests the integrity of the visual system when trying to maintain postural stability. Even on firm surfaces there was a trend of greater postural sway speed in the

glaucoma patient group, thus even with proprioceptive input, the reduction in vision does have an effect on postural sway instability, this finding supports previous research (Shabana, Cornilleau-Pérès et al. 2005, Black, Wood et al. 2008).

From the results it can be suggested that in the foam surface conditions, glaucoma participants are more stable in a visual scene where stimuli are located in both the central and peripheral visual field. It could be argued that in this condition, there is a higher frequency of visual targets and a larger 'dosage' of visual environment reference cues for feedback of body sway. There was little difference found between the central only and central and peripheral visual scene. This finding suggests that visual information located in the central visual field (within 60°) is more important for postural sway stability. The peripheral stimuli only condition produce greater postural instability then the other conditions with central stimuli, suggesting that peripheral stimuli located between 60 to 90 degrees did not contribute greatly to standing stability. This finding supports the role of central vision for controlling postural stability (O'connell, Mahboobin et al. 2017), however with little research on the role of far periphery on standing balance, we cannot directly compare our results against previous findings.

The control group also showed the lack of contribution that peripheral stimuli have on stability in the foam condition compared to the other visual cue conditions, this suggests that cues the peripheral visual field outside of 60 degrees do not contribute towards standing balance. In this study we did not undertake a blank visual scene on foam condition due to patient safety. However before undertaking the peripheral scene on foam and firm conditions, participants were asked if they were aware of dots in the side of their vision. All participants reported that they were aware of

them, thus it can be suggested that these results of the peripheral stimuli only scene are not a replication of a no visual stimuli condition. This result further suggest that peripheral visual stimuli outside of 60 degrees do not contribute to standing balance.

An important part of this study was to investigate the different roles central and peripheral vision play in angular directions of postural sway, potentially supporting the functional sensitivity hypothesis (Warren and Kurtz 1992). Our findings do not directly support this theory that the peripheral visual field controls postural sway in the pitch direction, and central controls sway in the roll direction (Warren and Kurtz 1992, Agostini, Sbrollini et al. 2016). Glaucoma participants sway more in both roll and pitch angular directions compared to controls. This is expected considering they had overall greater sway speed than controls, however glaucoma participants overall swayed more in the roll direction than pitch. In accordance to the functional sensitivity theory, central vision is responsible for sway in the roll direction. With a reduction of vision in the central visual field within 60 degrees by glaucoma, our results showed an increase of sway in this roll direction. This confirms previous research which found a significant effect on roll directional sway with vision loss in the central (Black, Wood et al. 2008, de Luna, Mihailovic et al. 2017). However the definition of central field loss differs between studies, with some defining it as within 10° or less (Straube, Krafczyk et al. 1994, Nougier, Bard et al. 1997), and others within the central 30° of visual field (Black, Wood et al. 2011). This pilot study defined central vision within 60°, thus to determine the area of vision loss in this visual region, which has the greatest effect of postural sway in the roll direction, is unclear.

To further support the functional sensitivity theory the differences between the glaucoma and control groups in angular sway was observed. The results identified that in the roll direction there were significant differences between the groups in the peripheral only visual scene conditions, on foam and firm surfaces. In the pitch sway direction there was a significant difference between groups in the central visual scene, foam condition only. From these findings there does seem to be a trend towards the functional sensitivity theory (Berencsi, Ishihara et al. 2005, Agostini, Sbrollini et al. 2016), within the glaucoma group, but not the control group, possible as a result of the pattern of visual field loss. Glaucomatous visual field loss tends to develop paracentral and arch round following the path of the retinal fibers. This vison loss then progresses outward with the very central visual field being the last to go. Due to our results it could be interpreted that vision loss within 60 degrees but outside of the central say between 10 to 20 degrees may control pitch sway. This theory would also compare to previous research and their definitions of central and peripheral visual fields (Nougier, Bard et al. 1997, Black, Wood et al. 2008).

A Romberg's test was used to access the input of proprioceptive measures. This was undertaken by measuring the performance between participant groups in conditions with no visual stimuli to help stabilise oneself, and comparing postural sway speed under eyes open and eyes closed conditions. The results found that there was no significant difference between groups. However the control group did reach the threshold, with a ratio of 1. This result suggests that the control group are more reliant on their vision to control postural stability. In the glaucoma group there was not as much difference between eyes open and eyes closed. This confirms

previous findings (Agostini, Sbrollini et al. 2016, de Luna, Mihailovic et al. 2017), where individuals with vision loss rely more on their proprioceptive somatosensory system to maintain postural stability. This also supports previous work which has found glaucoma groups to be more stable than their healthy counter parts when on firm surfaces, potentially explained by the theory of compensatory up-weighting of the proprioceptive somatosensory systems (Kotecha, Chopra et al. 2013).

The results of the mean deviation from the central visual field test found a weak correlation between the visual field loss, found in the central 30 degrees of vision, with postural instability. This does not comply with previous findings, where a greater mean deviation was associated with greater postural sway instability (Black, Wood et al. 2008, Black, Wood et al. 2011, de Luna, Mihailovic et al. 2017). However these studies had much larger recruitment numbers, thus is a limitation to this study due to the small numbers. The extent of the peripheral visual field boundary, estimated using a partial isopter in the temporal inferior region, also did not have a strong correlation with postural instability. This differs from results by Yamamoto (2001) and Black (2008), again due to the small recruitment numbers, this pilot study cannot be directly compared to previous research.

There were a number of limitations of this study, with one of the main ones small sample size. Although trends were found in results, there were few significant findings. During sample measurements participants were barefoot, with their feet close together (4cm), this does not accurately replicate everyday real world conditions. The surface conditions were limited to two varieties firm/foam. Other surface conditions such as grass or tiled flooring have been suggested as conditions where an individual may lose balance more frequently. This pilot study also only

investigated static standing measures of postural sway, whereas dynamic balance has been shown as more indicative of falls (Winter 1995, Bird, Hill et al. 2012). It has been shown that the peripheral visual field is more useful for identifying situational awareness, and motion perception (Brandt, Dichgans et al. 1973, Finlay 1982). Thus future research may find that the extent of the peripheral visual field in glaucoma participants may be more predictive of postural instability in dynamic balance tests. Finally, this study did not take fitness levels of patients into account. Individuals who work our regularly have been shown to have better balance (Daley and Spinks 2000, Messier, Royer et al. 2000, Ray, Melton et al. 2012).

An additional limitation of this study if the defining degrees of the central and peripheral visual field. In this study we defined the central vision as within 60 degrees and the periphery 60 degrees outward. A large amount of research on postural sway in glaucoma patients have only examined the visual field within 30 degrees monocular or 60 degrees binocularly (Black, Wood et al. 2008, Kotecha, Richardson et al. 2012). This difference makes our results incomparable to previous research and may explain contradicting findings, however also builds the case that the visual field as a whole should be examined, as remaining vision outside of 60 degrees may be crucial for postural stability in individuals with extensive visual field loss.

In this study we were also limited by the range of visual field loss participants had. Participants were categorised by the results of the central visual field test, with a MD of -6 classed as moderate damage and -12 as advanced damage. Approximately 50% of the glaucoma participants had a MD of -20 or worst in the worst eye, however this percentage reduced to 27% of participants who had a best eye MD of -

15 or more. A larger participant sample size would allow for comparisons between moderate and advanced glaucomatous participants, and also comparisons between extend of damage binocularly and monocularly.

With increasing age having good balance is essential for preventing falls (Scuffham, Chaplin et al. 2003). In glaucoma participants it has been shown that there is an increased risk of falling (Ramulu, Van Landingham et al. 2012). As previous research, including this study, has found a relationship between vision loss and increased postural sway instability. With this study also identifying that visual cues in the far periphery do not contribute to standing balance. Further research is needed to establish the impact of advanced glaucomatous vision loss, and more specifically the role of the peripheral visual field in everyday conditions such as walking, and the impact this could have on quality of life for these population. Additionally further research in required to define the roles different visual regions, from the very central 10 degrees, out to 100 degrees, contribute to postural sway stability during either standing or dynamic balance. This could be undertaken by conducting tests of visual field as a whole and comparing the patterns of visual field loss in a large scale sample of glaucoma participants, and the impact this pattern of vision loss has on postural sway under a number of visual scene and surface conditions. The contribution of this work could warn clinicians when there may be a greater risk on quality of life for a glaucomatous population, when their vision loss encroaches on a certain area of the visual field. This type of research could influence the role of the peripheral visual field regions on balance impairment, and could also influence the monitoring of the peripheral visual field on a regular basis, which at current is not undertaken regularly due to the limitations of peripheral visual field tests.

Chapter 8: Conclusions

8 Conclusions

The development of peripheral visual field tests could contribute to the better understanding of retinal degenerations such as advanced glaucoma. They could also be used to evaluate the impact that peripheral visual field loss has on everyday life activities, and the effect that certain types of ocular surgery, such as cataracts, can have on them. These tests should be easy and fast to complete and provide clinically relevant information. These tests should also provide clinical relevant information, which could contribute to treatment and intervention decisions.

Currently, peripheral visual field tests are highly variable and not participant friendly in terms of test duration. Thus, the aim of this thesis was to access methods of measuring the peripheral visual field, and develop a kinetic perimetry test which was robust to participant errors, but easy and fast to complete.

8.1 Chapters 2 & 3: The outer limits of the far peripheral visual field

In commercial perimeters, measurements of the far-peripheral visual field are currently limited to 90°. However, research conducted using manual perimetry methods a century ago found responses even beyond 100° (Rönne 1915). Visual field tests today are computerised and conducted using commercial perimeters bowls such as the Humphrey field analyser and the Octopus 900. Due to the design of these perimeters, measurements beyond 90° are not possible. Therefore, this study aimed to adapt an Octopus 900, to allow for measurements of the outer limits of the far-peripheral visual field, replicating findings from a century ago, but using a computerised standardised method.

This study found responses to kinetic perimetry stimuli up to 108° in the temporal inferior visual field, confirming previous manual perimetry findings. The results from this simple adaption allowed for the distribution of responses to kinetic perimetry to be investigated, and the evaluation of different methods of limits: ascending and descending (Blackwell 1946, Herrick 1965). This kinetic distribution of responses was then used in further studies (Chapter 3) to develop a robust and fast kinetic perimetry visual field test.

8.2 Chapter 4: Measuring the extent of the peripheral visual field and identifying negative dysphotopsia in pseudophakic patients.

The exact cause and position of the visual phenomenon known as negative dysphotopsia in the visual field is poorly understood. It occurs after uncomplicated cataract surgery in approximately 15 to 20% of patients (Davison 2000), however after several weeks or months the phenomenon disappears and is only bothersome in around 2% of patients (Osher 2008). A number of theories have been established as to the exact cause of negative dysphotopsia, however none have been proven thus far (Osher 2008). Manual and automated perimetry methods have been used to measure the position of the “shadow” reported by patients, however these are lengthy tests and have high variability (Makhotkina, Berendschot et al. 2016). The new lens placed in the eye is smaller and thinner than the crystalline lens, thus the ability to produce images at large visual angles may be reduced (Simpson 2016). This study used the novel technique of extended fixation to allow the full extent of the temporal visual field to be measured. It also used ascending and descending methods to estimate the outer boundary of the visual field, and to detect the possible presence of a shadow in the temporal peripheral visual field. The findings of this study reported that the temporal peripheral visual field in patients who have

undergone cataract surgery is reduced by approximately 10°. The presence of negative dysphotopsia was identified in two patients, supporting the use of descending in conjunction with the usual ascending kinetic perimetry method as a novel and fast technique to estimate the position of the visual phenomena, and measure the overall effect of the new smaller lens. This study influences the measurement of the peripheral visual field in all populations and not only those with retinal degeneration of the periphery. It also suggests that future design of new IOLs should take the size of the lens into account due to the possible clinical implications. A possible example of a clinical implication would be the effect a smaller peripheral visual field could have on dynamic balance.

8.3 Chapter 5: Simulating response behaviours to kinetic perimetry: An adaptive algorithm.

Kinetic perimetry tests take a relatively long time to undertake, and are susceptible to outlier responses, resulting in “spikes” in isopters. Previous research has tried to develop strategies to account for these responses, e.g., Program K (Hashimoto, Matsumoto et al. 2015), or adding additional stimulus presentations (Mönter, Crabb et al. 2017). However, with this gain in precision, a longer test is the end result. A great deal of research has been undertaken to develop static perimetry strategies which are robust to patient errors, and can be undertaken within a clinically relevant time (Bengtsson and Heijl 1998, Heijl, Patella et al. 2019). Thus, the aim of this study was to create simulations to evaluate kinetic perimetry strategies, using the distribution of responses to kinetic perimetry stimuli collected in Chapter 3. The simulations found that between 2 and 5 responses were required to estimate a precise isopter position, depending on the response variability of the individual. The criterion to decide when to add additional presentations was based upon the

distance between the first two responses. If this distance between responses was greater than 5° then additional presentations were made until either the distance between any two responses was less than 5° or a maximum of 5 presentations was used. The median was found to produce the most precise estimate to quantify the isopter position. The results of these simulations found that by using the designed strategy, measuring only a partial isopter of the temporal inferior visual field, consisting of 7 positions, a test could be estimated to take approximately 3 minutes. This is comparable to current static visual field test durations. This simulation could be implemented in a clinical test, as a fast method to quantify whether there is intact vision left is certain areas of the peripheral visual field. This would improve upon the manual option of identifying fingers in the periphery and could be used to monitor progression of retinal diseases such as glaucoma.

8.4 Chapter 6: An automated kinetic perimetry algorithm: Test-Retest variability of measures of the inferior temporal visual field in glaucomatous visual field loss.

Previous research has found that central and peripheral fields can be remarkably different in patients with advanced glaucoma (Mönter, Crabb et al. 2017). The aim of this study was to apply the newly developed kinetic perimetry strategy (see in Chapter 5) in a group of patients with moderate to advanced glaucoma and evaluate the performance. This study also aimed to highlight the importance of measuring the peripheral visual field in individuals with advanced vision loss, as some vision may still be preserved, which is currently not monitored using central visual field tests. The results of this study found that the test-retest variability of the kinetic strategy was low and not affected by learning effects. The test estimated the inferior temporal visual field in approximately 2 minutes, improving upon simulation estimates. This test could be relevant in the clinical decisions for patients with

advanced glaucoma. Identifying areas of peripheral vision left unaffected by the disease could help to establish the importance of the peripheral visual field and why in patients with similar central visual field tests some can move around independently while others need a guide. By using a quick test like this progression of vision loss in the periphery could be monitored in populations with retinal diseases and also the effect of loss in certain peripheral visual field areas have on quality of life could be evaluated.

8.5 Chapter 7: Postural sway and the peripheral visual field in glaucoma.

Previous research found that glaucoma patients with vision loss can have poorer postural sway stability (Black, Wood et al. 2011, de Luna, Mihailovic et al. 2017) and are at a higher risk of falling (de Luna, Mihailovic et al. 2017). However there is conflicting evidence on the true effect of vision loss on balance, due to the up-weighting of responsibility to other balance systems, e.g., proprioceptive, in glaucoma patients (Peterka 2002). Previous studies have also only evaluated the role that central vision has on balance (Black, Wood et al. 2011, Kotecha, Richardson et al. 2012) and there is also limited evidence on the effects the peripheral visual field beyond 60° has on postural stability. This study investigated the difference in postural sway stability between advanced glaucoma and healthy controls. This was undertaken on a number of different surfaces and visual environments to establish the impact of vision loss and visual region on postural sway. In this study, the "functional sensitivity theory" was also examined. The results of this study found a trend in glaucoma patients having more postural sway instability. This was more noticeable in foam surface and when the better eye was occluded. This study found that glaucoma patients do up-weight more responsibility to other balance systems, however when these balance systems are compromised the impact of vision loss on

balance is more evident. Although there was no significant finding to support the "functional sensitivity theory" in this study, peripheral vision has been found to contribute towards motion perception (Finlay 1982), thus could be relevant for dynamic balance. These findings outline the importance of the monitoring the peripheral visual field in patients with advanced vision loss, as the remaining functional vision is crucial for guiding their way through everyday activities and maintaining their independence.

8.6 Limitations and additional considerations of current work.

There were several potential sources of error throughout these studies that were not controlled, including small sample sizes and small range of participants' ages. Additional sources of error could have arisen from the fatigue effects of repeated measurements of kinetic perimetry stimuli and undisclosed medical histories.

In Chapter 3, the distribution of kinetic responses was collected from a group of participants with a relatively low age range. It has been found in previous studies that response variability can increase with age (Schiefer, Strasburger et al. 2001). This distribution of responses from a young population was used to simulate a kinetic strategy for a group of patients with advanced glaucoma. The age range of an advanced glaucoma population is generally older than 60 years. However, in the simulations, differing levels of response variability were accounted for, thus the age range of this kinetic distribution should not have had a significant effect on strategy development. Repeated measurements using kinetic perimetry can incur fatigue effects, or loss of concentration by subjects which can result in unreliable kinetic visual field results. To minimise this effect, participants were given regular rest breaks in between tests.

In Chapter 4, two participants out of 30 identified having bothersome negative dysphotopsia. For one of these participants the phenomenon disappeared after they had cataract surgery on the other eye; this occurred during the study time duration. Thus, we were only able to undertake a test-retest of the kinetic perimetry method on this patient. A larger cohort of participants who report negative dysphotopsia would allow a more reliable result of the test and help to determine the position of the shadow in the visual field.

In chapter 6 and 7, the sample sizes were relatively small. This was due to the balance and test-retest study sharing the same participants and conducted during the same study session, thus if a participant did not meet the inclusion and exclusion criteria for both studies, they were excluded. Approximately 18 glaucoma participants were recruited, however a few participants had undisclosed vision and balance issues, thus making them ineligible to complete all the study assessments. Control participant numbers aimed to be kept even with the number of glaucoma to reduce bias of results. Both of these studies had newly developed stimuli designs/tests and as a result, they were defined as pilot studies. As a result, there were not predetermined recruitment numbers. Future larger scales trials would be useful to identify the true effect of these studies.

8.7 Clinical implications and future work.

8.7.1 Chapter 2 & 3: The outer limits of the far peripheral visual field

The adapted Octopus perimeter allowed for the outer extent of the peripheral visual field to be estimated using the conventional ascending kinetic perimetry method. This extended fixation method could be used to evaluate the role the far-peripheral visual field in certain tasks such as motion detection or colour perception. Future work could develop on the design of the laser to allow for smoother, more

standardised movements. This could also be incorporated into the experimental coding, thus that the program and laser work together, rather than controlled individually. This device incorporation with the kinetic strategy designed in this thesis could be used clinically for the early visual field loss detection in individuals with retinitis pigmentosa which often starts in the far-periphery.

8.7.2 Chapter 4: Measuring the extent of the peripheral visual field and identifying negative dysphotopsia in pseudophakic patients.

The results of this pilot study could allow for a better understanding of the position and size of negative dysphotopsia. In doing so, possible future links could be made to determine the exact cause. Applying this kinetic method in a larger group of patients with negative dysphotopsia would allow for further verification of the method. This information gathered could then be applied in ray tracing, to form a better understanding of the cause of negative dysphotopsia and allow simulations to be generated and see if the shadow does occur in the position measure in experimental set-ups.

8.7.3 Chapter 6: An automated kinetic perimetry algorithm: Test-Retest variability of measures of the inferior temporal visual field in glaucomatous visual field loss.

The findings from this study demonstrate that the kinetic adaptive strategy designed is reliable and fast. This strategy has the ability to measure the temporal and inferior visual field within approximately 2 minutes. Future work could incorporate supra-threshold static perimetry methods within the measured isopter position, to possess an overall view of the peripheral visual field in patients with advanced glaucoma.

8.7.4 Chapter 7: Postural sway and the peripheral visual field in glaucoma.

This study found that individuals with advanced glaucoma sway more compared to their control counterparts, particularly when the feedback of the proprioceptive

system is reduced and they are more reliant on their vision. The results from this study suggests that the far peripheral visual field beyond 60 degrees does not contribute towards standing balance, however it may be more involved in dynamic balance, which could be investigated in future work. This study also identified a possible link to the “functional sensitivity theory” with vision loss within the central 60 degrees of vision causing greater postural sway in the roll direction. The results of this study supports the importance of visual system for standing balance. Future work should examine vision loss in specific visual regions in both the peripheral, and central visual field in advanced glaucoma participants, and how this effects both standing and dynamic balance. The contribution of this kind of work could warn clinicians when there may be a greater risk on quality of life for a glaucomatous population, and can also influence the importance of measuring the peripheral visual field in this population on a regular basis.

9 Bibliography

Abu-Amero, K. K., et al. (2006). "Mitochondrial abnormalities in patients with primary open-angle glaucoma." Investigative ophthalmology & visual science **47**(6): 2533-2541.

Agostini, V., et al. (2016). "The role of central vision in posture: Postural sway adaptations in Stargardt patients." Gait & posture **43**: 233-238.

Alfonso, J. F., et al. (2007). "Correlation of pupil size with visual acuity and contrast sensitivity after implantation of an apodized diffractive intraocular lens." Journal of Cataract & Refractive Surgery **33**(3): 430-438.

Allison, K., et al. (2020). "Epidemiology of glaucoma: The past, present, and predictions for the future." Cureus **12**(11).

Anderson, D. R. and V. M. Patella (1992). "Automated static perimetry."

Anson, E., et al. (2017). "Loss of peripheral sensory function explains much of the increase in postural sway in healthy older adults." Frontiers in aging neuroscience **9**: 202.

Artes, P. H. and B. C. Chauhan (2005). "Longitudinal changes in the visual field and optic disc in glaucoma." Progress in retinal and eye research **24**(3): 333-354.

Artes, P. H., et al. (2010). "Longitudinal and cross-sectional analyses of visual field progression in participants of the Ocular Hypertension Treatment Study." Archives of Ophthalmology **128**(12): 1528-1532.

Artes, P. H., et al. (2002). "Properties of perimetric threshold estimates from Full Threshold, SITA Standard, and SITA Fast strategies." Investigative ophthalmology & visual science **43**(8): 2654-2659.

Artes, P. H., et al. (2014). "Visual field progression in glaucoma: what is the specificity of the Guided Progression Analysis?" Ophthalmology **121**(10): 2023-2027.

Arundale, K. (1978). "An investigation into the variation of human contrast sensitivity with age and ocular pathology." British journal of ophthalmology **62**(4): 213-215.

Åsman, P. and A. Heijl (1992). "Glaucoma hemifield test: automated visual field evaluation." Archives of Ophthalmology **110**(6): 812-819.

Aulhorn, E. and H. Harms (1972). Visual perimetry. Visual psychophysics, Springer**:** 102-145.

Balestrucci, P., et al. (2017). "Effects of visual motion consistent or inconsistent with gravity on postural sway." Experimental brain research **235**(7): 1999-2010.

Bardy, B. G., et al. (1999). "The role of central and peripheral vision in postural control duringwalking." Perception & psychophysics **61**(7): 1356-1368.

Barela, J. A., et al. (2014). "Explicit and implicit knowledge of environment states induce adaptation in postural control." Neuroscience letters **566**: 6-10.

Barford, A., et al. (2006). "Life expectancy: women now on top everywhere: during 2006, even in the poorest countries, women can expect to outlive men." BMJ: British Medical Journal **332**(7545): 808.

Bengtsson, B. and A. Heijl (1998). "Evaluation of a new perimetric threshold strategy, SITA, in patients with manifest and suspect glaucoma." Acta Ophthalmologica Scandinavica **76**(3): 268-272.

Bengtsson, B. and A. Heijl (2008). "A visual field index for calculation of glaucoma rate of progression." American journal of ophthalmology **145**(2): 343-353.

Bengtsson, B., et al. (1998). "Evaluation of a new threshold visual field strategy, SITA, in normal subjects." Acta Ophthalmologica Scandinavica **76**(2): 165-169.

Bengtsson, B., et al. (1997). "A new generation of algorithms for computerized threshold perimetry, SITA." Acta Ophthalmologica Scandinavica **75**(4): 368-375.

Berencsi, A., et al. (2005). "The functional role of central and peripheral vision in the control of posture." Human movement science **24**(5-6): 689-709.

Berry, V., et al. (1966). "An evaluation of differences between two observers plotting and measuring visual fields." Canadian journal of ophthalmology. Journal canadien d'ophtalmologie **1**(4): 297.

Bird, M.-L., et al. (2012). "A randomized controlled study investigating static and dynamic balance in older adults after training with Pilates." Archives of physical medicine and rehabilitation **93**(1): 43-49.

Black, A. A., et al. (2011). "Inferior field loss increases rate of falls in older adults with glaucoma." Optometry and vision science **88**(11): 1275-1282.

Black, A. A., et al. (2008). "Visual impairment and postural sway among older adults with glaucoma." Optometry and vision science **85**(6): 489-497.

Blackwell, H. R. (1946). "Contrast thresholds of the human eye." JOSA **36**(11): 624-643.

Bland, J. M. and D. Altman (1986). "Statistical methods for assessing agreement between two methods of clinical measurement." The Lancet **327**(8476): 307-310.

Boland, M. V. and H. A. Quigley (2007). "Risk factors and open-angle glaucoma: classification and application." Journal of glaucoma **16**(4): 406-418.

Bournas, P., et al. (2007). "Dysphotopsia after cataract surgery: comparison of four different intraocular lenses." Ophthalmologica **221**(6): 378-383.

Brandt, T., et al. (1973). "Differential effects of central versus peripheral vision on egocentric and exocentric motion perception." Experimental brain research **16**(5): 476-491.

Brigell, M., et al. (1998). "Guidelines for calibration of stimulus and recording parameters used in clinical electrophysiology of vision." Documenta ophthalmologica **95**(1): 1-14.

Broadway, D. C. (2012). "Visual field testing for glaucoma–a practical guide." Community Eye Health **25**(79-80): 66.

Broman, A. T., et al. (2008). "Estimating the rate of progressive visual field damage in those with open-angle glaucoma, from cross-sectional data." Investigative ophthalmology & visual science **49**(1): 66-76.

Burton, R., et al. (2012). "Glaucoma and reading: exploring the effects of contrast lowering of text." Optometry and vision science **89**(9): 1282-1287.

Bussel, I. I., et al. (2014). "OCT for glaucoma diagnosis, screening and detection of glaucoma progression." British journal of ophthalmology **98**(Suppl 2): ii15-ii19.

Chang, R. T. and K. Singh (2013). "Myopia and glaucoma: diagnostic and therapeutic challenges." Current opinion in ophthalmology **24**(2): 96-101.

Chauhan, B., et al. (2005). "Central corneal thickness and progression of the visual field and optic disc in glaucoma." British journal of ophthalmology **89**(8): 1008-1012.

Chauhan, B. C., et al. (2008). "Practical recommendations for measuring rates of visual field change in glaucoma." British journal of ophthalmology.

Chauhan, B. C., et al. (2009). "Incidence and rates of visual field progression after longitudinally measured optic disc change in glaucoma." Ophthalmology **116**(11): 2110-2118.

Chen, T.-Z., et al. (2014). "Postural sway in idiopathic rapid eye movement sleep behavior disorder: A potential marker of prodromal Parkinson' s disease." Brain research **1559**: 26-32.

Collins, C. C., et al. (1975). "Muscle tension during unrestrained human eye movements." The Journal of physiology **245**(2): 351-369.

Cook, C. and P. Foster (2012). "Epidemiology of glaucoma: what's new?" Canadian Journal of Ophthalmology **47**(3): 223-226.

Cooke, D. L., et al. (2013). "Resolution of negative dysphotopsia after laser anterior capsulotomy." Journal of Cataract & Refractive Surgery **39**(7): 1107-1109.

Crabb, D. P., et al. (2013). "How does glaucoma look?: patient perception of visual field loss." Ophthalmology **120**(6): 1120-1126.

Cretual, A. (2015). "Which biomechanical models are currently used in standing posture analysis?" Neurophysiologie Clinique/Clinical Neurophysiology **45**(4-5): 285-295.

Crundall, D., et al. (2002). "Attending to the peripheral world while driving." Applied Cognitive Psychology: The Official Journal of the Society for Applied Research in Memory and Cognition **16**(4): 459-475.

Daley, M. J. and W. L. Spinks (2000). "Exercise, mobility and aging." Sports medicine **29**(1): 1-12.

Damgaard-jensen, l. (1977). "Vertical steps in isopters at the hemiopic border—in normal and glaucomatous eyes." Acta ophthalmologica **55**(1): 111-122.

Davison, J. A. (2000). "Positive and negative dysphotopsia in patients with acrylic intraocular lenses2." Journal of Cataract & Refractive Surgery **26**(9): 1346-1355.

de Luna, R. A., et al. (2017). "The Association of Glaucomatous Visual Field Loss and Balance." Translational Vision Science & Technology **6**(3): 8-8.

De Moraes, C. G., et al. (2017). "Detection and measurement of clinically meaningful visual field progression in clinical trials for glaucoma." Progress in retinal and eye research **56**: 107-147.

De Moraes, C. G., et al. (2013). "Visual field progression outcomes in glaucoma subtypes." Acta ophthalmologica **91**(3): 288-293.

de Moraes, C. G., et al. (2016). "Management of advanced glaucoma: characterization and monitoring." Survey of ophthalmology **61**(5): 597-615.

Dhital, A., et al. (2010). "Visual loss and falls: a review." Eye **24**(9): 1437.

Drake, M. V. and D. Hetherington (1990). The visual fields: text and atlas of clinical perimetry, Mosby.

Drance, S., et al. (2001). "Risk factors for progression of visual field abnormalities in normal-tension glaucoma." American journal of ophthalmology **131**(6): 699-708.

Druault, A. (1898). "Sur la production des anneaux colorés autour des flammes; description d'un anneau physiologique." Arch d'Ophtalmol **18**: 312-321.

Elliott, D. B. (1987). "Contrast sensitivity decline with ageing: a neural or optical phenomenon?" Ophthalmic and Physiological Optics **7**(4): 415-419.

Engbert, R. and R. Kliegl (2004). "Microsaccades keep the eyes' balance during fixation." Psychological science **15**(6): 431-431.

Ernest, P. J., et al. (2016). "Prediction of glaucomatous visual field progression using baseline clinical data." Journal of glaucoma **25**(2): 228-235.

Fankhauser, F., et al. (1977). "Some aspects of the automation of perimetry." Survey of ophthalmology **22**(2): 131-141.

Farkas, R. H. and C. L. Grosskreutz (2001). "Apoptosis, neuroprotection, and retinal ganglion cell death: an overview." International ophthalmology clinics **41**(1): 111-130.

Finlay, D. (1982). "Motion perception in the peripheral visual field." Perception **11**(4): 457-462.

Flammer, J., et al. (2002). "The impact of ocular blood flow in glaucoma." Progress in retinal and eye research **21**(4): 359-393.

Fling, B. W., et al. (2014). "Associations between proprioceptive neural pathway structural connectivity and balance in people with multiple sclerosis." Frontiers in human neuroscience **8**: 814.

Folden, D. V. (2013). "Neodymium: YAG laser anterior capsulectomy: surgical option in the management of negative dysphotopsia." Journal of Cataract & Refractive Surgery **39**(7): 1110-1115.

Foster, P. J., et al. (2002). "The definition and classification of glaucoma in prevalence surveys." British journal of ophthalmology **86**(2): 238-242.

Fraser, S., et al. (1999). "Risk factors for late presentation in chronic glaucoma." Investigative ophthalmology & visual science **40**(10): 2251-2257.

Freeman, E. E., et al. (2007). "Visual field loss increases the risk of falls in older adults: the Salisbury eye evaluation." Investigative ophthalmology & visual science **48**(10): 4445-4450.

Friedman, D. S., et al. (2007). "Glaucoma and mobility performance: the salisbury eye evaluation project." Ophthalmology **114**(12): 2232-2237. e2231.

Friedman, D. S., et al. (2006). "The prevalence of open-angle glaucoma among blacks and whites 73 years and older: the Salisbury Eye Evaluation Glaucoma Study." Archives of Ophthalmology **124**(11): 1625-1630.

Gessesse, G. W. and K. F. Damji (2013). "Advanced glaucoma: management pearls." Middle East African journal of ophthalmology **20**(2): 131.

Gloor, B., et al. (1984). "Recent advances in the study of glaucomatous field defects using the Octopus Automated Perimeter." Klinische Monatsblätter für Augenheilkunde **184**(4): 249-253.

Goldmann, H. (1946). "Demonstration unseres neuen Projektionskugelperimeters samt theoretischen und klinischen Bemerkungen über Perimetrie." Ophthalmologica **111**(2-3): 187-192.

Gordon, M. O., et al. (2002). "The Ocular Hypertension Treatment Study: baseline factors that predict the onset of primary open-angle glaucoma." Archives of Ophthalmology **120**(6): 714-720.

Green, C. M., et al. (2007). "How significant is a family history of glaucoma? Experience from the Glaucoma Inheritance Study in Tasmania." Clinical & Experimental Ophthalmology **35**(9): 793-799.

Grødum, K., et al. (2005). "Risk of glaucoma in ocular hypertension with and without pseudoexfoliation." Ophthalmology **112**(3): 386-390.

Grover, S., et al. (1998). "Patterns of visual field progression in patients with retinitis pigmentosa." Ophthalmology **105**(6): 1069-1075.

Guo, Z., et al. (2017). "Optical coherence tomography analysis based prediction of Humphrey 24-2 visual field thresholds in patients with glaucoma." Investigative ophthalmology & visual science **58**(10): 3975-3985.

Gupta, N., et al. (2006). "Depth perception deficits in glaucoma suspects." British journal of ophthalmology **90**(8): 979-981.

Gwinn, O. S. and F. Jiang (2020). "Hemispheric asymmetries in deaf and hearing during sustained peripheral selective attention." The Journal of Deaf Studies and Deaf Education **25**(1): 1-9.

Haas, A., et al. (1986). "Influence of age on the visual fields of normal subjects." American journal of ophthalmology **101**(2): 199-203.

Hannibal, J., et al. (2017). "Melanopsin expressing human retinal ganglion cells: Subtypes, distribution, and intraretinal connectivity." Journal of Comparative Neurology **525**(8): 1934-1961.

Hartridge, H. (1919). "The limit to peripheral vision." Journal of Physiology **53**: 17.

Hashimoto, S., et al. (2015). "Development of a new fully automated kinetic algorithm (program K) for detection of glaucomatous visual field loss." Investigative ophthalmology & visual science **56**(3): 2092-2099.

Haymes, S. A., et al. (2007). "Risk of falls and motor vehicle collisions in glaucoma." Investigative ophthalmology & visual science **48**(3): 1149-1155.

Heebner, N. R., et al. (2015). "Reliability and validity of an accelerometry based measure of static and dynamic postural stability in healthy and active individuals." Gait & posture **41**(2): 535-539.

Heijl, A. (1987). The implications of the results of computerized perimetry in normals for the statistical evaluation of glaucomatous visual fields. Glaucoma update III, Springer**:** 115-122.

Heijl, A. and S. M. Drance (1981). A clinical comparison of three computerized automatic perimeters in the detection of glaucoma defects. Fourth International Visual Field Symposium Bristol, April 13–16, 1980, Springer.

Heijl, A. and C. Krakau (1975). "An automatic static perimeter, design and pilot study." Acta ophthalmologica **53**(3): 293-310.

Heijl, A., et al. (1989). "Test-retest variability in glaucomatous visual fields." American journal of ophthalmology **108**(2): 130-135.

Heijl, A., et al. (1987). A package for the statistical analysis of visual fields. Seventh International Visual Field Symposium, Amsterdam, September 1986, Springer.

Heijl, A., et al. (2012). The field analyzer primer: effective perimetry, Carl Zeiss Meditec Incorporated.

Heijl, A., et al. (2019). "A new sita perimetric threshold testing algorithm: construction and a multicenter clinical study." American journal of ophthalmology **198**: 154-165.

Henderson, B. A., et al. (2016). "New preventative approach for negative dysphotopsia." Journal of Cataract & Refractive Surgery **42**(10): 1449-1455.

Herndon, L. W., et al. (2004). "Central corneal thickness as a risk factor for advanced glaucoma damage." Archives of Ophthalmology **122**(1): 17-21.

Herrick, R. M. (1965). PSYCHOPHYSICAL METHODOLOGY I. COMPARISON OF THRESHOLDS OF THE METHOD OF LIMITS AND OF THE METHOD OF CONSTANT STIMULI, NAVAL AIR DEVELOPMENT CENTER JOHNSVILLE PA AEROSPACE MEDICAL RESEARCH DEPT.

Hirasawa, K. and N. Shoji (2014). "Learning effect and repeatability of automated kinetic perimetry in healthy participants." Current eye research **39**(9): 928-937.

Hodapp, E., et al. (1993). Clinical decisions in glaucoma, Mosby Inc.

Holladay, J. T. and M. J. Simpson (2017). "Negative dysphotopsia: causes and rationale for prevention and treatment." Journal of Cataract & Refractive Surgery **43**(2): 263-275.

Horak, F. B. (2006). "Postural orientation and equilibrium: what do we need to know about neural control of balance to prevent falls?" Age and Ageing **35**(suppl_2): ii7-ii11.

Hou, F., et al. (2016). "Evaluating the performance of the quick CSF method in detecting contrast sensitivity function changes." Journal of vision **16**(6): 18-18.

Howcroft, J., et al. (2013). "Review of fall risk assessment in geriatric populations using inertial sensors." Journal of neuroengineering and rehabilitation **10**(1): 91.

Huber, P. J. (1972). "The 1972 wald lecture robust statistics: A review." The Annals of Mathematical Statistics **43**(4): 1041-1067.

Huisingh, C., et al. (2015). "The driving visual field and a history of motor vehicle collision involvement in older drivers: a population-based examination." Investigative ophthalmology & visual science **56**(1): 132-138.

Hulsman, C. A., et al. (2001). "Is open-angle glaucoma associated with early menopause? The Rotterdam Study." American journal of epidemiology **154**(2): 138-144.

Investigators, A. G. I. S. (1994). "Advanced Glaucoma Intervention Study: 2. Visual field test scoring and reliability." Ophthalmology **101**(8): 1445-1455.

Jacobs, D. S., et al. (2016). "Open-angle glaucoma: epidemiology, clinical presentation, and diagnosis." In: UpToDate, UpToDate, Waltham, MA, USA, Accessed on May **14**.

Jacobs, N. and I. Patterson (1985). "Variability of the hill of vision and its significance in automated perimetry." British journal of ophthalmology **69**(11): 824-826.

Jampel, H. D., et al. (2002). "Correlation of the binocular visual field with patient assessment of vision." Investigative ophthalmology & visual science **43**(4): 1059-1067.

Jampel, H. D., et al. (2002). "Glaucoma patients' assessment of their visual function and quality of life." Journal of glaucoma **11**(2): 154-163.

Jeka, J., et al. (2000). "Multisensory information for human postural control: integrating touch and vision." Experimental brain research **134**(1): 107-125.

Johnson, C. A., et al. (1992). "Properties of staircase procedures for estimating thresholds in automated perimetry." Investigative ophthalmology & visual science **33**(10): 2966-2974.

Johnson, C. A. and J. L. Keltner (1987). "Optimal rates of movement for kinetic perimetry." Archives of Ophthalmology **105**(1): 73-75.

Johnson, C. A., et al. (1979). "Suprathreshold static perimetry in glaucoma and other optic nerve disease." Ophthalmology **86**(7): 1278-1286.

Johnson, C. A., et al. (2016). "Development and Reliability of the Tangent Corner Test (TCT) Visual Field Evaluation." Investigative ophthalmology & visual science **57**(12): 5977-5977.

Jonas, J. B., et al. (1992). "Human optic nerve fiber count and optic disc size." Investigative ophthalmology & visual science **33**(6): 2012-2018.

Ju, W.-K., et al. (2007). "Elevated hydrostatic pressure triggers mitochondrial fission and decreases cellular ATP in differentiated RGC-5 cells." Investigative ophthalmology & visual science **48**(5): 2145-2151.

Katz, J., et al. (1997). "Estimating progression of visual field loss in glaucoma." Ophthalmology **104**(6): 1017-1025.

Kessel, L., et al. (2016). "Indication for cataract surgery. Do we have evidence of who will benefit from surgery? A systematic review and meta-analysis." Acta ophthalmologica **94**(1): 10-20.

Khan, F. A., et al. (2017). "Comparison of the Long-term and Short-term Fluctuations of Frequency-Doubling Technology Perimetry Between Peripheral and Paracentral Zones of Visual Field." Journal of the College of Physicians and Surgeons--Pakistan: JCPSP **27**(3): 140-144.

Kim, J. A., et al. (2014). "Clinical Characteristics and Patient's Satisfaction in Pseudophakic Negative Dysphotopsia." Journal of the Korean Ophthalmological Society **55**(5): 669-678.

King, A. J., et al. (2011). "Treating patients presenting with advanced glaucoma—should we reconsider current practice?" British journal of ophthalmology **95**(9): 1185-1192.

Kiser, A. K., et al. (2005). "Reliability and consistency of visual acuity and contrast sensitivity measures in advanced eye disease." Optometry and vision science **82**(11): 946-954.

Kotecha, A., et al. (2013). "Dual tasking and balance in those with central and peripheral vision loss." Investigative ophthalmology & visual science **54**(8): 5408-5415.

Kotecha, A., et al. (2012). "Balance control in glaucoma." Investigative ophthalmology & visual science **53**(12): 7795-7801.

Krauzlis, R. J., et al. (2017). "Neuronal control of fixation and fixational eye movements." Philosophical Transactions of the Royal Society B: Biological Sciences **372**(1718): 20160205.

Kuo, A. D., et al. (1998). "Effect of altered sensory conditions on multivariate descriptors of human postural sway." Experimental brain research **122**(2): 185-195.

Kwon, Y. H., et al. (2001). "Rate of visual field loss and long-term visual outcome in primary open-angle glaucoma." American journal of ophthalmology **132**(1): 47-56.

LeBlanc, R. P., et al. (1985). Peripheral nasal field defects. Sixth International Visual Field Symposium, Springer.

Lee, P. P., et al. (2006). "A multicenter, retrospective pilot study of resource use and costs associated with severity of disease in glaucoma." Archives of Ophthalmology **124**(1): 12-19.

Lee, S. S.-Y., et al. (2017). "Effect of glaucoma on eye movement patterns and laboratory-based hazard detection ability." PloS one **12**(6): e0178876.

Leske, M. C. (2007). "Open-angle glaucoma—an epidemiologic overview." Ophthalmic epidemiology **14**(4): 166-172.

Leske, M. C., et al. (2003). "Factors for glaucoma progression and the effect of treatment: the early manifest glaucoma trial." Archives of Ophthalmology **121**(1): 48-56.

Leske, M. C., et al. (2008). "Risk factors for incident open-angle glaucoma: the Barbados Eye Studies." Ophthalmology **115**(1): 85-93.

Leske, M. C., et al. (2007). "Nine-year incidence of open-angle glaucoma in the Barbados Eye Studies." Ophthalmology **114**(6): 1058-1064.

Lewis, T. L. and D. Maurer (1992). "The development of the temporal and nasal visual fields during infancy." Vision Research **32**(5): 903-911.

Li, S. G., et al. (1979). "Clinical experiences with the use of an automated perimeter (otopus) in the diagnosis and management of patients with glaucoma and neurologic diseases." Ophthalmology **86**(7): 1302-1312.

Lopez, D., et al. (2011). "RelatedFalls, injuries from falls, health related quality of life and mortality in older adults with vision and hearing impairment—Is there a gender difference?" Maturitas **69**(4): 359-364.

Lynn, J. (1991). "Evaluation of automated kinetic perimetry (AKP) with the Humphrey Field Analyser." Perimetry update **1990**: 433-452.

Makhotkina, N. Y., et al. (2016). "Objective evaluation of negative dysphotopsia with Goldmann kinetic perimetry." Journal of Cataract & Refractive Surgery **42**(11): 1626-1633.

Makhotkina, N. Y., et al. (2018). "Effect of supplementary implantation of a sulcus-fixated intraocular lens in patients with negative dysphotopsia." Journal of Cataract & Refractive Surgery **44**(2): 209-218.

Mancini, M., et al. (2012). "Postural sway as a marker of progression in Parkinson's disease: a pilot longitudinal study." Gait & posture **36**(3): 471-476.

Marcus, M. W., et al. (2011). "Myopia as a risk factor for open-angle glaucoma: a systematic review and meta-analysis." Ophthalmology **118**(10): 1989-1994. e1982.

Marella, M., et al. (2010). "The psychometric validity of the NEI VFQ-25 for use in a low-vision population." Investigative ophthalmology & visual science **51**(6): 2878-2884.

Masket, S. and N. R. Fram (2011). "Pseudophakic negative dysphotopsia: surgical management and new theory of etiology." Journal of Cataract & Refractive Surgery **37**(7): 1199-1207.

Masket, S., et al. (2018). "Surgical management of negative dysphotopsia." Journal of Cataract & Refractive Surgery **44**(1): 6-16.

Masket, S., et al. (2019). "Neuroadaptive changes in negative dysphotopsia during contralateral eye occlusion." Journal of Cataract & Refractive Surgery **45**(2): 242-243.

Mckendrick, A. M. and A. Turpin (2005). "Combining perimetric suprathreshold and threshold procedures to reduce measurement variability in areas of visual field loss." Optometry and vision science **82**(1): 43-51.

McNaught, A. I., et al. (2000). "Accuracy and implications of a reported family history of glaucoma: experience from the Glaucoma Inheritance Study in Tasmania." Archives of Ophthalmology **118**(7): 900-904.

Mergner, T., et al. (2003). "A multisensory posture control model of human upright stance." Progress in brain research **142**: 189-202.

Messier, S. P., et al. (2000). "Long-term exercise and its effect on balance in older, osteoarthritic adults: results from the Fitness, Arthritis, and Seniors Trial (FAST)." Journal of the American Geriatrics Society **48**(2): 131-138.

Mills, R. P., et al. (1986). "Comparison of quantitative testing with the Octopus, Humphrey, and Tübingen perimeters." American journal of ophthalmology **102**(4): 496-504.

Mönter, V. M., et al. (2017). "Reclaiming the periphery: automated kinetic perimetry for measuring peripheral visual fields in patients with glaucoma." Investigative ophthalmology & visual science **58**(2): 868-875.

Morgan, R. K., et al. (1991). "Statpac 2 glaucoma change probability." Archives of Ophthalmology **109**(12): 1690-1692.

Munnerlyn, C. R., et al. (1981). Automated kinetic perimetry apparatus and method, Google Patents.

Murata, H., et al. (2013). "Identifying areas of the visual field important for quality of life in patients with glaucoma." PloS one **8**(3): e58695.

Narváez, J., et al. (2005). "Negative dysphotopsia associated with implantation of the Z9000 intraocular lens." Journal of Cataract & Refractive Surgery **31**(4): 846-847.

Nelson, P., et al. (2003). "Quality of life in glaucoma and its relationship with visual function." Journal of glaucoma **12**(2): 139-150.

Nevalainen, J., et al. (2008). "The use of semi-automated kinetic perimetry (SKP) to monitor advanced glaucomatous visual field loss." Graefe's archive for clinical and experimental ophthalmology **246**(9): 1331-1339.

Ng, W. S., et al. (2010). "The effect of socio-economic deprivation on severity of glaucoma at presentation." British journal of ophthalmology **94**(1): 85-87.

Niederhauser, S. and D. S. Mojon (2002). "In kinetic perimetry high refractive errors also influence the isopter position outside the central 30 degrees." Klinische Monatsblätter für Augenheilkunde **219**(4): 201-205.

Niederhauser, S. and D. S. Mojon (2002). "Normal isopter position in the peripheral visual field in Goldmann kinetic perimetry." Ophthalmologica **216**(6): 406-408.

Nitta, K., et al. (2017). "Is high myopia a risk factor for visual field progression or disk hemorrhage in primary open-angle glaucoma?" Clinical ophthalmology (Auckland, NZ) **11**: 599.

Nougier, V., et al. (1997). "Contribution of central and peripheral vision to the regulation of stance." Gait & posture **5**(1): 34-41.

Nouri-Mahdavi, K., et al. (2004). "Predictive factors for glaucomatous visual field progression in the Advanced Glaucoma Intervention Study." Ophthalmology **111**(9): 1627-1635.

Nowomiejska, K., et al. (2018). "Analysis of visual field defects obtained with semiautomated kinetic perimetry in patients with Leber hereditary optic neuropathy." Journal of Ophthalmology **2018**.

Nowomiejska, K., et al. (2005). "Comparison between semiautomated kinetic perimetry and conventional Goldmann manual kinetic perimetry in advanced visual field loss." Ophthalmology **112**(8): 1343-1354.

Nowomiejska, K., et al. (2015). "Semi-automated kinetic perimetry provides additional information to static automated perimetry in the assessment of the remaining visual field in end-stage glaucoma." Ophthalmic and Physiological Optics **35**(2): 147-154.

Ntim-Amponsah, C., et al. (2004). "Prevalence of glaucoma in an African population." Eye **18**(5): 491.

O'connell, C., et al. (2017). "Effects of acute peripheral/central visual field loss on standing balance." Experimental brain research **235**(11): 3261-3270.

Osaadon, P., et al. (2014). "A review of anti-VEGF agents for proliferative diabetic retinopathy." Eye **28**(5): 510-520.

Osher, R. H. (2008). "Negative dysphotopsia: long-term study and possible explanation for transient symptoms." Journal of Cataract & Refractive Surgery **34**(10): 1699-1707.

Owsley, C. (2003). "Contrast sensitivity." Ophthalmology Clinics **16**(2): 171-177.

Owsley, C., et al. (1983). "Contrast sensitivity throughout adulthood." Vision Research **23**(7): 689-699.

Owsley, C. and M. E. Sloane (1987). "Contrast sensitivity, acuity, and the perception of'real-world'targets." British journal of ophthalmology **71**(10): 791-796.

Patel, P., et al. (2018). "Effects of sex hormones on ocular blood flow and intraocular pressure in primary open-angle glaucoma: a review." Journal of glaucoma **27**(12): 1037-1041.

Paulus, W., et al. (1984). "Visual stabilization of posture: physiological stimulus characteristics and clinical aspects." Brain **107**(4): 1143-1163.

Pelli, D. G. (1985). "Uncertainty explains many aspects of visual contrast detection and discrimination." JOSA A **2**(9): 1508-1532.

Pelli, D. G. and P. Bex (2013). "Measuring contrast sensitivity." Vision Research **90**: 10-14.

Peterka, R. J. (2002). "Sensorimotor integration in human postural control." Journal of neurophysiology **88**(3): 1097-1118.

Peterka, R. J. (2003). "Simplifying the complexities of maintaining balance." IEEE Engineering in Medicine and Biology Magazine **22**(2): 63-68.

Peters, D., et al. (2013). "Lifetime risk of blindness in open-angle glaucoma." American journal of ophthalmology **156**(4): 724-730.

Peters, D., et al. (2015). "Visual impairment and vision-related quality of life in the Early Manifest Glaucoma Trial after 20 years of follow-up." Acta ophthalmologica **93**(8): 745-752.

Phu, J., et al. (2018). "Differences in static and kinetic perimetry results are eliminated in retinal disease when psychophysical procedures are equated." Translational Vision Science & Technology **7**(5): 22-22.

Pineles, S. L., et al. (2006). "Automated combined kinetic and static perimetry: an alternative to standard perimetry in patients with neuro-ophthalmic disease and glaucoma." Archives of Ophthalmology **124**(3): 363-369.

Polastri, P. F., et al. (2012). "Dynamics of inter-modality re-weighting during human postural control." Experimental brain research **223**(1): 99-108.

Posner, M. I. (1980). "Orienting of attention." Quarterly journal of experimental psychology **32**(1): 3-25.

Powell, S. K. and R. J. Olson (1995). "Incidence of retinal detachment after cataract surgery and neodymium: YAG laser capsulotomy." Journal of Cataract & Refractive Surgery **21**(2): 132-135.

Quigley, H. A., et al. (1991). "Larger optic nerve heads have more nerve fibers in normal monkey eyes." Archives of Ophthalmology **109**(10): 1441-1443.

Quigley, H. A. and S. Vitale (1997). "Models of open-angle glaucoma prevalence and incidence in the United States." Investigative ophthalmology & visual science **38**(1): 83-91.

Racette, L., et al. (2016). Visual field digest: a guide to perimetry and the Octopus perimeter, Köniz: Haag-Streit AG.

Racette, L., et al. (2016). "Visual field digest." A guide to perimetry and the Ocotpus perimeter **6**.

Racette, L., et al. (2003). "Primary open-angle glaucoma in blacks: a review." Survey of ophthalmology **48**(3): 295-313.

Ramirez, A. M., et al. (2008). "A comparison of semiautomated versus manual Goldmann kinetic perimetry in patients with visually significant glaucoma." Journal of glaucoma **17**(2): 111-117.

Ramulu, P. (2009). "Glaucoma and disability: which tasks are affected, and at what stage of disease?" Current opinion in ophthalmology **20**(2): 92.

Ramulu, P. Y., et al. (2012). "Real-world assessment of physical activity in glaucoma using an accelerometer." Ophthalmology **119**(6): 1159-1166.

Ramulu, P. Y., et al. (2013). "Difficulty with out-loud and silent reading in glaucoma." Investigative ophthalmology & visual science **54**(1): 666-672.

Ramulu, P. Y., et al. (2012). "Fear of falling and visual field loss from glaucoma." Ophthalmology **119**(7): 1352-1358.

Rao, H. L., et al. (2013). "Effect of cataract extraction on Visual Field Index in glaucoma." Journal of glaucoma **22**(2): 164-168.

Ratican, S. E., et al. (2018). "Progress in gene therapy to prevent retinal ganglion cell loss in glaucoma and leber's hereditary optic neuropathy." Neural plasticity **2018**.

Ray, C., et al. (2012). "The effects of a 15-week exercise intervention on fitness and postural control in older adults." Activities, Adaptation & Aging **36**(3): 227-241.

Redfern, M. S., et al. (2001). "Visual influences on balance." Journal of anxiety disorders **15**(1-2): 81-94.

Richman, J., et al. (2010). "Relationships in glaucoma patients between standard vision tests, quality of life, and ability to perform daily activities." Ophthalmic epidemiology **17**(3): 144-151.

Riddoch, G. (1917). "Dissociation of visual perceptions due to occipital injuries, with especial reference to appreciation of movement." Brain **40**(1): 15-57.

Robbins, S., et al. (1995). "Proprioception and stability: foot position awareness as a function of age and footware." Age and Ageing **24**(1): 67-72.

Røgind, H., et al. (2003). "Postural sway in normal subjects aged 20–70 years." Clinical physiology and functional imaging **23**(3): 171-176.

Ronne, H. (1915). "Ueber akute Retrobulbarneuritis, im Chiasma lokalisiert (Klinische und pathologisch-anatomische Untersuchungen)." Klin Monatsbl Augenheilkd **55**: 68-97.

Rönne, H. (1915). "Ueber akute Retrobulbärneuritis im Chiasma lokalisiert." Klin. Monatsbl. f. Augenh **55**: 68-97.

Runyal, D. and S. M. U. Din (2018). "Prevalence of Glaucoma among Family Members of Glaucoma Patients." Journal of Medical Science And clinical Research **6**(11).

Saunders, S. and F. Grum (1977). "Measurement of luminance factor." Color Research & Application **2**(3): 121-123.

Schiefer, U., et al. (2001). "Evaluation of advanced visual field loss with computer-assisted kinetic perimetry." Perimetry update: 131-138.

Schiefer, U., et al. (2001). "Reaction time in automated kinetic perimetry: effects of stimulus luminance, eccentricity, and movement direction." Vision Research **41**(16): 2157-2164.

Schmitt, C., et al. (2021). "Preattentive processing of visually guided self-motion in humans and monkeys." Progress in Neurobiology: 102117.

Schwartz, T. L., et al. (1987). "Kinetic perimetry assessment of binocular visual field shape and size in young infants." Vision Research **27**(12): 2163-2175.

Scuffham, P., et al. (2003). "Incidence and costs of unintentional falls in older people in the United Kingdom." Journal of Epidemiology & Community Health **57**(9): 740-744.

Shaarawy, T. M., et al. (2014). Glaucoma E-Book, Elsevier Health Sciences.

Shabana, N., et al. (2005). "Postural stability in primary open angle glaucoma." Clinical & Experimental Ophthalmology **33**(3): 264-273.

Short, H. (1976). "Metric notes." New Zealand Engineering **31**(3): 87.

Simpson, M. (2016). "Parameters affecting both Far Peripheral Vision in phakic eyes and Negative Dysphotopsia with Intraocular Lenses." Investigative ophthalmology & visual science **57**(12): 3118-3118.

Simpson, M. and M. Muzyka-Woźniak (2018). "Iris characteristics affecting far peripheral vision and negative dysphotopsia." Journal of cataract and refractive surgery.

Simpson, M. J. (2015). "Managing and understanding negative dysphotopsia." Journal of Cataract & Refractive Surgery **41**(2): 477.

Simpson, M. J. (2017). "Mini-review: far peripheral vision." Vision Research **140**: 96-105.

Skalicky, S. E. (2016). Ocular and visual physiology, Springer.

Smith, N. D., et al. (2011). "An exploratory study of visual search performance in glaucoma." Ophthalmic and Physiological Optics **31**(3): 225-232.

Smith, N. D., et al. (2014). "Using eye tracking to assess reading performance in patients with glaucoma: a within-person study." Journal of Ophthalmology **2014**.

Smith, S. D., et al. (1996). "Analysis of progressive change in automated visual fields in glaucoma." Investigative ophthalmology & visual science **37**(7): 1419-1428.

Smythies, J. (1996). "A note on the concept of the visual field in neurology, psychology, and visual neuroscience." Perception **25**(3): 369-371.

Sommerich, C. M., et al. (2001). "Effects of computer monitor viewing angle and related factors on strain, performance, and preference outcomes." Human factors **43**(1): 39-55.

Spaeth, G., et al. (2006). "Evaluation of quality of life for patients with glaucoma." American journal of ophthalmology **141**(1): 3-14.

Spry, P. G. and C. A. Johnson (2002). "Identification of progressive glaucomatous visual field loss." Survey of ophthalmology **47**(2): 158-173.

Stewart, W. C., et al. (1993). "Factors associated with visual loss in patients with advanced glaucomatous changes in the optic nerve head." American journal of ophthalmology **116**(2): 176-181.

Stewart, W. C., et al. (2006). "Mean intraocular pressure and progression based on corneal thickness in primary open-angle glaucoma." Journal of Ocular Pharmacology & Therapeutics **22**(1): 26-33.

Stoffregen, T. A., et al. (1987). "Use of central and peripheral optical flow in stance and locomotion in young walkers." Perception **16**(1): 113-119.

Strasburger, H., et al. (2011). "Peripheral vision and pattern recognition: A review." Journal of vision **11**(5): 13-13.

Straube, A., et al. (1994). "Dependence of visual stabilization of postural sway on the cortical magnification factor of restricted visual fields." Experimental brain research **99**(3): 501-506.

Sukumar, S., et al. (2009). "The influence of socioeconomic and clinical factors upon the presenting visual field status of patients with glaucoma." Eye **23**(5): 1038.

Susanna Jr, R. and R. M. Vessani (2009). "Staging glaucoma patient: why and how?" The open ophthalmology journal **3**: 59.

Swienton, D. J. and A. G. Thomas (2014). The visual pathway—functional anatomy and pathology. Seminars in Ultrasound, CT and MRI, Elsevier.

Syed, Z. A., et al. (2011). "Detection of progressive glaucomatous optic neuropathy using automated alternation flicker with stereophotography." Archives of Ophthalmology **129**(4): 512-526.

Syed, Z. A., et al. (2012). "Automated alternation flicker for the detection of optic disc haemorrhages." Acta ophthalmologica **90**(7): 645-650.

Tanna, A. P., et al. (2012). "Glaucoma Progression Analysis software compared with expert consensus opinion in the detection of visual field progression in glaucoma." Ophthalmology **119**(3): 468-473.

Taube, J. S. (2007). "The head direction signal: origins and sensory-motor integration." Annu. Rev. Neurosci. **30**: 181-207.

Thakur, N. and M. Juneja (2018). "Survey on segmentation and classification approaches of optic cup and optic disc for diagnosis of glaucoma." Biomedical Signal Processing and Control **42**: 162-189.

Tham, Y.-C., et al. (2014). "Global prevalence of glaucoma and projections of glaucoma burden through 2040: a systematic review and meta-analysis." Ophthalmology **121**(11): 2081-2090.

Tielsch, J. M., et al. (1994). "Family history and risk of primary open angle glaucoma: the Baltimore Eye Survey." Archives of Ophthalmology **112**(1): 69-73.

Tobimatsu, S. and G. G. Celesia (2006). "Studies of human visual pathophysiology with visual evoked potentials." Clinical Neurophysiology **117**(7): 1414-1433.

Traquair, H. M. (1924). "Essential considerations in regard to the field of vision: contraction or depression?" The British journal of ophthalmology **8**(2): 49.

Traquair, H. M. and G. I. Scott (1957). Clinical perimetry, London.

Turpin, A., et al. (2012). "The Open Perimetry Interface: an enabling tool for clinical visual psychophysics." Journal of vision **12**(11): 22-22.

Turpin, A., et al. (2002). "Development of efficient threshold strategies for frequency doubling technology perimetry using computer simulation." Investigative ophthalmology & visual science **43**(2): 322-331.

Turpin, A., et al. (2003). "Properties of perimetric threshold estimates from full threshold, ZEST, and SITA-like strategies, as determined by computer simulation." Investigative ophthalmology & visual science **44**(11): 4787-4795.

Uchiyama, M. and S. Demura (2008). "Low visual acuity is associated with the decrease in postural sway." The Tohoku journal of experimental medicine **216**(3): 277-285.

Urata, C. N., et al. (2020). "Comparison of short-and long-term variability in standard perimetry and spectral domain optical coherence tomography in glaucoma." American journal of ophthalmology **210**: 19-25.

Vonthein, R., et al. (2007). "The normal age-corrected and reaction time–corrected isopter derived by semi-automated kinetic perimetry." Ophthalmology **114**(6): 1065-1072. e1062.

Wall, M., et al. (2018). "The effective dynamic ranges for glaucomatous visual field progression with standard automated perimetry and stimulus sizes III and V." Investigative ophthalmology & visual science **59**(1): 439-445.

Warren, W. H. and K. J. Kurtz (1992). "The role of central and peripheral vision in perceiving the direction of self-motion." Perception & psychophysics **51**(5): 443-454.

Webster, R. G. and G. M. Haslerud (1964). "Influence on extreme peripheral vision of attention to a visual or auditory task." Journal of Experimental Psychology **68**(3): 269.

Weinreb, R. N., et al. (2014). "The pathophysiology and treatment of glaucoma: a review." Jama **311**(18): 1901-1911.

Weinreb, R. N. and P. T. Khaw (2004). "Primary open-angle glaucoma." The Lancet **363**(9422): 1711-1720.

Weleber, R. G., et al. (2015). "VFMA: topographic analysis of sensitivity data from full-field static perimetry." Translational Vision Science & Technology **4**(2): 14-14.

Wiggs, J. L. (2007). "Genetic etiologies of glaucoma." Archives of Ophthalmology **125**(1): 30-37.

Winter, D. A. (1995). "Human balance and posture control during standing and walking." Gait & posture **3**(4): 193-214.

Wolfs, R. C., et al. (1998). "Genetic risk of primary open-angle glaucoma: population-based familial aggregation study." Archives of Ophthalmology **116**(12): 1640-1645.

Wu, S.-Y., et al. (2006). "Nine-year changes in intraocular pressure: the Barbados Eye Studies." Archives of Ophthalmology **124**(11): 1631-1636.

Yanagi, M., et al. (2011). "Vascular risk factors in glaucoma: a review." Clinical & Experimental Ophthalmology **39**(3): 252-258.

Yang, C.-H. and T. Hung (1997). "Intraocular lens position and anterior chamber angle changes after cataract extraction in eyes with primary angle-closure glaucoma." Journal of Cataract & Refractive Surgery **23**(7): 1109-1113.

Yuki, K., et al. (2015). "Investigating the influence of visual function and systemic risk factors on falls and injurious falls in glaucoma using the structural equation modeling." PloS one **10**(6): e0129316.

Zeman, A., et al. (2017). "Simulating observer responses in kinetic perimetry using KANGA." Investigative ophthalmology & visual science **58**(8): 2876-2876.

Zhao, D., et al. (2015). "Diabetes, fasting glucose, and the risk of glaucoma: a meta-analysis." Ophthalmology **122**(1): 72-78.

10 Appendices

10.1 A1: Chapter 3 experimental R code

```
initials     <- "IMF"    # subject's initials
goldmannStim <- "III-4e" # options are I-4e, III-4e, and V-4e
testeye      <- "OS"     # eye to test
sector       <- "IT"     # eye to test
stim_speed   <- 5        # speed of the stimulus in deg/sec
nreps        <- 3        # number of repetitions
nfptrials    <- 3        # number of false positive trials
stim_intfp   <- 0.01     # intensity of the stimulus for false positives
stim_sizefp  <- 0.108    # size of the stimulus for false positives
randomize    <- TRUE     # randomize the trials or not
fkinvectrs   <- "kinvect_OS_IT.csv" # csv file with defined kinetic vectors

if( goldmannStim == "I-4e") {
  stim_int     <- 0      # intensity of the stimulus in dB
  stim_size    <- 0.108  # size of the stimulus in deg
}
if( goldmannStim == "III-4e") {
  stim_int     <- 0      # intensity of the stimulus in dB
  stim_size    <- 0.43   # size of the stimulus in deg
}
if( goldmannStim == "V-4e") {
  stim_int     <- 0      # intensity of the stimulus in dB
```

```
  stim_size    <- 1.73   # size of the stimulus in deg
}
if( goldmannStim == "VI-4e") {
  stim_int     <- 0     # intensity of the stimulus in dB
  stim_size    <- 3.47   # size of the stimulus in deg
}
if( goldmannStim == "III-1e") {
  stim_int     <- 15     # intensity of the stimulus in dB
  stim_size    <- 0.43   # size of the stimulus in deg
}
# preliminary analysis. Data distribution
setwd( "C:/OPIprojects/kineticPeripheryLimits" )
library( OPI )
source( "kinstim.r" )
fkinvectrs <- paste( "kinvectdef", fkinvectrs, sep = "/" ) # get vectors
kinvect <- read.csv( fkinvectrs, stringsAsFactors = FALSE )
#########################################################
# OPI connection parameters
#########################################################
serverPort            <- 50001
eyeSuiteSettingsLocation <- "C:\\Program Files (x86)\\Haag-Streit\\EyeSuite\\"
eye                   <- "right"
gazeFeed              <- 0
bigWheel              <- TRUE
```

```
pres_buzzer           <- 0

resp_buzzer           <- 1

zero_dB_is_10000_asb    <- TRUE

# construct name were to store the results

fname <- paste( "results/", initials, sep = "" )

fname <- paste( fname, goldmannStim, testeye, sector, sep = "_" )

fname <- paste( fname, gsub( "-", "", substr( Sys.time(), 1, 10 ) ), gsub( ":", "", substr(
Sys.time(), 12, 19 ) ), sep = "_" )

fname <- paste( fname, ".csv", sep = "" )


stimstack <- kinstim( kinvect,

                stim_int    = stim_int,

                stim_size   = stim_size,

                stim_speed  = stim_speed,

                nreps       = nreps,

                nfptrials   = nfptrials,

                stim_intfp  = stim_intfp,

                stim_sizefp = stim_sizefp,

                randomize   = randomize )


chooseOpi( "Octopus900" )

opiInitialize( serverPort = serverPort,

            eyeSuiteSettingsLocation = eyeSuiteSettingsLocation,

            eye = eye, gazeFeed = gazeFeed, bigWheel = bigWheel,
```

```
            pres_buzzer = pres_buzzer, resp_buzzer = resp_buzzer,
            zero_dB_is_10000_asb = zero_dB_is_10000_asb )
opiSetBackground( lum = .Octopus900Env$BG_10, fixation =
.Octopus900Env$FIX_CENTRE, fixIntensity = 0 )
len <- length( stimstack )
subj        <- NULL
subj$xstart  <- rep( NA, len )
subj$ystart  <- rep( NA, len )
subj$xend    <- rep( NA, len )
subj$yend    <- rep( NA, len )
subj$fptrial <- rep( NA, len )
subj$seen    <- rep( NA, len )
subj$x       <- rep( NA, len )
subj$y       <- rep( NA, len )
subj$restime <- rep( NA, len )
subj        <- as.data.frame( subj )
readline( prompt = "Press [enter] to continue" )
for( i in 1:len ) {
  # present stimulus
  if( !( i == len ) ) {
    res <- opiPresent( stimstack[[i]], nextStim = stimstack[[i+1]] )
  } else {
    res <- opiPresent( stimstack[[i]] )
  }
```

```
  # store results from presentation
  if( !is.null( res$err ) ) {
    print( paste( "error ocurred with code: ", res$err, sep = "" ) )
    warning( paste( "error ocurred with code: ", res$err, sep = "" ) )

    Sys.sleep( 1 )
    res$seen <- 0
    res$x    <- stimstack[[i]]$path$x[2]
    res$y    <- stimstack[[i]]$path$y[2]
  }
  if( res$seen == 0 ) {
    print( paste( i, " out of ", len, " (", round( 100 * i / len, 1 ), "%). Stimulus not seen",
sep = "" ) )
  } else {
    print( paste( i, " out of ", len, " (", round( 100 * i / len, 1 ), "%). Stimulus seen. (x,y)
= (",  res$x, ",", res$y, ")", sep = "" ) )
  }
  subj$xstart[i]  <- stimstack[[i]]$path$x[1]
  subj$ystart[i]  <- stimstack[[i]]$path$y[1]
  subj$xend[i]    <- stimstack[[i]]$path$x[2]
  subj$yend[i]    <- stimstack[[i]]$path$y[2]
  subj$fptrial[i] <- ( stimstack[[i]]$levels == stim_intfp )
  subj$seen[i]    <- res$seen
  subj$x[i]       <- res$x
  subj$y[i]       <- res$y
```

```
  subj$restime[i] <- substr( Sys.time(), 12, 19 )

}

opiClose()

write.csv( subj, file = fname, row.names = FALSE )
```

10.2 A2: Chapter 4 experimental R code

```
initials     <- "IMF"    # subject's initials
goldmannStim <- "III-4e" # options are I-4e, III-4e, and V-4e
testeye      <- "OD"     # eye to test
sector       <- "IL"     # eye to test
stim_speed   <- 5        # speed of the stimulus in deg/sec
nreps        <- 6        # number of repetitions
nfptrials    <- 4        # number of false positive trials
stim_intfp   <- 0.01     # intensity of the stimulus for false positives
stim_sizefp  <- 0.108    # size of the stimulus for false positives
randomize    <- TRUE     # randomize the trials or not
frevvec   <- "kinvect_OD_disrev.csv" # csv file with defined kinetic vectors
fnorvec   <- "kinvect_OD_disNORM.csv" # csv file with defined kinetic vectors

if( goldmannStim == "I-4e") {
  stim_int     <- 0      # intensity of the stimulus in dB
  stim_size    <- 0.108   # size of the stimulus in deg
}
if( goldmannStim == "III-4e") {
  stim_int     <- 0     # intensity of the stimulus in dB
  stim_size    <- 0.43   # size of the stimulus in deg
}
if( goldmannStim == "V-4e") {
  stim_int     <- 0     # intensity of the stimulus in dB
```

```
  stim_size    <- 1.73   # size of the stimulus in deg
}
if( goldmannStim == "VI-4e") {
  stim_int     <- 0     # intensity of the stimulus in dB
  stim_size    <- 3.47   # size of the stimulus in deg
}
if( goldmannStim == "III-1e") {
  stim_int     <- 15     # intensity of the stimulus in dB
  stim_size    <- 0.43   # size of the stimulus in deg
}
# preliminary analysis. Data distribution
setwd( "C:/OPIprojects/kineticPeripheryLimits" )
library( OPI )
source( "kinstim.r" )
runTrial <- function( stimstack ) {
  len <- length( stimstack )
  resp        <- NULL
  resp$xstart  <- rep( NA, len )
  resp$ystart  <- rep( NA, len )
  resp$xend    <- rep( NA, len )
  resp$yend    <- rep( NA, len )
  resp$fptrial <- rep( NA, len )
  resp$seen    <- rep( NA, len )
  resp$x       <- rep( NA, len )
```

```
 resp$y      <- rep( NA, len )
 resp$restime <- rep( NA, len )
 resp        <- as.data.frame( resp )
 readline( prompt = "Press [enter] to continue" )
 for( i in 1:len ) {
  # present stimulus
  if( !( i == len ) ) {
   res <- opiPresent( stimstack[[i]], nextStim = stimstack[[i+1]] )
  } else {
   res <- opiPresent( stimstack[[i]] )
  }
  # store results from presentation
  if( !is.null( res$err ) ) {
   print( paste( "error ocurred with code: ", res$err, sep = "" ) )
   warning( paste( "error ocurred with code: ", res$err, sep = "" ) )
   # patch to overcome the strange behavior of the OPI + Octopus 900
   Sys.sleep( 1 )
   res$seen <- 0
   res$x    <- stimstack[[i]]$path$x[2]
   res$y    <- stimstack[[i]]$path$y[2]
  }
  if( res$seen == 0 ) {
   print( paste( i, " out of ", len, " (", round( 100 * i / len, 1 ), "%). Stimulus not
seen", sep = "" ) )
```

```
    } else {
      print( paste( i, " out of ", len, " (", round( 100 * i / len, 1 ), "%). Stimulus seen.
(x,y) = (",  res$x, ",", res$y, ")", sep = "" ) )
    }
    resp$xstart[i]  <- stimstack[[i]]$path$x[1]
    resp$ystart[i]  <- stimstack[[i]]$path$y[1]
    resp$xend[i]    <- stimstack[[i]]$path$x[2]
    resp$yend[i]    <- stimstack[[i]]$path$y[2]
    resp$fptrial[i] <- ( stimstack[[i]]$levels == stim_intfp )
    resp$seen[i]    <- res$seen
    resp$x[i]       <- res$x
    resp$y[i]       <- res$y
    resp$restime[i] <- substr( Sys.time(), 12, 19 )
  }
  return( resp )
}
frevvec <- paste( "kinvectdef", frevvec, sep = "/" )
fnorvec <- paste( "kinvectdef", fnorvec, sep = "/" )
# get vectors
revvec <- read.csv( frevvec, stringsAsFactors = FALSE )
norvec <- read.csv( fnorvec, stringsAsFactors = FALSE )
revstack <- kinstim( revvec,
                     stim_int    = stim_int,
                     stim_size   = stim_size,
```

```
                stim_speed  = stim_speed,
                nreps       = nreps,
                nfptrials   = nfptrials,
                stim_intfp  = stim_intfp,
                stim_sizefp = stim_sizefp,
                randomize   = randomize )
norstack <- kinstim( norvec,
                stim_int    = stim_int,
                stim_size   = stim_size,
                stim_speed  = stim_speed,
                nreps       = nreps,
                nfptrials   = nfptrials,
                stim_intfp  = stim_intfp,
                stim_sizefp = stim_sizefp,
                randomize   = randomize )
#######################################################
# OPI connection parameters
#######################################################
serverPort            <- 50001
eyeSuiteSettingsLocation <- "C:\\Program Files (x86)\\Haag-Streit\\EyeSuite\\"
eye                 <- "right"
gazeFeed              <- 0
bigWheel              <- TRUE
pres_buzzer           <- 0
```

```
resp_buzzer            <- 1

zero_dB_is_10000_asb    <- TRUE

# construct name were to store the results

fname <- paste( "results/", initials, sep = "" )

fname <- paste( fname, goldmannStim, testeye, sector, sep = "_" )

fname <- paste( fname, gsub( "-", "", substr( Sys.time(), 1, 10 ) ), gsub( ":", "", substr(
Sys.time(), 12, 19 ) ), sep = "_" )

fname <- paste( fname, ".csv", sep = "" )

chooseOpi( "Octopus900" )

opiInitialize( serverPort = serverPort,

        eyeSuiteSettingsLocation = eyeSuiteSettingsLocation,

        eye = eye, gazeFeed = gazeFeed, bigWheel = bigWheel,

        pres_buzzer = pres_buzzer, resp_buzzer = resp_buzzer,

        zero_dB_is_10000_asb = zero_dB_is_10000_asb )

opiSetBackground( lum = .Octopus900Env$BG_10, fixation =
.Octopus900Env$FIX_CENTRE, fixIntensity = 0 )

# normal

norres <- runTrial( norstack )

revres <- runTrial( revstack )

opiClose()

norres$type <- "nor"

revres$type <- "rev"

write.csv( rbind ( norres, revres ), file = fname, row.names = FALSE )
```

10.3 A3: Chapter 5 Simulation R code

10.3.1 A3.1: Data fitting code

```
setwd ("C:/Users/cbain/Google
Drive/CB_PHD_Work/Projects/simulations/code/CBane/CBane")
library( mixtools )
library( e1071 )
vffiles <- read.csv(file ="data/vlengthall2.csv", header = TRUE, sep = ",")
med <- aggregate(vlength ~ angle + id, data = vffiles, FUN = median)
names(med)[3] <- "med"
vffiles <- merge(vffiles, med)
vffiles <- vffiles[order( vffiles$angle ),] # sort by angle
vffiles <- vffiles[order( vffiles$id ),]    # sort by id
vffiles$error <- vffiles$vlength - vffiles$med
vffiles$sderr <- vffiles$error / vffiles$mad
vffiles$id <- as.numeric( vffiles$id )
ids <- unique( vffiles$id )

for( i in 1:length( ids ) ) {
  fname <- paste0( "plots/hist", ids[i], ".png" )
  vf1 <- subset( vffiles, vffiles$id == ids[i] )
  vf1d <- density(vf1$error)
  png( fname, width=12, height=10, units="in", res=600, pointsize = 24)
  plot(vf1d, cex.lab = 1.2, main = "", mgp = c(2.5, 0.5, 0),
      xlim = c(-10, 10),
```

```
      ylim = c( 0, 0.6 ) )
  dev.off()
}
for( i in 1:length( ids ) ) {
  fname <- paste0( "plots/nhist", ids[i], ".png" )
  vf1 <- subset( vffiles, vffiles$id == ids[i] )
  vf1d <- density(vf1$sderr)
  png( fname, width=12, height=10, units="in", res=600, pointsize = 24)
  plot(vf1d, cex.lab = 1.2, main = "", mgp = c(2.5, 0.5, 0),
      xlim = c(-10, 10),
      ylim = c( 0, 0.6 ) )
  dev.off()
}
mixmdl <- normalmixEM( vffiles$sderr )
x  <- seq( -23, 31, by = 0.01 )
fx <- mixmdl$lambda[1] * dnorm( x, mixmdl$mu[1], mixmdl$sigma[1] ) +
mixmdl$lambda[2] * dnorm( x, mixmdl$mu[2], mixmdl$sigma[2] )
x2 <- dnorm( x, mixmdl$mu[1], mixmdl$sigma[1] ) + mixmdl$lambda[2] * dnorm( x,
mixmdl$mu[2], mixmdl$sigma[2] )
hist(x2)
png( "plots/pooledhist.png", width=12, height=10, units="in", res=600, pointsize =
24)
source ("./Artes.Graphics.R")
plot( x, fx, typ = "l", ylim = c( 0, 0.30 ), col = "blue", lty = "dotted", lwd = 3,
    ylab = "density", xlab = "Distribution of response error", mgp=c(2.4,0.5,0))
```

```
lines(density(vffiles$sderr), lwd=2, col = "black")

lines(density(dnorm(x), lwd = 2, col = "red", lty = "dashed"))

dev.off()

save( mixmdl, file = "mixmdl.rda" )

hist(vffiles$sderr, breaks = 50, col = "blue",  xlab = "Distribution of error", ylab = "",

    cex.lab = 1, xlim = c(-10, 10), ylim = c(0, 0.3), main = NULL, freq = FALSE)

curve(dnorm(x, mean = mean(err), sd = sd(err)), add = TRUE, lwd = 2, col = "red", lty
= "dashed")
```

10.3.2 A3.2: Strategy 1 simulation R code

```
setwd ("C:/Users/cbain/Google
Drive/CB_PHD_Work/Projects/simulations/code/CBane/CBane")

library( mixtools )

load( "mixmdl.rda" )

# input parameters

nt    <- 500 # max number of presentations per location

d     <- c((0.5), seq( 1, 20, by = 2 ) )

mad   <- 1

niter <- 12000

samplefun <- function(d, nt, mad){

  resp <- mad * rnormmix( nt, lambda = mixmdl$lambda, mu = mixmdl$mu, sigma =
mixmdl$sigma )

  trial <- resp[1]

  for( i in 2:nt ) {

    trial <- sort( c( trial, resp[i] ) )

    if( min( diff( trial[order( trial )] ) ) <= d ) break

  }

  return(data.frame( resmed = median( trial ), comb = length( trial ), criteria = d ) )

}

tmp <- samplefun( d[1], nt, mad )

nrunfunc <- function(d, nt, mad, nreps){

  results <- list()

  for(i in 1:nreps) {
```

```
   results[[i]] <- data.frame(samplefun(d, nt, mad))
  }
  resultsall <- (do.call(rbind, results))
  return(resultsall)
}
#tmp <- nrunfunc(d[1], nt, mad, niter)
criteria <- list()
for( i in 1:length(d)){
  criteria[[i]] <- data.frame(nrunfunc(d[i], nt, mad, niter))
}
criteria_results <-(do.call(rbind, criteria))
res <- data.frame( d = d, mn = NA, sn = NA, lbn = NA, ubn = NA, p500 = NA, p950 =
NA )
for(i in 1:length( d ) ){
  vf <- subset(criteria_results, criteria_results$criteria == d[i])
  res$mn[i]     <- mean( vf$comb )
  res$sn[i]     <- sd( vf$comb )
  res[i,c(4:5)]  <- quantile( vf$comb,   prob = c( 0.025, 0.975 ) )
  res[i,c(6:7)] <- quantile( abs( vf$resmed ), probs = c( 0.500, 0.950 ) )
}
png ("vfplot.png", width=12, height=10, units="in", res=600, pointsize = 24)
source ("./Artes.Graphics.R")
plot( res$d, res$p500, typ = "n", xlim = c( 0, 20 ), ylim = c( 0, 15 ),
     xlab = "Criterion",
```

```
    ylab = "Absolute error",
    xaxt = "n", yaxt ="n" )
axis( 1, at = c( 0, 5, 10, 15, 20 ), labels = c( "0°", "5°", "10°", "15°", "20°" ) )
axis( 2, at = c( 0, 5, 10, 15 ), labels = c( "0°", "5°", "10°", "15°" ) )
lines( res$d, res$p500, col = "black" , lwd = 2)
lines( res$d, res$p950, col = "red", lwd = 2 )
points( res$d, res$p500, pch = 22, cex = 2.25, col = "black", bg = "white" )
points( res$d, res$p950, pch = 22, cex = 2.25, col = "red", bg = "white"  )
text( res$d, res$p500, round( res$mn ),  cex = 10 / 12 )
text( res$d, res$p950, round( res$ubn ), cex = 10 / 12 )
dev.off()
write.csv(res, file = "res_MAD1.csv")
```

10.3.3 A3.3: Strategy 2 simulation R code

```
setwd ("C:/Users/cbain/Google
Drive/CB_PHD_Work/Projects/simulations/code/CBane/CBane")

library( mixtools )

load( "mixmdl.rda" )

# input parameters

nt    <- 500  # max number of presentations per location

d     <- c(seq(0.5, 5, by = 0.5), seq( 1, 20, by = 2 ) )

mad   <- 5

niter <- 10000

samplefun <- function(d, nt, mad){

 resp <- mad * rnormmix( nt, lambda = mixmdl$lambda, mu = mixmdl$mu, sigma =
mixmdl$sigma )

 trial <- resp[1]

 for( i in 2:nt ) {

  trial <- sort( c( trial, resp[i] ) )

  if( min( diff( trial[order( trial )] ) ) <= d ) break

 }

 med <- median(trial)

 idxd <- which.min(diff(sort(trial)))

 trial2 <- median(sort(trial) [c(idxd, idxd +1)])

 return(data.frame(med = med, resmed =  trial2, comb = length( trial ), criteria = d ) )

}

tmp <- samplefun( 4, nt, mad )

nrunfunc <- function(d, nt, mad, nreps){
```

```
  results <- list()
  for(i in 1:nreps) {
    results[[i]] <- data.frame(samplefun(d, nt, mad))
  }
  resultsall <- (do.call(rbind, results))
  return(resultsall)
}
#tmp <- nrunfunc(d[1], nt, mad, niter)

criteria <- list()
for( i in 1:length(d)){
  criteria[[i]] <- data.frame(nrunfunc(d[i], nt, mad, niter))
}
criteria_results <-(do.call(rbind, criteria))
res <- data.frame( d = d, mn = NA, sn = NA, lbn = NA, ubn = NA, p500 = NA, p950 =
NA )
for(i in 1:length( d ) ){
  vf <- subset(criteria_results, criteria_results$criteria == d[i])
  res$mn[i]     <- mean( vf$comb )
  res$sn[i]     <- sd( vf$comb )
  res[i,c(4:5)]  <- quantile( vf$comb,   prob = c( 0.025, 0.975 ) )
  res[i,c(6:7)] <- quantile( abs( vf$resmed ), probs = c( 0.500, 0.950 ) )
}
png ("vfplot.png", width=12, height=10, units="in", res=600, pointsize = 24)
```

```
source ("./Artes.Graphics.R")

plot( res$d, res$p500, typ = "n", xlim = c( 0, 20 ), ylim = c( 0, 15 ),

    xlab = "Criterion",

    ylab = "Absolute error",

    xaxt = "n", yaxt ="n" )

axis( 1, at = c( 0, 5, 10, 15, 20 ), labels = c( "0°", "5°", "10°", "15°", "20°" ) )

axis( 2, at = c( 0, 5, 10, 15 ), labels = c( "0°", "5°", "10°", "15°" ) )

lines( res$d, res$p500, col = "black" , lwd = 2)

lines( res$d, res$p950, col = "red", lwd = 2 )

points( res$d, res$p500, pch = 22, cex = 2.25, col = "black", bg = "white" )

points( res$d, res$p950, pch = 22, cex = 2.25, col = "red", bg = "white"  )

text( res$d, res$p500, round( res$mn ),  cex = 10 / 12 )

text( res$d, res$p950, round( res$ubn ), cex = 10 / 12 )

dev.off()
```

10.3.4 A3.4: Strategy 3 simulation R code

```
setwd ("C:/Users/cbain/Google
Drive/CB_PHD_Work/Projects/simulations/code/CBane/CBane")

library( mixtools )

load( "mixmdl.rda" )

# input parameters

nt    <- 500  # max number of presentations per location

#d     <- seq(0.5, to = 10, by = 0.5)  # threshold criterion

mad   <- 5 # median, use 0.4 for reliable patient and 1.2 for unreliable patient

niter <- 120000

nloc  <- 12

quan  <- 0.75

sample2responses <- function( nloc, mad, q ){

  tmp <- list()

  resp1 <- mad * rnormmix( nloc, lambda = mixmdl$lambda, mu = mixmdl$mu, sigma
= mixmdl$sigma )

  resp2 <- mad * rnormmix( nloc, lambda = mixmdl$lambda, mu = mixmdl$mu, sigma
= mixmdl$sigma )

  d <- as.numeric( quantile( abs( resp1 - resp2 ), q ) )

  resmed   <- rep( NA, nloc )

  lentrial <- rep( NA, nloc )

  for( i in 1:nloc ) {

    trial <- c( resp1[i], resp2[i] )

    if( abs(resp1[i] - resp2[i] ) <= d ) {

      resmed[i] <- median( trial )
```

```
      lentrial[i] <- length( trial )
      next
    }
    for( j in 3:nt ) {
      trial <- c( trial, mad * rnormmix( 1, lambda = mixmdl$lambda, mu = mixmdl$mu,
sigma = mixmdl$sigma ) )
      if( min( diff( trial[order( trial )] ) ) <= d ) break
    }
    resmed[i]   <- median( trial )
    lentrial[i] <- length( trial )
  }
  return( data.frame( resmed = resmed, comb = lentrial, criteria = d ) )
}
#tmp <- sample2responses(nloc, mad)
nrunfunc <- function( nloc, mad, nreps, q ){
  results <- list()
  for( i in 1:nreps ) {
    results[[i]] <- data.frame( sample2responses( nloc, mad, q) )
  }
  resultsall <- ( do.call( rbind, results ) )
  return( resultsall )
}
tmp2 <- nrunfunc( nloc, mad, niter, quan )
tmp2$resmed <- abs( tmp2$resmed )
```

```
tmp2$criteria <- round(tmp2$criteria)

criteria <- unique(tmp2$criteria)

cri <- criteria

res <- list()

for(i in 1:length(cri)){

  res2 <- subset(tmp2, tmp2$criteria == cri[i])

  med <- quantile( res2$resmed, probs = c( 0.500))

  upmed <- quantile( res2$resmed, probs = c( 0.950))

  lbn  <- quantile( res2$comb,  probs = c( 0.025) )

  ubn  <- quantile( res2$comb,  probs = c( 0.975 ) )

  mn      <- round(mean( res2$comb ))

  sn      <- round(sd( res2$comb ))

  res[[i]] <- data.frame(d = cri[i], med = med, upmed = upmed, lbn = lbn, ubn = ubn,
mn = mn, sn = sn)

}

res <- (do.call(rbind, res))

res <- res[order(res$d),]


png ("vfplot.png", width=12, height=10, units="in", res=600, pointsize = 24)

source ("./Artes.Graphics.R")

plot( res$d, res$p500, typ = "n", xlim = c( 0, 20 ), ylim = c( 0, 15 ),

     xlab = "Criterion",

     ylab = "Absolute error",

     xaxt = "n", yaxt ="n" )
```

```
axis( 1, at = c( 0, 5, 10, 15, 20 ), labels = c( "0°", "5°", "10°", "15°", "20°")) #, "25Â°",
"30Â°", "35Â°", "40Â°") )

axis( 2, at = c( 0, 5, 10, 15), labels = c( "0°", "5°", "10°", "15°" )) #, "20Â°" ) )

lines( res$d, res$med, col = "black" , lwd = 2)

lines( res$d, res$upmed, col = "red", lwd = 2 )

points( res$d, res$med, pch = 22, cex = 2.25, col = "black", bg = "white" )

points( res$d, res$upmed, pch = 22, cex = 2.25, col = "red", bg = "white"  )

text( res$d, res$med, round( res$mn ),  cex = 10 / 12 )

text( res$d, res$upmed, round( res$ubn ), cex = 10 / 12 )

dev.off()

write.csv(res, file = "resadap_MAD3.csv")
```

10.4 A4: Chapter 6 experimental R code

```
setwd( "C:/OPIprojects/New kinetic test/New kinetic test/code" )

library( OPI )

source( "kinstim.r" )

source( "kinetic_criterion.r" )

source( "Oct900_17.Bain.r")

#####################################################

# experiment parameters

#####################################################

initials    <- "CB_OS"  # subject's initials

stim_int    <- 0     # intensity of the stimulus in dB

stim_size   <- 1.72   # size of the stimulus in deg

stim_speed  <- 5     # speed of the stimulus in deg/sec

minreps     <- 2     # minimum number of repetitions

maxreps     <- 5     # maximum number of repetitions

nfptrials   <- 5     # number of false positive trials

stim_intfp  <- 0.1    # intensity of the stimulus for false positives

stim_sizefp <- 0.108  # size of the stimulus for false positives

randomize   <- TRUE   # randomize the trials or not

criterion   <- "mindif" # criterion to finish adaptive algorith

threshold   <- 5        # threshold to finish adaptive algorith. Typically modulus
difference in degrees

fkinvectrs <- "kinvectdef/CBReducedOS2.csv" # csv file with defined kinetic vectors

# get vectors

kinvect <- read.csv( fkinvectrs, stringsAsFactors = FALSE )
```

```
kinvect$angle   <- round(Oct900.VectorAngle(kinvect$xstart, kinvect$ystart))

#####################################################

# OPI connection parameters

#####################################################

serverPort            <- 50001

eyeSuiteSettingsLocation <- "C:\\Program Files (x86)\\Haag-Streit\\EyeSuite\\"

eye                   <- "right"

gazeFeed              <- 0

bigWheel              <- FALSE

pres_buzzer           <- 0

resp_buzzer           <- 1

zero_dB_is_10000_asb    <- TRUE

# construct name were to store the results

fname  <- paste( "results/", initials, "_", criterion, "_", threshold, sep = "" )

fname  <- paste( fname, gsub( "-", "", substr( Sys.time(), 1, 10 ) ), gsub( ":", "", substr(
Sys.time(), 12, 19 ) ), sep = "_" )

fnamec <- paste( fname, "_control.csv", sep = "" )

fnamed <- paste( fname, ".csv", sep = "" )

stimstack <- kinstim( kinvect,

                stim_int    = stim_int,

                stim_size   = stim_size,

                stim_speed  = stim_speed,

                nreps       = maxreps,

                nfptrials   = nfptrials,
```

```
                stim_intfp  = stim_intfp,
                stim_sizefp = stim_sizefp,
                randomize   = randomize )

# adaptive run control table
kinvect$ntrials  <- 0
kinvect$finished <- FALSE
chooseOpi( "Octopus900" )
opiInitialize( serverPort = serverPort,
          eyeSuiteSettingsLocation = eyeSuiteSettingsLocation,
          eye = eye, gazeFeed = gazeFeed, bigWheel = bigWheel,
          pres_buzzer = pres_buzzer, resp_buzzer = resp_buzzer,
          zero_dB_is_10000_asb = zero_dB_is_10000_asb )
opiSetBackground( lum = .Octopus900Env$BG_10, fixation =
.Octopus900Env$FIX_CENTRE )
len <- length( stimstack )
subj       <- NULL
subj$xstart  <- rep( NA, len )
subj$ystart  <- rep( NA, len )
subj$xend    <- rep( NA, len )
subj$yend    <- rep( NA, len )
subj$fptrial <- rep( NA, len )
subj$seen    <- rep( NA, len )
subj$x       <- rep( NA, len )
```

```
subj$y      <- rep( NA, len )
subj$vlength <- rep( NA, len )
subj$angle   <- rep( NA, len )
subj$restime <- rep( NA, len )
subj        <- as.data.frame( subj )

readline( prompt = "Press [enter] to continue" )
for( i in 1:len ) {
 # check status of kinetic vector to present
 idx <- which( kinvect$xstart == stimstack[[i]]$path$x[1] &
               kinvect$xend   == stimstack[[i]]$path$x[2] &
               kinvect$ystart == stimstack[[i]]$path$y[1] &
               kinvect$yend   == stimstack[[i]]$path$y[2] )
 # present stimulus?
 # if the current trial is not for false positive, then check
 if( stimstack[[i]]$levels != stim_intfp ) {
  if( kinvect$finished[idx] ) {
   print( paste( i, " out of ", len, " (", round( 100 * i / len, 1 ), "%). Stimulus not
shown. Adaptive algorithm finished", sep = "" ) )
   next
  }
 }
 # present stimulus
 if( !( i == len ) ) {
```

```
  res <- opiPresent( stim = stimstack[[i]], nextStim = stimstack[[i+1]] )
 } else {
  res <- opiPresent( stim = stimstack[[i]] )
 }
 # store results from presentation
 if( is.null( res$err ) ) {
  if( res$seen == 0 ) {
   print( paste( i, " out of ", len, " (", round( 100 * i / len, 1 ), "%). Stimulus not
seen", sep = "" ) )
  } else {
   print( paste( i, " out of ", len, " (", round( 100 * i / len, 1 ), "%). Stimulus seen.
(x,y) = (",  res$x, ",", res$y, ")", sep = "" ) )
  }
  subj$xstart[i]  <- stimstack[[i]]$path$x[1]
  subj$ystart[i]  <- stimstack[[i]]$path$y[1]
  subj$xend[i]    <- stimstack[[i]]$path$x[2]
  subj$yend[i]    <- stimstack[[i]]$path$y[2]
  subj$fptrial[i] <- ( stimstack[[i]]$levels == stim_intfp )
  subj$seen[i]    <- res$seen
  subj$x[i]       <- res$x
  subj$y[i]       <- res$y
  subj$vlength[i] <- sqrt (( subj$x[i] - subj$xend[i] )^2 + ( subj$y[i] - subj$yend[i] )^2)
  subj$angle[i]   <- round(Oct900.VectorAngle(subj$xstart[i], subj$ystart[i]))
  subj$restime[i] <- substr( Sys.time(), 12, 19 )
 } else {
```

```
    warning( paste( "error ocurred with code: ", res$seen, sep = "" ) )
  }
  if( subj$fptrial[i] == TRUE ) next # if FP trial, then skip.
  # accummulate number of trials and see if max num of trials have been reached
  kinvect$ntrials[idx] <- kinvect$ntrials[idx] + 1
  if( kinvect$ntrials[idx] >= minreps ) {
    sidx <- which( subj$xstart == kinvect$xstart[idx] &
                   subj$xend   == kinvect$xend[idx]   &
                   subj$ystart == kinvect$ystart[idx] &
                   subj$yend   == kinvect$yend[idx]   &
                   !subj$fptrial                      )
    kinvect$finished[idx] <- kinadaptive( kinvect[idx,],
                                          subj[sidx,],
                                          criterion = criterion,
                                          threshold = threshold )
  }
  if( kinvect$ntrials[idx] == maxreps ) kinvect$finished[idx] <- TRUE
}
opiClose()
# remove lines with NA responses (nut run because of the adaptive algorithm)
idx <- which( is.na( subj$xstart ) )
if( length( idx ) != 0) subj <- subj[-idx,]
write.csv( subj, file = fnamed, row.names = FALSE )
kinvect$finished <- NULL
```

```
# remove all false positive trials before recording the estimated isopter

idx <- which( subj$fptrial == FALSE )

if( length( idx ) > 0 ) subj <- subj[idx,]

kinvect$vlength <- aggregate(vlength ~ angle, data = subj, FUN =  median, na.rm
=FALSE)$vlength

write.csv( kinvect, file = fnamec, row.names = FALSE )
```

10.4.1 A4.1: Chapter 6 patient plots

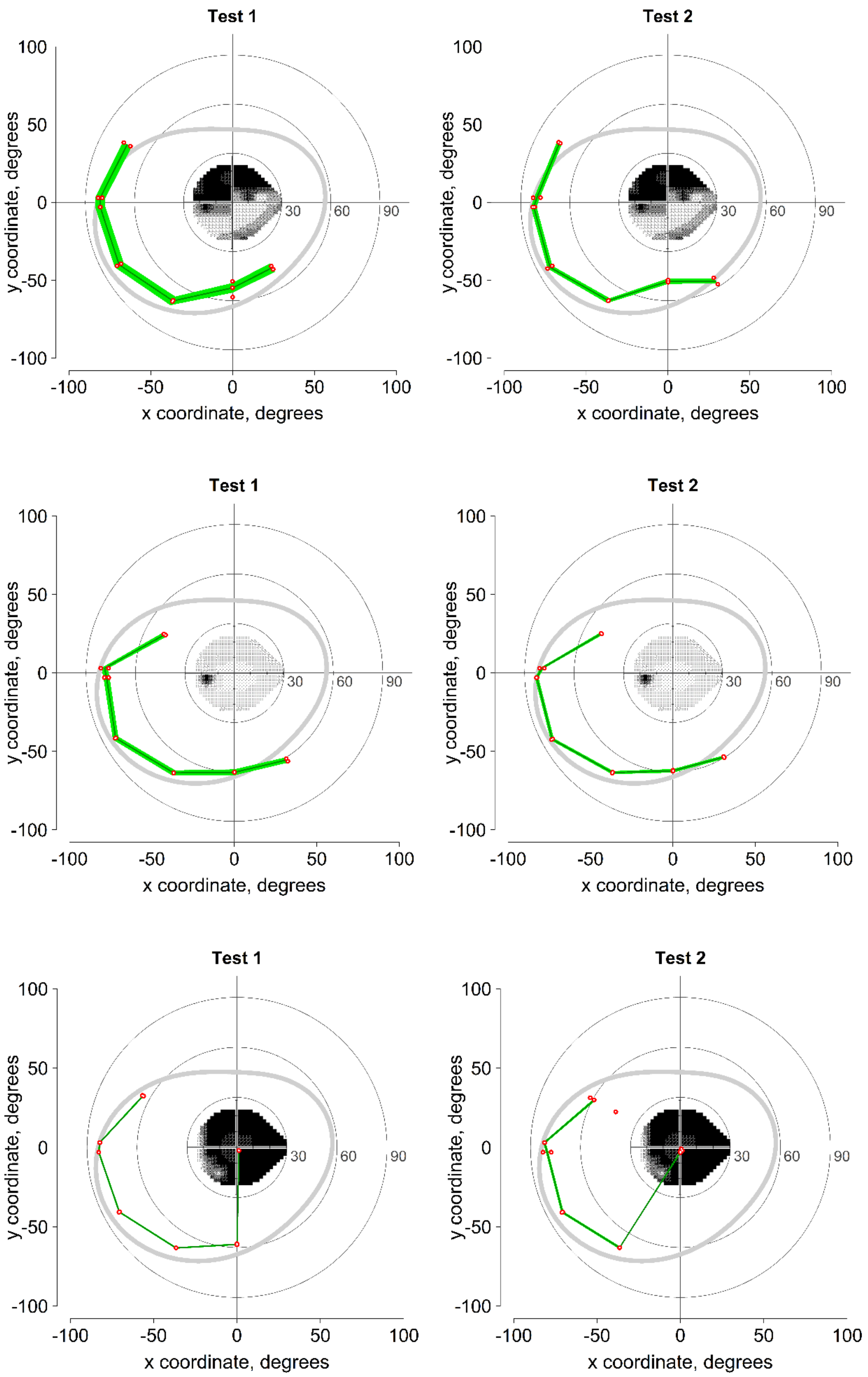

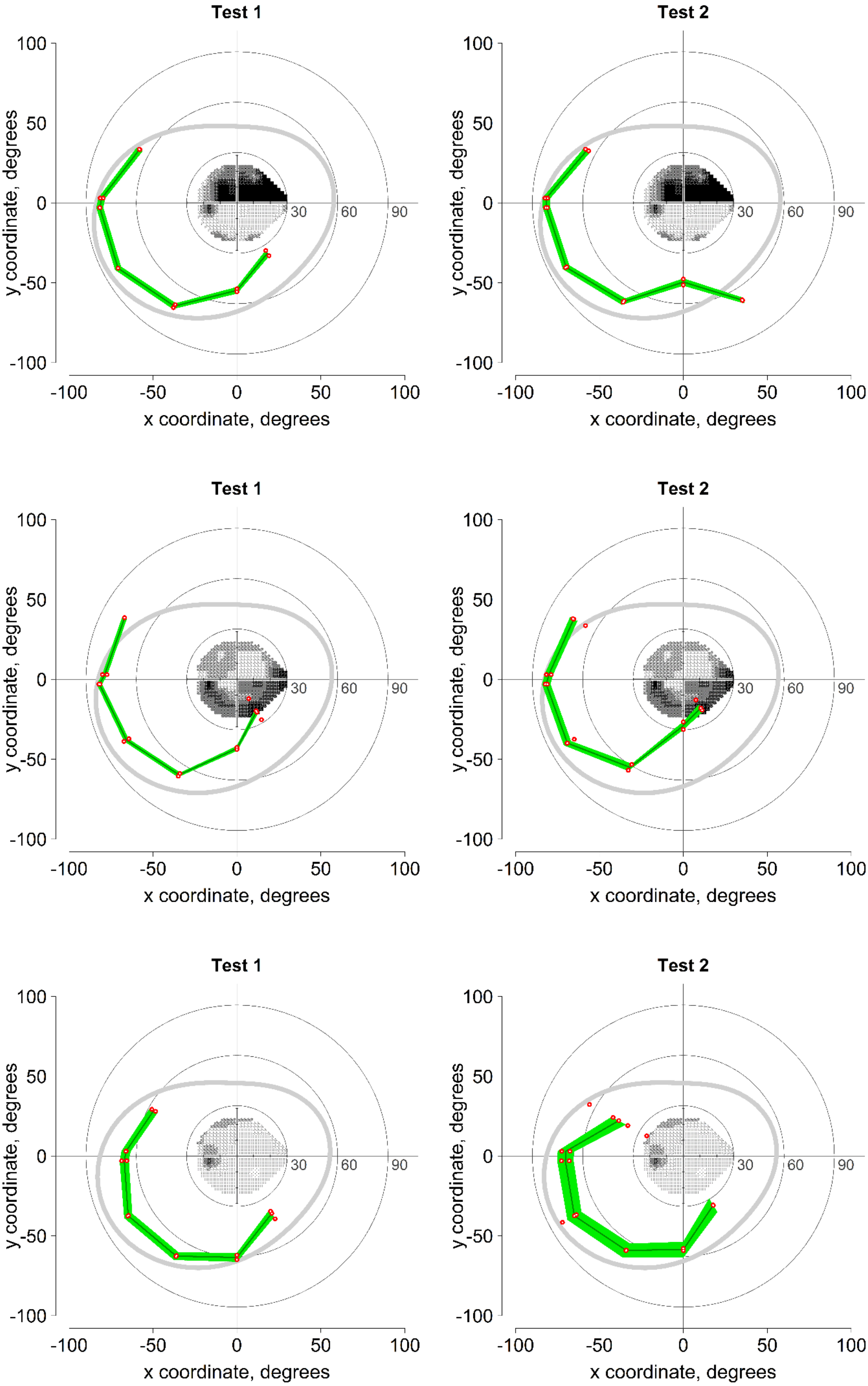

Test 1
Test 2
Test 1
Test 2
Test 1
Test 2
y coordinate, degrees
x coordinate, degrees
100
50
0
-50
-100
-100
-50
0
50
100
30
60
90

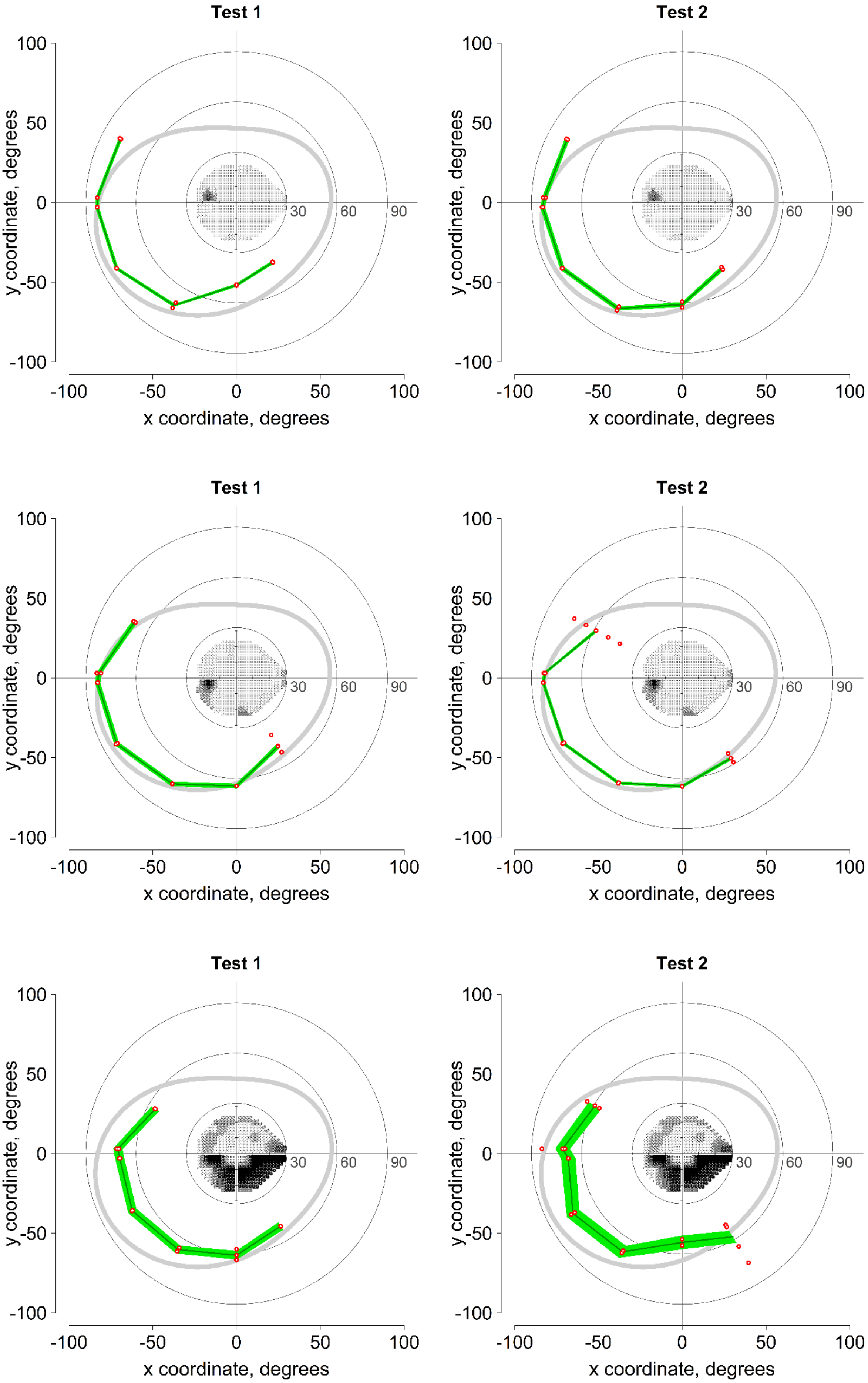
Test 1
Test 2
y coordinate, degrees
x coordinate, degrees
100
50
0
-50
-100
-100
-50
0
50
100
30
60
90

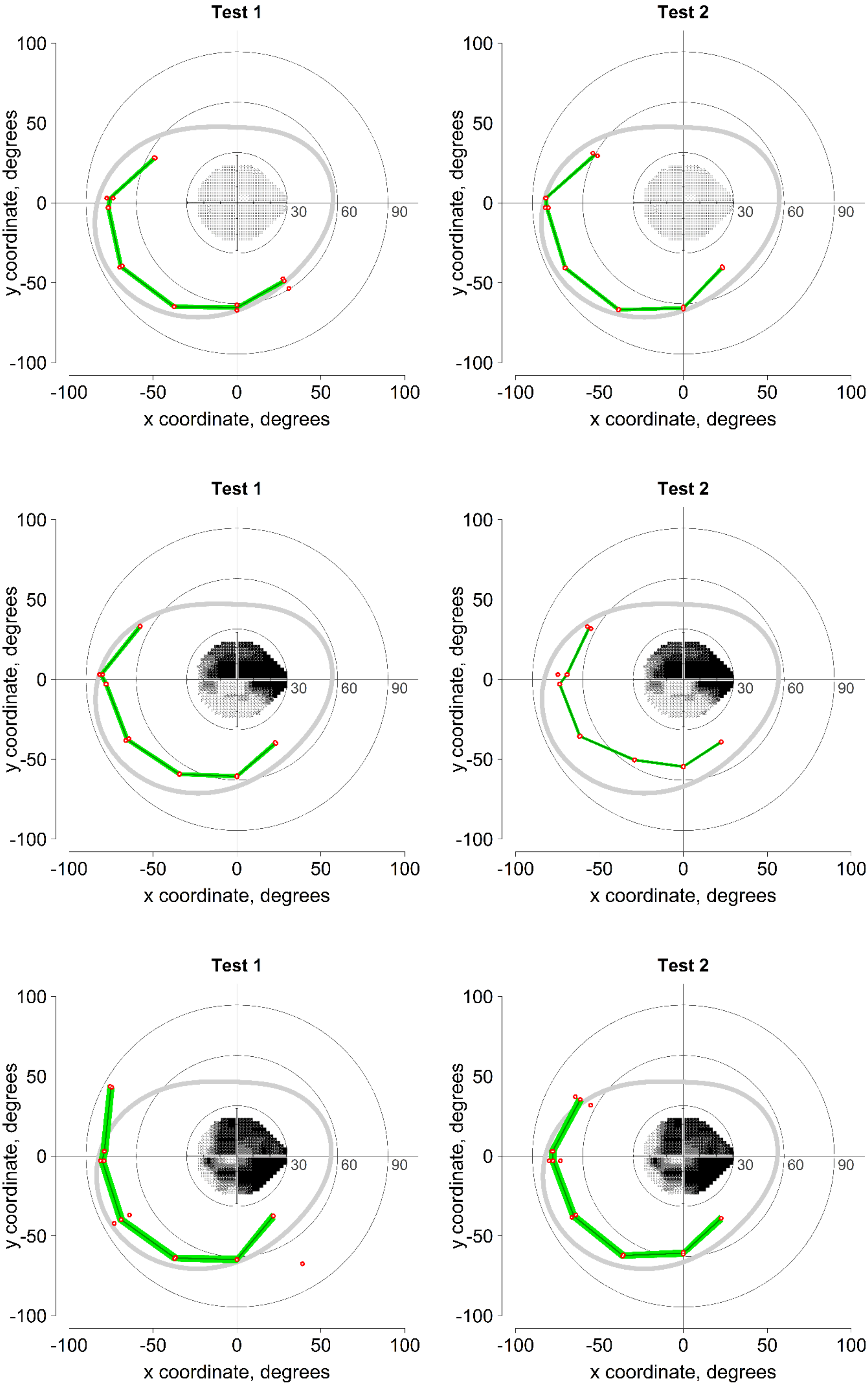
Test 1
Test 2
y coordinate, degrees
x coordinate, degrees
100
50
0
-50
-100
30
60
90
Test 1
Test 2
y coordinate, degrees
x coordinate, degrees
Test 1
Test 2
y coordinate, degrees
x coordinate, degrees

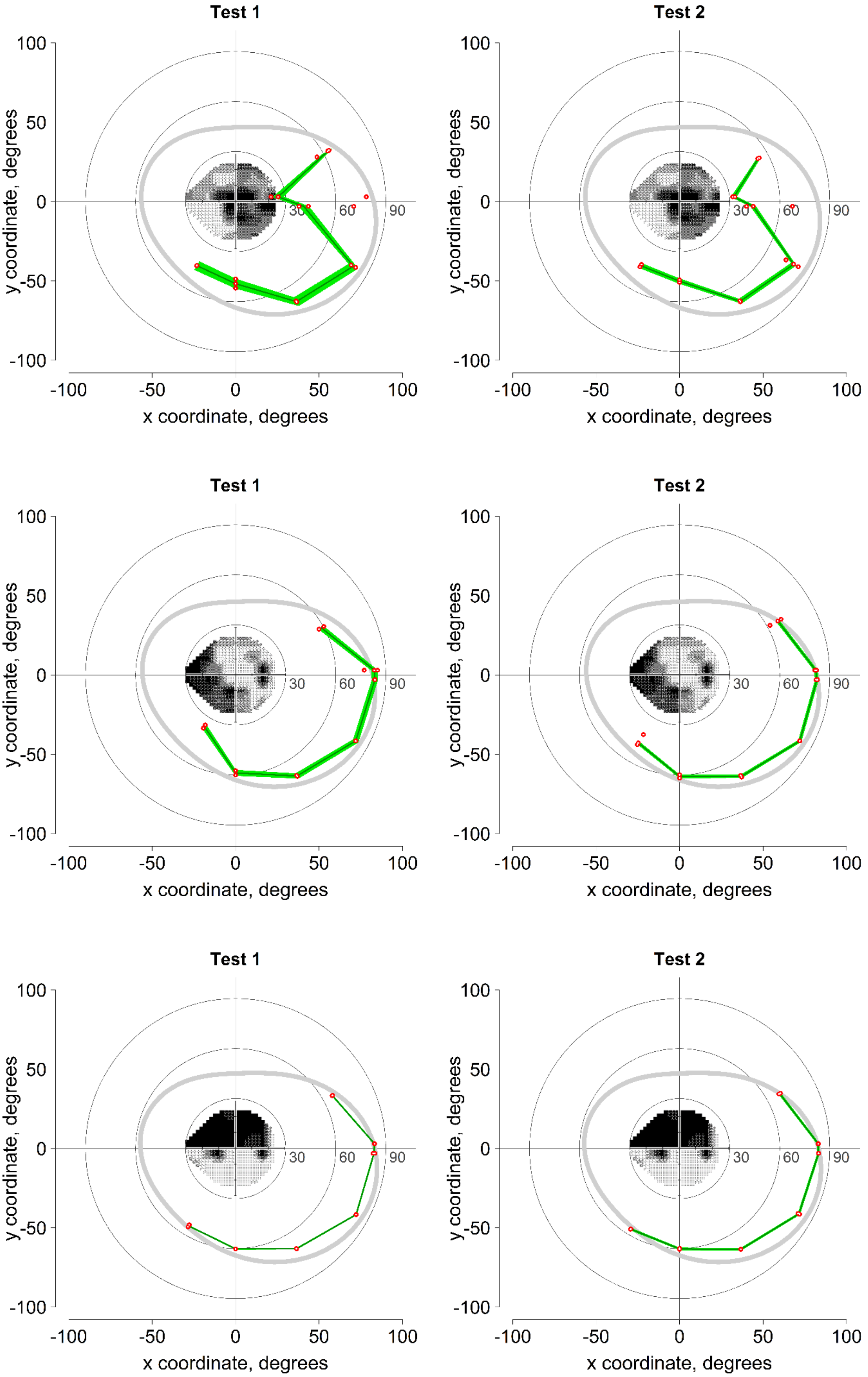
Test 1
Test 2
Test 1
Test 2
Test 1
Test 2
100
50
0
-50
-100
y coordinate, degrees
-100
-50
0
50
100
x coordinate, degrees
30
60
90

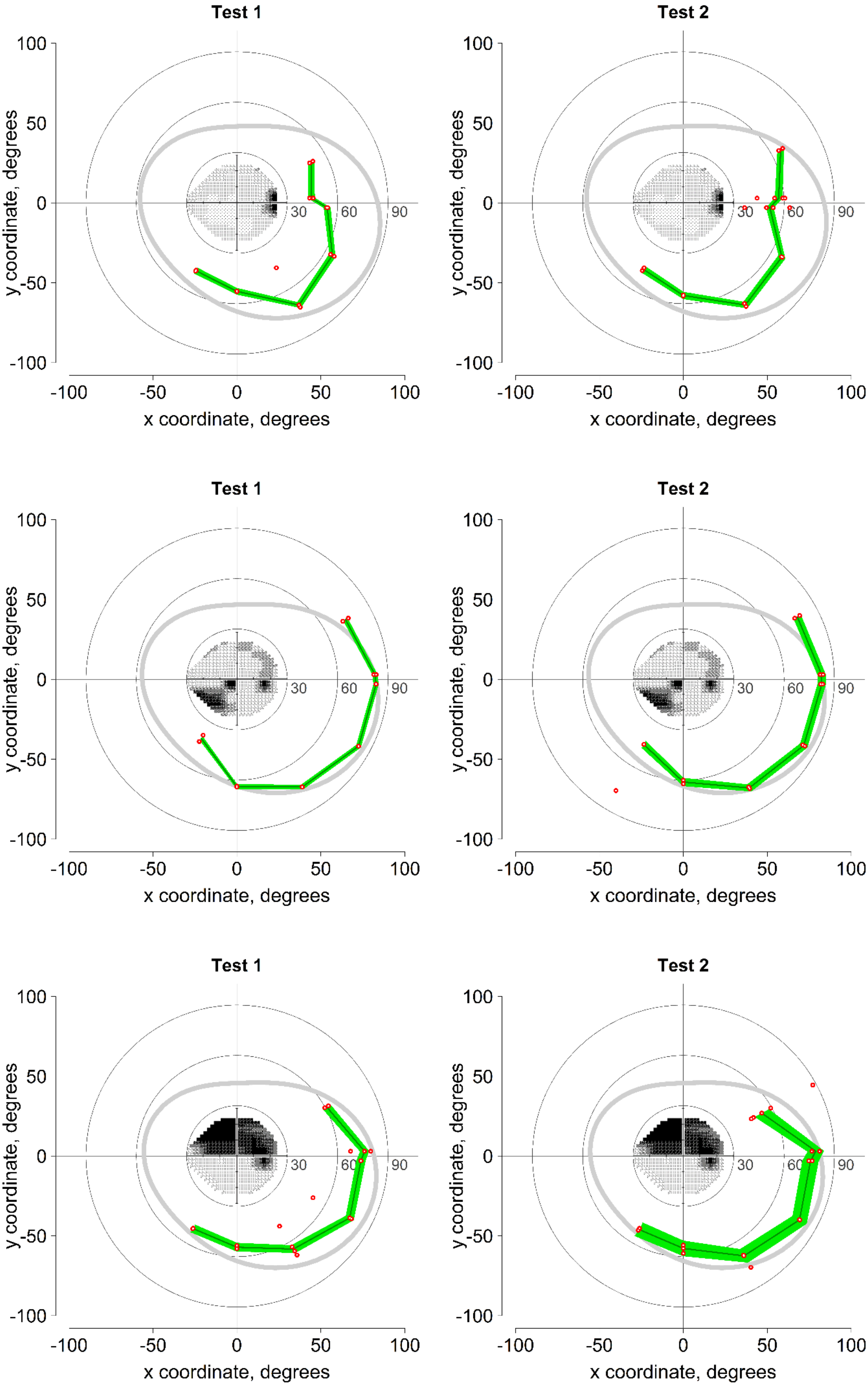
Test 1
Test 2
100
50
0
-50
-100
y coordinate, degrees
-100
-50
0
50
100
x coordinate, degrees
30
60
90
Test 1
Test 2
Test 1
Test 2

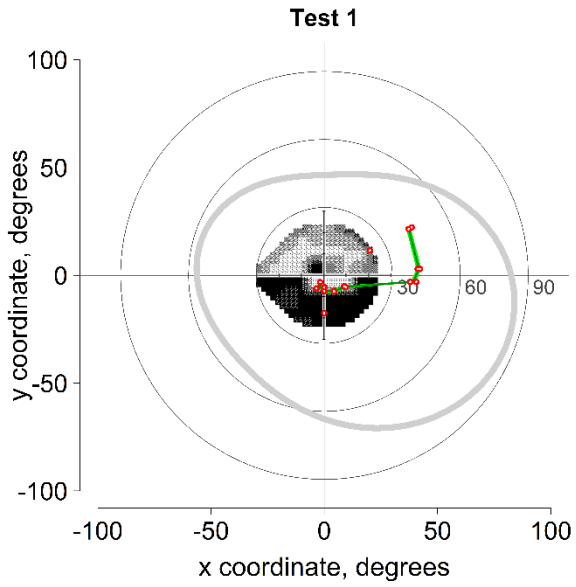
Test 1
100
50
0
-50
-100
y coordinate, degrees
30
60
90
-100
-50
0
50
100
x coordinate, degrees

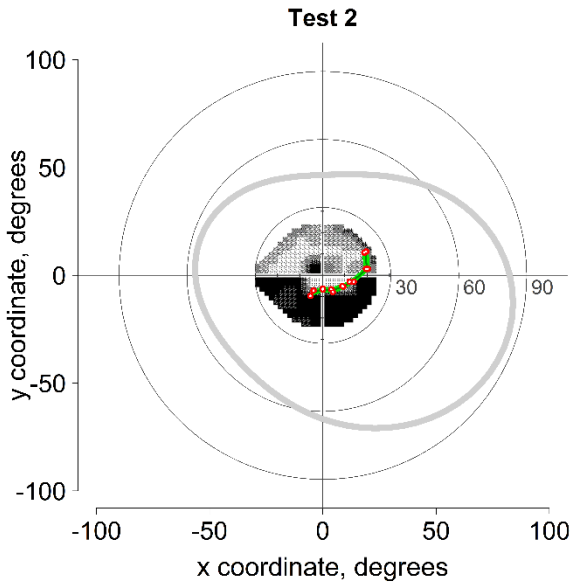
Test 2
100
50
0
-50
-100
y coordinate, degrees
30
60
90
-100
-50
0
50
100
x coordinate, degrees

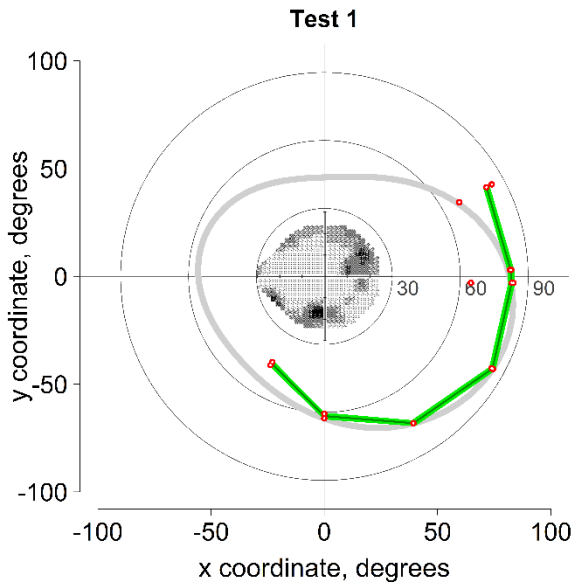
Test 1
100
50
0
-50
-100
y coordinate, degrees
30
60
90
-100
-50
0
50
100
x coordinate, degrees

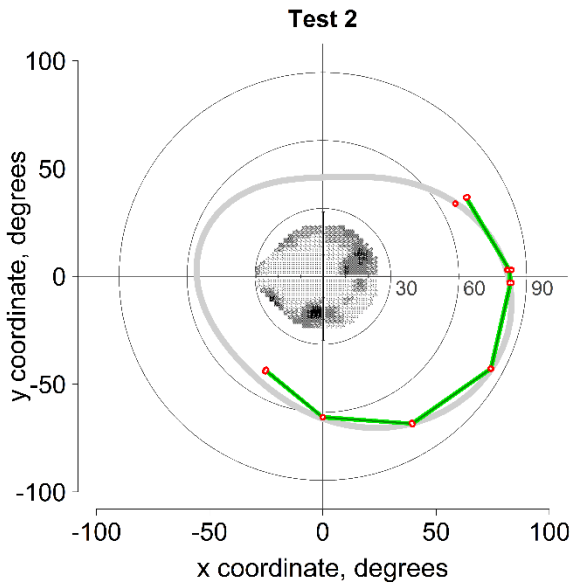
Test 2
100
50
0
-50
-100
y coordinate, degrees
30
60
90
-100
-50
0
50
100
x coordinate, degrees

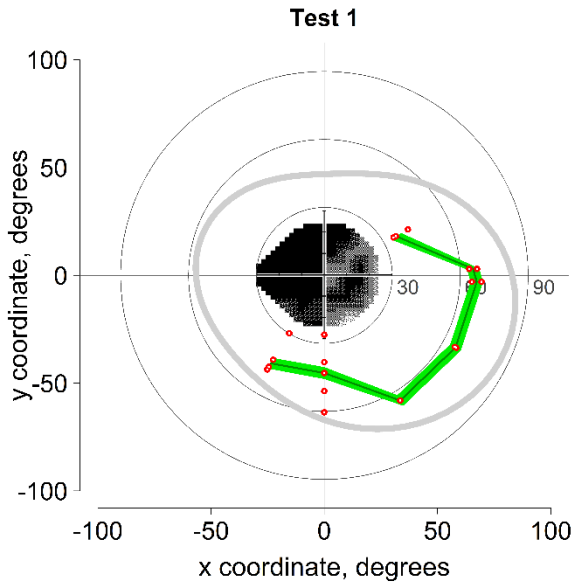
Test 1
100
50
0
-50
-100
y coordinate, degrees
30
90
-100
-50
0
50
100
x coordinate, degrees

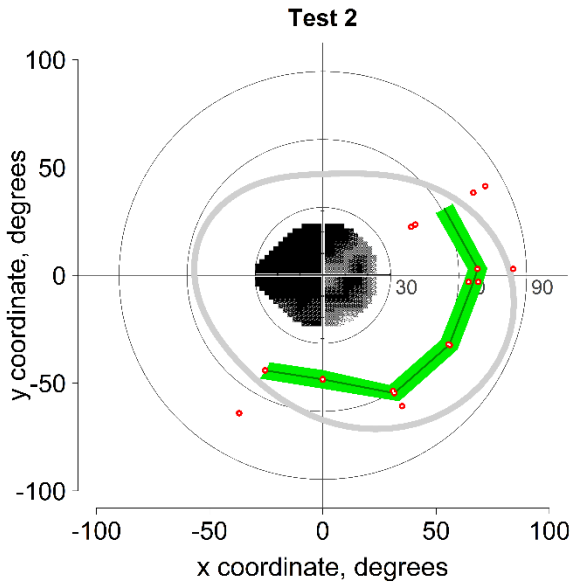
Test 2
100
50
0
-50
-100
y coordinate, degrees
30
90
-100
-50
0
50
100
x coordinate, degrees

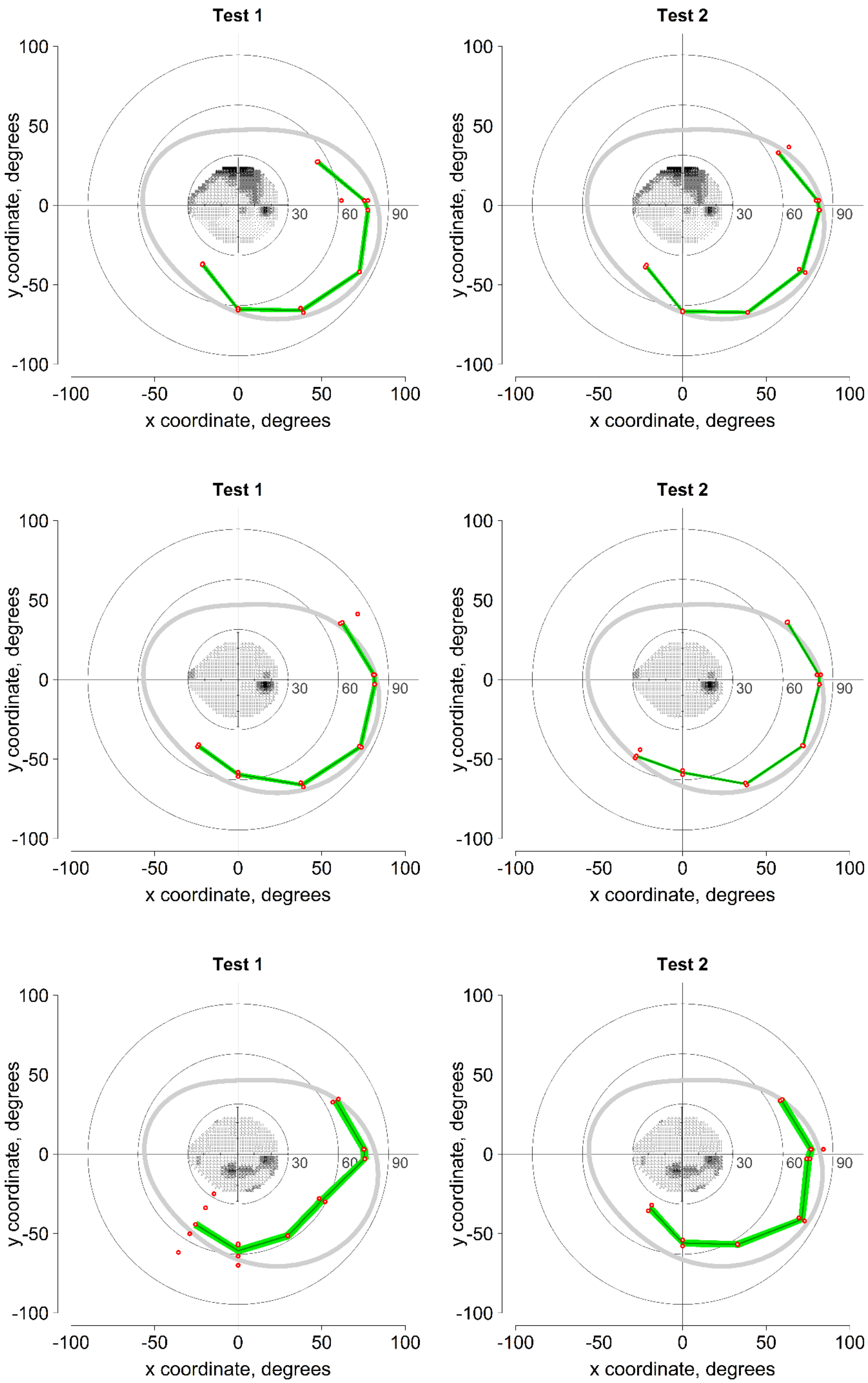
Test 1
Test 2
Test 1
Test 2
Test 1
Test 2
y coordinate, degrees
x coordinate, degrees
100
50
0
-50
-100
30
60
90

10.5 A5: Chapter 7 balance analysis R code

```
setwd ("C:/Users/cbain/Google Drive/CB_PHD_Work/Projects/Balance study/Real Patient data")

rm(list=ls())

require(lattice)

require(Hmisc)

require(plotrix)

require(signal)

vffiles <- dir ("./GP08/", ".csv", full.names = TRUE)

vfdata <- data.frame ()

for (i in 1 : length(vffiles)) {

 tmp <- read.csv (vffiles[i], sep = ",", head=TRUE)


 tmp.id <- gsub ("_", " ", basename (vffiles[i]))

 tmp.id.2 <- sub (".csv", "", tmp.id)

 tmp <- cbind (fname = tmp.id.2, tmp)

 tmp$id <- "GP08"

 tmp$Trialtype <- substr(tmp$fname, 1, 6)

 tmp$Trialnumber <- substr(tmp$fname, 18, 20)

 tmp$fname <- NULL

 bf <- butter(3, 0.1)

 tmp$Roll <- filtfilt(bf, tmp$Roll)

 tmp$Pitch <- filtfilt(bf, tmp$Pitch)

 tmp$Velroll <- filtfilt(bf, tmp$VelInc_Z)

 tmp$Velpitch <- filtfilt(bf, tmp$VelInc_X)
```

```
tmp$Accroll <- filtfilt(bf, tmp$Acc_Z)

tmp$Accpitch <- filtfilt(bf, tmp$Acc_X)

tmp$Yaw <- filtfilt(bf, tmp$Yaw)


tmp <- tmp[-c(1:100),]

if(nrow(tmp) < 2900) {

  tmp <- NULL

}

tmp <-tmp[c(1:3000),]

tmp$Rollstart <- tmp[1, 20]

tmp$Pitchstart <- tmp[1, 21]

tmp$Accpitchstart <- tmp[1, 7]

tmp$Accrollstart <- tmp[1, 9]

tmp$Velpitchstart <- tmp[1, 13]

tmp$Velrollstart <- tmp[1, 15]

tmp$Yawstart <- tmp[1, 22]


tmp$rollerror <- abs(tmp$Roll - tmp$Rollstart)

tmp$rollrmse <- sqrt(mean(tmp$rollerror^2))

tmp$Pitcherror <- abs(tmp$Pitch - tmp$Pitchstart)

tmp$Pitchrmse <- sqrt(mean(tmp$Pitcherror^2))

tmp$Velrollerror <- abs(tmp$Velroll - tmp$Velrollstart)

tmp$velrollrmse <- sqrt(mean(tmp$Velrollerror^2))

tmp$Velpitcherror <- abs(tmp$Velpitch - tmp$Velpitchstart)
```

```
  tmp$velpitchrmse <- sqrt(mean(tmp$Velpitcherror^2))
  tmp$Accrollerror <- abs(tmp$Accroll - tmp$Accrollstart)
  tmp$Accrollrmse <- sqrt(mean(tmp$Accrollerror^2))
  tmp$Accpitcherror <- abs(tmp$Accpitch - tmp$Accpitchstar)
  tmp$Accpitchrmse <- sqrt(mean(tmp$Accpitcherror^2))
  tmp$Yawerror <- abs(tmp$Yaw - tmp$Yawstart)
  tmp$Yawrmse <- sqrt(mean(tmp$Yawerror^2))

  tmp$diffx <- ave(tmp$rollerror, FUN=function(x) c(0, diff(x)))
  tmp$diffy <- ave(tmp$Yawerror, FUN=function(x) c(0, diff(x)))
  tmp$diffz <- sqrt( tmp$diffx^2 + tmp$diffy^2 )
  tmp$vflength <- sum(tmp$diffz)
  tmp$vfspeed <- tmp$vflength/30
  vfdata <- rbind (vfdata, tmp)
}
rollmean <- aggregate(rollrmse ~ Trialtype, data = vfdata, FUN = mean)
pitchmean <- aggregate(Pitchrmse ~ Trialtype, data = vfdata, FUN = mean)
yawmean <- aggregate(Yawrmse ~ Trialtype, data = vfdata, FUN = mean)
rollsd <- aggregate(rollrmse ~ Trialtype, data = vfdata, FUN = sd)
pitchsd <- aggregate(Pitchrmse ~ Trialtype, data = vfdata, FUN = sd)
yawsd <- aggregate(Yawrmse ~ Trialtype, data = vfdata, FUN = sd)
Speedmean <- aggregate(vfspeed ~ Trialtype, data = vfdata, FUN = mean)
vfdistance <- aggregate(vflength ~ Trialtype, data = vfdata, FUN = mean)
Speedsd <- aggregate(vfspeed ~ Trialtype, data = vfdata, FUN = sd)
```

```
vfdistancesd <- aggregate(vflength ~ Trialtype, data = vfdata, FUN = sd)

results <- cbind(rollmean, pitchmean)

results <- cbind(results, yawmean)

results <- cbind(results, Speedmean)

results <- cbind(results, vfdistance)

results[3] <- NULL

results[4] <- NULL

results[5] <- NULL

results[7] <- NULL

write.csv(results, file = "GP08results.csv")
```

10.5.1 A5.1 Postural sway stability, all conditions

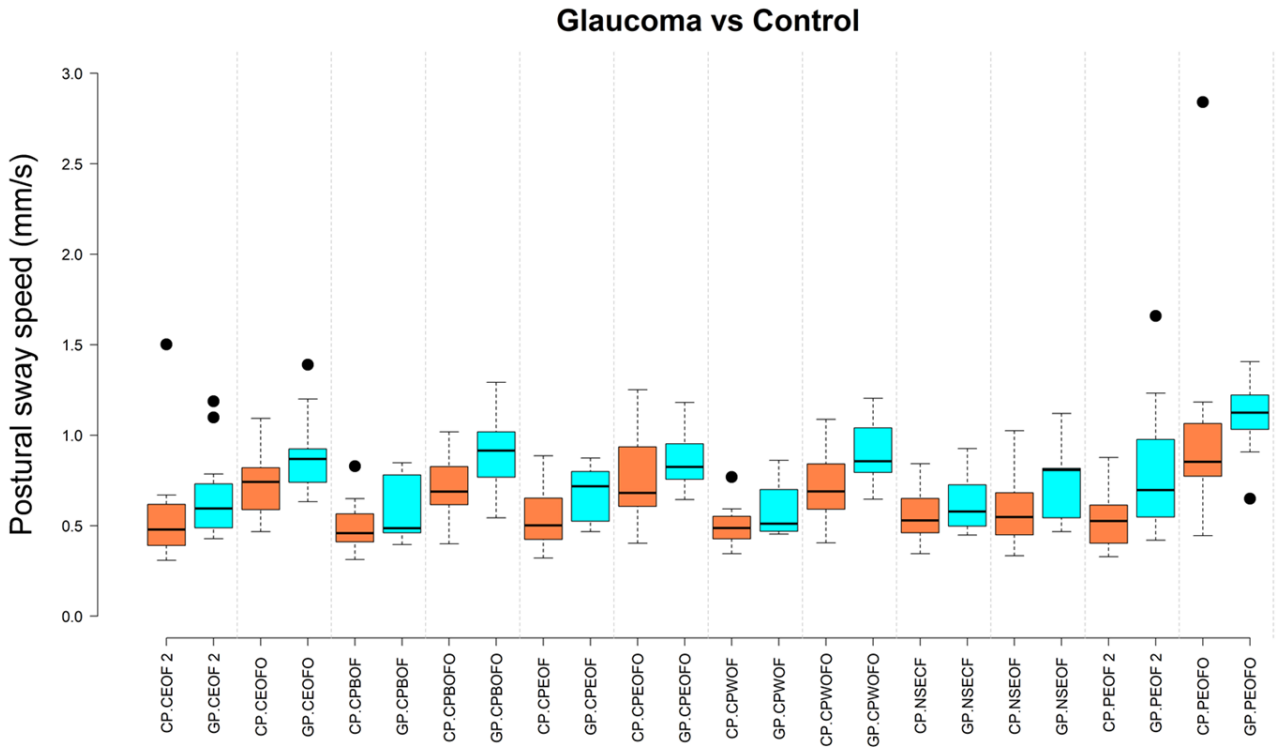

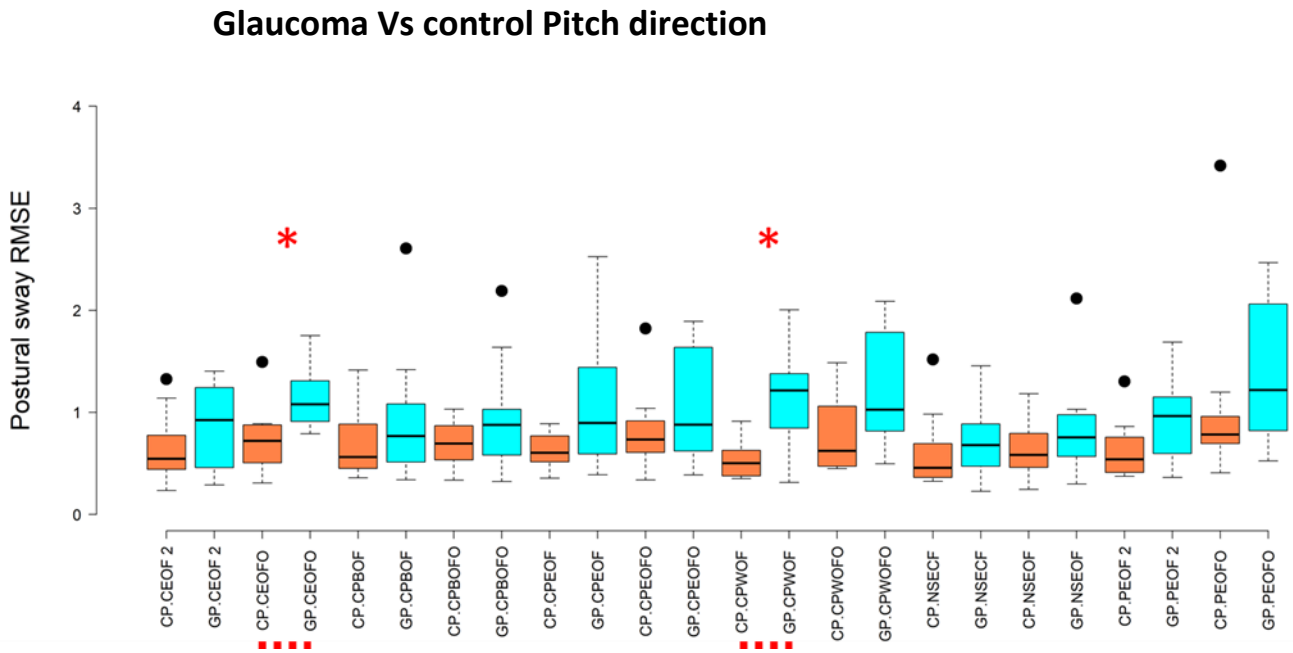

Glaucoma Vs control roll direction